LATERAL VARIATION OF THE ELECTRICAL CONDUCTIVITY STRUCTURE ACROSS SOUTH SCOTLAND

Malcolm Robert Ingham

Doctor of Philosophy
University of Edinburgh
1981

DECLARATION

I hereby declare that the work presented in this thesis is my own, unless otherwise stated in the text, and that the thesis has been composed by myself.

Malcolm Ingham

ABSTRACT.

Magnetotelluric measurements in the period range 10 - 1000 seconds have been made at ten new sites in South Scotland and the data analysed to give apparent resistivities and phases and induction vectors for each site.

Nine of the sites lie on a linear traverse stretching from Kinloch Rannoch in the Highlands to Borthwickbrae in the Borders. The apparent resistivities and phases from these sites have been modelled by both one and two-dimensional apparent resistivity structures. The technique of modelling averaged resistivity and phase values as a first approximation,has been found to be a useful way of simplifying the initial modelling procedure.

The final two dimensional model across the traverse shows horizontal discontinuities in electrical conductivity at both the Highland Boundary and Southern Uplands Faults, with a highly conducting zone extending to a depth of 90km below the Southern Uplands.Heat flow measurements and thermal conductivity estimates have been used to predict temperature-depth profiles for the Highlands,the Midland Valley and the Southern Uplands. These in turn have been used to interpret the electrical conductivity model in terms of the possible causes of high conductivity. In the Highlands and Midland Valley the conducting zones have been identified with electronic conduction in hydrated rocks and the process of dehydration at the boundary between amphibolitic and granulitic facies. As well as these mechanisms it is possible that beneath the Southern Uplands, partial melting may occur at depths around 70km.

The two-dimensional model has also been fitted to the verti-

cal magnetic field data across the traverse. However, additional data from other sites in the South of Scotland have been analysed also, and an interpretation of the vertical magnetic field in terms of an equivalent line current has been made. The depth to the line current, and its position beneath the Southern Uplands, agrees with the depth and position of the highly conducting zone in the two-dimensional induction model. It is likely though that both conduction and induction contribute to the measured vertical field.

The results of the modelling tend to support the suggestion that the anomalously high conductivity beneath the Southern Uplands is a result of the tectonic processes involved in the closing of the Iapetus Ocean. There is also some indication of the possibility of an ancient subduction zone beneath the Highland Boundary Fault.

ACKNOWLEDGEMENTS.

I would like to express my thanks to the following people without whose help the writing of this thesis would have been much more difficult if not impossible.

Primarily, to Dr. Rosemary Hutton, my supervisor, for the initial impetus for the project and for her continuing support and guidance thereafter.

To Drs. Ebong Mbipom and David McKirdy for their companionship in sharing an office and for the various helpful discussions.

Also to the many other members of the geomagnetic induction group, both past and present, for discussions and suggestions on many areas of the work.

To Grahame Dawes, for his invaluable assistance on many aspects of computing, particularly for the programs associated with the reading of the cassette tape data, likewise to Ian MacDonald for his advice and help in all matters concerning electronics and his good fellowship on fieldwork.

To Alex Jackson and Helmut Jakubowicz for their assistance in the field at various times, and also the many landowners, factors and farmers on whose property the fieldwork was carried out and without whose patience and forbearance nothing would have been possible.

To the Department of Geophysics of the University of Edinburgh for the facilities for this work to be carried out, and to the Natural Environmental Research Council for the provision of a postgraduate studentship.

And finally, last but not least, to my wife Gillian, not only for typing this thesis but for her help and support in many other ways also.

LIST OF CONTENTS.

LIST OF TABLES.

LIST OF FIGURES.

CHAPTER 1: INTRODUCTION.

The Earth's magnetic field varies with time and since 1889, when Schuster first separated it into internal and external parts, this characteristic of the field has provided a means of inferring the electrical conductivity of the Earth. However until comparatively recently, research concentrated on the determination of a global electrical conductivity distribution. It was Caignard (1953) who first suggested that simultaneous measurements of the electric and magnetic fields at the surface of the Earth could be used to investigate more localized conductivity structures. Since then this branch of geophysics, known as magnetotellurics (MT), has progressed steadily until today it is accepted as an important method of geophysical exploration of the crust and mantle.

Price (1962) adapted Caignard's theory to non-uniform and finite source fields and Berdichevsky (1960, 1963) introduced the concept of an impedance tensor for the evaluation of two-dimensional problems. In recent years advances have also been made (Haak, 1978; Jones and Vozoff, 1978) in the analysis of three-dimensional structures. The electrical structure of the Earth can also be studied by means of geomagnetic deep sounding (GDS) which invloves the measurement of all three components of the magnetic field. It was Parkinson (1959, 1962) who showed the importance of the vertical magnetic field in induction work and this is now routinely measured as part of MT studies.

Although a knowledge of the source field is in no way a prerequisite for the use of magnetotelluric and geomagnetic deep sounding techniques; indeed they can be used to make inferences

about the source field (e.g. Bannister and Gough, 1977, 1978); it is helpful to have an understanding of the kinds of magnetic variations to be expected. The frequency spectrum of the geomagnetic field is shown in figure 1.1. Table 1.1 gives a breakdown of the main peaks of the spectrum, their characteristics and causes. This thesis reports the use of induction studies (particularly MT) to construct a geoelectric section along a traverse across South Scotland. The period range involved is about 20-1000 seconds and therefore the majority of the magnetic activity recorded was due to micropulsations. The theory, outlined in chapter 2, makes the assumption that the dimensions of the source field are greater than the skin depth of the Earth. Fortunately, in this period range, Scotland is far enough south of the electrojet region for this assumption to be valid, particularly as the high conductivities modelled in chapter 6 mean that the skin depth is relatively small.

Chapter 2 also discusses the derivation, meaning and usefulness of the various functions which represent the response of the Earth to an impulse in the form of a magnetic field variation. The tectonic history, geology and geophysics of South Scotland are discussed in chapter 3. The complex structure and evolution of the area(and how it is important because it represents the site of closure of the Iapetus or proto-Atlantic Ocean)is emphasized.

The fourth chapter describes the equipment used in this study and the sites at which measurements were made, including the problems encountered at particular sites. It also describes the data analysis routines used and likely sources of error in the results. The results themselves are presented in chapter 5.

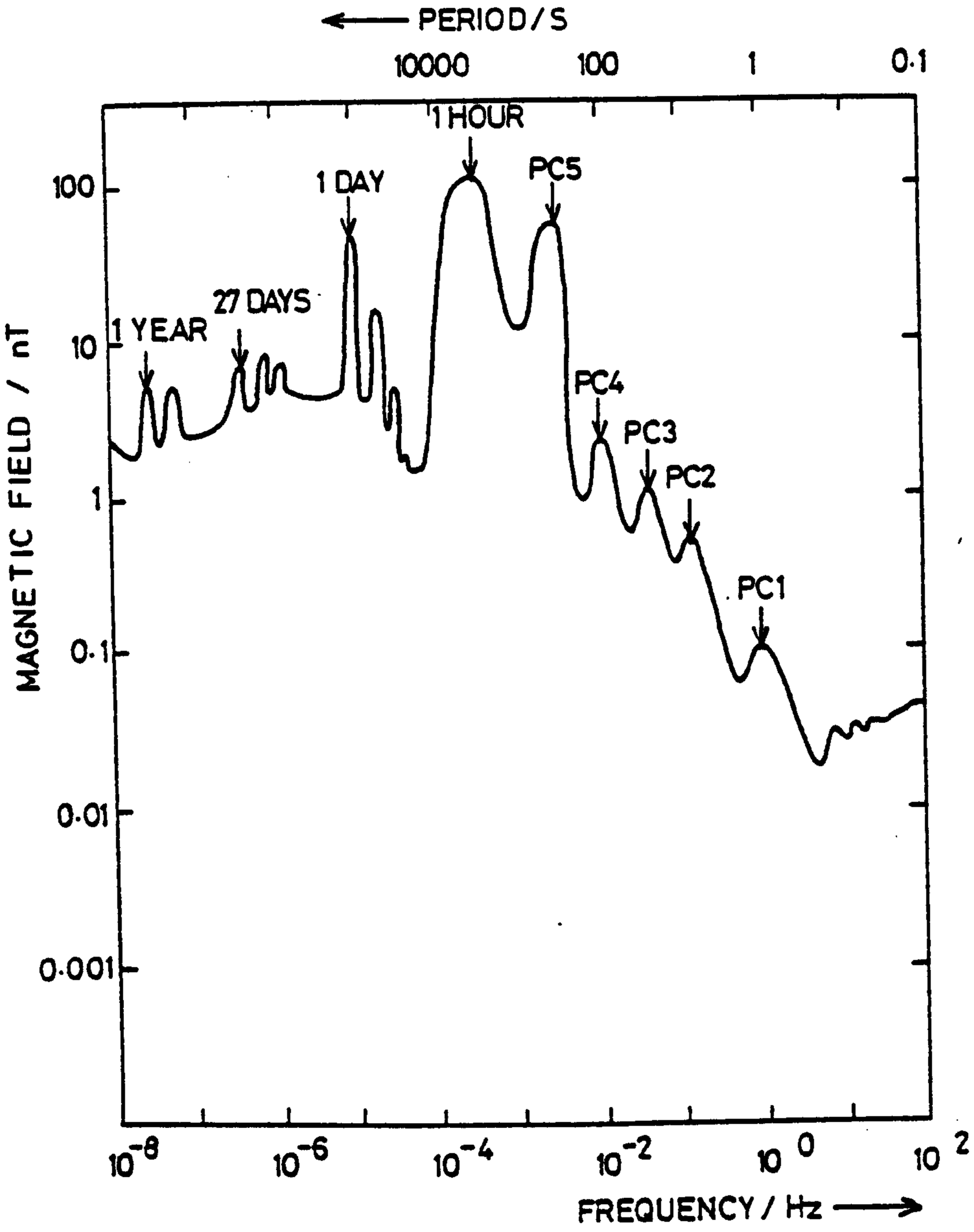

Figure 1·1.

Natural variations in the horizontal magnetic field of the Earth which are used in induction studies.

(after Serson , 1973)

Table 1.1

Peaks in the geomagnetic spectrum.

Variation	Period	Origin	Comments	References
	1 year	Earth's rotation around the sun.		
	27 days	Solar rotation.		Matsushita (1967) & Campbell
Daily variation (Sq)	24 hours and harmonics	Rotation of the Earth -ionospheric dynamo action.	Observed best during geomagnetically quiet periods.	Mishin et al. (1975)
Bays	1 hour	Simplest type of worldwide magnetic storms.		
Micropulsations	1-200 seconds	Originate as hydro-magnetic waves due to the interaction between the solar wind and the magnetosphere.	Either continuous harmonic pulsations (pc's) or transient phenomena (pi's), usually observed around local midnight.	Orr (1973)

Chapter 6 deals with the modelling studies (both one and two-dimensional) carried out on the magnetotelluric results. The final geoelectric section is presented in figure 6.15 with estimates of both resistivity and depth ranges. The chapter also deals with attempts to model the vertical magnetic field by means of equivalent line currents.

In chapter 7 the geoelectric section is compared with both the results of similar studies in other parts of the world and with other geophysical results from South Scotland. There is then a review of the literature concerned with the causes of zones of anomalously high electrical conductivity in the Earth. The second part of the chapter applies these results and also the results of heat flow measurements to the interpretation of the geoelectric section. The interpretation is discussed in the light of the geological structure and tectonic history of the area and various conclusions are drawn and suggestions made.

Thunderstorm activity is the source of magnetic variations of period less than 1 second and these can be used in audiomagnetotellurics (AMT) to study the structure of the first few kilometres of the crust. The appendix describes such an investigation into the surface sedimentary cover along the geoelectric section and is an extension of the orginal work.

CHAPTER 2: THE THEORY OF THE MAGNETOTELLURIC METHOD AND EARTH RESPONSE FUNCTIONS.

2.1: The basic theory of the magnetotelluric method.

The basic theory of the magnetotelluric method can be derived from Maxwell's equations:

$$\underline{\nabla}_{\wedge}\underline{E} = -\mu\frac{\partial \underline{H}}{\partial t} \qquad 2.1$$

$$\underline{\nabla}_{\wedge}\underline{H} = \underline{j} + \frac{\partial \underline{D}}{\partial t} \qquad 2.2$$

$$\underline{\nabla}.\underline{D} = \rho \qquad 2.3$$

$$\underline{\nabla}.\underline{H} = 0 \qquad 2.4$$

where the different parameters are:

$\underline{E}$ - the electric field vector;

$\underline{D}$ - the electric displacement vector;

$\underline{H}$ - the magnetic field intensity vector;

$\underline{j}$ - the electric current density;

ρ - the space electric charge density;

and μ - the magnetic permeability of the medium.

Applying the constitutive relationships

$$\underline{D} = \varepsilon\underline{E} \qquad 2.5$$

$$\underline{j} = \sigma\underline{E} \qquad 2.6$$

(where ε and σ are respectively the permittivity and conductivity of the medium) and taking the curl of equation 2.1 gives, using 2.2;

$$\underline{\nabla}_{\wedge}(\underline{\nabla}_{\wedge}\underline{E}) = -\mu\sigma\frac{\partial \underline{E}}{\partial t} - \mu\varepsilon\frac{\partial^2 \underline{E}}{\partial t^2} \qquad 2.7$$

In a conducting medium any initial space charge density decays with time according to

$$\rho(t) = \rho_o e^{-\sigma t/\varepsilon}$$

and for the rocks of the earth's crust and mantle $\sigma/\varepsilon \gg 1$, thus $\rho(t) \approx 0$ and 2.3 becomes

$$\underline{\nabla}.\underline{D} = 0 \qquad 2.8$$

Expanding $\underline{\nabla}_\wedge(\underline{\nabla}_\wedge\underline{E})$ as

$$\underline{\nabla}_\wedge(\underline{\nabla}_\wedge\underline{E}) = \underline{\nabla}(\underline{\nabla}.\underline{E}) - \nabla^2\underline{E} \qquad 2.9$$

and using 2.8 gives

$$\nabla^2\underline{E} - \mu\sigma\frac{\partial\underline{E}}{\partial t} - \mu\varepsilon\frac{\partial^2\underline{E}}{\partial t^2} = 0 \qquad 2.10$$

A further simplification is possible. Typical values of σ and ε are $\sigma \sim 10^{-5}$ to 10^{-1} S m^{-1} and $\varepsilon \sim 9 \times \varepsilon_o$ where ε_o, the permittivity of free space, is 8.85×10^{-12} F.m^{-1}. For the periods of magnetic field variation involved, $T \gtrsim 1$s so that

$$\left|\sigma\frac{\partial E}{\partial t}\right| \gg \left|\varepsilon\frac{\partial^2 E}{\partial t^2}\right|$$

Using this result 2.10 reduces to

$$\nabla^2\underline{E} = \mu_o\sigma\frac{\partial\underline{E}}{\partial t} \qquad 2.11$$

where μ has been put equal to the permeability of free space μ_o ($=4\pi \times 10^{-7}$ H.m^{-1}).

The problem can therefore be treated as one of diffusion of the incident field into the Earth, as suggested by Price (1962).

2.1.1: Induction in one-dimensional structures.

A one-dimensional structure is one in which the conductivity of the Earth varies only as a function of depth into the Earth.

If in Cartesian co-ordinates z is measured vertically downwards, $\sigma = \sigma(z)$, and $\underline{E}$ may be expressed as

$$\underline{E}\,(t,x,y,z) = T(t).Z(z).\underline{F}(x,y) \qquad 2.12$$

The diffusion equation 2.11 then becomes

$$\frac{\partial^2 \underline{F}}{\partial x^2} + \frac{\partial^2 \underline{F}}{\partial y^2} = \left\{ \mu_0 \sigma \frac{1}{T} \frac{\partial T}{\partial t} - \frac{1}{Z} \frac{\partial^2 Z}{\partial z^2} \right\} \underline{F} \qquad 2.13$$

in which the term in brackets is independent of x and y and can be set equal to a constant, $-\nu^2$, for example. Thus

$$\frac{\partial^2 \underline{F}}{\partial x^2} + \frac{\partial^2 \underline{F}}{\partial y^2} = -\nu^2 \underline{F} \qquad 2.14$$

and

$$\frac{\partial^2 Z}{\partial z^2} = \mu_0 \sigma \frac{1}{T} \frac{\partial T}{\partial t} Z + \nu^2 Z \qquad 2.15$$

If it is assumed that the time variation of the field is harmonic with a period $2\pi/\omega$, then

$$\frac{\partial^2 Z}{\partial z^2} = (\nu^2 + i\omega\mu_0\sigma) Z \qquad 2.16$$

Combining equations 2.8 and 2.12 gives

$$Z\left(\frac{\partial F_x}{\partial x} + \frac{\partial F_y}{\partial y}\right) + F_z \frac{\partial Z}{\partial z} = 0 \qquad 2.17$$

which is soluble if either

$$-\left(\frac{\partial F_x}{\partial x} + \frac{\partial F_y}{\partial y}\right) \Big/ F_z = \frac{\partial Z}{\partial z} \Big/ Z \qquad 2.18$$

or $F_z = 0$ and

$$\frac{\partial F_x}{\partial x} + \frac{\partial F_y}{\partial y} = 0 \qquad 2.19$$

The solutions corresponding to condition 2.18 have been shown by Price (1950) to be associated with varying electric currents which produce no external magnetic field, and are of no interest in induction studies. However, from condition 2.19, it is possible to deduce that $\underline{F}$ must have the form $\underline{F} = \left(\frac{\partial P}{\partial y}, -\frac{\partial P}{\partial x}, 0\right)$

where P is a scalar satisfying

$$\frac{\partial^2 P}{\partial x^2} + \frac{\partial^2 P}{\partial y^2} + \nu^2 P = 0 \qquad 2.20$$

in order that $\underline{F}$ satisfies 2.19.

Solutions for Z can be found from 2.16 by putting $\theta^2 = \nu^2 + i\mu_o\omega\sigma$; these have the form

$$Z(z) = C_1 e^{\theta z} + C_2 e^{-\theta z} \qquad 2.21$$

For the region external to the Earth $\sigma = 0$ and $\theta = \nu$ so that

$$\frac{\partial^2 Z}{\partial z^2} = \nu^2 Z \qquad 2.22$$

and thus

$$Z(z) = C_1 e^{\nu z} + C_2 e^{-\nu z} \qquad 2.23$$

From 2.20 ν can be understood as being representative of the horizontal dimensions of the inducing field. For regions inside the Earth, if

$$\nu^2 \ll \mu_o\omega\sigma \qquad 2.24$$

then $\theta^2 = i\mu_o\omega\sigma$ and

$$\theta = \pm(1 + i)\left(\frac{\mu_o\omega\sigma}{2}\right)^{1/2} \qquad 2.25$$

This complex number when inserted in 2.21 gives the solution for Z. When condition 2.24 is met it is clear that the electric field decays exponentially into the Earth, penetrating a distance characterized by the "skin depth"

$$\delta = \left(\frac{2}{\mu_o\omega\sigma}\right)^{1/2} \qquad 2.26$$

at which the amplitude is reduced to 1/e of its value at the surface.

The condition 2.24 is equivalent to the wavelength of the inducing field being greater than the skin depth of the medium.

From 2.26 it is apparent that the skin depth varies with conductivity and period. For the range of conductivities found in the Earth, analysis of different periods of variation allows penetration into the Earth to the different depths illustrated in figure 2.1 to be studied. The skin depth defined by 2.26 is only strictly true for a constant conductivity, where $\sigma = \sigma(z)$ Sims and Bostick (1969) defined a generalized skin depth:

$$\mathrm{Re}\left\{\int_0^{\delta(\omega)} \sqrt{\{i\mu\,\omega\sigma(z)\}}\; dz\right\} = 1 \qquad 2.27$$

where δ is representative of the depth of penetration of the field.

Putting together the expressions for T(t), Z(z) and $\underline{F}(x,y)$, $\underline{E}$ can now be written as

$$\underline{E}(t,x,y,z) = e^{i\omega t} Z(z)\left(\frac{\partial P}{\partial y}, -\frac{\partial P}{\partial x}, 0\right) \qquad 2.28$$

and using equation 2.1 an expression for $\underline{H}$ is also obtained.

$$\underline{H}(t,x,y,z) = -e^{i\omega t} \frac{1}{i\mu_0\omega}\left(\frac{\partial Z}{\partial z}\frac{\partial P}{\partial x}, \frac{\partial Z}{\partial z}\frac{\partial P}{\partial y}, \nabla^2 ZP\right) \qquad 2.29$$

In magnetotelluric studies orthogonal components of $\underline{E}$ and the magnetic field $\underline{H}$ are measured. An impedance (also normally denoted by $\underline{\underline{Z}}$), the ratio of orthogonal components of $\underline{E}$ and $\underline{H}$ is calculated and the conductivity structure is usually modelled to fit the observed variation of $\underline{\underline{Z}}$ with period, T.

In a one-dimensional situation it is possible to obtain an analytical expression for the impedance from 2.28 and 2.29. This was done by Weaver (1973), the result being

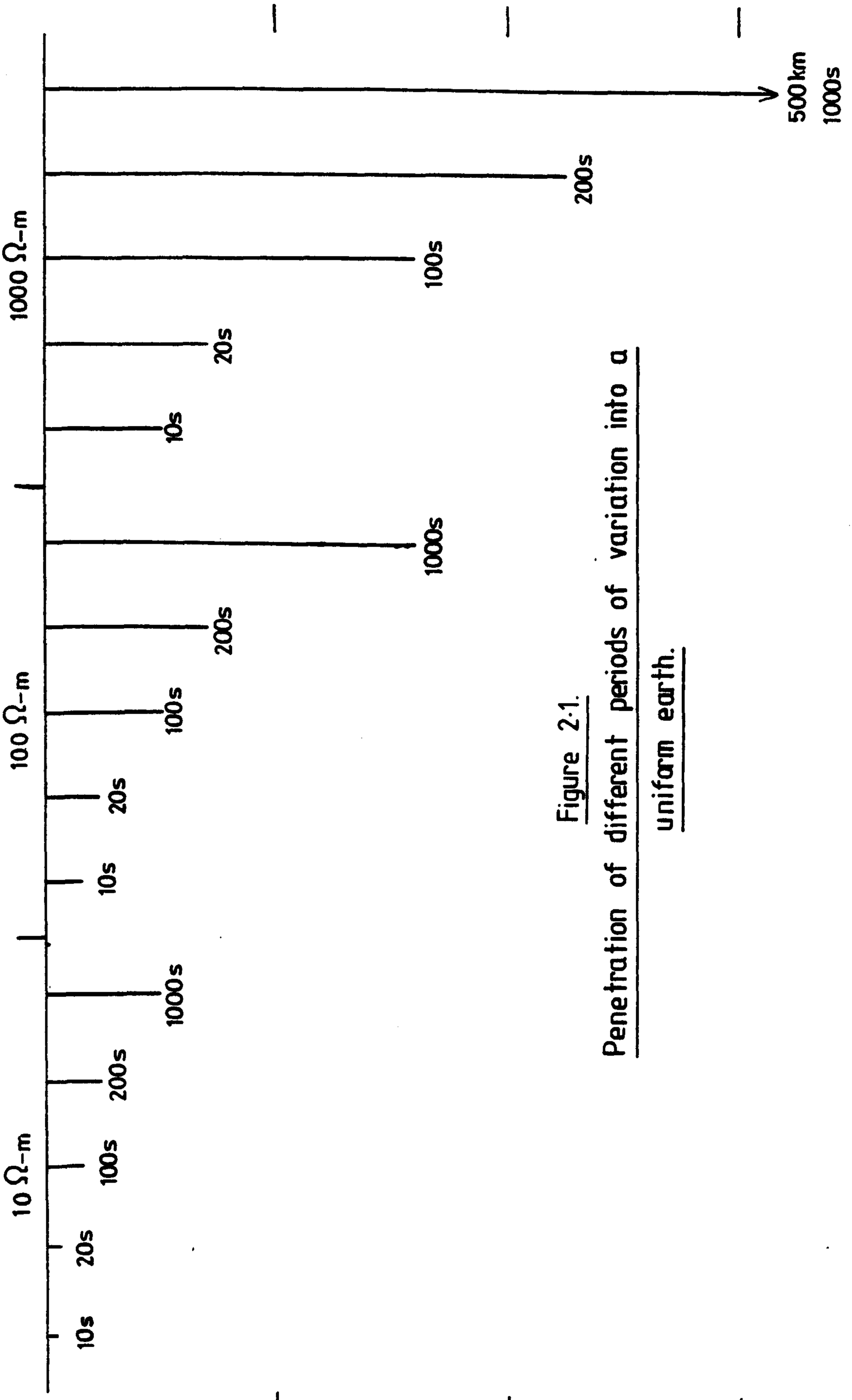

Figure 2.1.

Penetration of different periods of variation into a uniform earth.

$$Z_1(0) = \frac{i\mu_0\omega}{\theta_1} \coth\left\{\theta_1 h_1 + \coth^{-1}\left\{\frac{\theta_1}{\theta_2}\coth\left\{\theta_2 h_2 + \ldots\ldots + \coth^{-1}\frac{\theta_{n-1}}{\theta_n}\right\}\right\}\right\} \qquad 2.30$$

where $Z_1(0)$ is the impedance at the Earth's surface above a layered structure of n layers of conductivities σ_n and layer interface depths h_n. The θ_n's are given by

$$\theta_n^2 = \nu^2 + i\mu_0\omega\sigma_n$$

or, for the plane wave approximation, by equation 2.25. Various workers have devised one-dimensional inversion schemes for magnetotelluric data using equation 2.30, (Jones, 1977).

2.1.2: Induction in two-dimensional structures.

Whereas analytical solutions for $\underline{E}$ and $\underline{H}$ are obtainable in the one-dimensional case this is not so for two dimensions. For such a situation, where $\sigma = \sigma(y,z)$ Maxwell's equations 2.1 and 2.2 can be written, assuming the simplifications made in the last section, as

$$\underline{\nabla}_\wedge(\underline{\nabla}_\wedge\underline{E}) = -\mu_0\frac{\partial}{\partial t}(\underline{\nabla}_\wedge\underline{H}) \qquad 2.31$$

and $$\underline{\nabla}_\wedge(\underline{\nabla}_\wedge\underline{H}) = \underline{\nabla}_\wedge(\sigma\underline{E}) \qquad 2.32$$

Using 2.9 and taking the time variations of the fields to be harmonic 2.31 becomes

$$\nabla^2\underline{E} = i\mu_0\omega\sigma\underline{E} \qquad 2.33$$

which is equivalent to 2.11. However, because σ is a function of y as well as z, 2.32, using 2.4 and the equation for $\underline{\nabla}_\wedge(\underline{\nabla}_\wedge\underline{H})$ corresponding to 2.9, gives

$$-\nabla^2\underline{H} = \sigma\underline{\nabla}_\wedge\underline{E} + \underline{\nabla}\sigma_\wedge\underline{E} \qquad 2.34$$

This is simpilfied using 2.1 and the abbreviated form of 2.2 ($\underline{\nabla}_\wedge\underline{H}$

$= \sigma \underline{E}$) to

$$- \sigma \nabla^2 \underline{H} = -i\mu_o \omega \sigma^2 \underline{H} + \underline{\nabla} \sigma_\wedge (\underline{\nabla}_\wedge \underline{H}) \qquad 2.35$$

A general two-dimensional field obeying 2.33 and 2.35 can be separated, assuming invariance with x, into two fields which represent $\underline{E}$ and $\underline{H}$ - polarization fields. The $\underline{E}$-polarization field is

$$\underline{E} = E\underline{x} \quad ; \quad \underline{H} = \frac{i}{\mu_o \omega} \left(\underline{y} \frac{\partial E}{\partial z} - \underline{z} \frac{\partial E}{\partial y} \right) \qquad 2.36$$

and the $\underline{H}$ -polarization case

$$\underline{H} = H\underline{x} \quad ; \quad \underline{E} = \frac{1}{\sigma} \left(\underline{y} \frac{\partial H}{\partial z} - \underline{z} \frac{\partial H}{\partial y} \right) \qquad 2.37$$

$\underline{x}$, $\underline{y}$ and $\underline{z}$ are unit vectors along the axes of Cartesian co-ordinates.

Equations 2.33 and 2.35 cannot be solved analytically. However, numerical solutions are obtainable subject to the boundary conditions that;

1) both $\underline{E}$ and $\underline{H}$ parallel to any discontinuity are continuous across it;

2) electric current density perpendicular to a boundary is continuous across it;

3) both $\underline{E}$ and $\underline{H}$ go to zero at infinite depth into the Earth; and

4) $\underline{H}$ is constant at and above the Earth's surface.

Algorithms which compute numerical solutions to two-dimensional induction problems have been produced by various authors using a number of different methods. These include the finite element method of Reddy and Rankin (1972), the transmission line analogy of Maddon and Swift (1969) and the finite difference method of Jones and Pascoe (1971) and Pascoe and Jones (1972).

The latter method has been quite widely used and involves the representation of the conducting space by a mesh of points and the calculation of field differences between points by finite differences. A disadvantage of the method is that it has to fit field values across sharp transitions in conductivity rather than over a smoothly varying function as would be observed in the Earth. A modified finite difference method which uses a smooth transition in conductivity has been produced by Brewitt-Taylor and Weaver (1976) and it is this method which has been used for the two-dimensional modelling carried out in this study (see chapter 6).

2.1.3: Induction in three-dimensional structures.

In the vast majority of geophysical problems, although a two-dimensional approximation can often be made, the conductivity structure is in fact three-dimensional. For such a conductivity distribution Maxwell's equations do not reduce to a simple form and analytical solutions are not possible. Numerical solutions to three-dimensional problems have been proposed by various workers (Lines and Jones, 1973, a, b; Raiche, 1974; Weidelt, 1975; Haak, 1978) and Dosso (1973) has used laboratory analogue models to investigate particular problems (including that of induction in the seas around the British Isles).

Haak treated the case of an anomalous, thin surface layer over a stratified medium and related the measured electric field (E_x, E_y) to the homogeneous field (E_{x_o}, E_{y_o}) above the layered medium by

$$\begin{pmatrix} E_x(x,y,z=0,T) \\ E_y(x,y,z=0,T) \end{pmatrix} = \begin{pmatrix} t_x(x,y) & t_y(x,y) \\ p_x(x,y) & p_y(x,y) \end{pmatrix} \begin{pmatrix} E_{x_o}(y,z=0,T) \\ E_{y_o}(y,z=0,T) \end{pmatrix} \qquad 2.38$$

The electric fields are then related to the magnetic field $\underline{H}$ by the measured impedances Z_{xx}, Z_{xy}, Z_{yx}, Z_{yy} and the homogeneous impedance Z over the layered structure.

Thus

$$E_{x_o}(y,z=0,T) = Z(T)H_y(y,z=0,T)$$
$$E_{y_o}(y,z=0,T) = -Z(T)H_x(y,z=0,T) \qquad 2.39$$

$$\text{and} \begin{pmatrix} E_x(x,y,z=0,T) \\ E_y(x,y,z=0,T) \end{pmatrix} = \begin{pmatrix} Z_{xx}(x,y,T) & Z_{xy}(x,y,T) \\ Z_{yx}(x,y,T) & Z_{yy}(x,y,T) \end{pmatrix} \begin{pmatrix} H_x \\ H_y \end{pmatrix} \qquad 2.40$$

where
$$Z_{xx}(x,y,T) = -Z(T)t_y(x,y)$$
$$Z_{xy}(x,y,T) = Z(T)t_x(x,y)$$
$$Z_{yx}(x,y,T) = -Z(T)p_y(x,y) \qquad 2.41$$
$$Z_{yy}(x,y,T) = Z(T)p_x(x,y)$$

It is not possible to determine the five unknowns Z(T), t_x, t_y, p_x, and p_y completely from the measured impedances, but model calculations do allow non-unique solutions to be found for these parameters.

Dawson and Weaver (1979) have also used the approximation of an anomalous thin sheet over a stratified medium to solve three-dimensional induction problems. They have applied their method to the problem of an island off an irregularly shaped coastline, and found that, as well as channeling around the island, electric currents also flow vertically between the lower crust , beneath the land, and the ocean. This result indicates that the channeling of electric currents, induced in the seas, through relatively conducting areas of land, is a much more complicated process than the modelling of such currents by a single line current would suggest. (e.g. Babour et al., 1976)

In general it would appear that a three-dimensional conductivity structure, even confined to a thin surface layer, can have

a marked effect on the distribution of electric and magnetic fields at much greater depths. Even so, although the detailed conductivity structure may be three-dimensional in many cases, the larger scale features of the problem are two-dimensional. However, in localized areas of plane layering, a one-dimensional treatment can give meaningful results.

2.2: Earth response functions.

Magnetotelluric studies involve the measurement of the orthogonal components of the Earth's electric and magnetic fields at the surface. The five components normally measured are:

N - the component of $\underline{E}$ in the direction of magnetic north;

E - the component of $\underline{E}$ in the direction of magnetic east;

H - the component of $\underline{H}$ in the direction of magnetic north;

D - the component of $\underline{H}$ in the direction of magnetic east;

and Z - the vertical component of H.

The time variations of these quantities and their relationships are used to calculate various Earth response functions which indicate the possible electrical conductivity structure of the Earth, beneath the recording site.

2.2.1: Impedance and apparent resistivity.

Because the conductivity within the Earth is much greater than that outside, it is possible, for a horizontally layered Earth, to consider all the currents and fields as being horizontal. Even when this is not the case it is usual to assume that only the horizontal components of the magnetic fields cause induction, in which case the following holds.

The electric field variations with time N'(t) and E'(t) are

given by the convolutions of response functions Z_1, Z_2, Z_3 and Z_4 with the magnetic fields $H'(t)$ and $D'(t)$

$$N'(\tau) = \int Z_1(t-\tau)H'(t)dt + \int Z_2(t-\tau)D'(t)dt \qquad 2.42$$

$$E'(\tau) = \int Z_3(t-\tau)H'(t)dt + \int Z_4(t-\tau)D'(t)dt \qquad 2.43$$

The equations 2.42 and 2.43 are easier to use in the frequency or period domain, after Fourier transformation, when $\underline{E}$ is related to $\underline{H}$ by an impedance tensor $\underline{\underline{Z}}$.

$$\underline{E} = \underline{\underline{Z}}.\underline{H} \qquad 2.44$$

More specifically this is

$$N = Z_{xx}H + Z_{xy}D \qquad 2.45$$

$$E = Z_{yx}H + Z_{yy}D \qquad 2.46$$

where Z_{xx}, Z_{xy}, Z_{yx} and Z_{yy}, the components of $\underline{\underline{Z}}$, are the Fourier transforms of Z_1, Z_2, Z_3 and Z_4.

In a one-dimensional situation the electric field components are related only to their respective orthogonal magnetic field component. That is, Z_{xx} and Z_{yy} are zero (Caignard, 1953). When this is the case the ratios of orthogonal electric and magnetic fields are used to define an apparent resistivity (ρ_a) and a phase (φ_a).

$$\rho_a = \frac{1}{\mu_o \omega} \left| Z_{\substack{xy \\ (yx)}} \right|^2 \qquad 2.47$$

$$\varphi_a = \arg \left(Z_{\substack{xy \\ (yx)}} \right) \qquad 2.48$$

Both the apparent resistivity and the phase vary with the period (T) of the inducing field and curves of ρ_a and φ_a plotted against T can be matched with theoretical curves produced from model conductivity distributions using equation 2.30. The variation of ρ_a with T is indicative of how the real resistivity of a structure varies with depth, as illustrated in figure 2.2, having

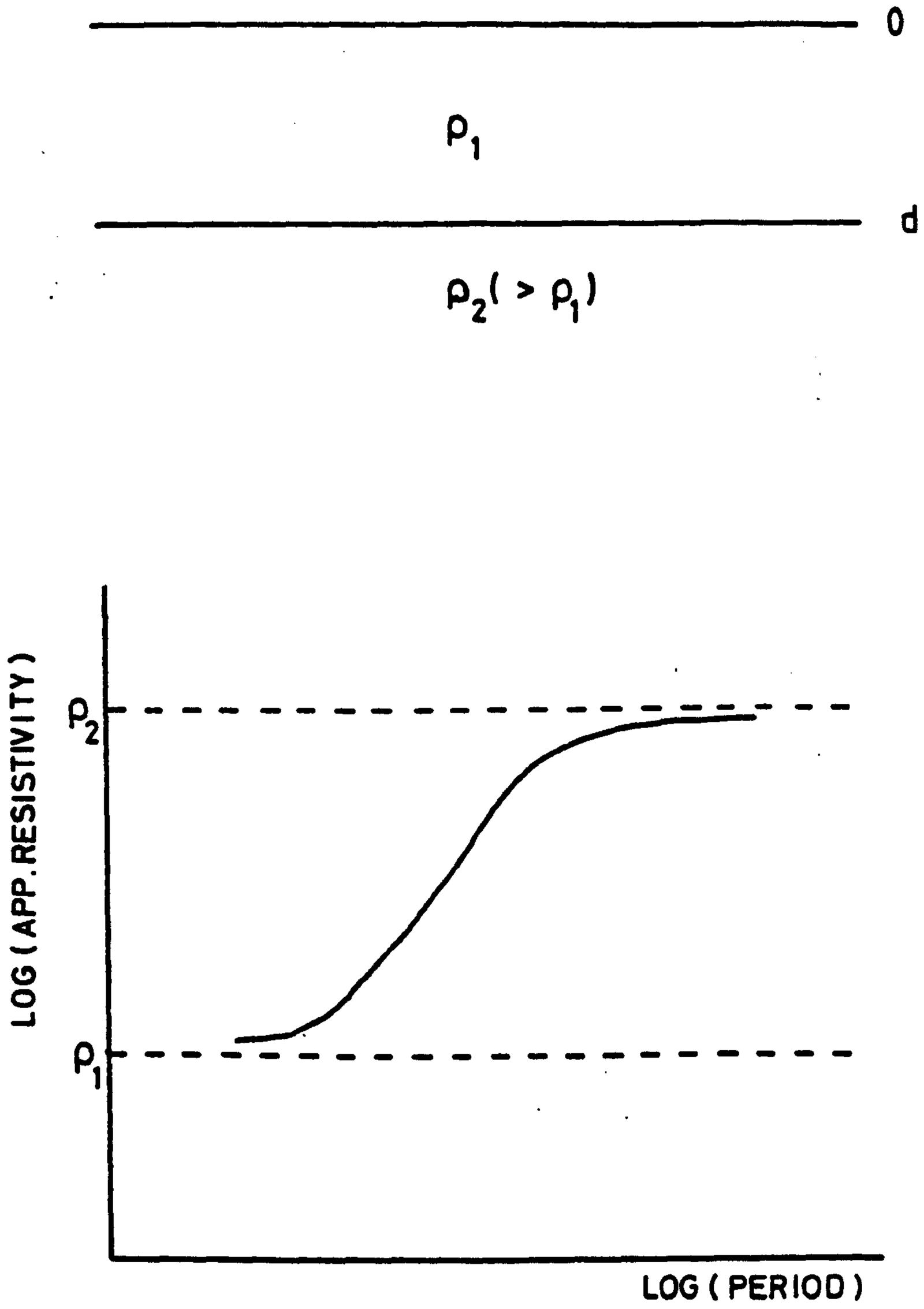

Figure 2·2.

Schematic representation of the relationship between real and apparent resistivity for a simple two layer case.

maxima and minima corresponding to the actual resistivity variation. The phase, φ_a, represents the phase difference between the magnetic and electric fields.

For a two-dimensional structure Z_{xx} and Z_{yy} are, in general, non-zero and vary as the measurement frame is rotated with respect to the direction in which the conductivity is invariant (the strike direction). When the axes of the measurement frame are parallel and perpendicular to the strike Z_{xx} and Z_{yy} do in fact equal zero, and in this situation the impedances Z_{xy} and Z_{yx} can be written as $Z_{/\!/}$ and $Z_{\perp}$, the impedances parallel and perpedicular to the strike. $Z_{/\!/}$ and $Z_{\perp}$ are characteristic of $\underline{E}$ and $\underline{H}$ - polarization (section 2.1.2) respectively. To see how the impedance tensor elements vary with rotation, consider the measurement frame to be rotated an angle γ clockwise from the strike direction. By expressing the electric and magnetic fields, $\underline{E}'$ and $\underline{H}'$, in this orientation in terms of the fields parallel and perpendicular to the strike it is easy to show that

$$Z_{xx} = \left(\frac{Z_{/\!/} - Z_{\perp}}{2}\right) \sin 2\gamma \qquad 2.49$$

$$Z_{xy} = \left(\frac{Z_{/\!/} + Z_{\perp}}{2}\right) + \left(\frac{Z_{/\!/} - Z_{\perp}}{2}\right) \cos 2\gamma \qquad 2.50$$

$$Z_{yx} = -\left(\frac{Z_{/\!/} + Z_{\perp}}{2}\right) + \left(\frac{Z_{/\!/} - Z_{\perp}}{2}\right) \cos 2\gamma \qquad 2.51$$

$$Z_{yy} = -\left(\frac{Z_{/\!/} - Z_{\perp}}{2}\right) \sin 2\gamma \qquad 2.52$$

From these equations it is evident that when $\gamma=0$: $Z_{xx} = Z_{yy} = 0$ and Z_{xy} and Z_{yx} are either at a maximum or a minimum.

In practice the direction of strike is unknown and has to be found from the measured impedances. To do this, consider the

action of the rotation tensor $\underline{\underline{T}}$

$$\underline{\underline{T}} = \begin{pmatrix} \cos\theta & \sin\theta \\ -\sin\theta & \cos\theta \end{pmatrix} \qquad 2.53$$

on equation 2.44

$$\begin{aligned} \underline{E}' &= \underline{\underline{T}}.\underline{E} = \underline{\underline{T}}.\underline{\underline{Z}}.\underline{H} \\ &= \underline{\underline{T}}.\underline{\underline{Z}}.\underline{\underline{T}}^{-1}\underline{H}' \\ &= \underline{\underline{Z}}'\underline{H}' \end{aligned} \qquad 2.54$$

Where $\underline{\underline{Z}}' = \underline{\underline{T}}.\underline{\underline{Z}}.\underline{\underline{T}}^{-1}$ 2.55

Expanding 2.55 relates the impedance tensor in the original co-ordinate system to its rotated value.

$$Z'_{xx}(\theta) = \frac{1}{2}\left\{Z_{xx}+Z_{yy}+(Z_{xx}-Z_{yy})\cos 2\theta +(Z_{xy}+Z_{yx})\sin 2\theta\right\} \qquad 2.56$$

$$Z'_{xy}(\theta) = \frac{1}{2}\left\{Z_{xy}-Z_{yx}+(Z_{xy}+Z_{yx})\cos 2\theta -(Z_{xx}-Z_{yy})\sin 2\theta\right\} \qquad 2.57$$

$$Z'_{yx}(\theta) = \frac{1}{2}\left\{-Z_{xy}+Z_{yx}+(Z_{xy}+Z_{yx})\cos 2\theta -(Z_{xx}-Z_{yy})\sin 2\theta\right\} \qquad 2.58$$

$$Z'_{yy}(\theta) = \frac{1}{2}\left\{Z_{xx}+Z_{yy}-(Z_{xx}-Z_{yy})\cos 2\theta -(Z_{xy}+Z_{yx})\sin 2\theta\right\} \qquad 2.59$$

In theory maximum and minimum values of $Z'_{xy}(\theta)$ and $Z'_{yx}(\theta)$ can be found from 2.57 and 2.58 which correspond to the principal impedances $Z_{/\!/}$ and $Z_{\perp}$ and identify the strike direction. However, as the impedances are complex numbers, it is usual to maximize some suitable function of $Z'_{xy}(\theta)$ and $Z'_{yx}(\theta)$. Several such functions have been used by different authors, the two main ones being $|Z'_{xy}(\theta)|$ (Everett and Hyndman, 1967) and $|Z'_{xy}(\theta)|^2 + |Z'_{yx}(\theta)|^2$ (Swift, 1967). The latter can be maximized analytically giving a result for the direction of strike of

$$\theta_0 = \frac{1}{4}\tan^{-1}\left\{\frac{(Z_{xx}-Z_{yy})(Z_{xy}+Z_{yx})^* + (Z_{xx}-Z_{yy})^*(Z_{xy}+Z_{yx})}{|Z_{xx}-Z_{yy}|^2 - |Z_{xy}+Z_{yx}|^2}\right\} \qquad 2.60$$

The resulting value of θ is ambiguous in that $\theta = \theta_0 + \pi/2$ also satisfies equation 2.60, thus, it is not immediatly clear which of the impedances $Z'_{xy}(\theta_0)$ and $Z'_{yx}(\theta_0)$ refers to $Z_{/\!/}$ and which to $Z_{\perp}$. The change in the relative magnitudes of the

apparent resistivities, calculated from the maximized/minimized impedances, across a simple two-dimensional structure, is shown by considering two quarter spaces of different resistivities (figure 2.3). From this it can be seen that on the resistive side of the structure, close to the boundary, $\rho_{\perp}$ is greater than $\rho_{//}$, the reverse being true on the conducting side. As a result of this the maximum value ρ'_{xy} or ρ'_{yx} can be identified as $\rho_{//}$ or $\rho_{\perp}$ depending on whether the measurement is taken over a relative resistor or conductor respectively.

A more realistic two-dimensional structure is that represented in figure 2.4, in which the status of a given site as being relatively resistive or conductive with respect to another changes with depth. Neither the maximum or minimum apparent resistivity can be consistently identified with $\rho_{//}$ or $\rho_{\perp}$. However, as can be seen from both figures 2.3 and 2.4 a better estimate of the true resistivity is given by the average of the values ρ'_{xy} and ρ'_{yx} or $\rho_{//}$ and $\rho_{\perp}$.

Because of the three-dimensionality of real structures in the Earth, field data rarely give values of $Z'_{xx}(\emptyset)$ and $Z'_{yy}(\emptyset)$ which reduce to zero on rotation. Jones and Vozoff (1978) have shown however, that in a three-dimensional situation equation 2.60 still defines the gross two-dimensional strike of the feature (section 2.1.3). It is often still useful therefore, to treat such a situation as being two-dimensional.

2.2.2: Dimensionality indicators.

As such variation in the behaviour of the impedance tensor elements is to be expected, depending on the dimensionality of the problem, it is useful to have some parameter which can easily

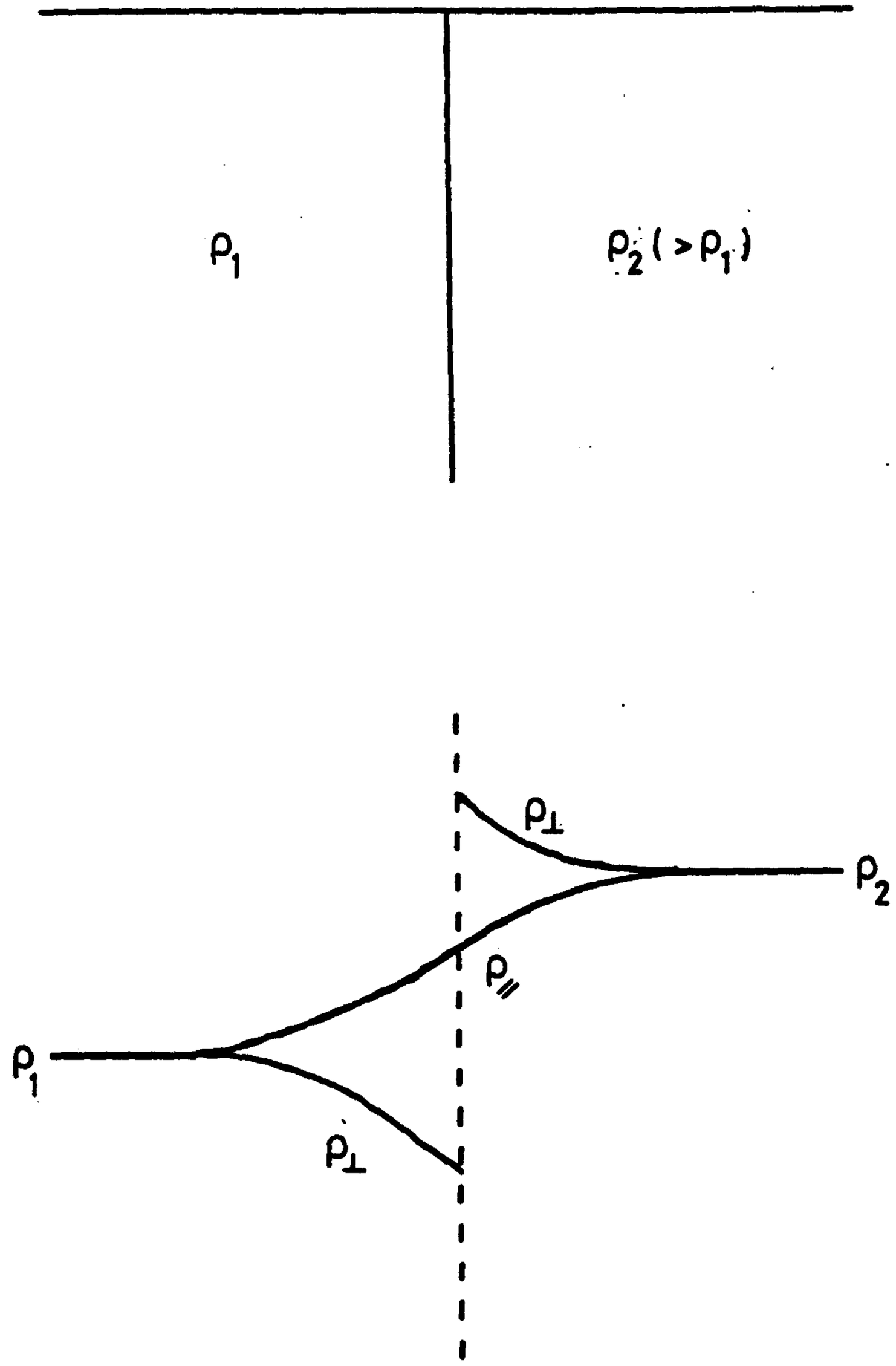

Figure 2·3.

Schematic representation of the variation in apparent resistivity across a vertical discontinuity.

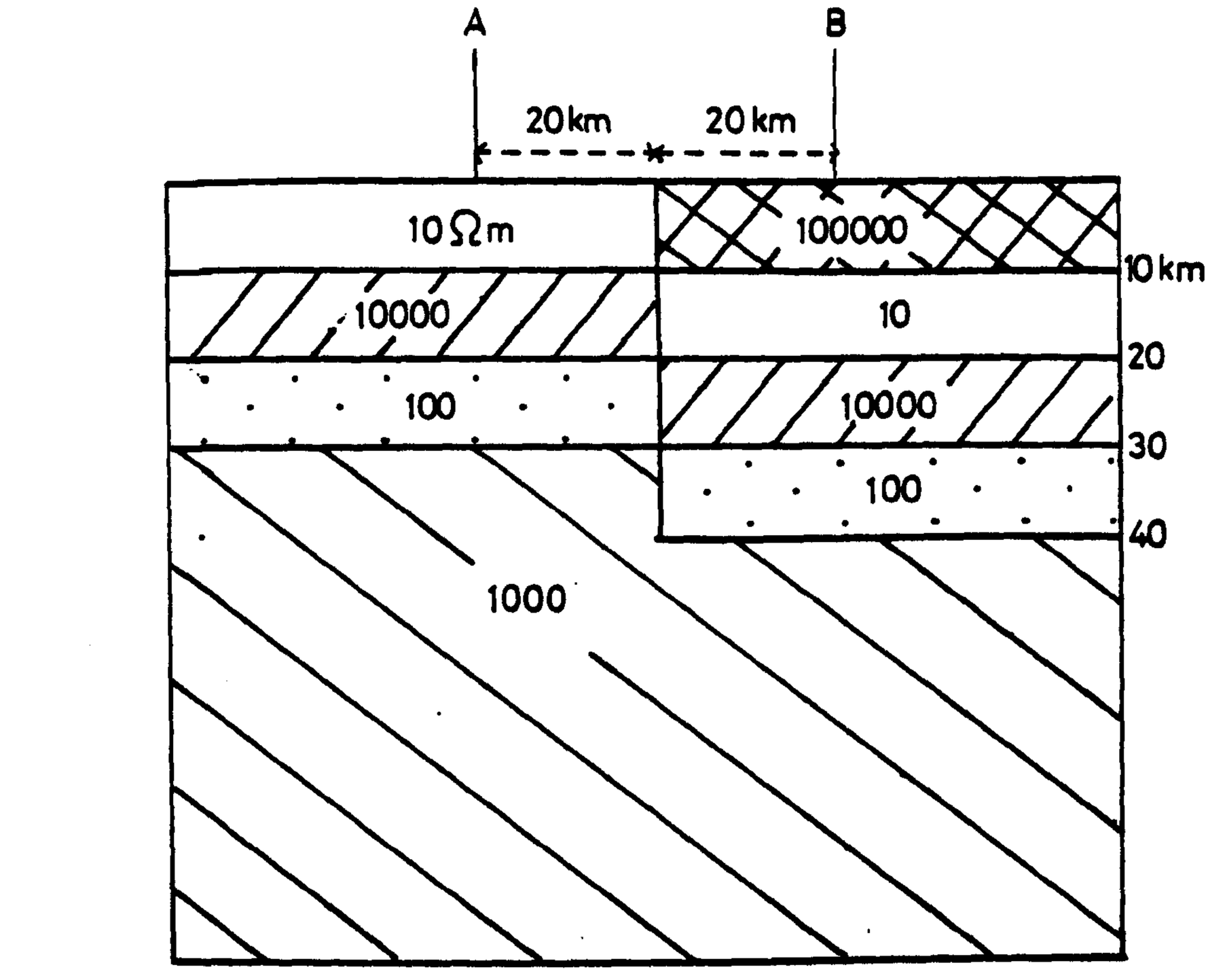

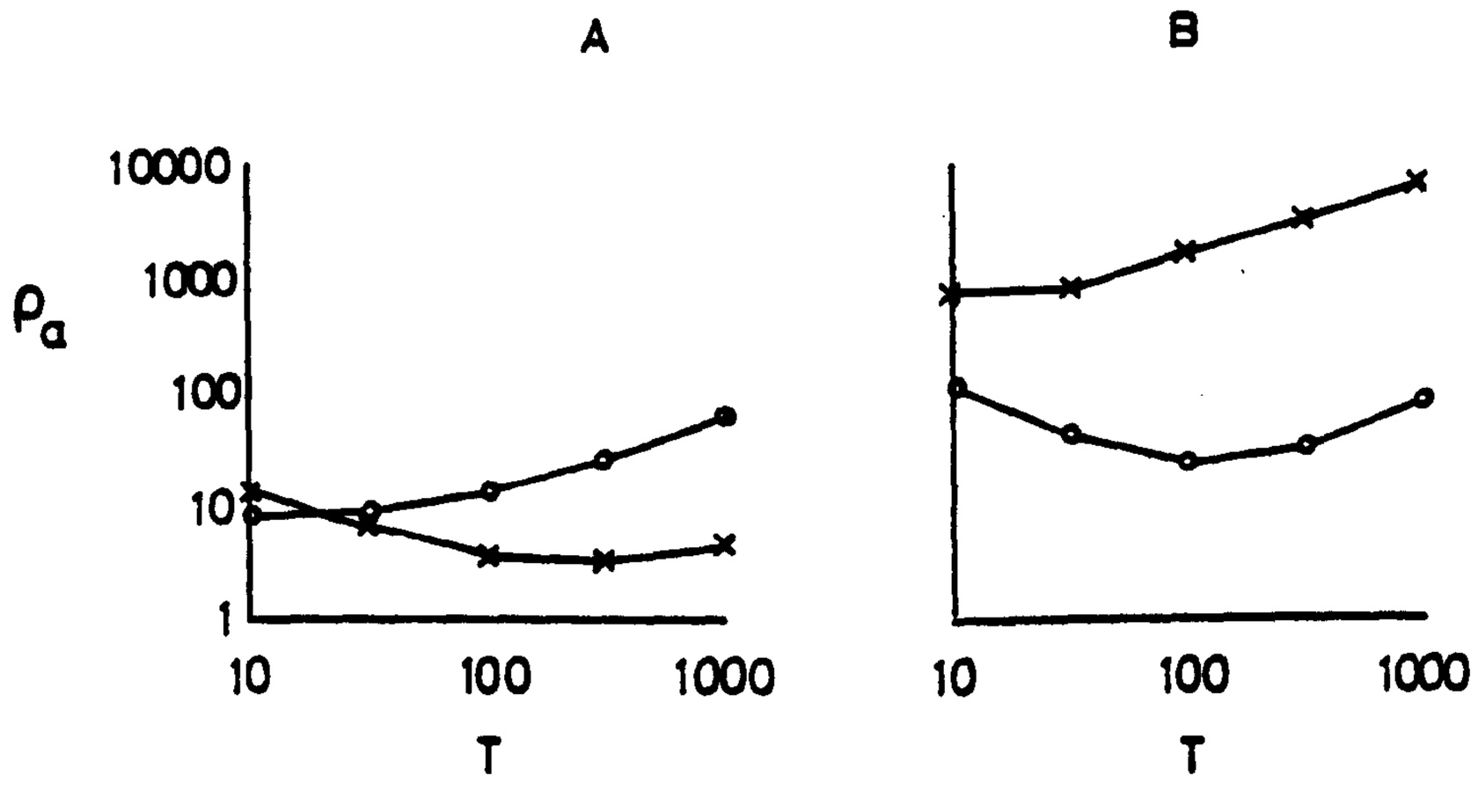

• E-pol
× H-pol

Figure 2·4.

Variation of apparent resistivity close to a fault in a layered earth.

be calculated and gives an indication of the complexity of the case being dealt with.

The most frequently used parameter which indicates the dimensionality of a structure is the skew, defined as

$$S = \frac{|Z_{xx} + Z_{yy}|}{|Z_{xy} - Z_{yx}|} \qquad 2.61$$

The skew can be seen, from equations 2.56 to 2.59 to be independent of θ and equal to zero in the perfect two-dimensional case. However, for real data considerable care is required in its interpretation.

For the one-dimensional case the impedance tensor has diagonal elements which are zero and equal off-diagonal elements. Hence the skew, allowing for noise, should approximate to zero, and when plotted, Z_{xy} and Z_{yx} should show little variation with angle.

In a two-dimensional situation the impedance elements Z_{xy} and Z_{yx} should maximize and minimize at the strike angle, where Z_{xx} and Z_{yy} go to zero. The skew should therefore approach zero also. It is possible however that if the resistivity contrast across the structure is low, i.e. $|Z_{xy} - Z_{yx}| \approx 0$, then the skew given by 2.61 can still be large even for a two-dimensional stucture.

For the general three-dimensional structure $|Z_{xy}|$ and $|Z_{yx}|$ will not have coincident maxima and minima and Z_{xx} and Z_{yy} will not be small. Thus, unless $|Z_{xy}| >> |Z_{yx}|$, or vice-versa, the skew will not be zero. Figures 2.5, 2.6 and 2.7 show the variations of the impedance tensor elements for real data, in each of these three cases.

Some authors have placed an upper limit on the value of the

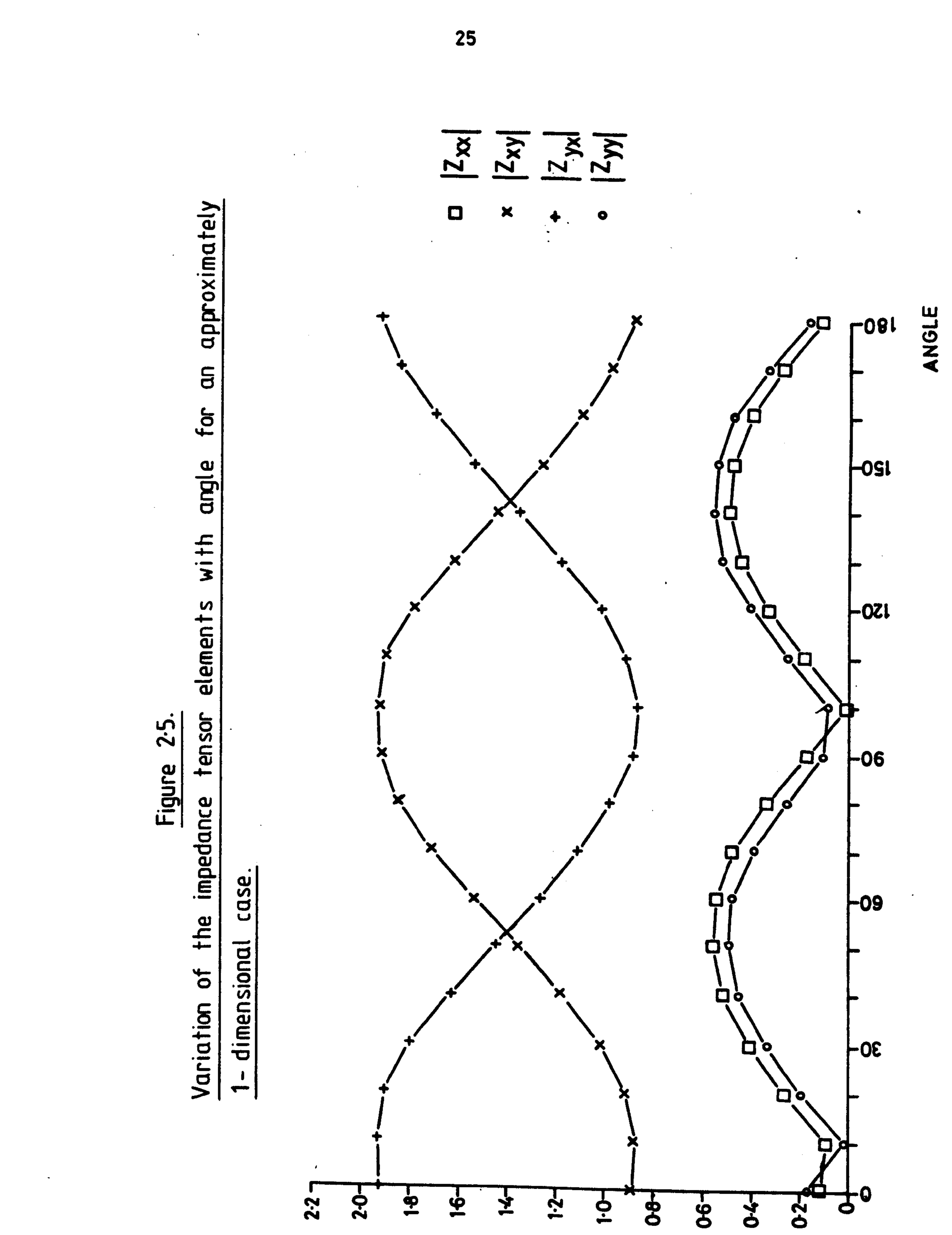

Figure 2·5. Variation of the impedance tensor elements with angle for an approximately 1- dimensional case.

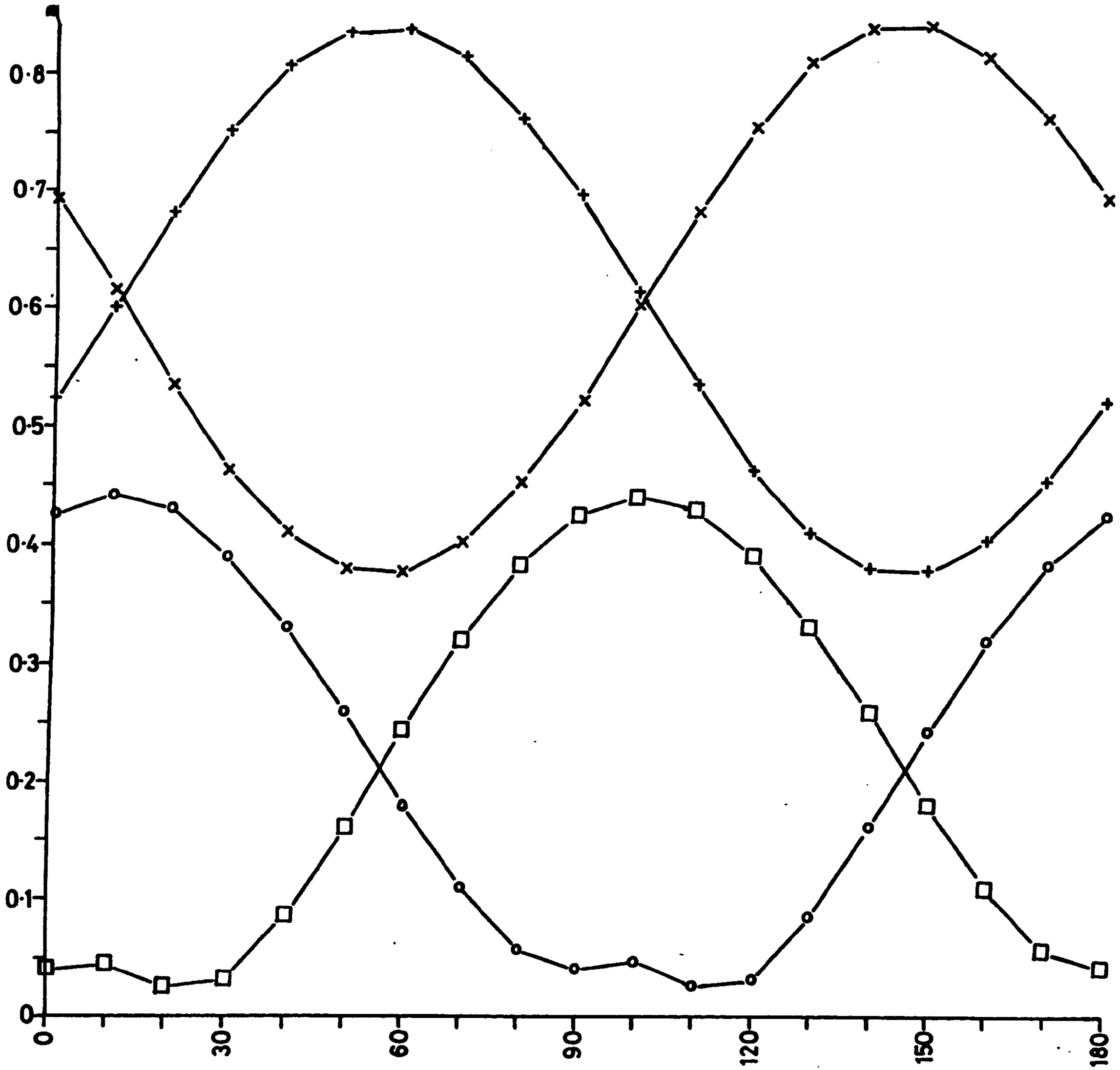

Figure 2·6.
Variation of the impedance tensor elements with angle for a 2-dimensional case.

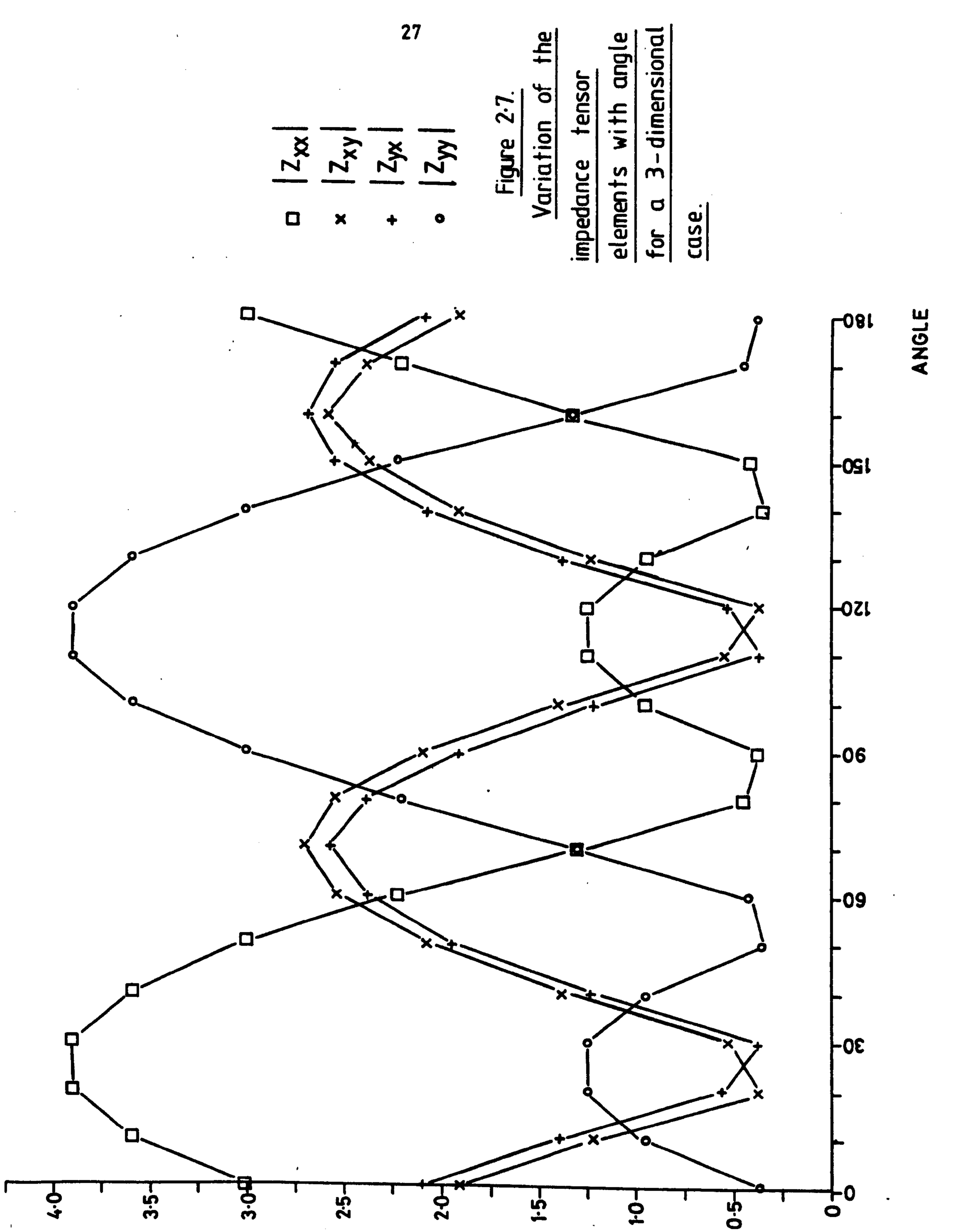

Figure 2·7.
Variation of the impedance tensor elements with angle for a 3-dimensional case.

skew for a two-dimensional interpretation to be valid. However, because of the possibility of other factors affecting the magnitude, in this study it has only been used qualitatively, together with plots like those of figures 2.5, 2.6 and 2.7, to give an indication of dimensionality.

2.2.3: Single station transfer functions.

So far only four of the quantities (N, E, H and D) measured in magnetotelluric studies have been mentioned. The fifth component, Z - the vertical magnetic field, can also be used, in terms of its relationship with H and D, to give information on the electrical conductivity structure.

The measured magnetic fields H(T), D(T) and Z(T) at a particular period T and station can be represented by the sum of a normal inducing field $H_n(T)$, $D_n(T)$, $Z_n(T)$ and an anomalous induced field $H_a(T)$, $D_a(T)$, $Z_a(T)$; (Banks, 1973). Hence

$$Z_a(T) = W_{ZH}(T)H_n(T) + W_{ZD}(T)D_n(T) + W_{ZZ}(T)Z_n(T) \qquad 2.62$$

$$D_a(T) = W_{DH}(T)H_n(T) + W_{DD}(T)D_n(T) + W_{DZ}(T)Z_n(T) \qquad 2.63$$

$$H_a(T) = W_{HH}(T)H_n(T) + W_{HD}(T)D_n(T) + W_{HZ}(T)Z_n(T) \qquad 2.64$$

To solve these equations fully it is necessary to define a field station at which measurements are considered as normal. Simultaneous measurements at other field stations are then relative to this "normal" station, (Schmucker, 1970).

Where simultaneous recordings at a number of stations are not available a simplification of this approach can be made by making the following assumptions:

1) the normal vertical field Z_n is small compared to Z_a;

2) the anomalous fields D_a and H_a are small, so that $H = H_n + H_a \approx H_n$ and $D = D_n + D_a \approx D_n$;

and 3) there is no correlation between Z_n and H_n or D_n.

The equations 2.62 and 2.64 can now be replaced by

$$Z(T) = A(T)H(T) + B(T)D(T) + \mathcal{E}(T) \qquad 2.65$$

where Z(T), H(T) and D(T) are the measured magnetic fields at period T, A(T) and B(T) are geomagnetic single-station transfer functions and $\mathcal{E}(T)$ is a residual. The transfer functions are complex quantities which on the basis of the third assumption above can be calculated from cross-spectral estimates.

Equation 2.65 defines a preferred plane in which variations of the magnetic field with a period of T tend to take place (Parkinson, 1959, 1962). The "Parkinson" vector, which points towards anomalous currents in the Earth, is the horizontal projection of a unit vector perpendicular to this plane. Another means of expressing this is to calculate real and imaginary induction vectors

$$|R| = (A_r^2 + B_r^2)^{1/2} \qquad \theta_r = \tan^{-1}\frac{B_r}{A_r} \qquad 2.66$$

$$|I| = (A_i^2 + B_i^2)^{1/2} \qquad \theta_i = \tan^{-1}\frac{B_i}{A_i} \qquad 2.67$$

where A_r, A_i, B_r and B_i are the real and imaginary parts of A and B. When the direction of the real arrow $\underline{R}$ is reversed it is equivalent to the "Parkinson" vector and points towards current concentrations. The amplitude of $\underline{R}$ corresponds to the amplitude of the induced vertical field associated with a unit amplitude variation in the horizontal field.

An alternative form of single station transfer function may be found by rotating the measuring frame to find new values H′ and D′ along which the magnitudes of the response functions are maximum and minimum, (Banks and Ottey, 1974). In this situation

$$Z(T) = G_p(T)H'(T) + G_l(T)D'(T) \qquad 2.68$$

In a two-dimensional structure vertical field variations do

not correlate with horizontal variations parallel to the strike; for such a case $G_l(T)$ would be zero and the H′ axis would be perpendicular to the strike of the structure. The relative magnitudes of G_p and G_l thus indicate the degree of two-dimensionality of the structure and their azimuths the direction of strike.

Jones and Vozoff (1978) also use a "tipper" to indicate the direction of strike. For a general three-dimensional conductivity anomaly,by considering the variation of Z as the direction of the horizontal field is changed, they conclude that the direction of most rapidly varying conductivity is given by

$$\theta = \tan^{-1}(|B| / |A|) \qquad 2.69$$

It has also been suggested (Beamish, 1979; Sik, 1980) that the source field configuration can severely bias transfer function estmiates. This is considered in more detail in chapter 4.

2.3: Summary.

1) The solution of problems of electromagnetic induction in the Earth depends on the validity of various assumptions concerning the nature of the source field and the induced fields.

2) For a one-dimensional problem an analytical solution is obtainable.

3) In a two-dimensional situation the problem can be divided up into two distinct polarizations, E and H. These cases are soluble numerically.

4) Three-dimensional problems can be solved numerically with the approximation that the anomalous structure is confined to a thin surface layer.

5) Various earth response functions are defined and the conductivity structure is modelled to fit the observed variation of these parameters with the period of electromagnetic variation.

CHAPTER 3: THE TECTONIC HISTORY, GEOLOGY AND GEOPHYSICS OF THE SOUTH OF SCOTLAND.

A simplified tectonic map of the South of Scotland is shown in figure 3.1. The main tectonic features of the area are the Highland Boundary and the Southern Uplands Faults which divide the region up into three geomorphological provinces: the Highlands, the Midland Valley and the Southern Uplands.

The Highland Boundary Fault strikes approximately SW-NE from Helensburgh, on the Clyde, to Stonehaven, on the east coast. The Highlands, to the north, are a rugged mass, of mainly metamorphic and igneous rocks, characterized by high mountains and deep, narrow valleys. There are many wrench faults in the region, running principally SSW-NNE, parallel to the third major fault in Scotland, the Great Glen Fault.

Lying between the Highland Boundary and the Southern Uplands Faults, the Midland Valley is about 80 km. wide, and has a very varied relief although, in general, the land is lower than that to the north or the south. The sedimentary basins close to the two faults are separated by a series of igneous hills across the centre of the valley. A large number of dykes and sills and many minor faults also criss-cross the valley floor.

Whereas the Highland Boundary Fault is generally a very well defined boundary between lowland and highland, the same cannot be said of the Southern Uplands Fault. At the northern end in particular the exact line is complicated by the existence of several faults rather than one principal one. The Southern Uplands are much more rounded, gentler hills than those of the Highlands,

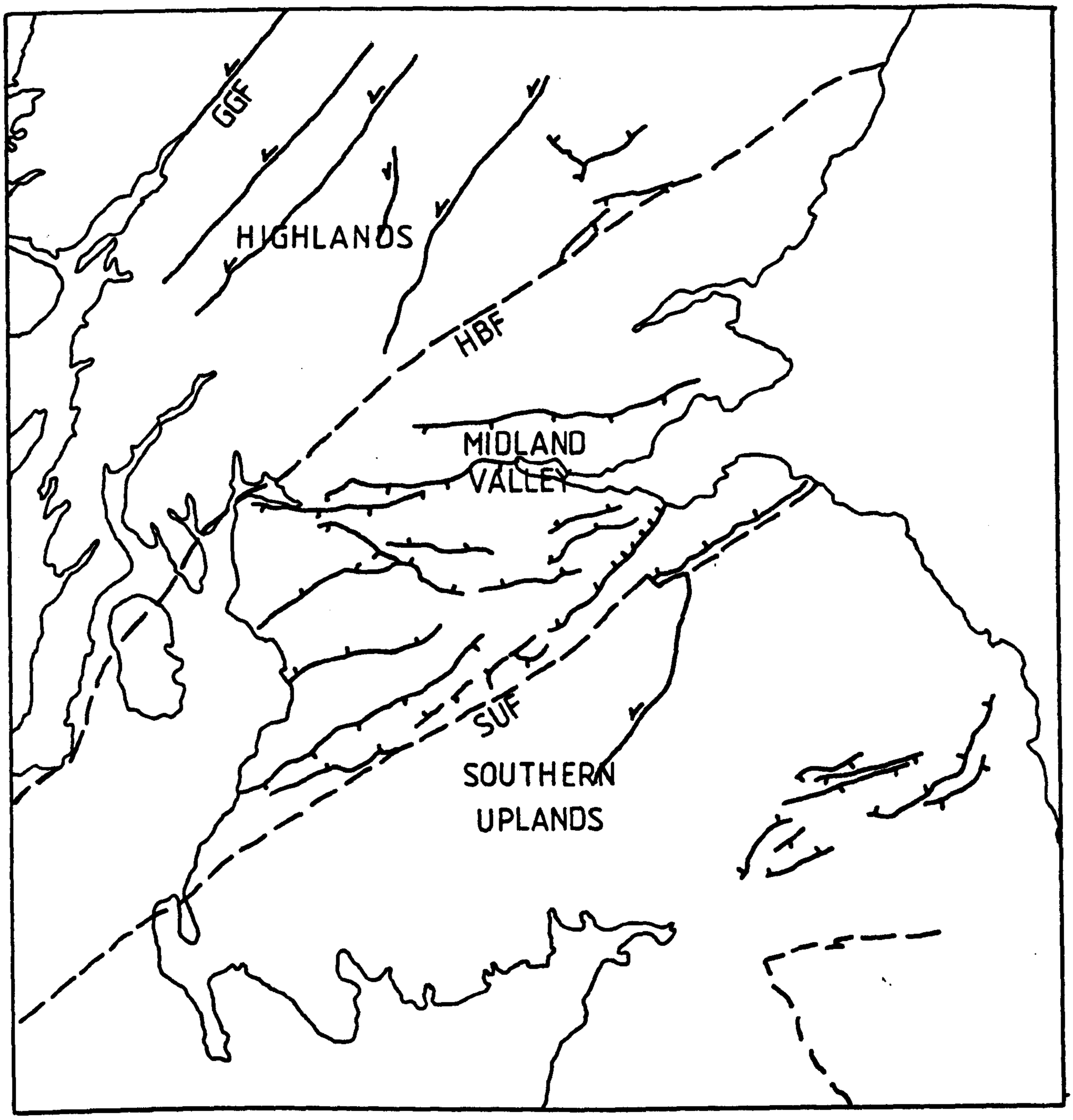

— — — major faults

——— normal faults

——— thrust faults

——— wrench faults

GGF Great Glen Fault

HBF Highland Boundary Fault

SUF Southern Uplands Fault

Figure 3·1.

Simplified tectonic map of S.Scotland.

although still punctuated by deep valleys. The only other fault cutting across the region is the Ettrick Thrust, striking SSW from where it joins the Southern Uplands Fault north-east of Peebles.

3.1: The tectonic history of South Scotland.

The tectonic history of the south of Scotland is of great interest as it is now widely accepted that the region marks the point of closure of the Cambrian Iapetus or proto-Atlantic Ocean. The Iapetus separated the north of Scotland, on an American plate, from England and the Scottish Borders which were on a European plate to the south-east.

The idea that such an ocean existed throughout Cambrian and Ordovician times was first put forward by Wilson (1966). Dewey (1969, 1971) and Dewey and Pankhurst (1970) suggested that the Girvan-Ballantrae ophiolite region was the result of an upthrust relic of a subduction zone dipping northwards towards the Midland Valley. The Southern Uplands, to the south, would therefore be underlain by oceanic crust, figure 3.2a. Fitton and Hughes (1970) and Church and Gayer (1973) agreed with the general conclusions of this model although differing in detail. However, Powell (1971) used arguements based on seismic, magnetic, resistivity and gravity observations, to refute the Dewey model, suggesting that the Southern Uplands are in fact underlain by continental crust.

To account for this Gunn (1973) and Jeans (1973) proposed that the Midland Valley could be the site of any remnants of the Iapetus oceanic crust. Jeans' model (figure 3.2b) had subduction zones beneath both the Highlands and the Southern Uplands, which

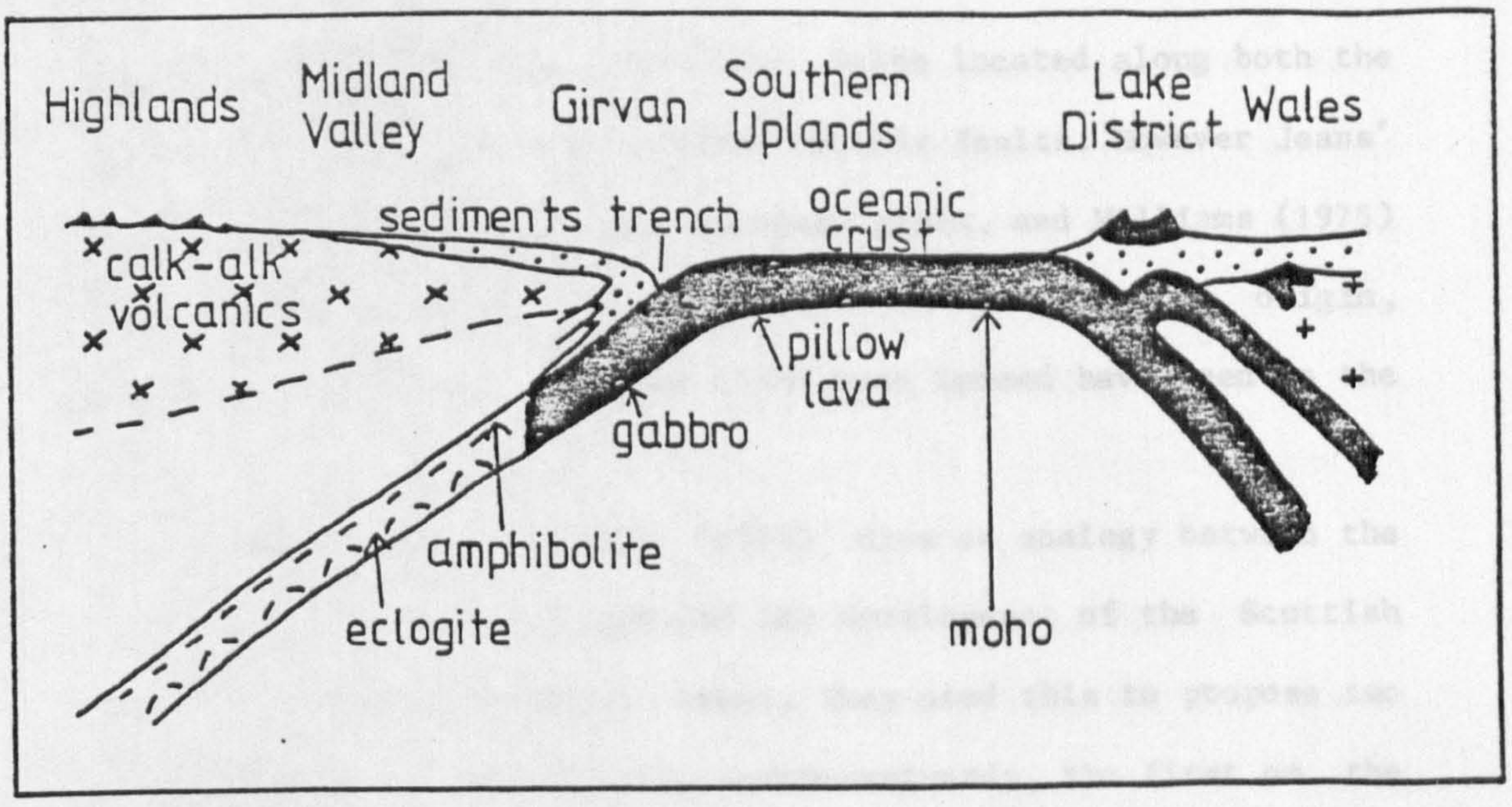

(a) Dewey.

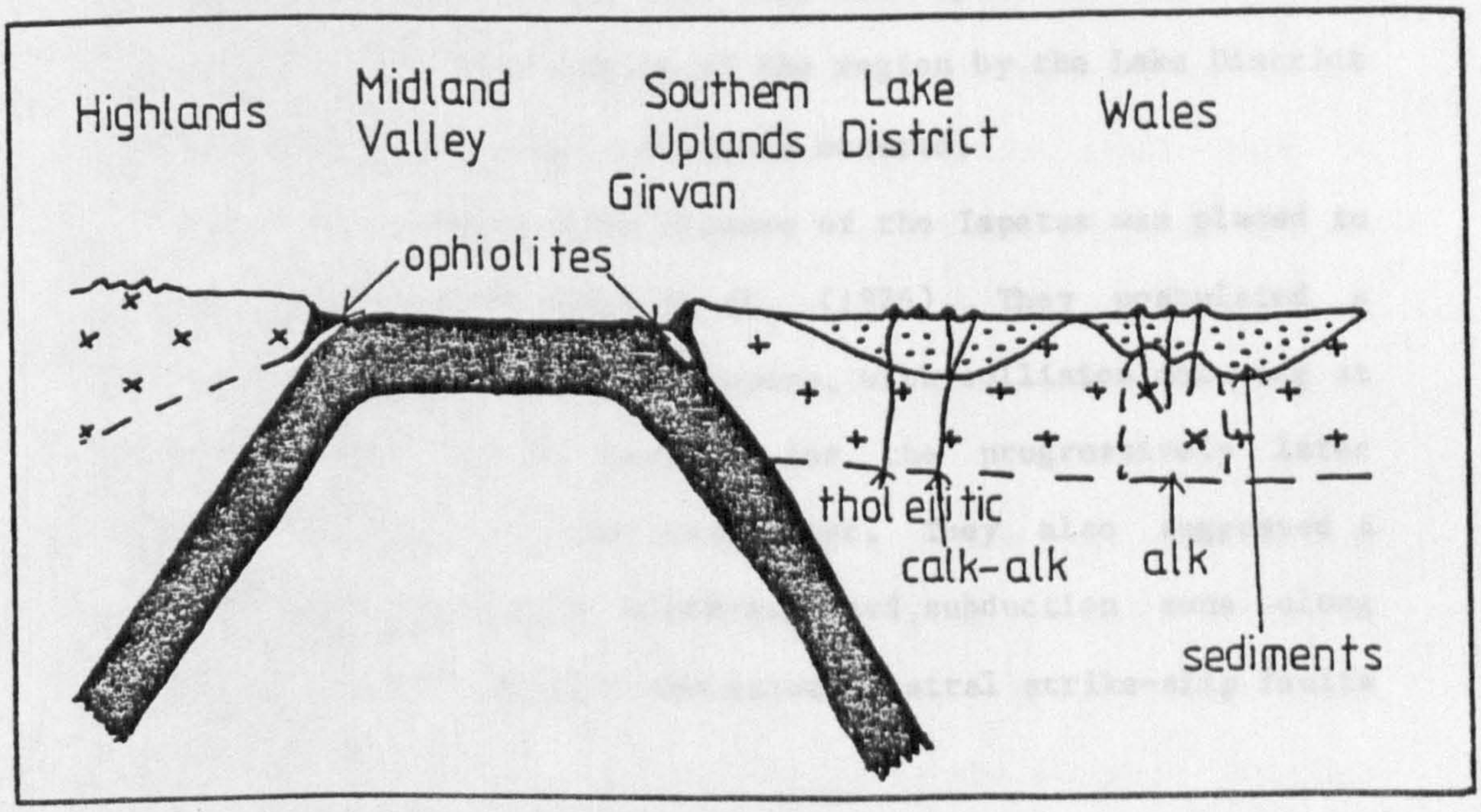

(b) Jeans.

Figure 3·2.

Tectonic models of the evolution of S. Scotland.

(after Moseley (1977)).

would account for the ophiolite belts located along both the Highland Boundary and the Southern Uplands Faults. However Jeans' model places Girvan on the European plate, and Williams (1975) showed that the fauna in this area is of American origin, suggesting that the Iapetus Ocean must indeed have been to the south.

Mitchell and McKerrow (1975) drew an analogy between the Burma Orogen of Tertiary age and the development of the Scottish Caledonides in Ordovician times. They used this to propose two subduction zones, both dipping north-westwards, the first on the northern margin of the Midland Valley, followed by a later, second zone south of the Southern Uplands. Both the Southern Uplands and Girvan would therefore be underlain by oceanic crust and the 30 km. depth to the Moho suggested by Powell could then be explained by under-riding of the region by the Lake District when the final continental collision occured.

The final position of closure of the Iapetus was placed in the Solway Firth by Phillips et al. (1976). They postulated a very complicated pattern of closure, with collision occuring at an angle of about 14° to account for the progressively later volcanic activity to the south-west. They also suggested a simultaneous, continental, south-eastward subduction zone along the Moine Thrust to explain the major sinstral strike-slip faults in Scotland.

Most of these models, and others, were reviewed by Moseley (1977) who indicated in conclusion that it is possible that no actual remnant of oceanic crust remains to identify the final position of suture. However, the proposal of Phillips et al., siting the suture in the Solway Firth, has now gained widespread

support. Leggett et al. (1979) used this position of the suture to account for many of the geological phenomena in the Southern Uplands, including the differences in stratigraphy and the occurrence of reverse strike faults. Anderton et al. (1979) used a process of elimination to conclude that the suture is along the Solway Firth and can be extended to the Shannon Estuary in Ireland.

The varied geological structure which is the result of the complicated tectonic history of the South of Scotland will now be described.

3.2: The geological structure of the South of Scotland.

The surface geology of the South of Scotland is shown in figure 3.3. The area is divided into three regions; the Highlands, the Midland Valley and the Southern Uplands; by the two major faults (figure 3.1), and each region is dealt with in detail in the respective handbook of the British Regional Geology Series by Johnstone (1966), MacGregor and MacGregor (1948) and Greig (1971). Only a brief outline of the features of each region is given here.

The rocks immediatly to the north of the Highland Boundary Fault are of the Dalradian metamorphic series, probably dating to Cambrian times. Current bedding of quartzites, limestones and pelites indicates that the earlier part of the sequence possibly originated in shallow seas. The graded bedding of thick slate and schistose grit above this is more likely to be of deep water origin. The Highlands are not however comprised entirely of metamorphics; along the line of the Highland Boundary Fault are small areas of Cambrian and Ordovician sediments, and, further

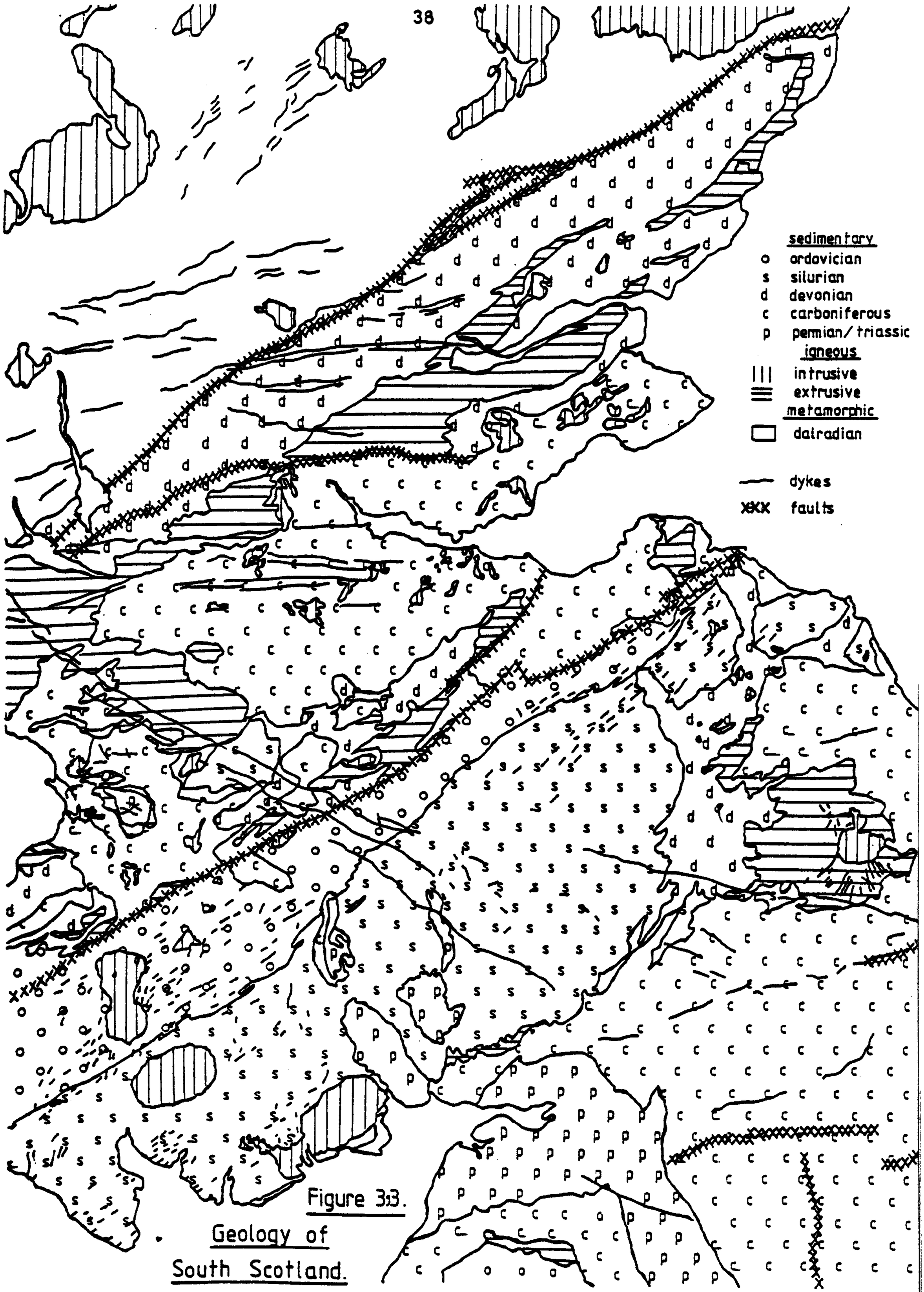

Figure 3:3.

Geology of South Scotland.

north, but outside the scope of the present study, are the vast granitic intrusions of the Central Highland Massif.

The geological stucture of the Midland Valley is principally sedimentary, although a large area is covered by basalt lavas of various ages. There are also many small igneous intrusions. Devonian and Carboniferous sediments are predominant though a considerable part of the south-western margin is Ordovician and there are several Silurian inliers in the central region.

To the north, sandwiched between the Highland Boundary Fault and the line of the hills across the centre of the valley, is up to 6-8 km. of Lower Old Red Sandstone. The Ochil Hills to the south-east of this depression are basalt lavas of Devonian age, contemporary with the Pentland Hills just north of the central part of the Southern Uplands Fault. Much of the rest of the Midland Valley is covered by greatly varying thicknesses of Carboniferous sediments which include the productive coal measures of Mid-Lothian and Ayrshire. The olivine-basalt lavas of the Campsie Fells, the Bathgate Hills and in west central Scotland are all of this era and indicate intense volcanic activity in the Carboniferous. The large numbers of dykes which intrude the Midland Valley are also predominantly of Carboniferous and Permian age.

The rocks of the Southern Uplands are mainly Lower Palaeozoic sediments with small outcrops of Devonian, Carboniferous and Permian series and two distinct regions of volcanic activity. The broad areas of Ordovician and Silurian sediments are principally greywackes and shales, probably deposited on the floor of a marine trough. The Devonian sediments in the north-east are of Upper Old Red Sandstone and show a marked unconformity at the

base. There is very little Lower Old Red Sandstone although the large igneous intrusions in the south-west - the Loch Doon, Cairnsmore of Fleet and Criffell granites - are all of this age. The lava flows of the north Cheviots provide evidence for Carboniferous volcanic activity also.

3.3: Previous geophysical studies in the South of Scotland.

Many of the previous geophysical studies carried out in South Scotland have been magnetovariational studies of the Eskdalemuir geomagnetic anomaly. This was first identified by Osemeikhian and Everett (1968) who took measurements at ten locations, using 3-component proton magnetometers, and found attenuation of the vertical magnetic field, at frequencies of 10 Hz, at Eskdalemuir and Glenlee. Edwards, Law and White (1971) took further measurements in the area, as part of a wider array study of the British Isles, and confirmed the existence of an anomalous region centred on Eskdalemuir. They suggested that this was caused by electric currents in the North Sea, leaking, through a lower crustal conductor under the Southern Uplands, into the Irish Sea. The existence of such a conductor at Eskdalemuir had been proposed by Jain and Wilson (1967) on the basis of magnetotelluric maesurements made there. Bailey et al. (1974) and Bailey and Edwards (1976) reinterpreted Edwards' magnetometer data using a hypothetical event technique and suggested that the lower crustal conductor could be the remains of the oceanic crust of the Iapetus.

A shorter period study, using micropulsations, was carried out by Green (1975), with two sites - Eskdalemuir and Earlyburn - in the Southern Uplands. The behaviour of the in-phase induction

arrow at Earlyburn suggested a resistivity contrast across the Southern Uplands Fault with the more conducting region to the north.

Jones (1977) carried out extensive magnetotelluric measurements in the South of Scotland. The results, reported in Jones and Hutton (1979 a, b) indicated a conductor underlying the Midland Valley at, at most, 12 km. depth, with a deep conductor at a depth of at least 24 km. under the Southern Uplands. Further south, under the Northumberland Basin the conductor is within 5 km. of the surface (figure 3.4).

The 1974 Lithospheric Seismic Profile in Britain (LISPB) has led to the construction of a north-south section through Scotland and into northern England. The part of the section pertaining to the South of Scotland is summarized by Bamford et al. (1978) and Faber and Bamford (1979) as having the following structure:

1) A superficial layer comprising of Upper Palaeozoic and more recent sediments.

2) An upper crustal structure to a depth of between 8 and 15 km. which has a velocity varying from north to south.

3) A sequence which defines the pre-Caledonian basement north of the Southern Uplands Fault but which is much more ill-defined to the south of it, there being horizontal discontinuity between the Midland Valley and the Southern Uplands.

4) A lower crustal layer which is also absent or less well developed beneath the Southern Uplands.

5) A uniform sub-Moho layer.

This structure is shown in the schematic cross section of figure 3.5. It shows a major discontinuity in structure under the Southern Uplands and also an unresolved zone just north of the

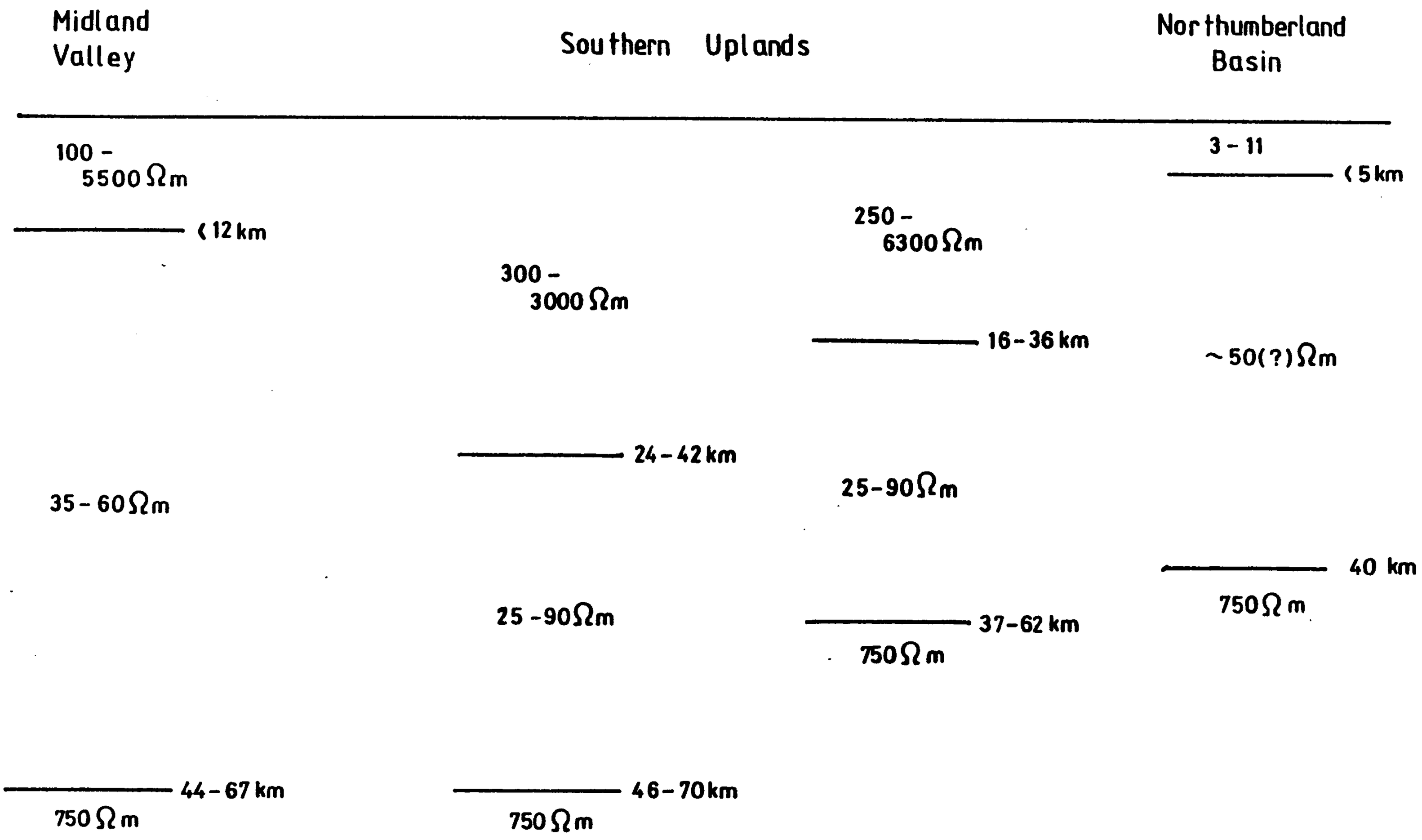

Figure 3-4.

One-dimensional resistivity profiles across S.Scotland (Jones (1977)).

Figure 3·5.

Schematic cross-section across the Scottish Midland Valley (after Bamford et al. (1978)).

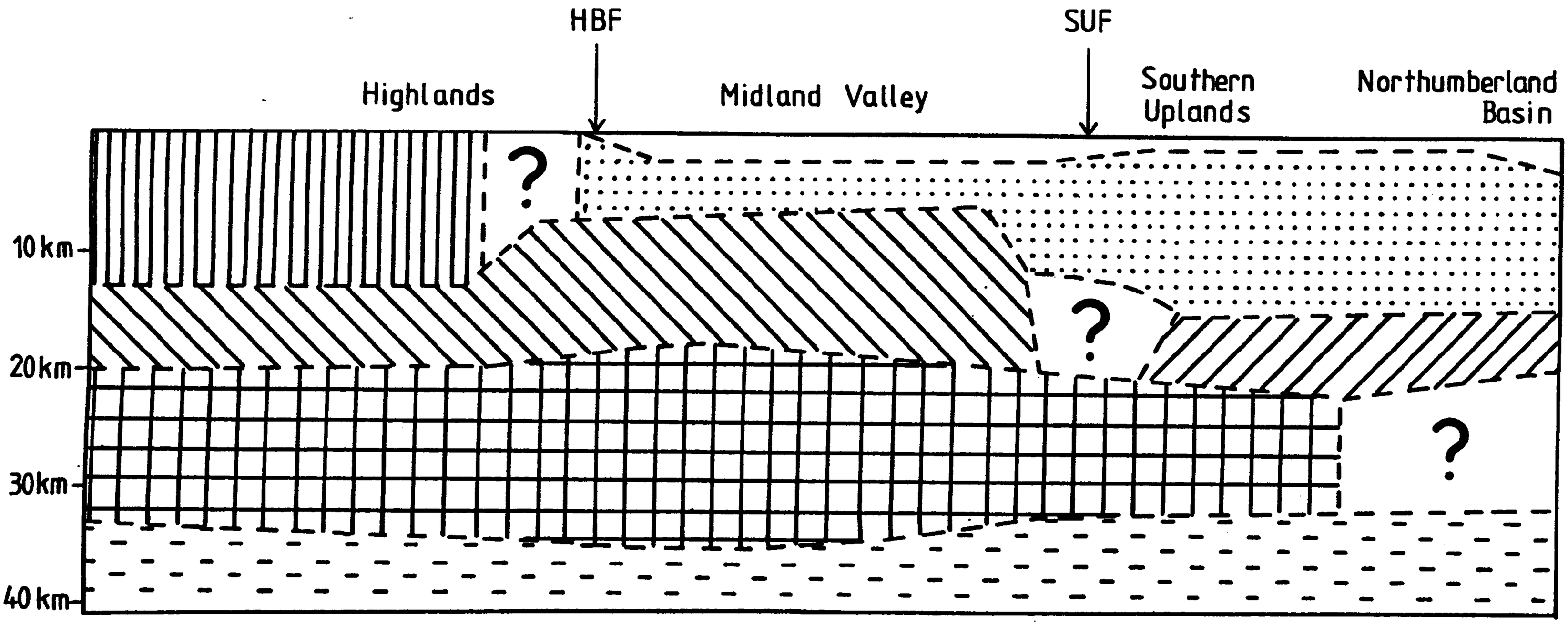

Highland Boundary Fault.

Blaxland et al (1979) carried out Pb isotope analyses of feldspar separates from granites from different regions of Scotland and found that the samples from under the Southern Uplands were consistently more radiogenic than those from other areas. They interpreted this as meaning that the rocks to the north of the Southern Uplands Fault contain a significant component of Lewisian crust whereas those under the Southern Uplands are younger and have a composition close to either underlying mantle or a mixture of mantle and overlying sediment. Hall and Simmons (1979) have carried out seismic velocity tests on rocks representative of the structural profile of LISPB for the Highlands. They reached the conclusions that 1) the upper crustal layer is a mixture of Lewisian-like quartzo-feldspathic gneisses with granitic additions; 2) the middle crustal layer is made up of pyroxene granulites with an average composition of andesite-diorite; 3) the lower crustal layer may be equivalent to basic igneous rocks metamorphosed to garnet granulite facies, but cannot be mainly serpentized peridotite or amphibolite facies rock.

The step in the lower crust which is indicated by LISPB across the Southern Uplands Fault was previously detected by a gravity survey in the western part of the Midland Valley by McLean and Gureshi (1966). The granitic masses of south-west Scotland have also been investigated by gravity methods and El-Batroukh (1975) concluded that the Loch Doon, Cairnsmore of Fleet and Criffell granites are all connected at depth. A recent, very detailed gravity survey in the south-east of Scotland has led to the detection of a similar granitic body, extending south

and east from around Peebles under the Southern Uplands (Lagios, 1979; Lagios and Hipkin, 1979). The proposed extent of the intrusion, which in places comes very close to the surface, is shown in figure 3.6. Using data from the same survey Hipkin and Lagios (1978) have concluded that the part of the Southern Uplands Fault west of Earlyburn (the Leadburn Fault) originated in the lower Devonian and that there has been no significant strike-slip displacement on the Fault as a whole, since the Silurian.

Of the work decribed above, only the LISPB profile refers to the area north of the Midlothian coalfields. This is representative of the fact that very little geophysical work has been carried out north of the Forth-Clyde line. A magnetometer survey carried out by Hutton et al. (1977) covering the whole of Scotland, identified the Eskdalemuir anomaly and also an anomalous region associated with the Great Glen, but yielded little information about the Southern Highlands and the northern part of the Midland Valley. The Great Glen region is now being studied in more detail by Mbipom (pers. comm.) using magnetotelluric and magnetovariational methods, but there is still a lack of geophysical data from around the Highland Boundary Fault.

3.4: The tectonic continuation of the Iapetus suture in North America.

Various workers in Canada and the United States have identified a geomagnetic anomaly close to the Atlantic coast of North America which has been interpreted as the North American continuation of the Iapetus suture. Hyndman and Cochrane (1971) found that the Z transfer function at Sable Island, off Novia

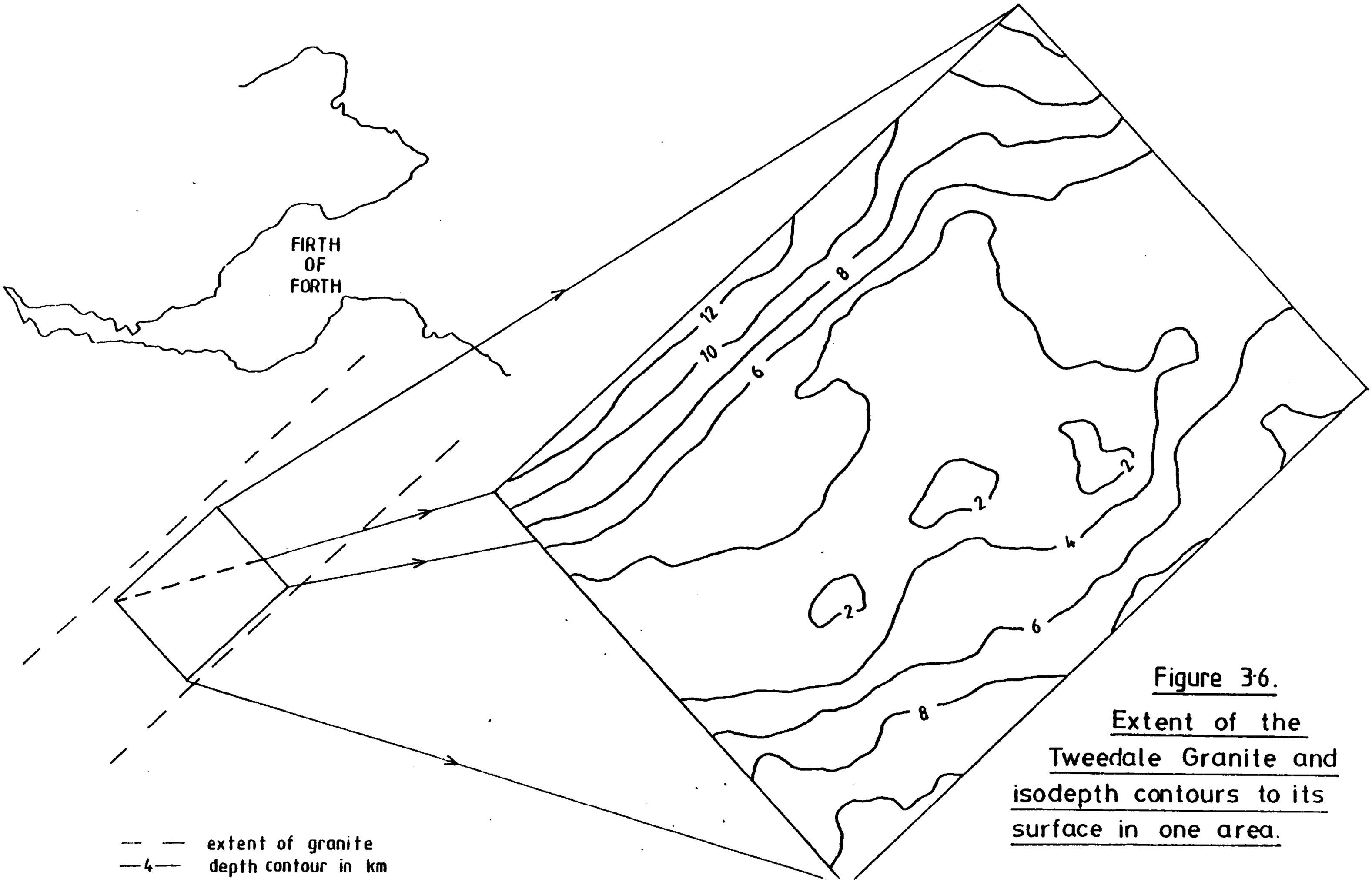

Figure 3·6.
Extent of the Tweedale Granite and isodepth contours to its surface in one area.

Scotia, was strongly attenuated and they explained this as being due to a highly conducting lower crust beneath Nova Scotia. In a later paper (Cochrane and Hyndman, 1974) the same authors suggested that this could be caused by either water saturation of granites or the incorporation of ancient oceanic crust into a continental margin geosyncline. Measurements near the American Appalachians by Edwards and Greenhouse (1975) indicated that the anomaly extended down the coast and Honkura et al. (1977) identified its extension to the north-east of Quebec. Further work by Cochrane and Wright (1977), Nekut et al. (1977) and Bailey et al. (1978) all gave somewhat similar results at different positons along the Atlantic coast.

Kurtz and Garland (1976) took magnetotelluric measurements in the Grenville Province and Appalachian System of Eastern Canada. They reported a considerable conductivity contrast between sites in the two regions, with a relatively conducting lower crust (200 Ω-m) in the Grenville Shield and a conducting (100Ω-m) upper mantle in the Appalachians to the south-east.

Finally, support for the correlation of the geomagnetic anomaly with the Iapetus suture also comes from geological evidence. McKerrow and Cocks (1977) mapped the suture, geologically, through Newfoundland and reported that it coincided with the low resistivity zone of 20Ω-m at lower crustal depths.

3.5: Summary.

1) The position of closure of the proto-Atlantic or Iapetus Ocean is now generally taken to be along the line of the Solway Firth.

2) The suture has been traced through Newfoundland into the

north-east of the United States and Canada.

3) The closure may well have been a complex process involving several subduction zones.

4) Previous geomagnetic studies have identified an anomalous region around Eskdalemuir in the Southern Uplands.

5) Both gravity and seismic surveys indicate a step down in the crust on passing across the Southern Uplands Fault from north to south. The LISPB seismic profile also showed a thickening of the upper crustal layer beneath the Highlands but could not resolve the deeper structure beneath the Southern Uplands.

CHAPTER 4: FIELDWORK AND DATA ANALYSIS.

This chapter deals with the instrumentation, fieldwork and data analysis involved in this project. In section 4.1 the instrumentation used is described, with particular reference to a major improvement in the data recording since earlier projects. The field sites are dealt with in section 4.2, including those sites from earlier investigations from which results are referred to here. Finally, section 4.3 deals with the basic analysis of the field data.

4.1: Instrumentation.

The five-component magnetotelluric system used in this project was the same, with one important exception, as the FVS system of Jones (1977). The electrodes used were hollow cylinders of lead sheet about 18 inches in length and 6 inches in diameter; these were arranged in an L-shaped array, with the electrode at the apex of the array common to both directions. The arms of the electrode array were usually approximatly 75-100 metres in length, although the availability of sufficient amplification for the signals meant that a shorter electrode spacing could be used if the nature of the terrain (e.g. a narrow valley) precluded a longer spread. To reduce the effect of temperature change on the electrode potential, the electrodes were buried, usually vertically, with the top of the cylinder 6-8 inches beneath the surface.

The telluric signals were first fed into a Trigg amplifier (Trigg, 1972) which also contained a low pass filter of 10 s cut-off. After passing through a high-pass ($\sim$1200 s) filter the

signals were then amplified for a second time, before recording.

The magnetometers used in the project were of the kind developed by Jolivet (1966) and improved by Albouy et al. (1971). The "Jolivet" is a magnetic balance magnetometer, the magnet being suspended, by a thin wire, in a fluid of the same density. The magnet lies between two feedback coils which have their axes oriented parallel to the component of the magnetic field which is to be measured. Any change in this component of the field causes the magnet to rotate. A mirror attached to the magnet then reflects light from a bulb onto a photo-resistor, the output of which drives the feedback circuit so that the coils produce a magnetic field sufficient to cancel out the change and bring the magnet back to its original position. The response of the Jolivet magnetometer is constant above a period of 5 seconds, so that it is ideal for recording variations in the period range 10-1200 seconds.

The output of the magnetometer is the drop in voltage across a 1k resistor produced by the feedback current which is itself proportional to the change in the magnetic field. The deployment of the three magnetometers (one for each component of the magnetic field), described by Rooney (1976), uses a zero-centred Keithley Microvoltmeter to detect the null position of the magnetometer. The microvoltmeter also provides a variable amplification before the output signals are filtered and undergo a second stage of amplification.

In previous studies the Edinburgh University magnetotelluric system used a five-channel Watanabe paper chart recorder. The analogue record obtained was then hand digitized on a Ferranti Freescan Digitizer table, a process which invariably introduced

noise into the data through both human inaccuracy and the finite width of the ink trace on the paper. In this project, to remove the problem of hand digitization, recording was carried out on digital tape cassette using the N.E.R.C. Datel geologger developed by M.J. Valiant. The difference in the errors associated with each manner of recording has been commented on by Mbipom and Hutton (1978) and can be seen in figure 4.1.

The geologger can record on up to 15 channels simultaneously, the first four channels having a range of ±10V and the others a range of ±5V. Although the rate of recording can be varied from 1 reading per second up to one reading every 10 minutes, in this project a recording interval of 5 seconds was used at all sites. Recording was carried out on eight channels, the three magnetic components being recorded twice (channel 1-Z; 2-D; 3-H; 4-EW; 5-NS; 6-Z; 7-D; 8-H), once on each range. Using eight channels at a 5 second recording interval each tape lasted for approximately 20 hours.

As a means of keeping a visual check on the incoming data, the Watanabe chart recorder was run in parallel with the geologger. The chart record obtained was also used to select possible events of good signal to noise ratio, high activity and a variety of polarizations.

A block diagram of the complete M.T. system is shown in figure 4.2.

Since spring 1978 the filters, amplifiers and recording equipment for the magnetotelluric system have been mounted inside a caravan. In general this was parked relatively close to a power supply and as well as providing shelter and security for the equipment, by retaining the living quarters in the caravan, full

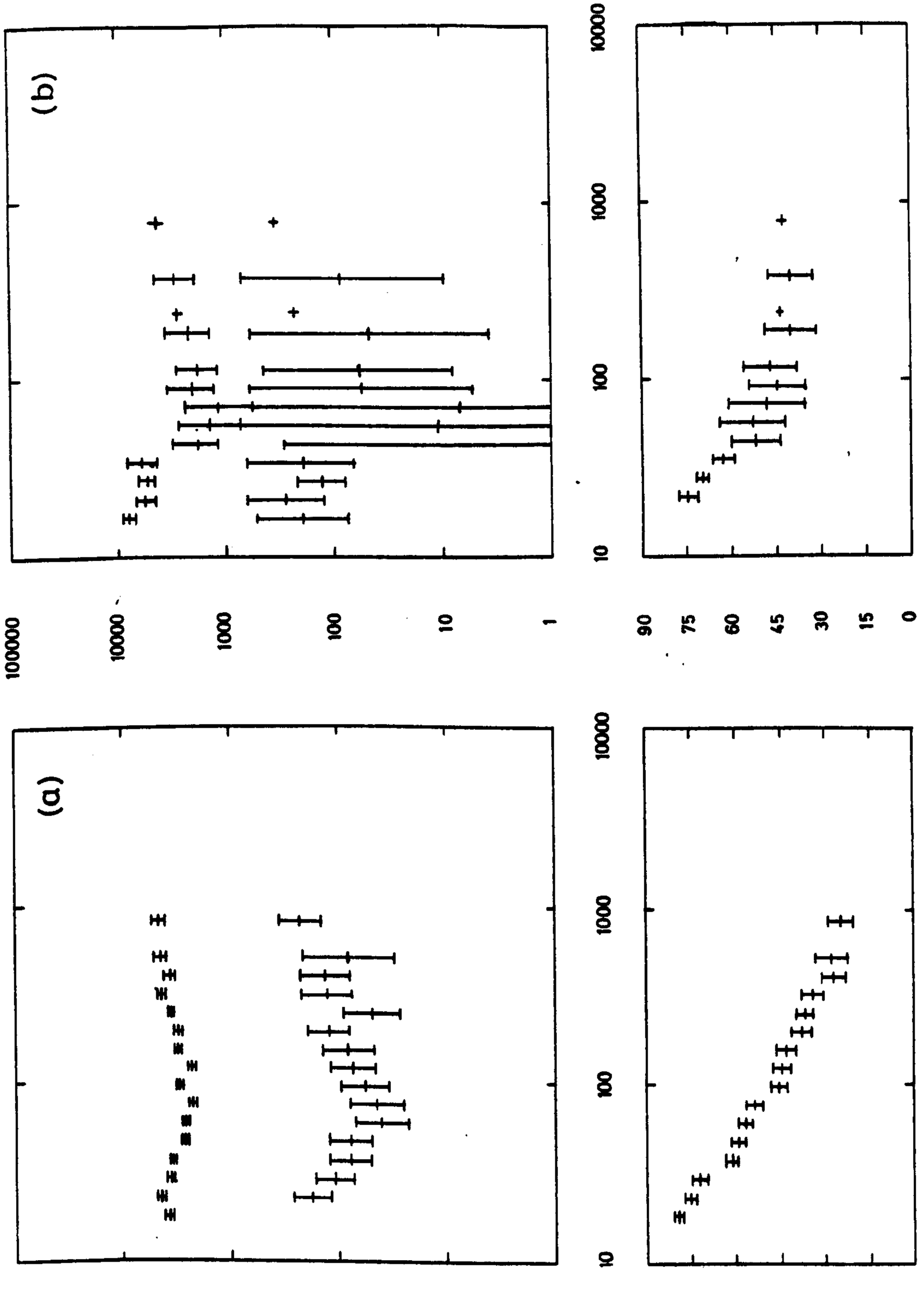
Comparison of max. and min. apparent resistivities and max. phase
calculated from a) digital tape data and b) hand digitized chart data.
(a)
(b)
100000
10000
1000
100
10
1
90
75
60
45
30
15
0
PERIOD / S
APPARENT RESISTIVITY / OHM.M
PHASE

Figure 4·1.

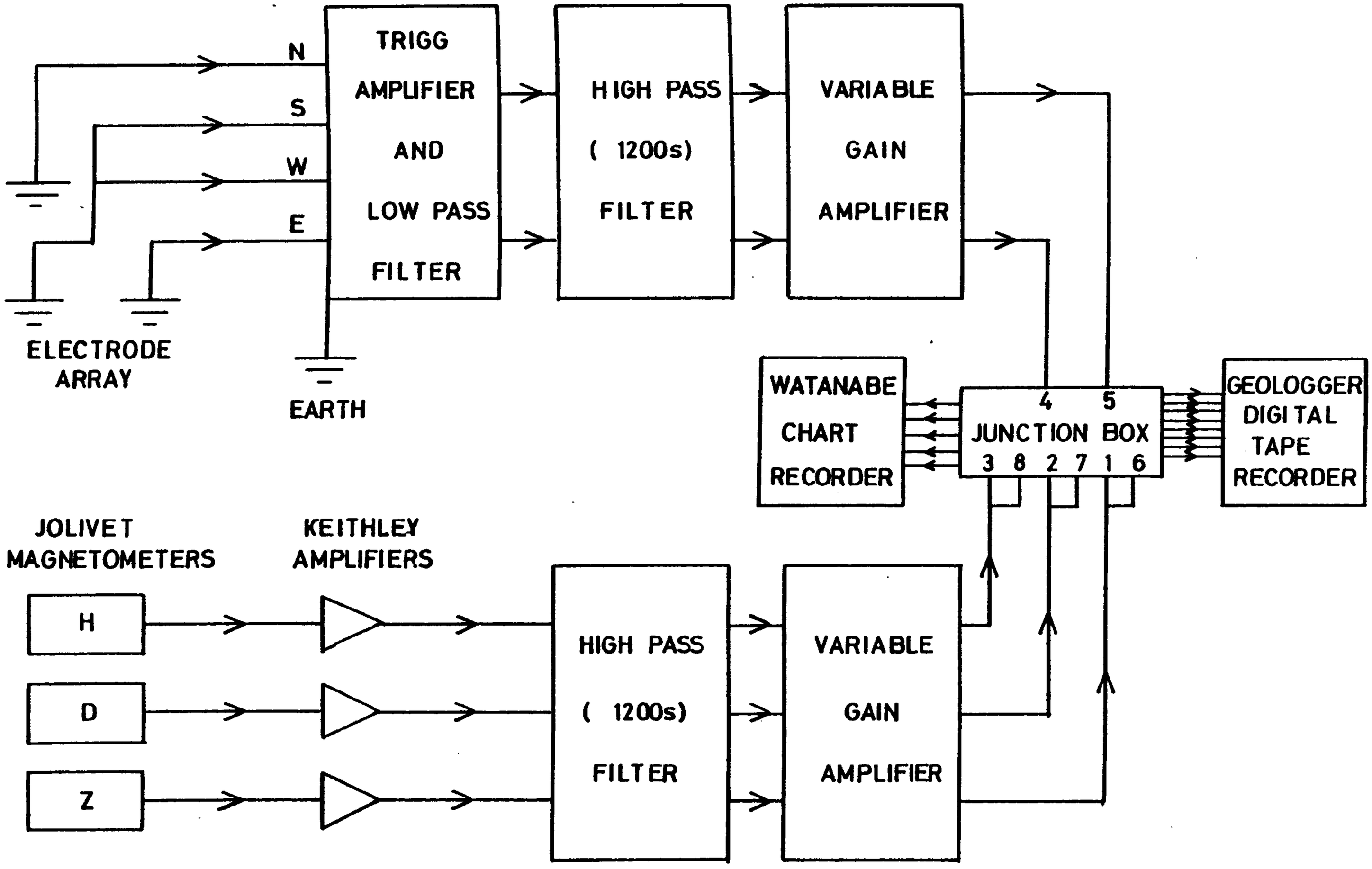

Figure 4·2.
The magnetotelluric system.

time supervision of the sites was possible.

4.2: Field sites.

The new field sites at which recordings were made during this project are listed in table 4.1 which also shows the grid reference of each site and the dates over which recording was carried out. The physical characteristics of, and the problems encountered at each site are listed below.

1) Bonnybridge (BON).

Because of cultural noise encountered regularly from 6 a.m. to 12 p.m. the site at BON had to be abandoned without obtaining any data. The actual source of the noise was not tracked down, but it was probably due either to the relative proximity of the site to industrial works, or, more locally, to some source within the farmhouse from which power was obtained.

2) Borthwichbrae (BOW).

The site at BOW was situated at the edge of an open moor on rough, poorly drained land. The remoteness meant that no cultural noise was evident apart from occasional disturbances due to activity around the farm. Except for chart recorder pens drying up, no problems were encountered.

3) Crieff (CRF).

The position of the site on a narrow wedge of pastureland between fields of crops meant that one electrode separation was considerably shortened. However the main problem was considerable thunderstorm activity which affected the magnetometers and caused loss of power supply on several occasions.

4) Earlyburn (EAR).

The site at Earlyburn was at the old satellite tracking

Table 4.1

Magnetotelluric sites.

Station	Abbreviation	Grid ref.	Date
Bonnybridge	BON	28346784	02/05/78 - 09/05/78
Borthwickbrae	BOW	33666163	02/06/78 - 08/06/78
Crieff	CRF	29047208	11/08/78 - 16/08/78
Earlyburn	EAR	32286496	20/04/78 - 02/05/78
			and 29/05/78 - 02/06/78
Glen Quaich	GQU	28857366	06/08/78 - 11/08/78
Kinloch Rannoch	KLR	26837587	01/08/78 - 06/08/78
Kinross	KRS	30757003	16/08/78 - 21/08/78
Peebles	PEE	32746405	18/05/78 - 24/05/78
Penicuik	PEN	32176609	25/09/78 - 29/09/78
Strathyre	STY	25807110	23/11/77 - 11/12/77
Yarrow	YAR	32996244	11/05/78 - 18/05/78

station owned by the Institute of Geological Sciences; positioned strategically, in terms of this project, in the proposed kink in the Southern Uplands Fault. The data recorded at EAR were relatively noisy, possibly because of the magnetic debris lying around the site from its previous usage. However a contibutary factor may also have been the use of shortened telluric lines which would tend to magnify any noise due to electrode potentials. Because of a failure of the geologger the site had to be visited twice.

5) Glen Quaich (GQU).

GQU was situated on rough, marshy land in the flat bottom of Glen Quaich, at the south-eastern end of Loch Freuchie. As at EAR, the main source of noise was debris, in this case in the old farmyard from which power was obtained.

6) Kinloch Rannoch (KLR).

The site at KLR, on good, flat land in the bottom of a relatively narrow E-W valley, was noise-free and gave good data.

7) Kinross (KRS)

The field station was also situated on good pastureland at KRS. Some slight cultural noise was encountered from the many battery chicken farms in the area.

8) Peebles (PEE).

At PEE the site was situated on the north side of the River Tweed valley, a few miles to the east of Peebles itself. The town was therefore far enough away so as not to cause interference on the magnetics, there was however, slight cultural noise from the small-holdings around the site.

9) Penicuik (PEN).

Leakage across the signal wires from the magnetic sensors

was a problem at PEN. This presumably arose through the three-core signal cable used getting wet, and thus allowing electrical conduction through imperfections in the insulation. The problem was eliminated by replacing the cable.

10) Strathyre (STY).

The logistics at STY were made difficult because of the narrowness of the valley. Eventually the site was established on the narrow band of pasture between the edge of Loch Lubnaig and the eastern slopes of Ben Ledi. Despite the imperfect situation the data obtained were good.

11) Yarrow (YAR).

The site at YAR was situated on the flood plain of the Yarrow Water, close to the line of the Ettrick Thrust. The main problem was the stoney nature of the flood plain which meant that the electrodes had to be buried horizontally rather than vertically. The telluric signals recorded at YAR were generally of very low power.

Overall the principal restrictions during the fieldwork were 1) the difficulty of getting away from cultural noise, particularly in the Midland Valley; and 2) the problem of finding suitable power supplies in the Upland areas without situating all the sites on the floors of valleys which may channel telluric currents.

The magnetotelluric sites are shown in figure 4.3. Also marked on the map are other field stations from which the results have been used in this project. These include several magnetotelluric sites of Jones (1977) and the sites used in a magnetometer array study of Scotland by Hutton et al. (1977), and are also listed in table 4.2.

Figure 4·3.

Magnetotelluric (×) and geomagnetic deep sounding (□) sites in South Scotland.

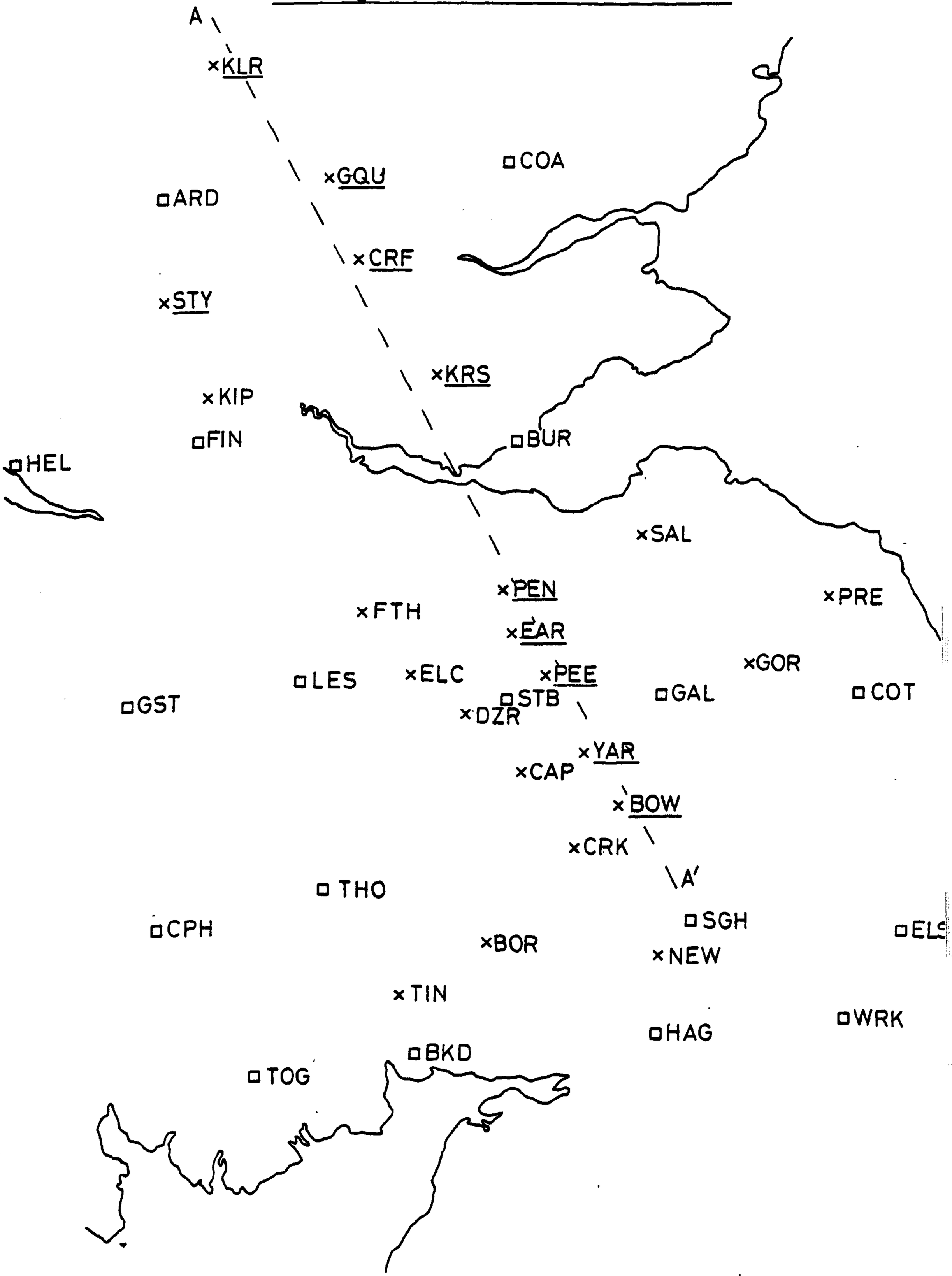

Table 4.2

Additional data used.

Station	Abbreviation	Type of data	Year
Ardeonaig	ARD	GDS	1973
Bankend	BKD	GDS	1973
Borland	BOR	MT	1976
Burntisland	BUR	GDS	1973
Cappercleuch	CAP	MT	1976
Carsphain	CPH	GDS	1973
Castle Douglas	TOG	GDS	1973
Coldstream	COT	GDS	1973
Coupar Angus	COA	GDS	1973
Craik	CRK	MT	1976
Drumelzier	DZR	MT	1976
Elsrickle	ELC	MT	1976
Elsdon	ELS	GDS	1973
Fintry	FIN	GDS	1973
Forth	FTH	MT	1976
Galashiels	GAL	GDS	1973
Galston	GST	GDS	1973
Gordon	GOR	MT	1976
Helensburgh	HEL	GDS	1973
Hethersgill	HAG	GDS	1973
Kippen	KIP	MT	1977
Larriston	SGH (?)	GDS	1973
Lesmahagow	LES	GDS	1973
Newcastleton	NEW	MT	1976
Preston	PRE	MT	1976
Saltoun	SAL	MT	1976
Stobo	STB	GDS	1973
Thornhill	THO	GDS	1973
Tinwald	TIN	MT	1976
Towhouse	TOW	MT	1976
Wark	WRK	GDS	1973

The type of magnetic activity recorded at each site, within the bandwidth of the system, consisted primarily of micropulsational activity with periods ranging from 10 to 600 seconds. The shorter period, continuous micropulsations, typically Pc3 and Pc4 were generally dominant during the daytime with more longer period (bay type) and transient phenomena around local midnight. Examples of the data recorded are shown in figures 4.4 to 4.7

4.3: Data analysis.

4.3.1: Event selection.

The first stage in the data analysis involved the visual examination of the chart records obtained on the Watanabe pen recorder for events exhibiting the following characteristics.

1) High magnetic and telluric activity at as large a range of periods as possible. This ensures a good power level in the signal.

2) Clean traces, free from extraneous noise.

3) A low degree of polarization, which is important for reasons discussed in section 4.3.4.

An interactive program TEK, written in IMP by Graham Dawes was then used to select these events from the cassette tape recordings and view them on a Tektronix 4014 console. In this way each event could be checked to ensure that it had been satisfactorily recorded on the magnetic tape and rejected if for some reason it was not available. If selected, an event was filed by the program TEK in digital form with a suitable heading identifying the date, time, site name and digitization interval for each channel.

Figure 4·4.

Example of recorded data.

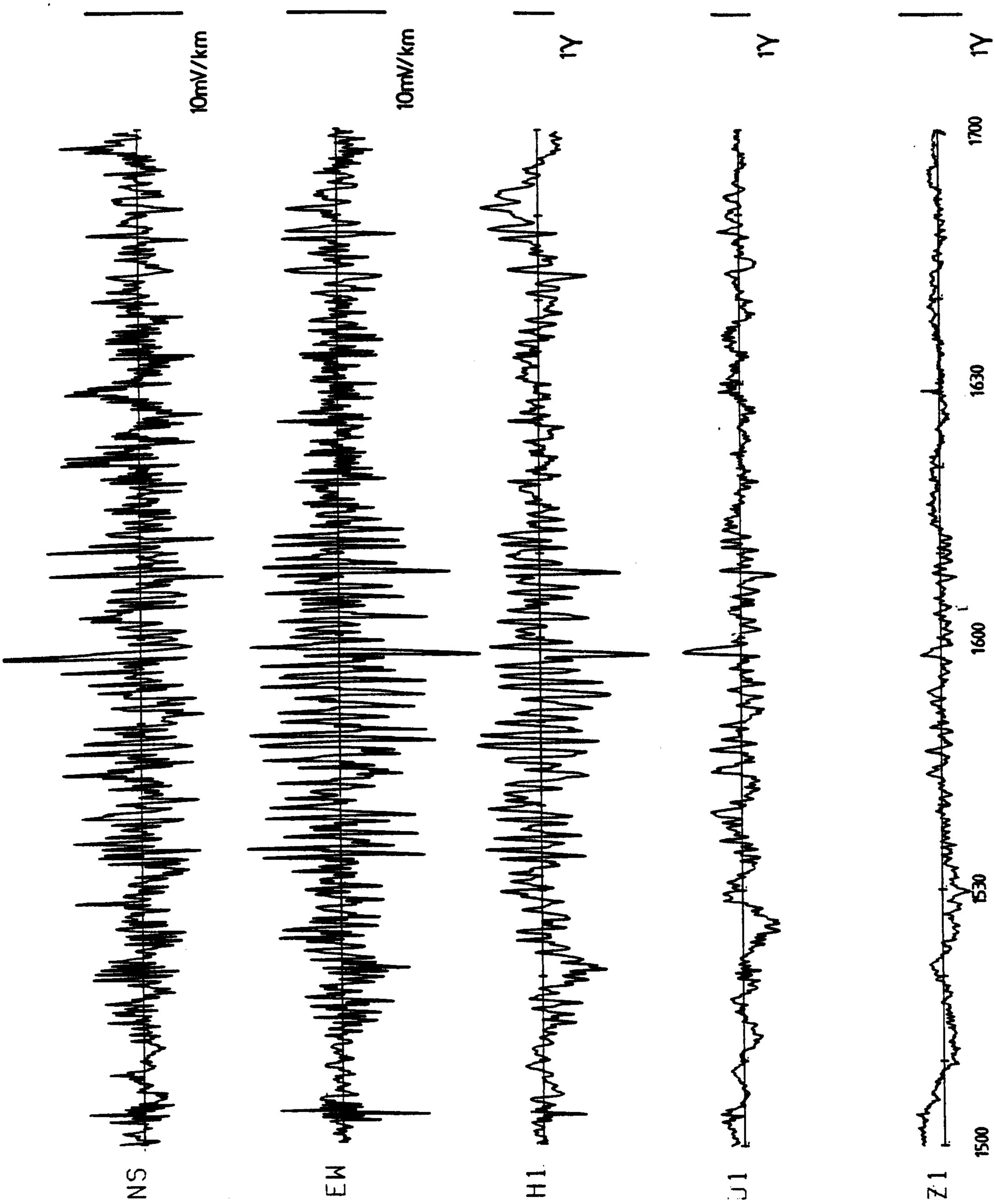

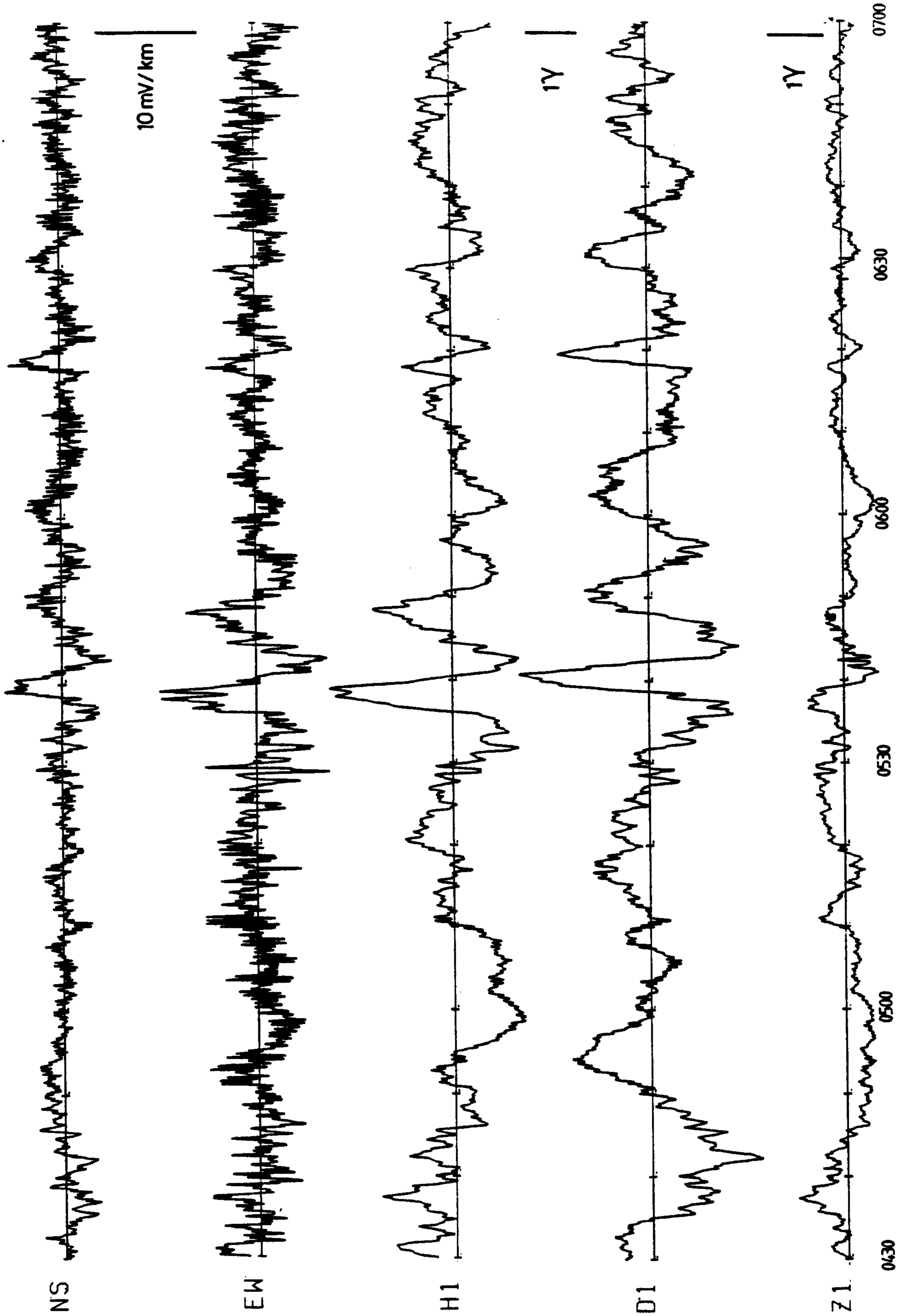

Figure 45.

Example of recorded data.

Figure 4·6.

Example of recorded data.

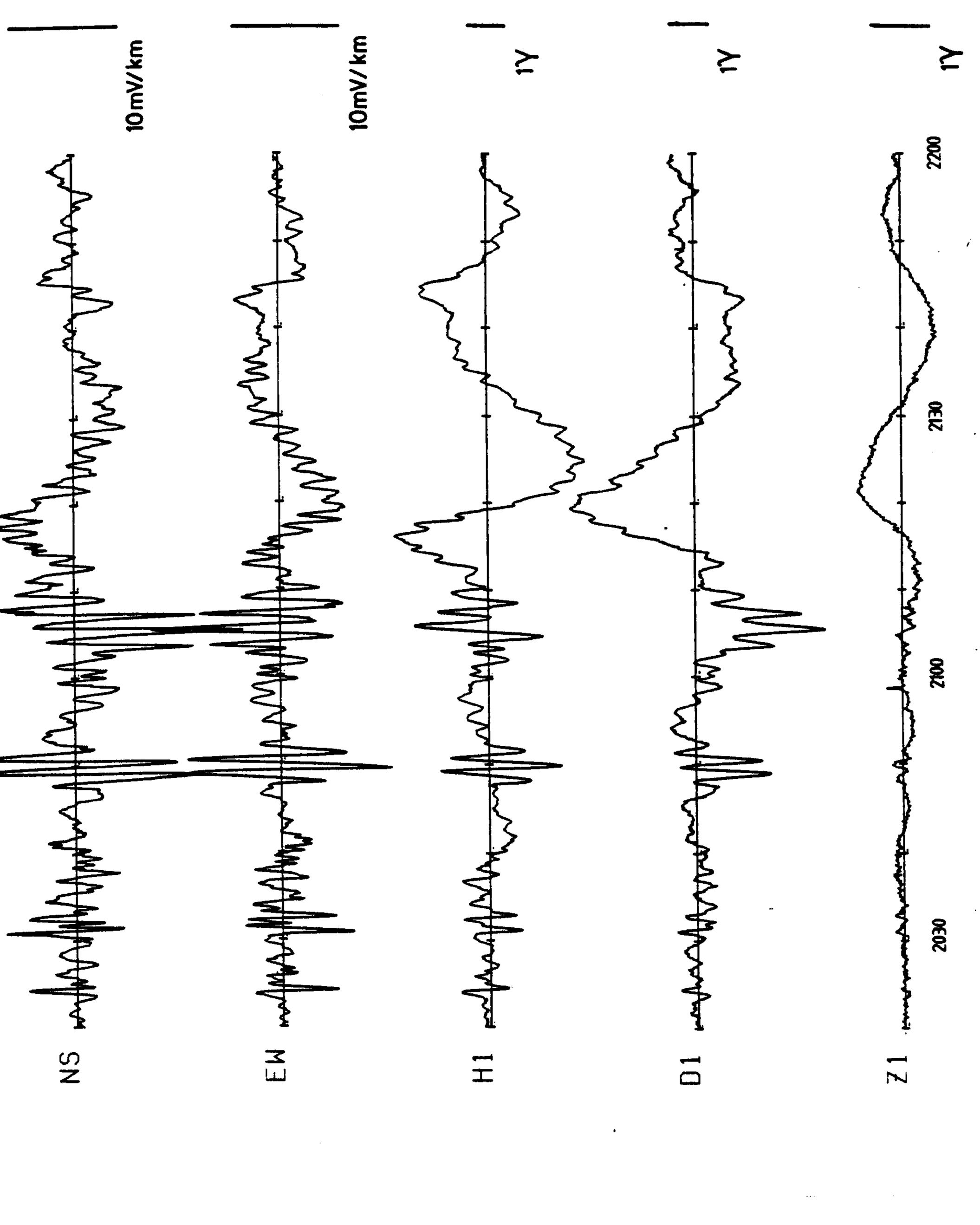

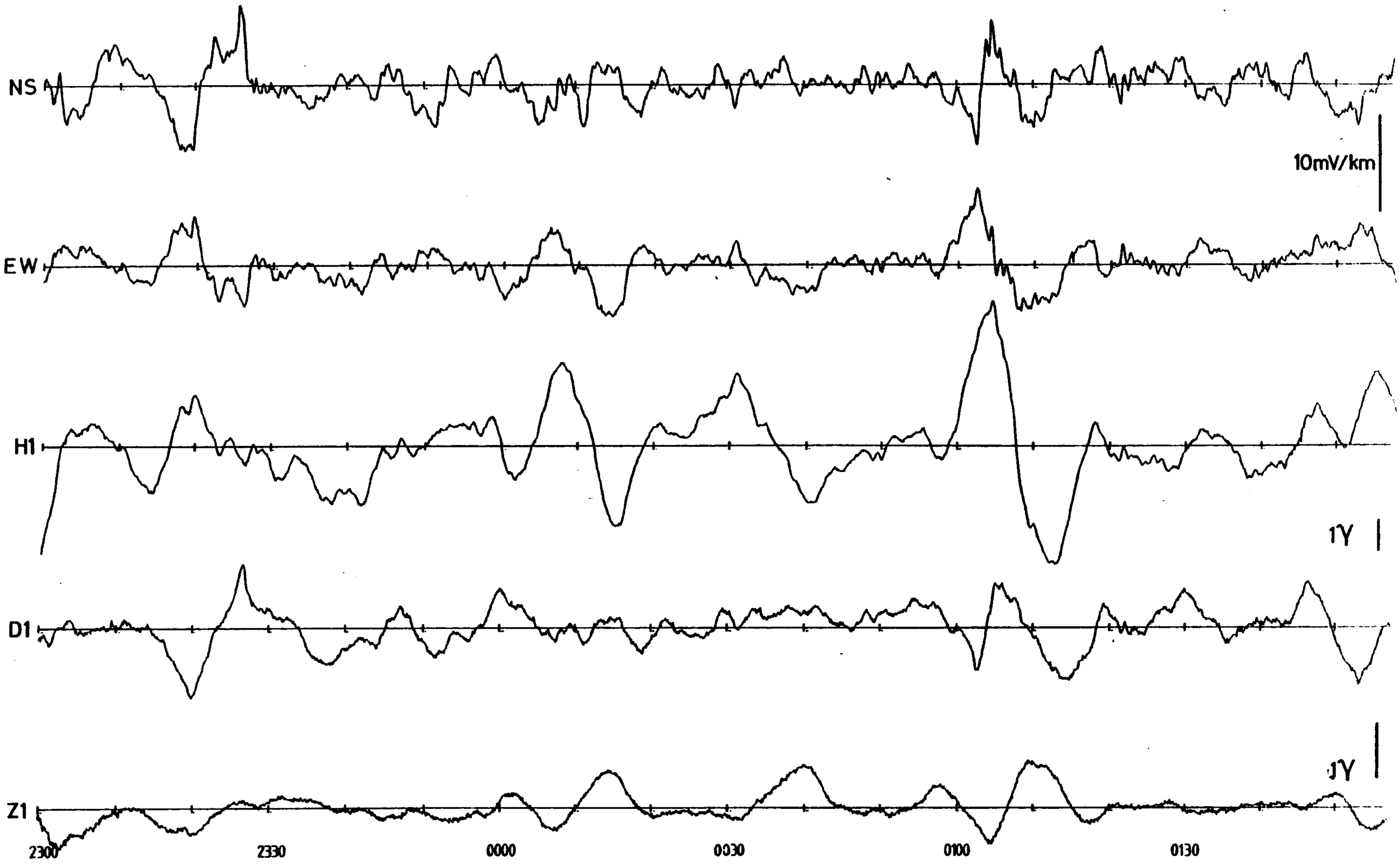

Figure 4·7.

Example of recorded data.

4.3.2: Single event processing.

Each event selected in the manner described above was processed using the single event analysis program MAGMI2. The following operations are executed by the program (Rooney, 1976)

1) Any underlying long period trend in each componet is removed by subtracting a linear least squares line from the data.

2) A cosine bell is applied to the first and last 10% of the data points of each component to reduce power leakage into the side lobes of the Fourier Transformation. For example, an estimate, $X_f(w)$, of the Fourier Transform of a finite time series $x(t)$ $(0<t<T)$ is given by

$$X_f(\omega) = \frac{1}{2\pi_0}\int^{T} x(t)\ e^{-i\omega t}\,dt \qquad 4.1$$

Such a finite time series is the equivalent of an infinite series multiplied by a viewing window (or "box-car" function) given by

$$u(t) = \begin{cases} 1 & 0<t<T \\ 0 & t<0,\ t>T \end{cases} \qquad 4.2$$

and shown in figure 4.8a.

Thus

$$X_f(\omega) = \frac{1}{2\pi}\int_{-\infty}^{\infty} x(t)\ u(t)\ e^{-i\omega t}\,dt \qquad 4.3$$

$$= X_i(\omega) * U(\omega)$$

which is the convolution of the Fourier Transform of $x(t)$ and the Fourier Transform, $U(\omega)$, of the window function 4.2. The power spectrum of this function is shown in figure 4.8b. The large side lobes of the transform mean that much of the power at the central frequency is lost; evidently a more suitable window

(a)

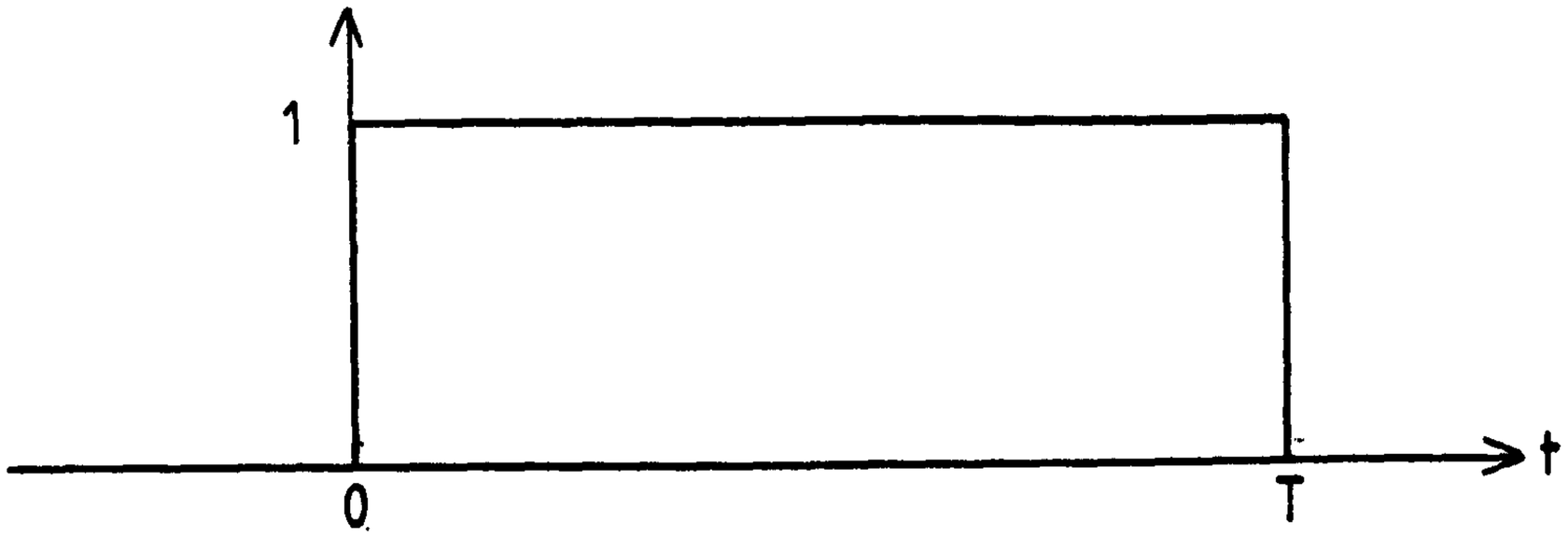

(b)

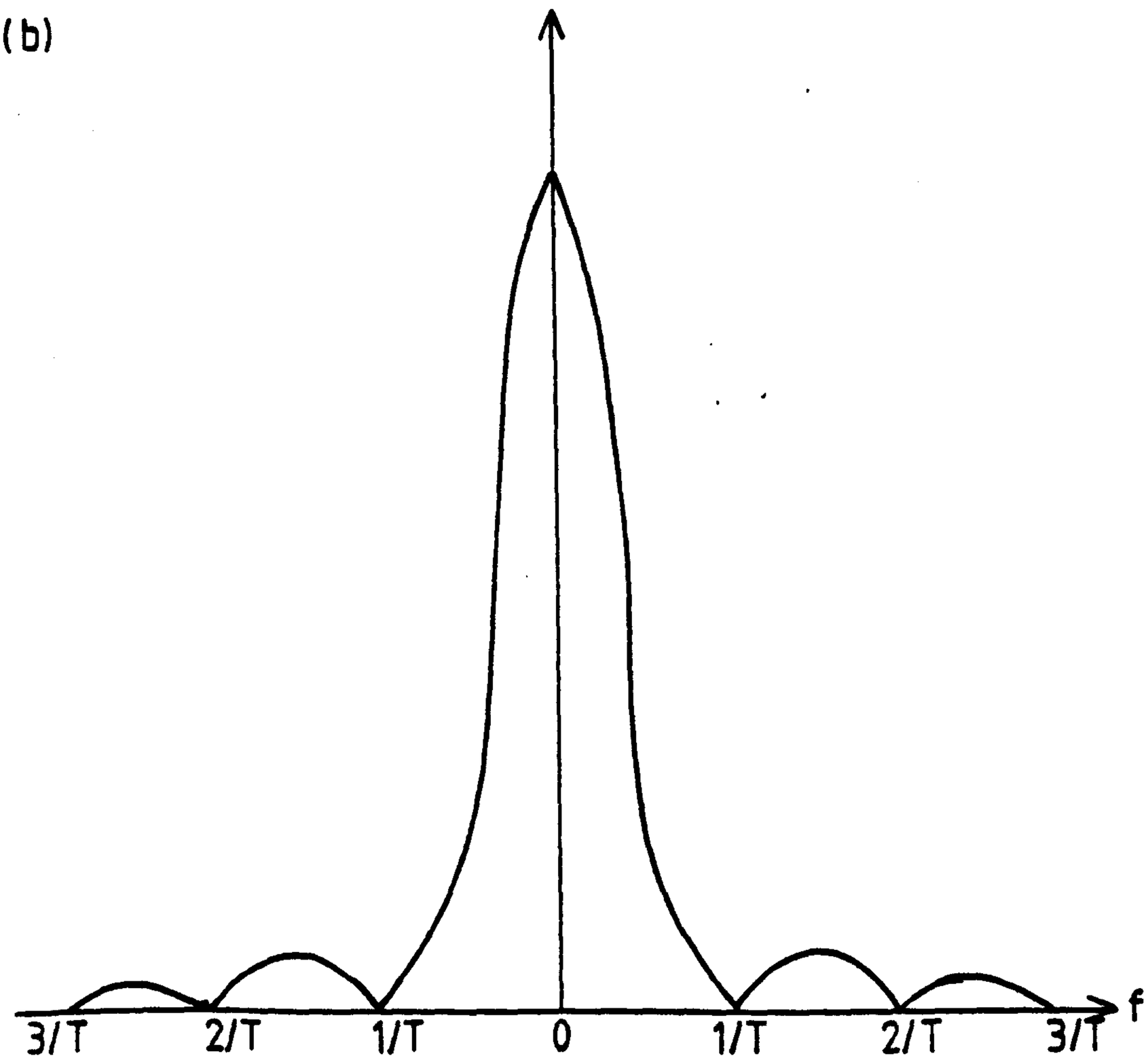

Figure 4·8.

The box-car window and its power spectrum.

function is required. Although there are many such windows, the performances of which have been reviewed by Harris (1978), the one which is generally used is the cosine taper or Tukey window (Kanasewich, 1973) defined by

$$C(t) = \begin{cases} 0 & t<0 \\ \frac{1}{2}(1 + \cos(\frac{10t}{T} - 1)\pi) & 0<t<T/10 \\ 1 & T/10<t<9T/10 \\ \frac{1}{2}(1 + \cos(10(\frac{T-t}{T}) - 1)\pi) & 9T/10<t<T \\ 0 & t>T \end{cases} \quad 4.4$$

The function C(t) is shown in figure 4.9a and the power spectrum of its Fourier Transform in figure 4.9b. It is apparent from comparing figures 4.8b and 4.9b that the power leakage is less using the cosine tapered window of 4.4 than using the "box-car" window of 4.2

3) Zeros are added to the data to bring the total number of data points to 2^m - a requirement of the Fast Fourier Transformation algorithm of Cooley and Tukey (1965).

4) Each component is Fourier Transformed using the above algorithm.

5) The auto- and cross-power spectral estimates of the components are calculated and band averaged over 8 adjoining estimates. The averaged estimates are then corrected for the frequency response of the high pass filter used in the data recording.

6) The following parameters are calculated from the spectral estimates:

i) the polarization parameters of both the horizontal magnetic and electric fields and the coherencies between H and D and N and E.

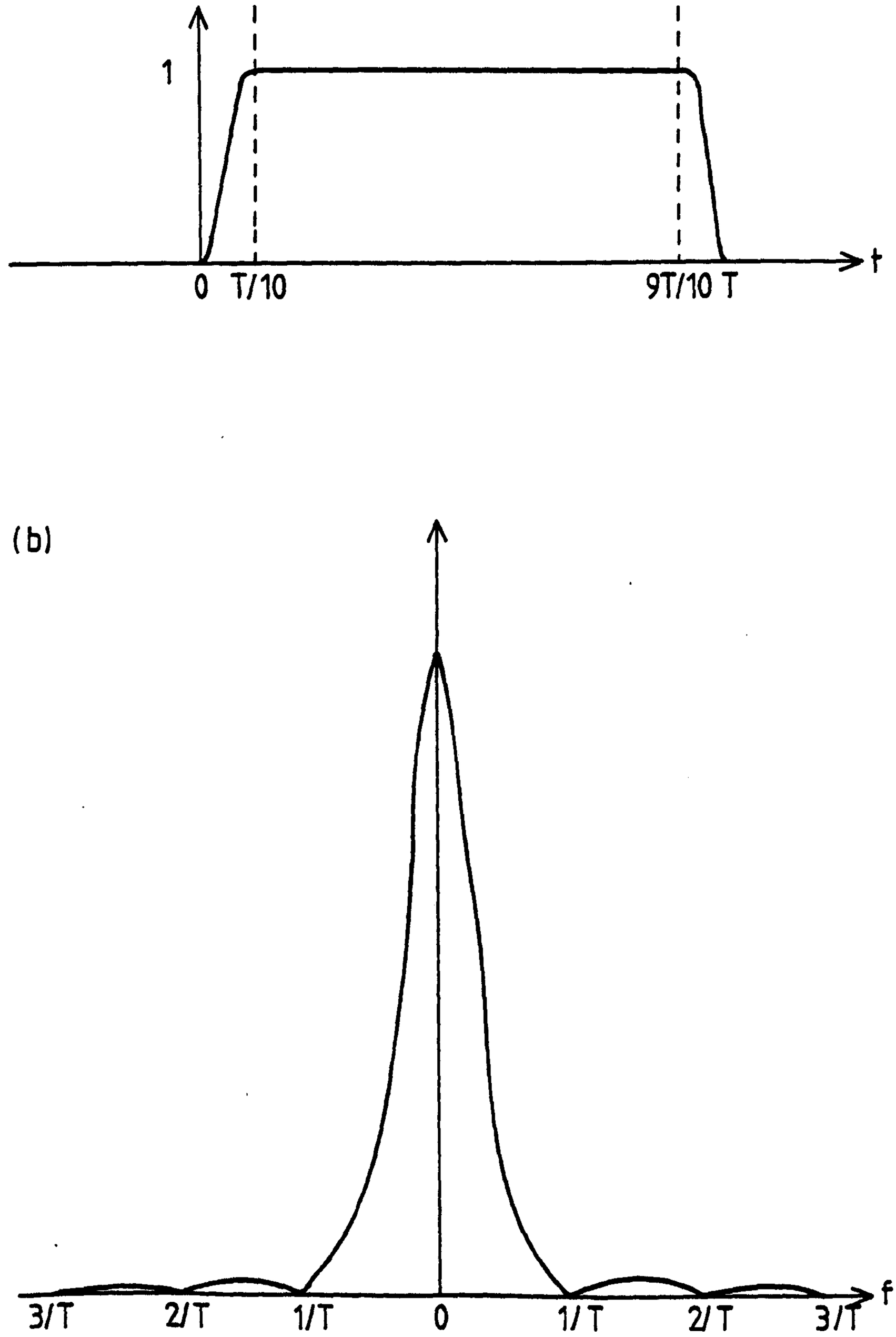

Figure 4·9.

The cosine-tapered window and its power spectrum.

ii) The transfer functions $A, B, Z_{xx}, Z_{xy}, Z_{yx}$ and Z_{yy}, by the solution of equations such as

$$Z_{xy} = \frac{\langle H\ H^* \rangle \langle N\ D^* \rangle - \langle H\ D^* \rangle \langle N\ H^* \rangle}{\langle H\ H^* \rangle \langle D\ D^* \rangle - \langle H\ D^* \rangle \langle D\ H^* \rangle} \qquad 4.5$$

which can be obtained from the relations 2.45 and 2.46.

iii) The predicted coherencies between the measured Z, N and E fields and the Z, N and E fields respectively calculated from H, D and the transfer functions A, B, Z_{xx}, Z_{xy}, Z_{yx}, Z_{yy}. Predicted coherency for a given transfer function relation provides a guide to the contamination of the transfer function estimates by random noise (Kurtz,1973), uncontaminated estimates have high coherencies. The predicted coherencies calculated were used as a selection criterion in the event averaging program.

iv) The transfer functions are used to obtain values for the induction arrows, apparent resistivities and phases for the single event, from equations 2.66, 2.67, 2.47 and 2.48.

4.3.3: Event averaging.

The event averaging program, LASTMI2, was used to calculate average values of all the relevant earth response functions over several single events. The basic operation of this program is the same as that described by Rooney (1976).

1) The values of the parameters calculated, as above, for several single events are read in.

2) For any given event, only those transfer function estimates are accepted for which the predicted Z coherency is greater than 0.8 and either the predicted N or the predicted E coherency is greater than 0.9.

3) An estimate of the signal to noise ratio is made and an

additional selection criterion, that this should be greater than 5, is applied.

4) The accepted values of each transfer function are averaged to give estimates which are equally spaced on a logarithmic period scale.

5) The averaged values of the following quantities are calculated, and both printed and plotted out:

i) the magnitudes and unreversed directions of the induction arrows (equations 2.66 and 2.67).

ii) the maximum and minimum induction arrows of Banks (1973) which correspond to the new axes H′ and D′ with respect to which the response of the vertical magnetic field is respectively a maximum and a minimum (section 2.2.3).

iii) The azimuth (equation 2.60) of the principal impedance axis.

iv) The maximum and minimum apparent resistivities and phases corresponding to the elements of the impedance tensor at this orientation (equations 2.56, 2.57, 2.58 and 2.59).

v) The skew parameter (equation 2.61).

vi) The apparent resistivities and phases corresponding to a rotation angle of $\theta = 60°$, i.e. the gross structural strike of the principal geological features in the South of Scotland.

vii) A simple one-dimensional inversion of the results, following Schmucker (1970). This assumes a resistive surface layer, overlying a conductor; thus θ_1 in equation 2.30 can be replaced by ν, the wave number of the inducing field and θ_2 by $(1+i)/\delta_2$, which is equation 2.25, using equation 2.26 for the skin depth. If the thickness, h, of the upper layer is such that $h\nu \ll 1$ then 2.30 reduces to

$$\frac{Z(0)}{i\omega\mu_0} = h + \frac{\delta_2}{2} - i\frac{\delta_2}{2} = C \qquad 4.6$$

and

$$\rho_2 = 2\omega\mu_0(Im(C))^2 \qquad 4.7$$

$$h = Re(C) - Im(C) \qquad 4.8$$

A multilayered substratum can thus be represented in its response at any period by a substitute conductor ρ_2 at a depth of h. In general the real part of C represents the depth of in-phase eddy currents in the conductor (Wiedelt, 1972) and a plot of ρ_2 against the real part of h gives an approximation to the structure.

6) As a further guide to the dimensionality of each site the magnitudes of the four elements of the impedance tensor at different angles of rotation are calculated from equations 2.56 to 2.59 inclusively.

4.3.4 Error analysis.

The error bars plotted for all of the quantities discussed above are the standard deviations about each average, assuming a normal distribution, except for those plotted on a logarithmic scale for which a lognormal distribution is used (Bentley, 1973). What the error estimates do not take into account is the possible biasing effect of source polarization on the transfer functions. As Fowler et al. (1967) have shown that any band averaged Fourier estimate can be considered as the sum of a polarized signal and an unpolarized signal, such an effect is present, to a certain extent, in all the estimates.

Consider, for example, the case in which the measured signals are composed of the true signal plus a random noise

component

$$H_M = H + n_H$$
$$D_M = D + n_D \qquad 4.9$$
$$X_M = X + n_X$$

and that the source field is polarized such that

$$H = P + h$$
$$D = CP + d \qquad 4.10$$

where h and d are the unpolarized contributions to the signal. For the simplified random noise cases, when cross-powers of the type $n_H n_D^*$ and $n_H H^*$ can be put to zero when averaged, the estimates A′ and B′ of the transfer functions A and B which relate X to H and D

$$X = A\,H + B\,D \qquad 4.11$$

are given by equations similar to 4.5, which reduce to

$$A' = \frac{((d^2 + n_D^2)(p^2 + h^2) + C^2h^2p^2)A + C^*P^2n_D^2B}{(d^2 + n_D^2)(P^2 + h^2 + n_H^2) + C^2P^2(h^2 + n_H^2)} \qquad 4.12$$

and

$$B' = \frac{C^*P^2n_H^2A + ((P^2 + h^2 + n_H^2)d^2 + C^2P^2(h^2 + n_H^2)B}{(d^2 + n_D^2)(P^2 + h^2 + n_H^2) + C^2P^2(h^2 + n_H^2)} \qquad 4.13$$

If there is strong polarization of the signal and a good signal to noise ratio then for a N-S polarization

$$A' = A; \quad B' = \frac{d^2}{d^2 + n_D^2}\,B \qquad 4.14$$

and for a E-W polarization

$$A' = \frac{h^2}{h^2 + n_H^2}\,A; \quad B' = B \qquad 4.15$$

It is possible to minimize the biasing evident in equations 4.14 and 4.15 by choosing events which are not strongly polarized. However, when this is not possible, because of shortage of

suitable events, although the process of event averaging will reduce the effect, there will be a biasing down of transfer functions. For a worst case of signal to noise ratio of 5 and 80% polarization, the factors $d^2/(d^2 + n_D^2)$ and $h^2/(h^2 + n_H^2)$ are equal to 0.5. Thus, one transfer function would be reduced by 50% and the other would be a good estimate of the true value. For the case of the impedance tensor (i.e. X is E or N) then the apparent resistivity may be biased down by a factor of up to 4.

If coherent rather than random noise is considered, then assuming that $n_H^* n_D \neq 0$ when averaged, for N-S polarization B′ is given by

$$B' = \frac{d^2}{d^2 + n_D^2} B - \frac{n_H n_D^*}{d^2 + n_D^2} A \qquad 4.16$$

and for E-W polarization

$$A' = \frac{h^2}{h^2 + n_H^2} A - \frac{n_D n_H^*}{h^2 + n_H^2} B \qquad 4.17$$

Thus there is leakage between the transfer functions. Although no estimate of the bias in the transfer functions was attempted in this project it should be appreciated that such effects may be present in some of the results. This is most likely to be the case at short and long periods at which the signal power is lower.

4.4: Summary.

1) The five-component magnetotelluric system used was similar to that employed in previous projects, except that digital recording was used for this study. This greatly improved the quality of the data by eliminating the stage of hand digitization.

2) Ten new sites were occupied on a traverse across the Midland

Valley of Scotland, penetrating into both the Highlands and the Southern Uplands.

3) Single events were analysed using standard techniques and the results averaged to give final values of the earth response functions at each site.

CHAPTER 5:RESULTS.

The results from the ten new magnetotelluric sites are presented in figures 5.1 to 5.17 and are discussed briefly below.

5.1:Magnetotelluric results.

The magnetotelluric results for the three regions, the Highlands, the Midland Valley and the Southern Uplands, are discussed separately. For each site the results shown are

a)the maximum and minimum apparent resistivities and phases;

b)the azimuth, skew and number of events averaged;

c)the Schmucker inversion of the maximum and minimum apparent resistivities and phases; and

d)the variation of the impedance tensor elements with angle for one representative period.

5.1.1:The Highlands.

The results from the three sites north of the Highland Boundary Fault, Kinloch Rannoch (KLR, figure 5.1), Glenquaich (GQU, 5.2) and Strathyre (STY, 5.3) are generally very similar.

The maximum apparent resistivity (ρ_a) curves all have a magnitude of about 1000Ω-m, only that from STY showing a slight rise with increasing period. The corresponding phase (φ_a) curves exhibit a decrease from 60° to around 40°. The φ_a curves for GQU are considerably scattered, probably due to the higher noise level encountered at the site. The three minimum ρ_a and φ_a curves are also all similar. The magnitude of ρ_a is around 200 Ω-m and fairly invariant with period.

At both STY and GQU the skew factor is 0.3 or less,

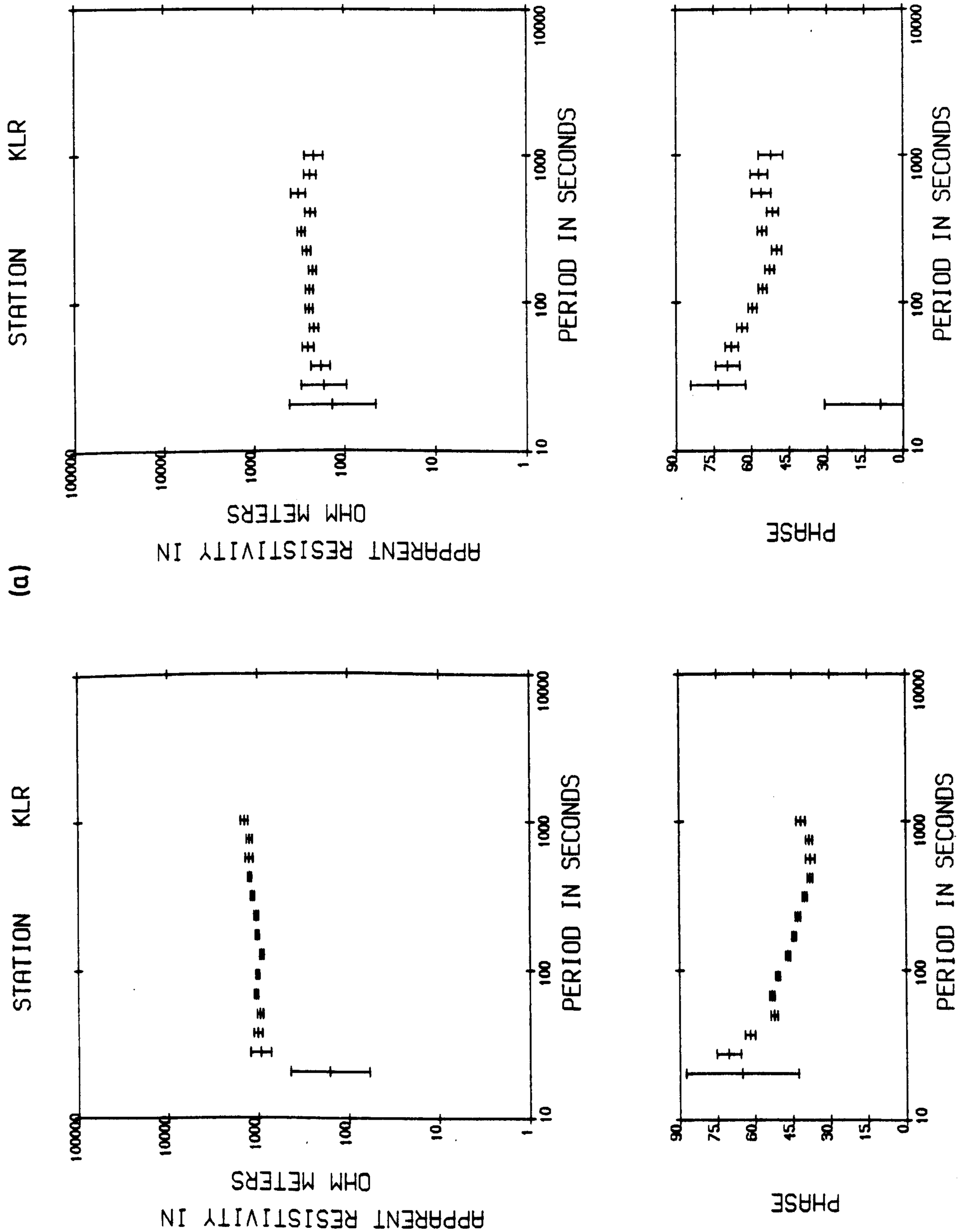
(a)
STATION KLR
APPARENT RESISTIVITY IN OHM METERS
100000
10000
1000
100
10
1
PERIOD IN SECONDS
10000
1000
100
10
PHASE
90
75
60
45
30
15
0
STATION KLR
APPARENT RESISTIVITY IN OHM METERS
100000
10000
1000
100
10
1
PERIOD IN SECONDS
10000
1000
100
10
PHASE
90
75
60
45
30
15
0

Figure 5·1.

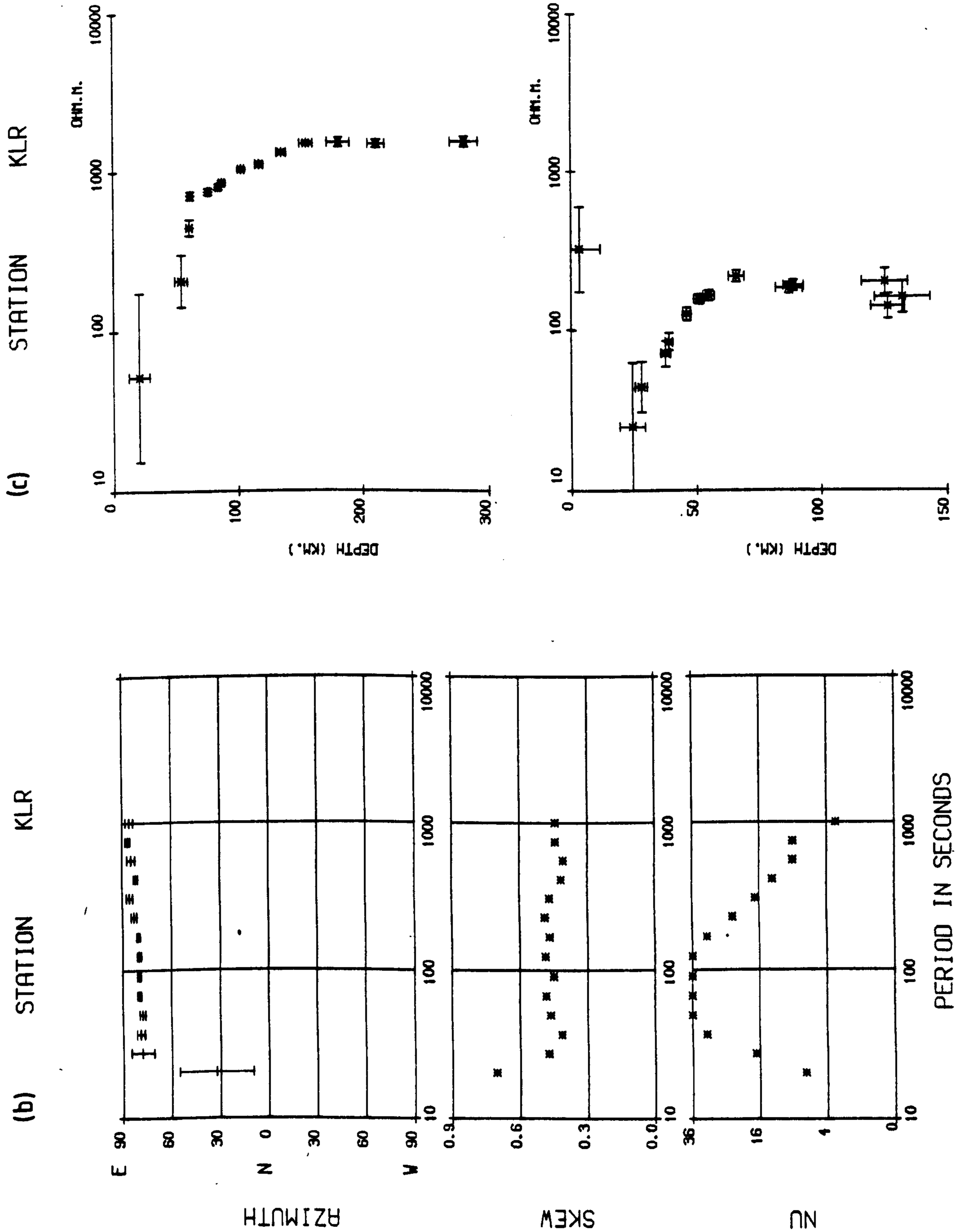
(c)
STATION KLR
OHM.M.
10000
1000
100
10
0
100
200
300
DEPTH (KM.)
OHM.M.
10000
1000
100
10
0
50
100
150
DEPTH (KM.)
(b)
STATION KLR
10000
1000
100
10
E 90
60
30
0
30
60
90
W
N
AZIMUTH
0.9
0.6
0.3
0.0
SKEW
36
16
4
0
NU
PERIOD IN SECONDS

Figure 5·1.

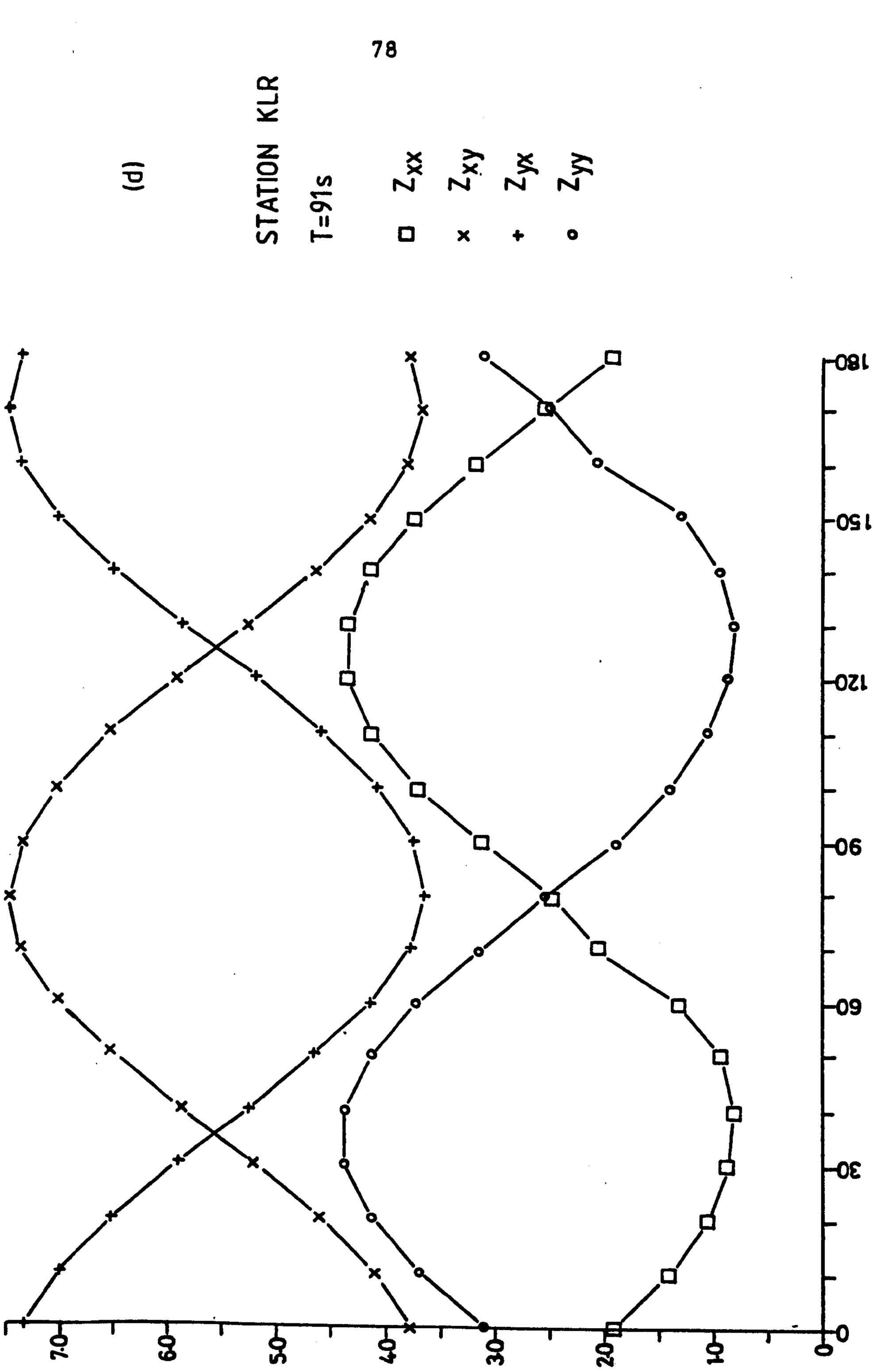
(d)
STATION KLR
T=91s
□ Zxx
× Zxy
+ Zyx
○ Zyy
ANGLE
180
150
120
06
09
30
0
70
60
50
40
30
20
10
0

Figure 5·1.

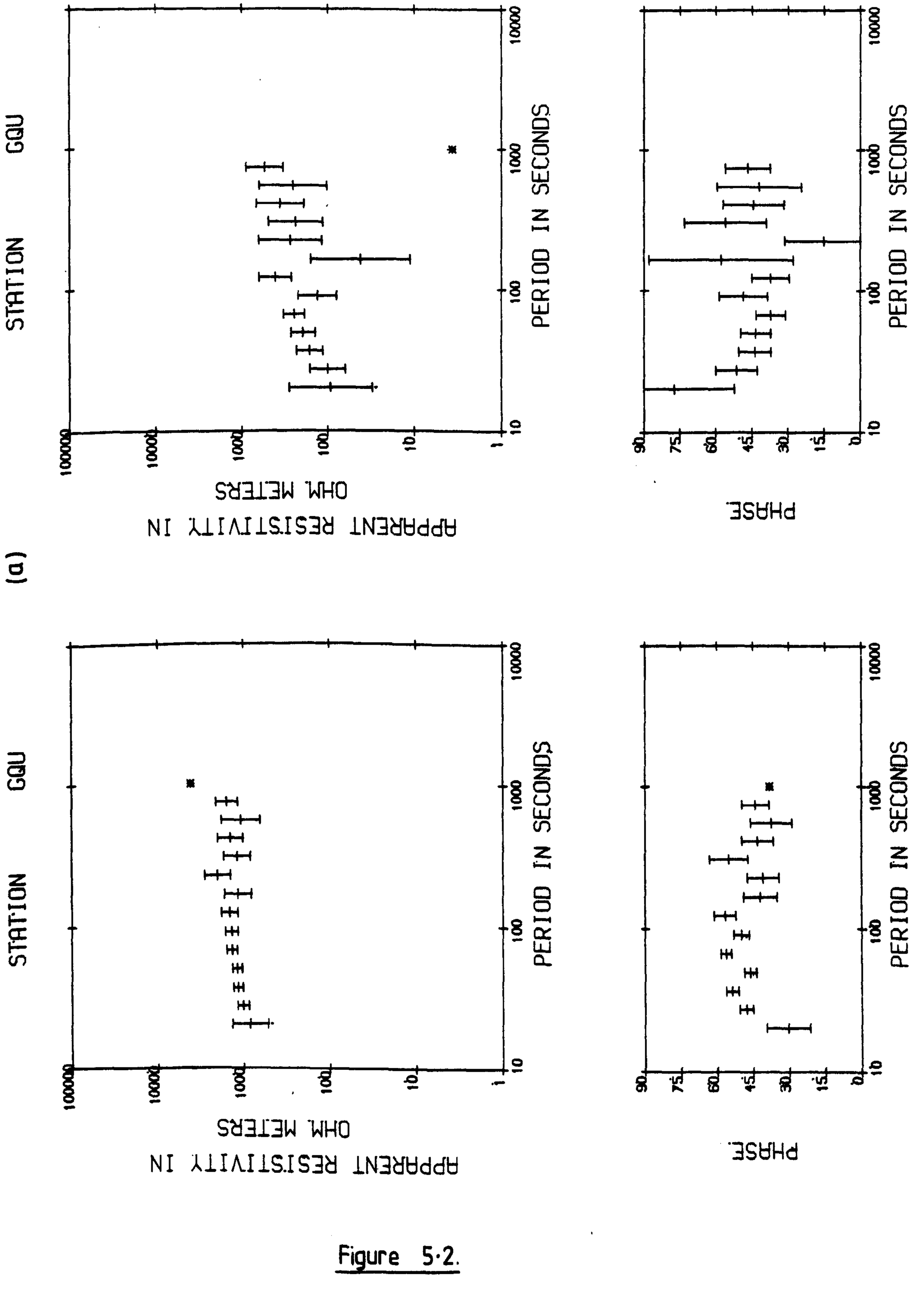
(a)
STATION GQU
APPARENT RESISTIVITY IN OHM METERS
PERIOD IN SECONDS
PHASE
PERIOD IN SECONDS
STATION GQU
APPARENT RESISTIVITY IN OHM METERS
PERIOD IN SECONDS
PHASE
PERIOD IN SECONDS

Figure 5·2.

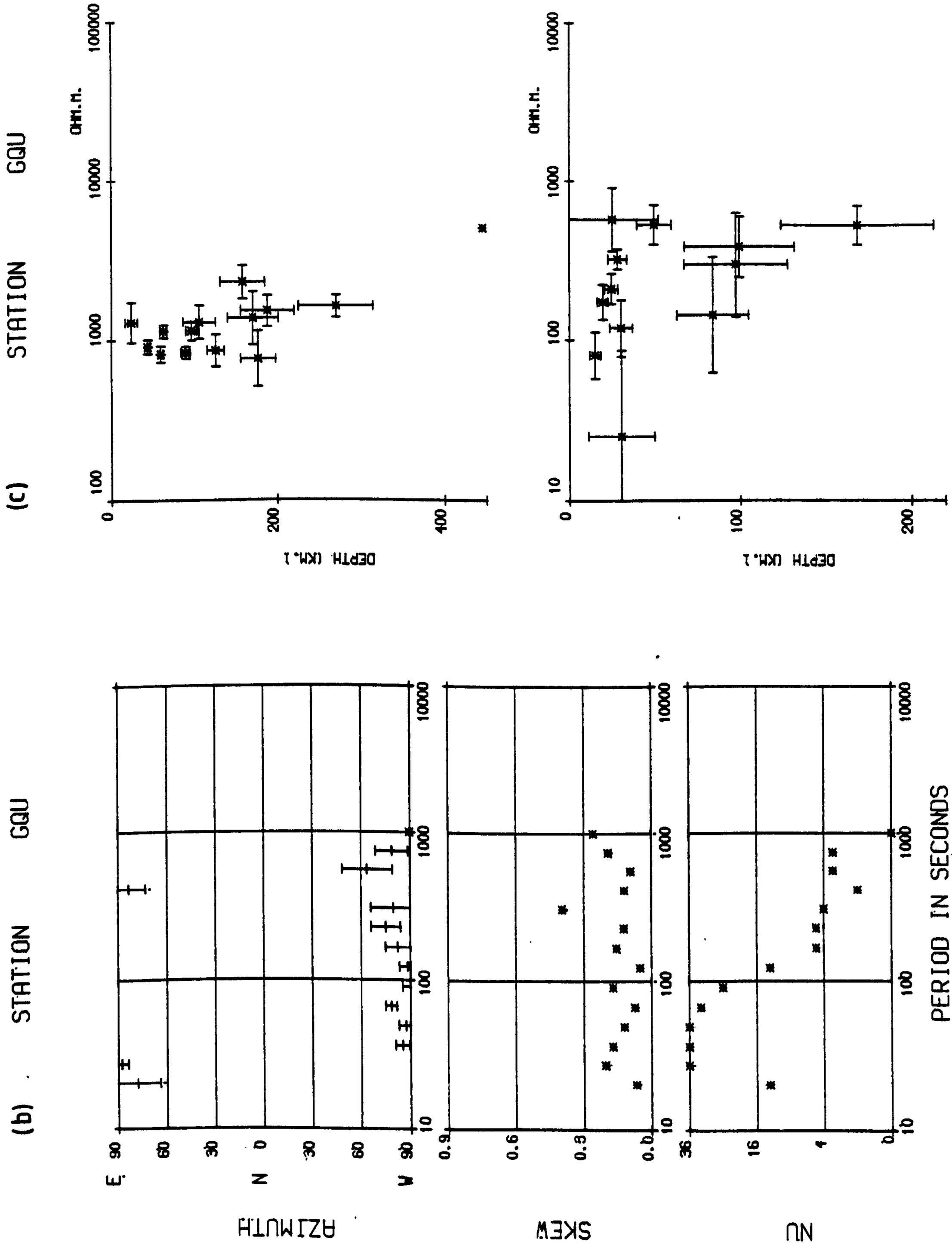
(c)
STATION GQU
OHM.M.
100000
10000
1000
100
0
200
400
DEPTH (KM.)
OHM.M.
10000
1000
100
10
0
100
200
DEPTH (KM.)
(b)
STATION GQU
10000
1000
100
10
E
90
60
30
0
30
60
90
N
W
AZIMUTH
0.9
0.6
0.3
0.0
SKEW
36
16
4
0
NU
PERIOD IN SECONDS

Figure 5·2.

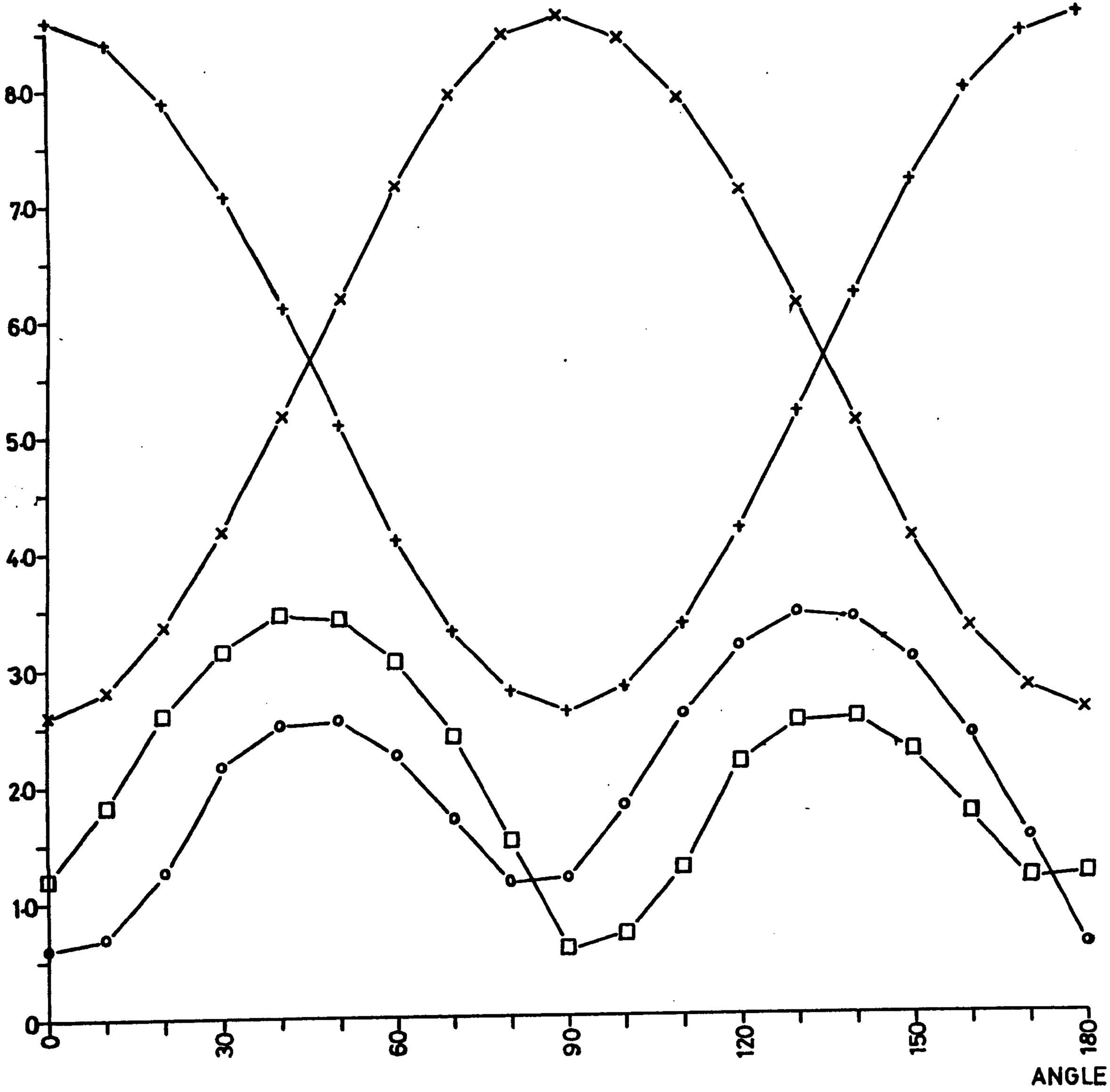
8.0
7.0
6.0
5.0
4.0
3.0
2.0
1.0
0
0
30
60
90
120
150
180
ANGLE
(d)
STATION GQU
T=95s
□ | Zxx |
× | Zxy |
+ | Zyx |
o | Zyy |

Figure 5.2.

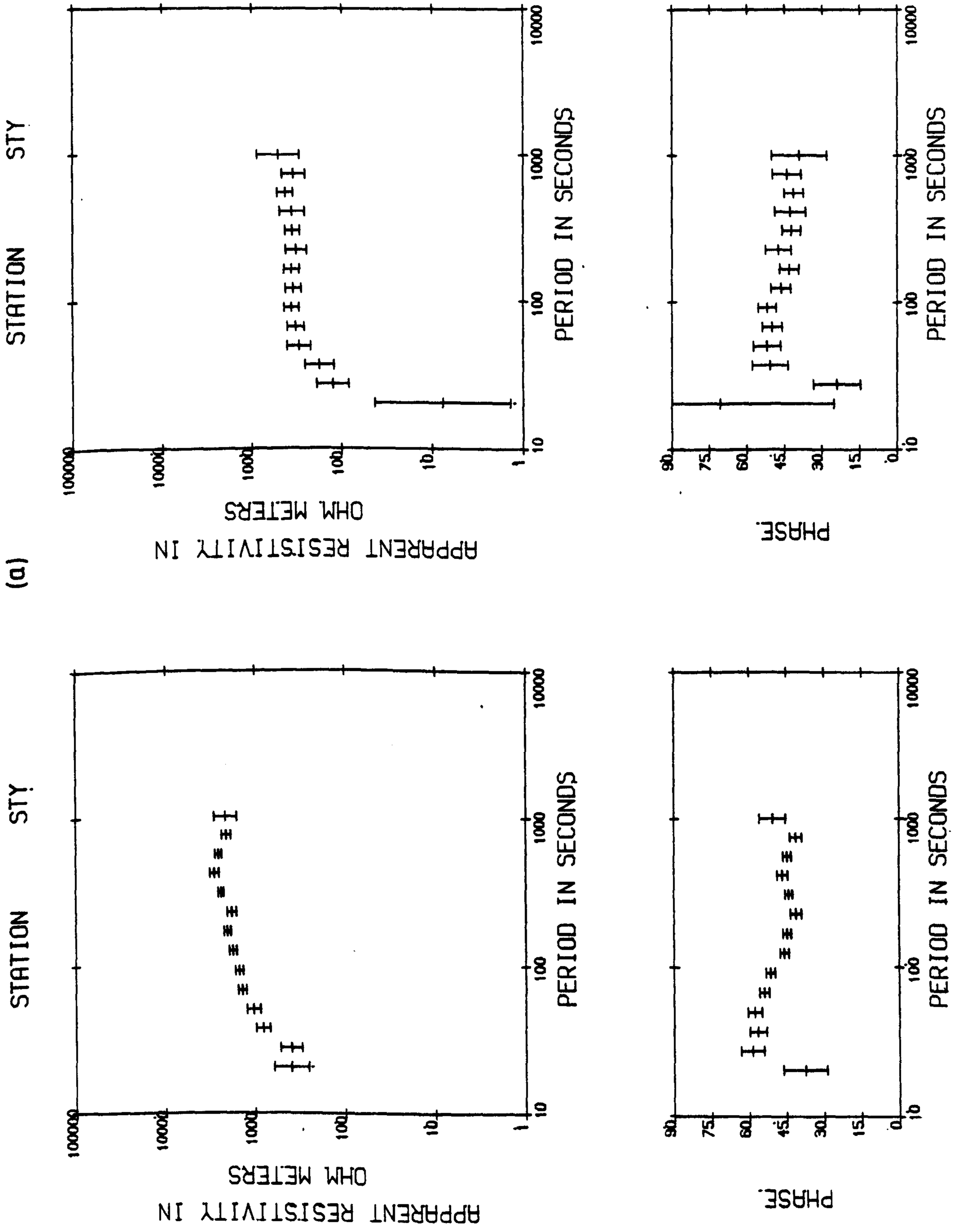
(a)
STATION STY
APPARENT RESISTIVITY IN OHM METERS
100000
10000
1000
100
10
1
PERIOD IN SECONDS
10000
1000
100
10
PHASE
90
75
60
45
30
15
0

Figure 5·3.

Figure 5.3.

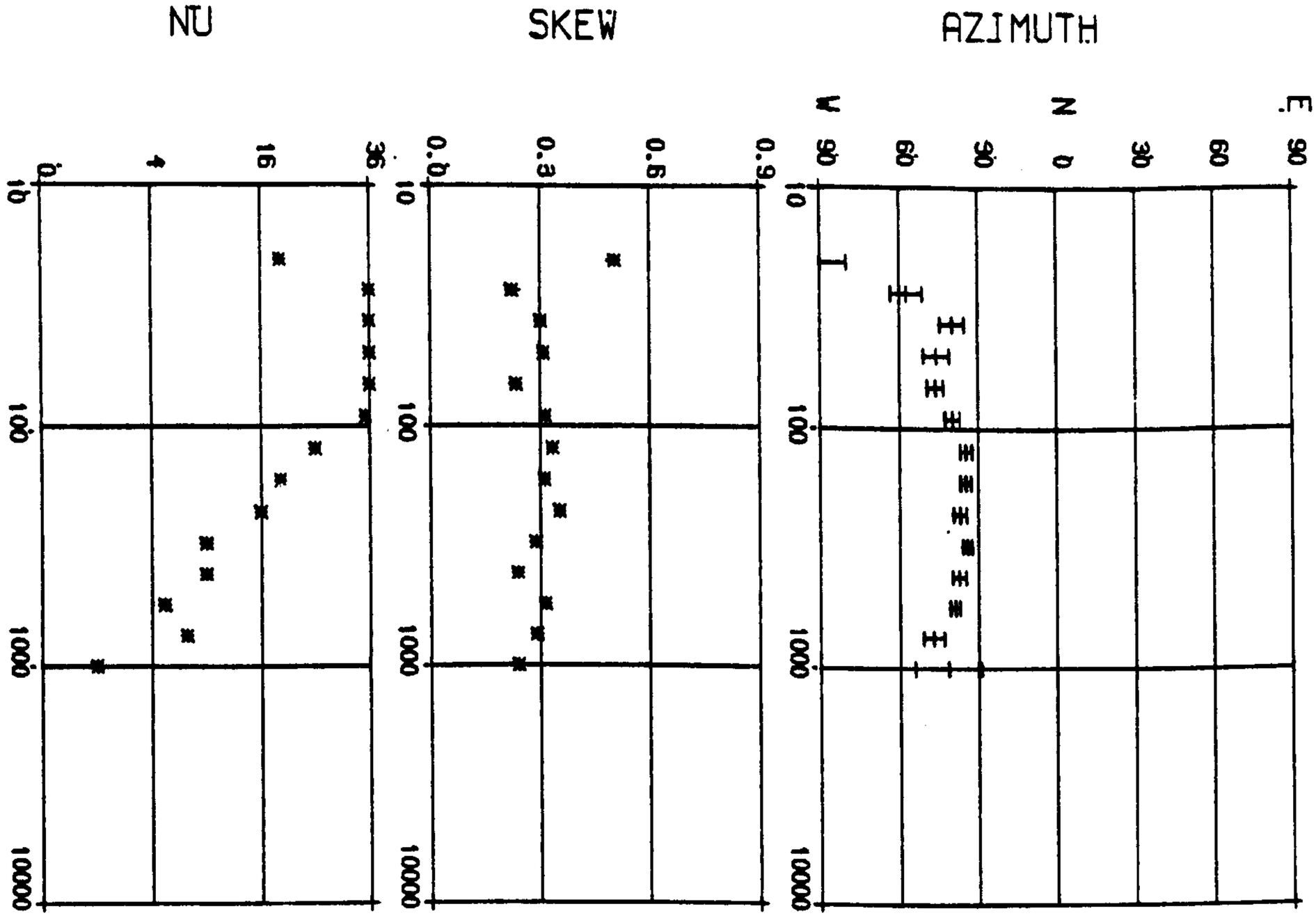
AZIMUTH
SKEW
NU
STATION STY
PERIOD IN SECONDS
(b)

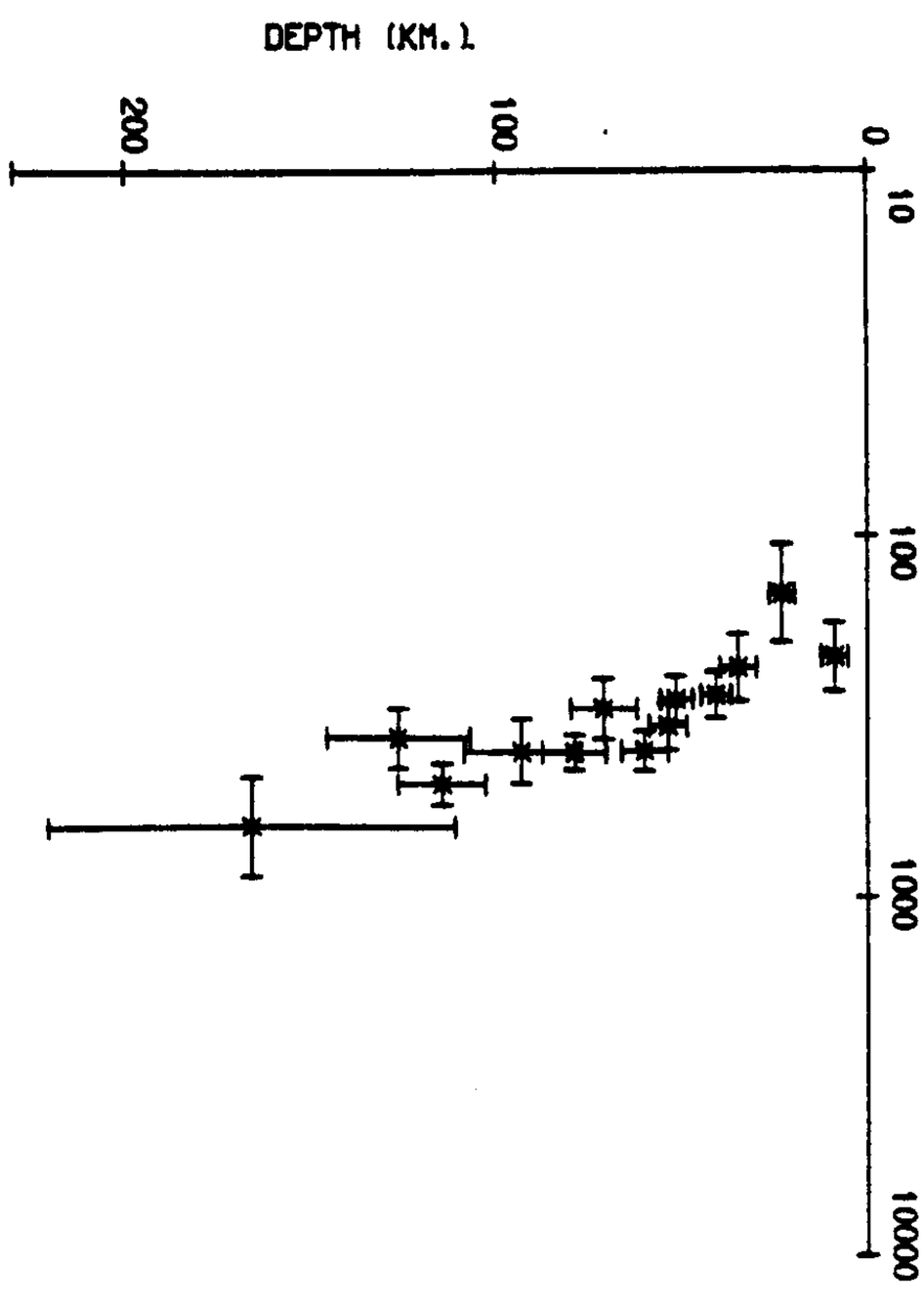
DEPTH (KM.)
OHM.M.
STATION STY
(c)

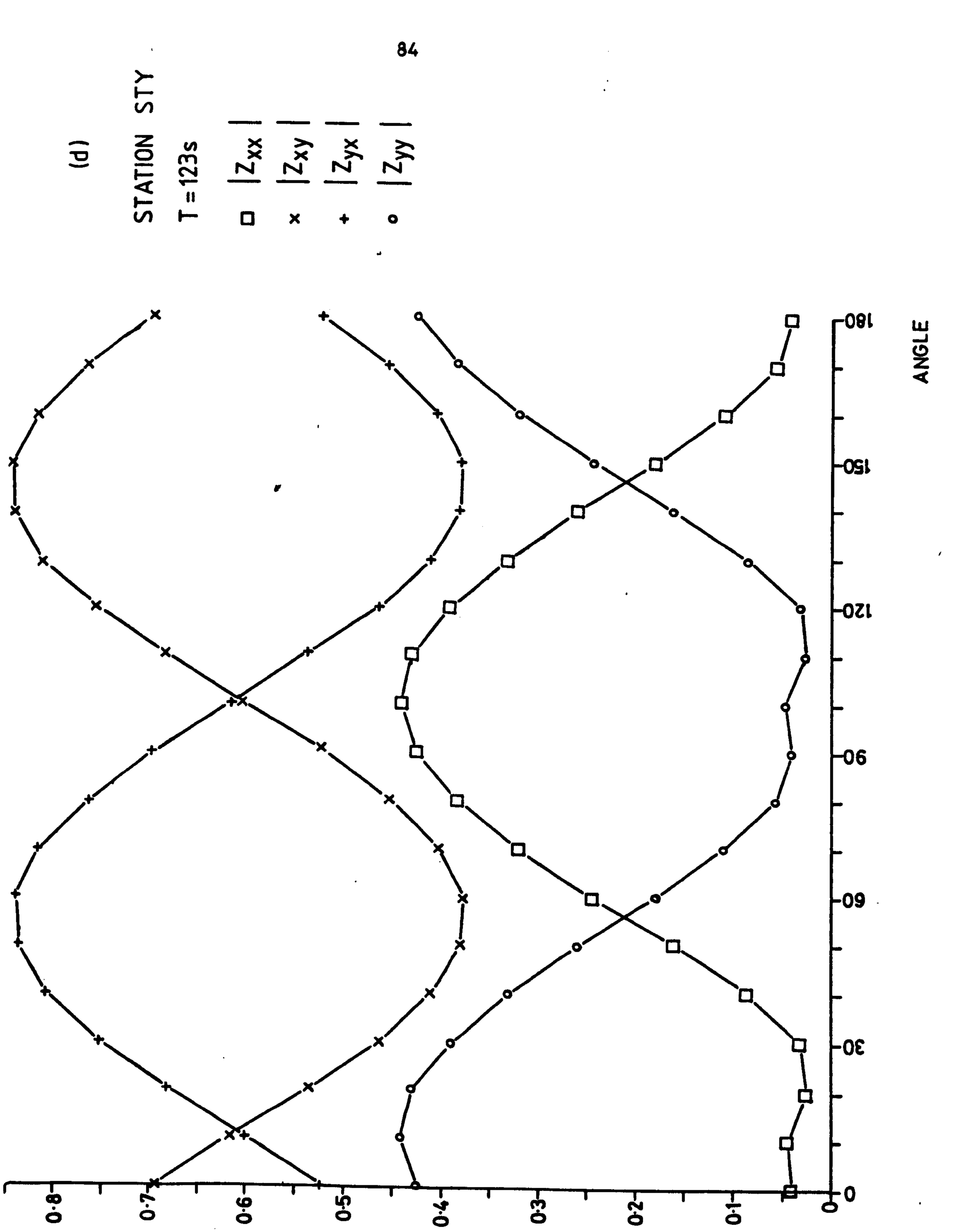
(d)
STATION STY
T=123s
□ |Zxx|
× |Zxy|
+ |Zyx|
o |Zyy|
ANGLE
180
150
120
06
09
30
0
0·8
0·7
0·6
0·5
0·4
0·3
0·2
0·1
0

Figure 5·3.

indicating reasonable two-dimensionality at the sites. This is supported by the variations of the impedance tensor elements with angle. At KLR, although the skew value is larger, the tensor element variation is also of reasonably two-dimensional character, however the differences in azimuth between the three sites do suggest that there may be local inhomogeneities in a general two-dimensional trend.

The Schmucker one-dimensional inversions for the Highland sites suggest a resistive structure extending to great depth beneath a more conducting zone in the upper thirty kilometres of the earth.

5.1.2:The Midland Valley.

The results from the Midland Valley demonstrate a considerable variation from Crieff (CRF, 5.4) in the north through Kinross (KRS, 5.5) to Penicuik (PEN, 5.6) in the south.

The maximum ρ_a curve has different characteristics at each site, the principal one being that at KRS it is an order of magnitude higher than at either CRF or PEN. The minimum curves do however all have the same order of magnitude of around 10-100Ω -m. PEN is in approximately the same situation relative to the Southern Uplands Fault as the sites of Jones (1977) at Forth and Saltoun. However, the results from these two sites (Jones and Hutton, 1979a) exhibit a steeper rise of the maximum ρ_a curve, from $\sim$20 Ω -m to$\sim$300Ω-m, over the same period range. This may well be indicative of some lateral variation in structure along the strike of the Midland Valley as well as across it. For example, the Pentland Hills extend into the valley between Penicuik and Forth.

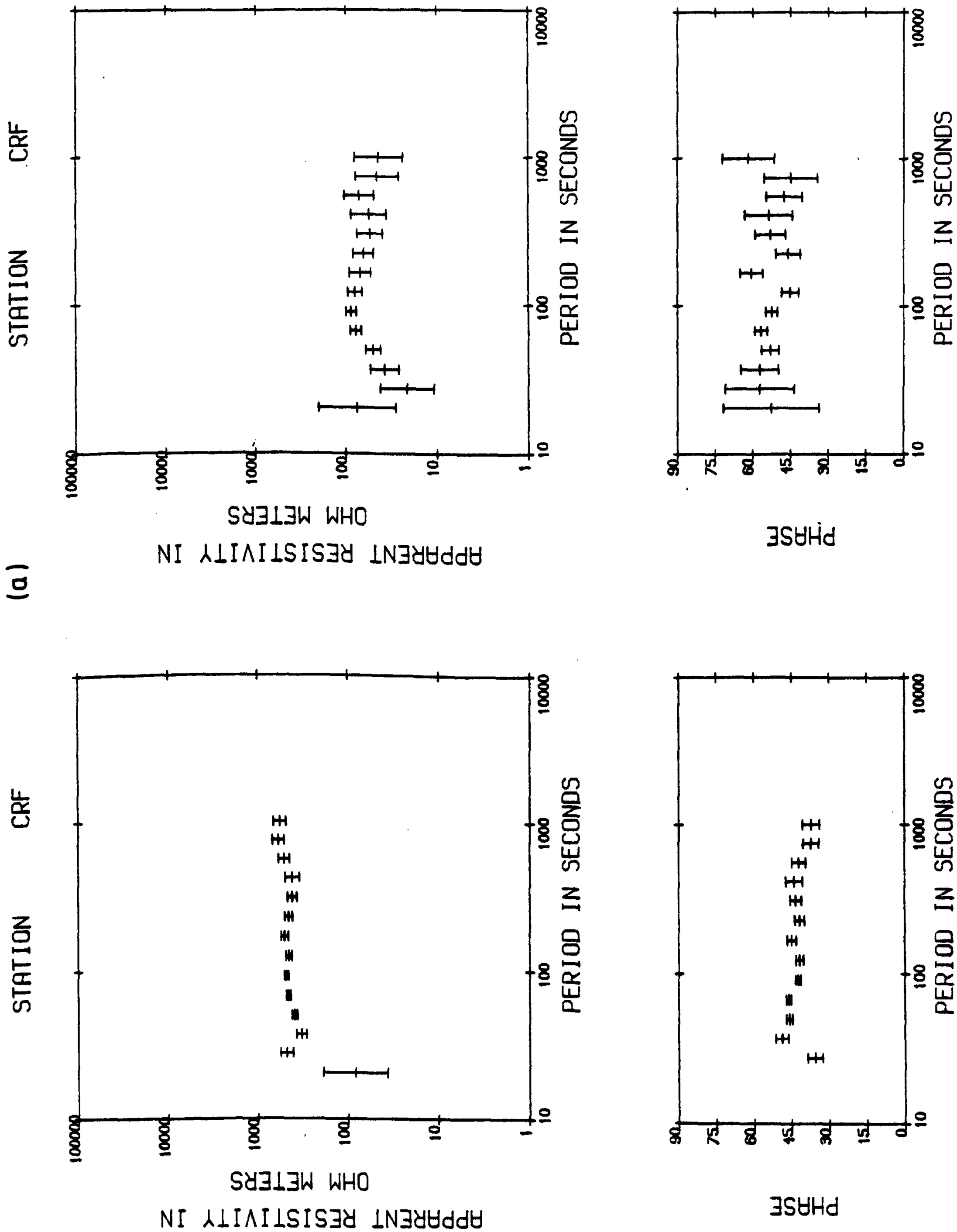
(a)
STATION CRF
APPARENT RESISTIVITY IN OHM METERS
100000
10000
1000
100
10
1
PERIOD IN SECONDS
10000
1000
100
10
PHASE
90
75
60
45
30
15
0

Figure 5·4.

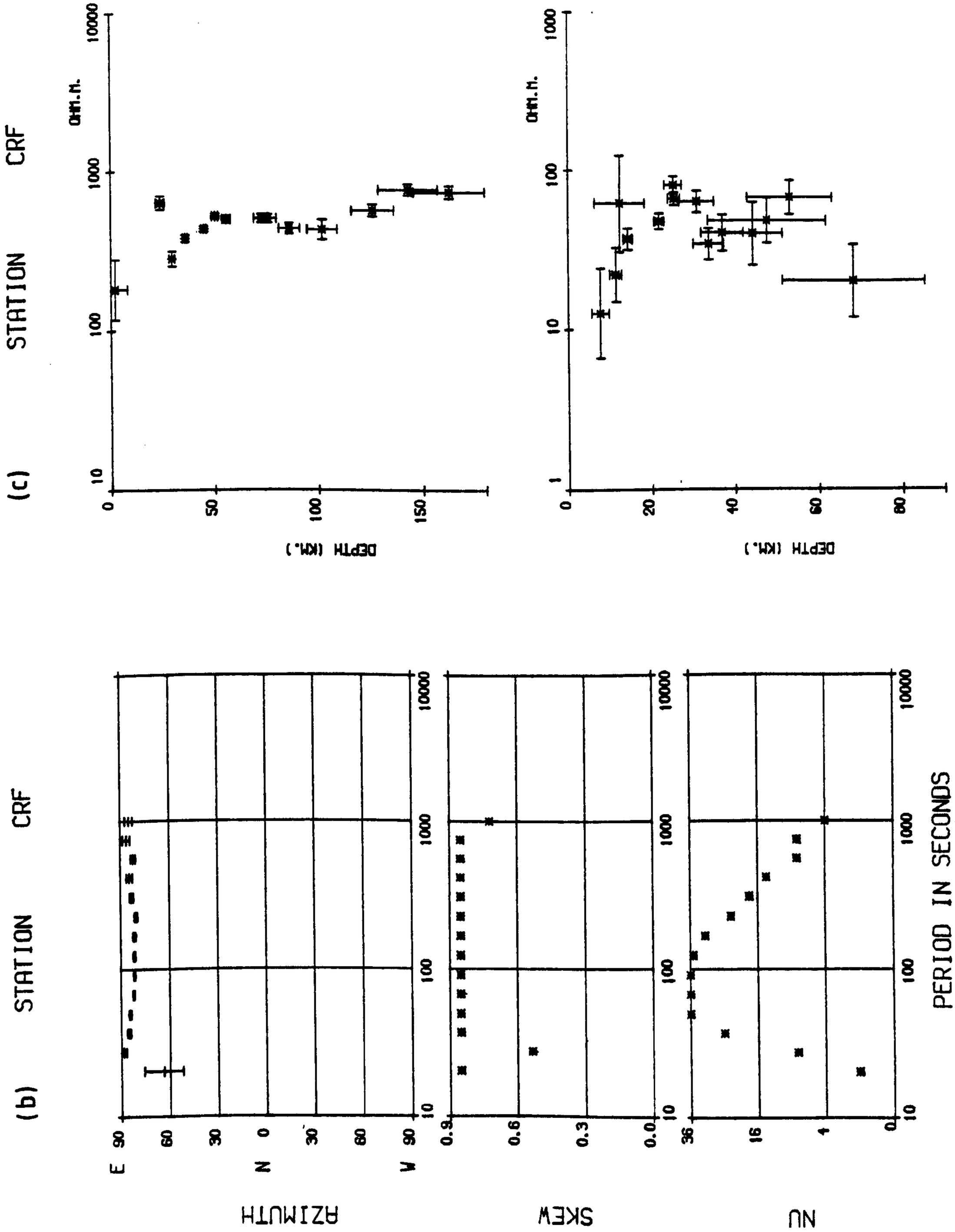
(c)
STATION CRF
OHM.M.
10000
1000
100
10
0
50
100
150
DEPTH (KM.)
1000
100
10
1
0
20
40
60
80
DEPTH (KM.)
(b)
STATION CRF
10000
1000
100
10
E 90
60
30
0
30
60
W 90
N
AZIMUTH
0.9
0.6
0.3
0.0
SKEW
36
16
4
0
NU
PERIOD IN SECONDS

Figure 5·4.

(d)

STATION CRF

T=166s

□ $|Z_{xx}|$ × $|Z_{xy}|$ + $|Z_{yx}|$ o $|Z_{yy}|$

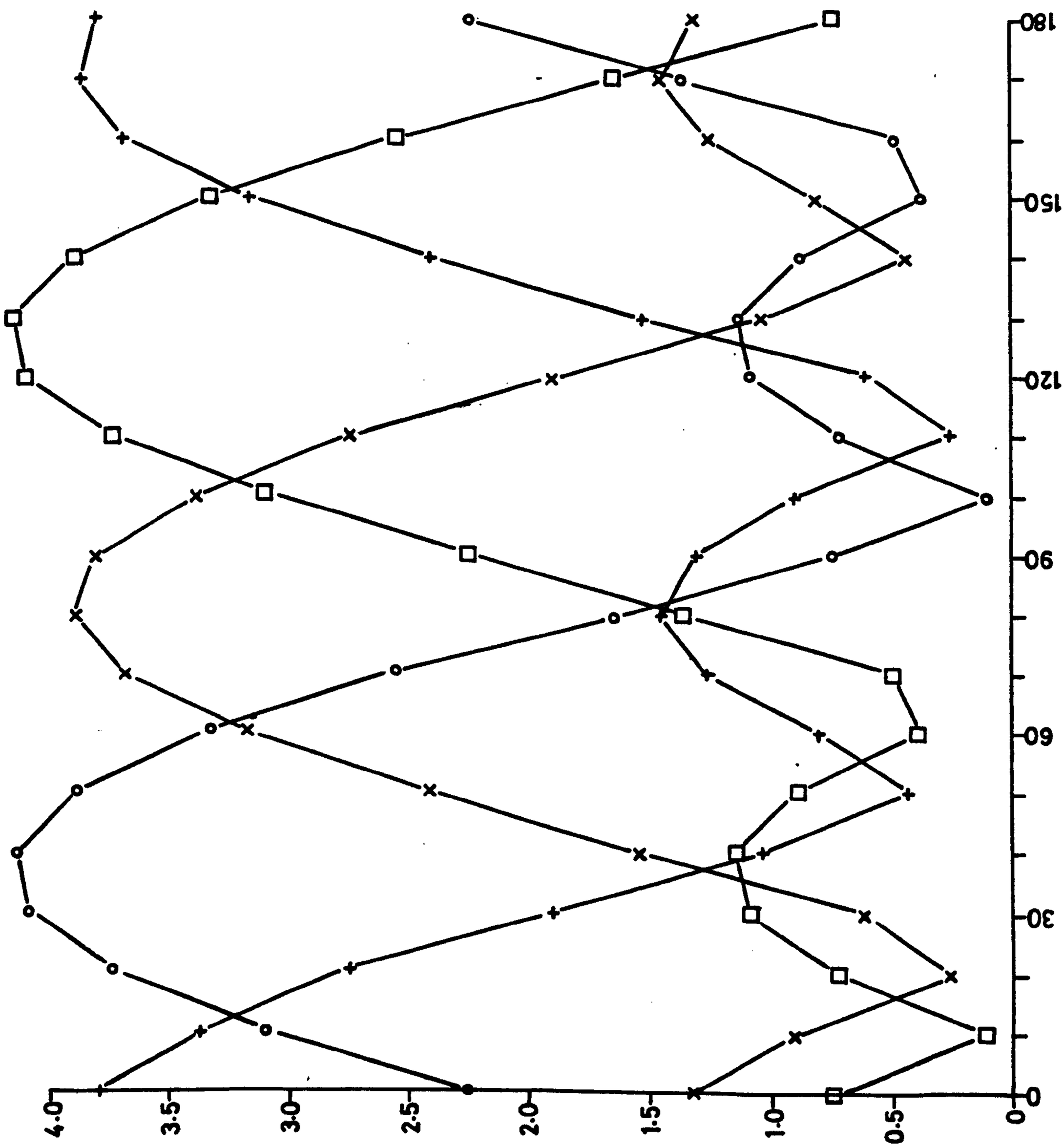

Figure 5·4.

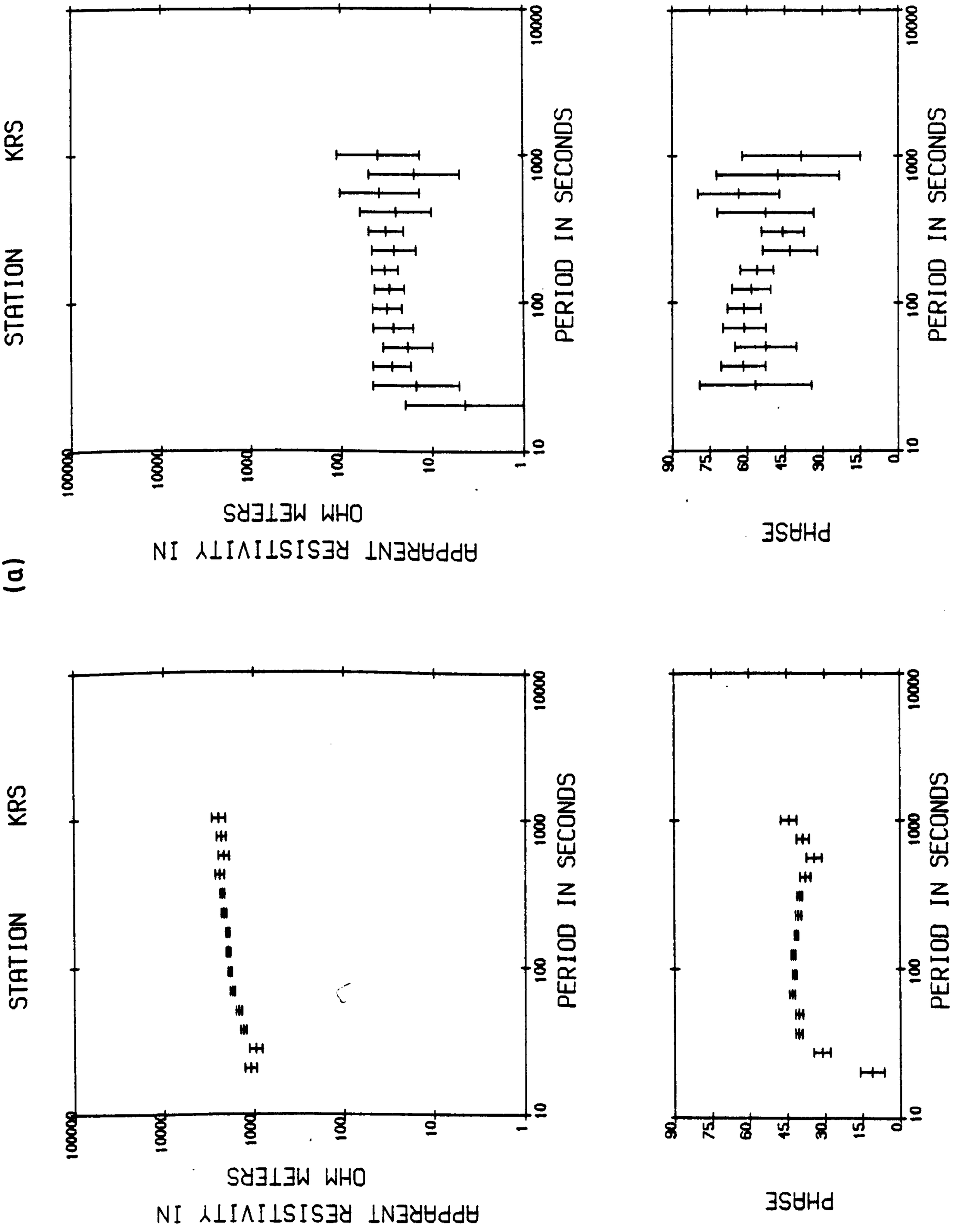
(a)
STATION KRS
APPARENT RESISTIVITY IN OHM METERS
100000
10000
1000
100
10
1
PERIOD IN SECONDS
10000
1000
100
10
PHASE
90
75
60
45
30
15
0

Figure 5·5.

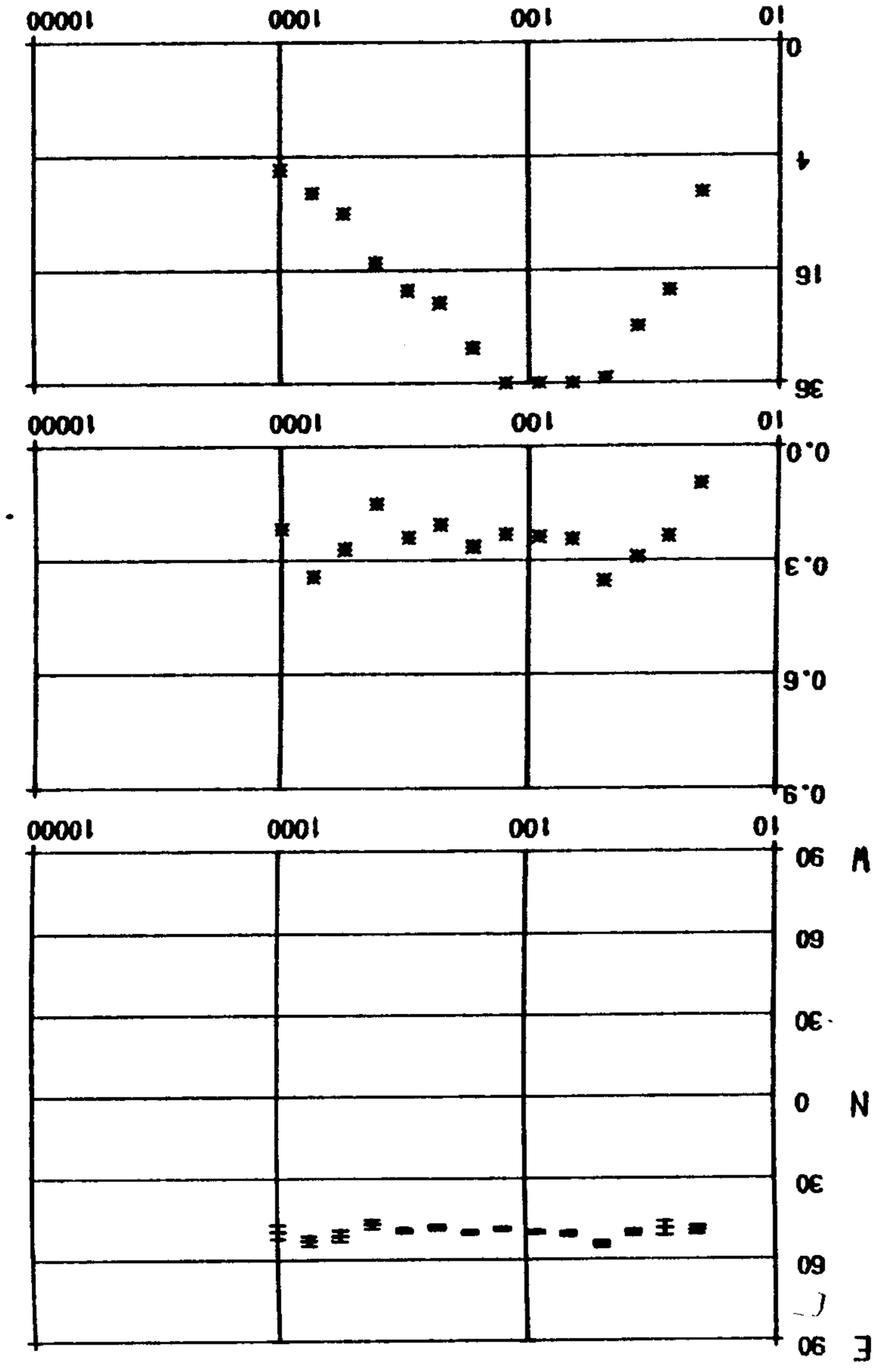
PERIOD IN SECONDS
10000
1000
100
10
0
4
16
36
NU
0.0
0.3
0.6
0.9
SKEW
W 90
60
30
0
N
30
60
E 90
AZIMUTH
(b)
STATION KRS

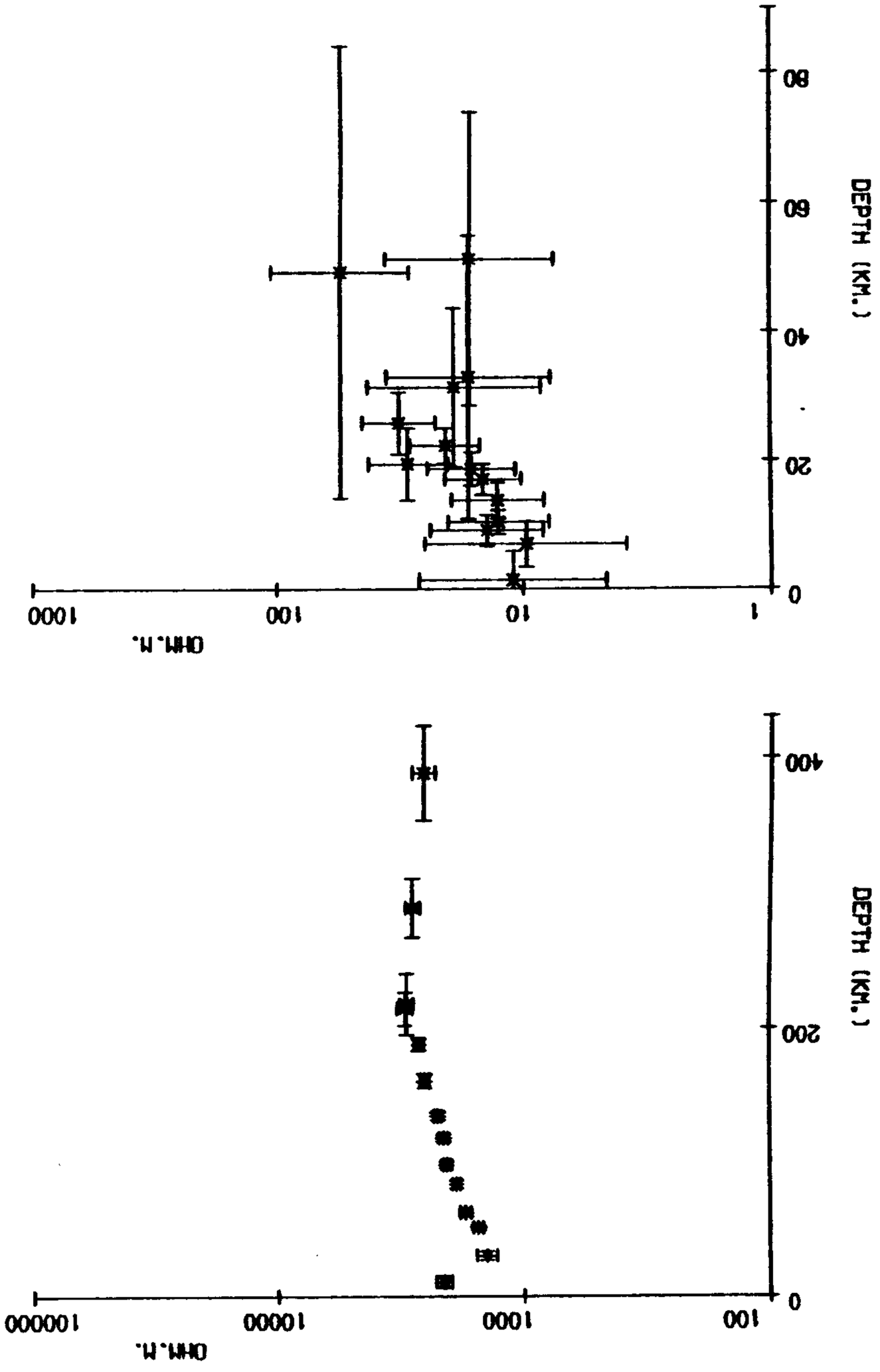
80
60
40
20
0
DEPTH (KM.)
1000
100
10
1
OHM.M.
90
400
200
0
DEPTH (KM.)
100000
10000
1000
100
OHM.M.
(c)
STATION KRS

Figure 5·5.

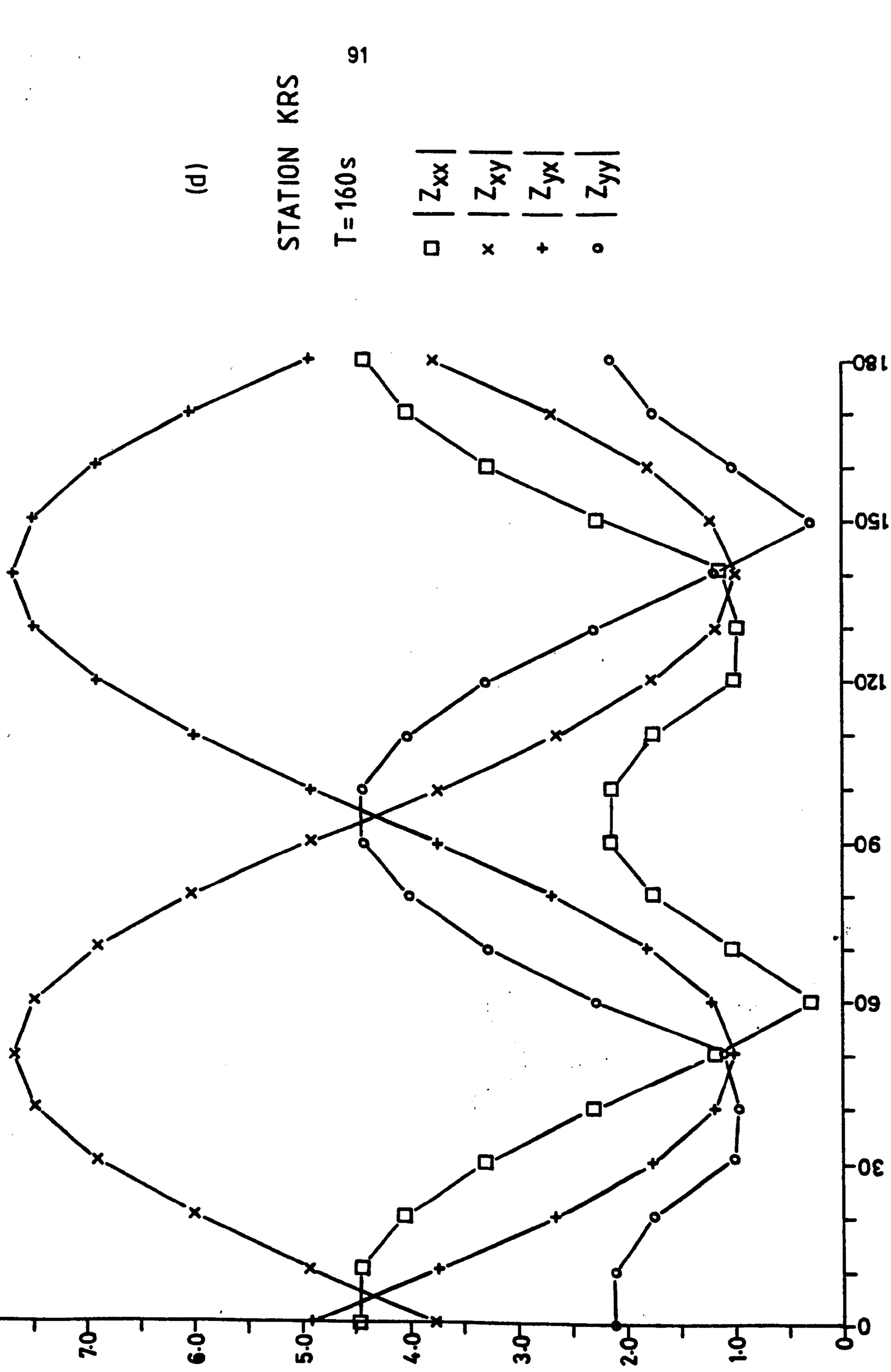
(d)
STATION KRS
T=160s
□ |Zxx|
× |Zxy|
+ |Zyx|
o |Zyy|
ANGLE
180
150
120
06
09
30
0
8.0
7.0
6.0
5.0
4.0
3.0
2.0
1.0
0

Figure 5·5.

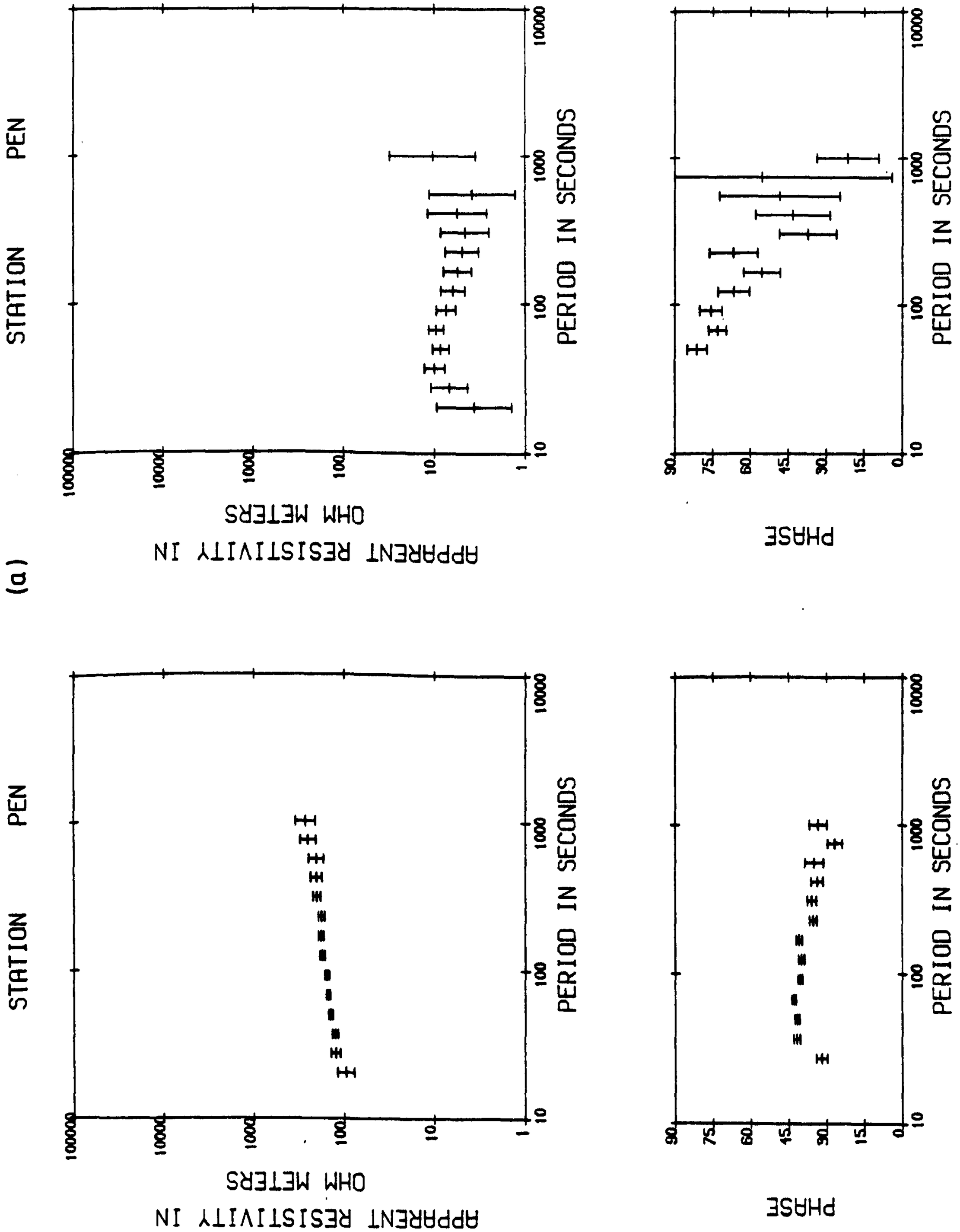
(a)
STATION
PEN
APPARENT RESISTIVITY IN
OHM METERS
100000
10000
1000
100
10
1
PERIOD IN SECONDS
10000
1000
100
10
PHASE
90
75
60
45
30
15
0
STATION
PEN
APPARENT RESISTIVITY IN
OHM METERS
PERIOD IN SECONDS
PHASE

Figure 5·6.

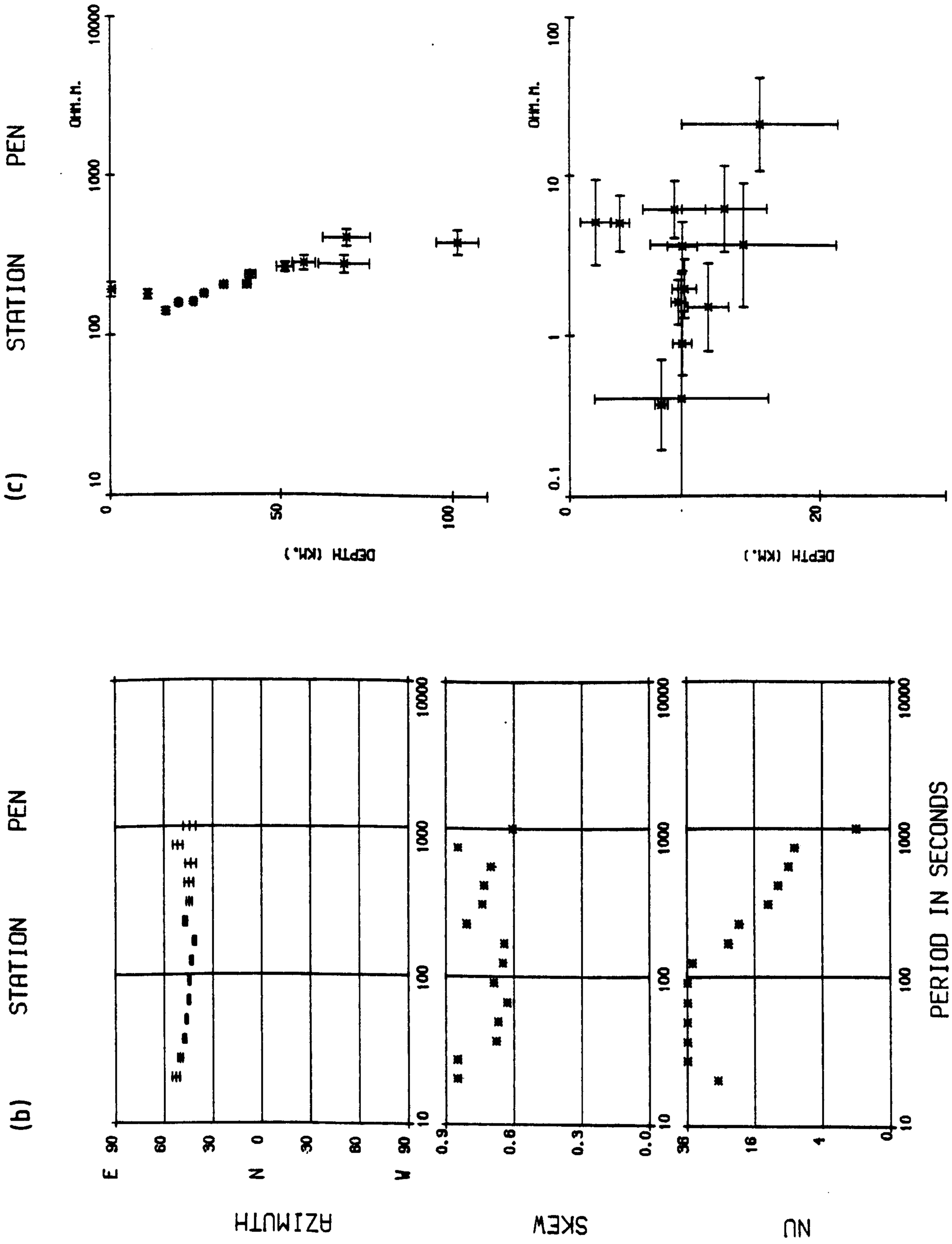
(c)
STATION
PEN
OHM.M.
10000
1000
100
10
0
50
100
DEPTH (KM.)
OHM.M.
100
10
1
0.1
0
20
DEPTH (KM.)
(b)
STATION
PEN
10000
1000
100
10
E 90
60
30
0
30
60
W 90
N
AZIMUTH
0.9
0.6
0.3
0.0
SKEW
98
16
4
0
NU
PERIOD IN SECONDS

Figure 5·6.

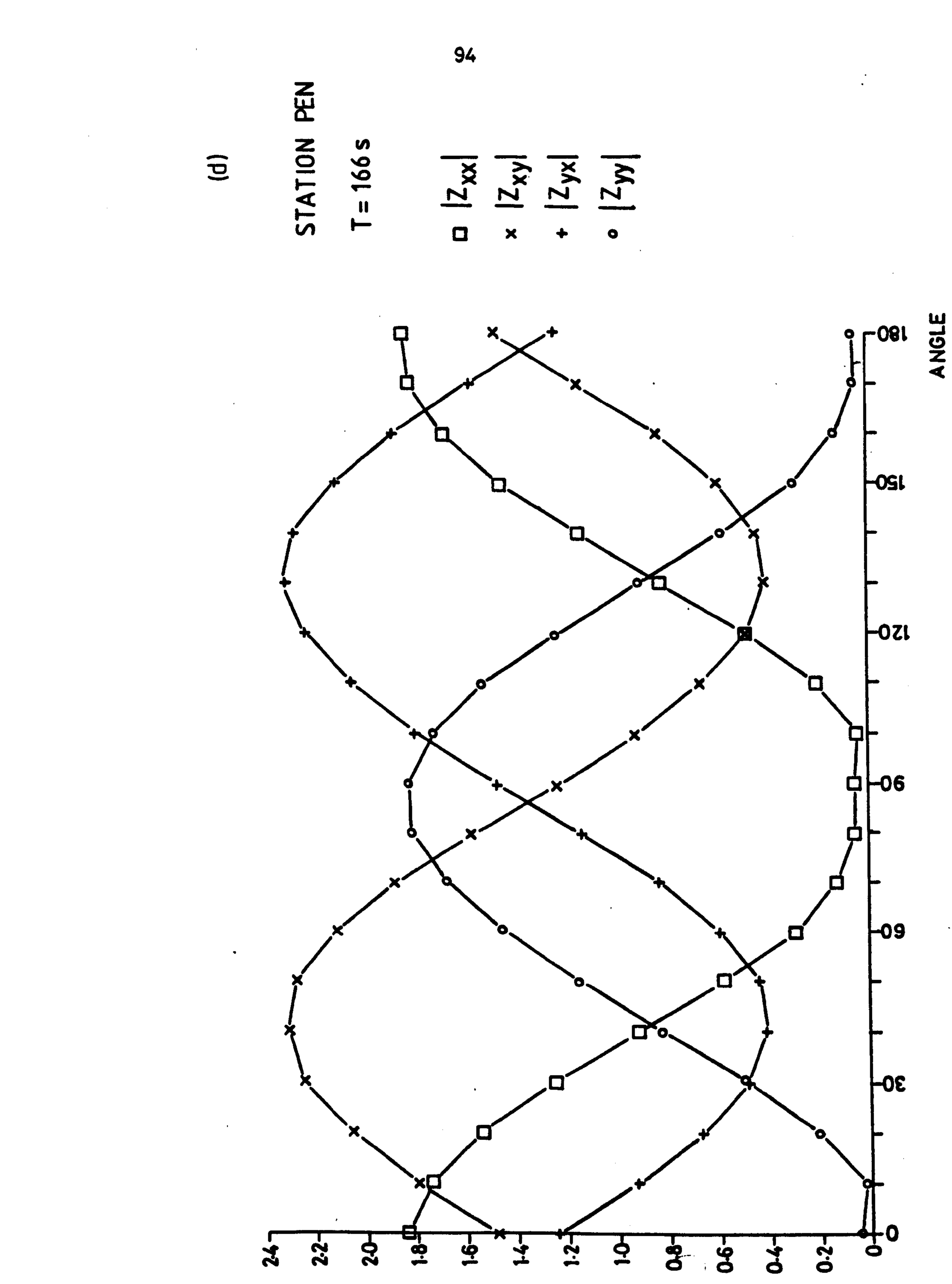
(d)
STATION PEN
T = 166 s
□ |Zxx|
× |Zxy|
+ |Zyx|
o |Zyy|
ANGLE
180
150
120
90
60
30
0
2·4
2·2
2·0
1·8
1·6
1·4
1·2
1·0
0·8
0·6
0·4
0·2
0

Figure 5·6.

At CRF and PEN which are relatively close to the two principal faults the value of skew is high enough to suggest three-dimensionality. At KRS however, both the skew and the variation of the impedance tensor with angle suggest two-dimensionality.

The one-dimensional inversions also show the variation across the Midland Valley. Relatively conducting structures are indicated beneath CRF and PEN, whilst at KRS the inversion reaches a depth of 400 km, suggesting a much more resistive structure.

5.1.3:The Southern Uplands.

Although some important differences do exist in the results from Borthwickbrae (BOW, 5.10), Earlyburn (EAR, 5.7), Peebles (PEE, 5.8) and Yarrow (YAR, 5.9), in general there is considerable similarity between the results from the four sites. The maximum and minimum ρ_a curves have values of approximately 200 Ω-m and 40Ω-m respectively, the maximum value having a slight decrease with period at the two most southerley sites YAR and BOW. The phase curves are also similar at the four sites, those at PEE being relatively scattered compared to the other three sites. These results agree very well with those obtained by Jones as generally representative of the Southern Uplands as a whole as far south as Newcastleton in the Borders (Jones, 1977; Jones and Hutton, 1979a).

The principal differences between the sites are in the azimuthal angles. At EAR and PEE these are between N15°W-S15°E and N-S whilst the orientation is more E-W at YAR and BOW. The effect of this is to change the relative magnitudes of the $\rho_{//}$

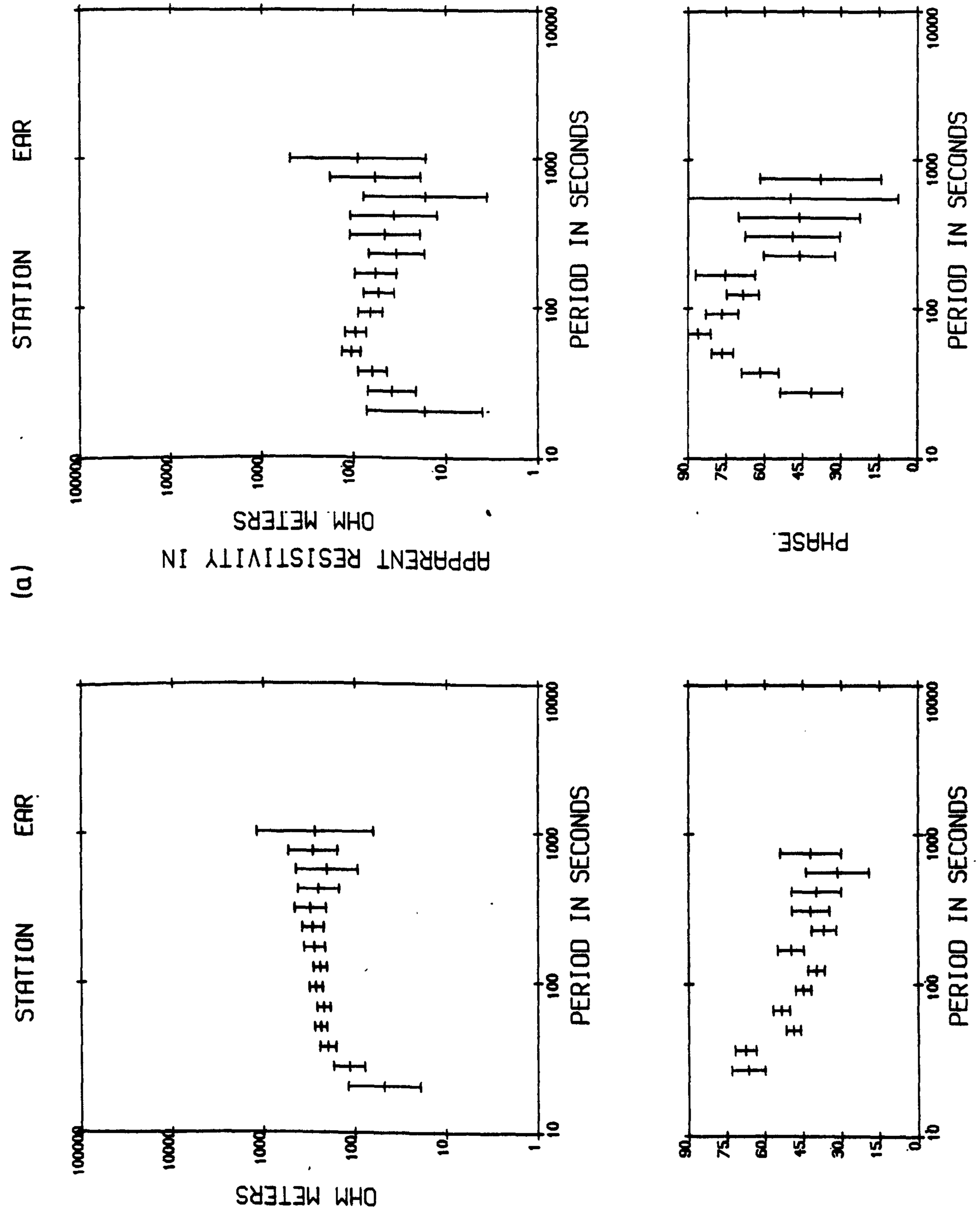
(a)
STATION EAR
APPARENT RESISTIVITY IN OHM METERS
100000
10000
1000
100
10
1
PERIOD IN SECONDS
10000
1000
100
10
PHASE
90
75
60
45
30
15
0
STATION EAR
APPARENT RESISTIVITY IN OHM METERS
PERIOD IN SECONDS
PHASE

Figure 5·7.

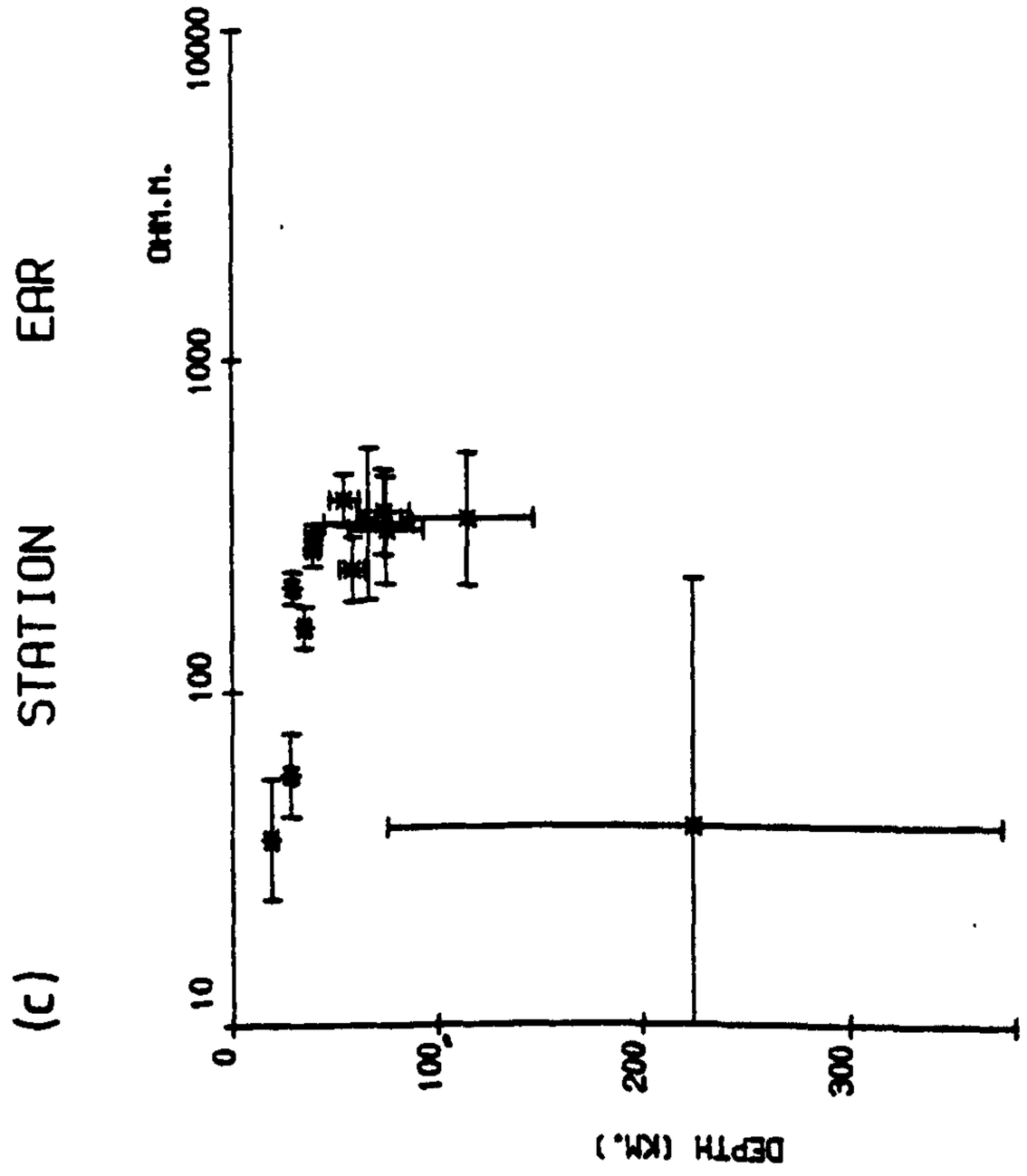
EAR
STATION
(c)
OHM.M.
10000
1000
100
10
0
100
200
300
DEPTH (KM.)

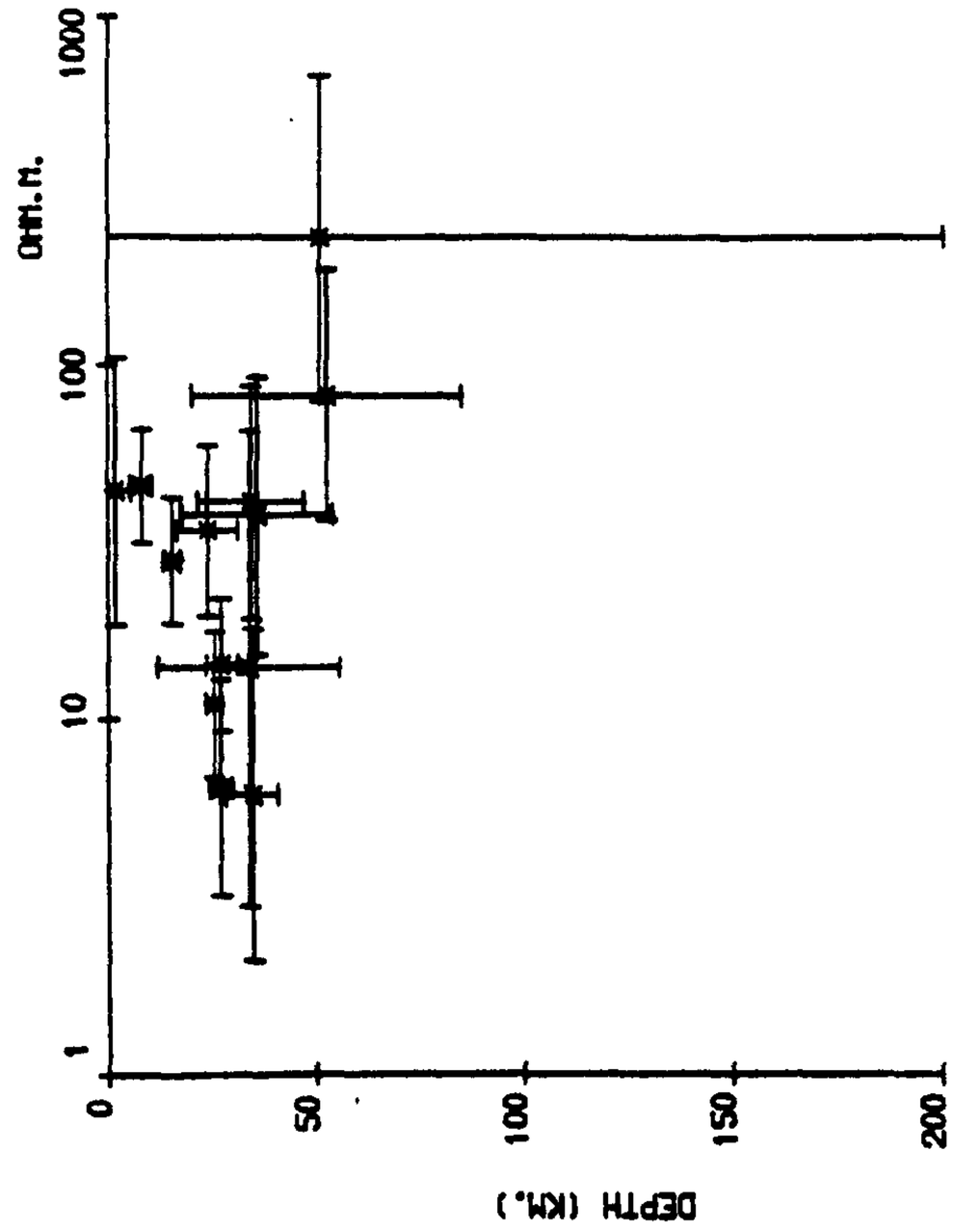
OHM.M.
1000
100
10
1
0
50
100
150
200
DEPTH (KM.)

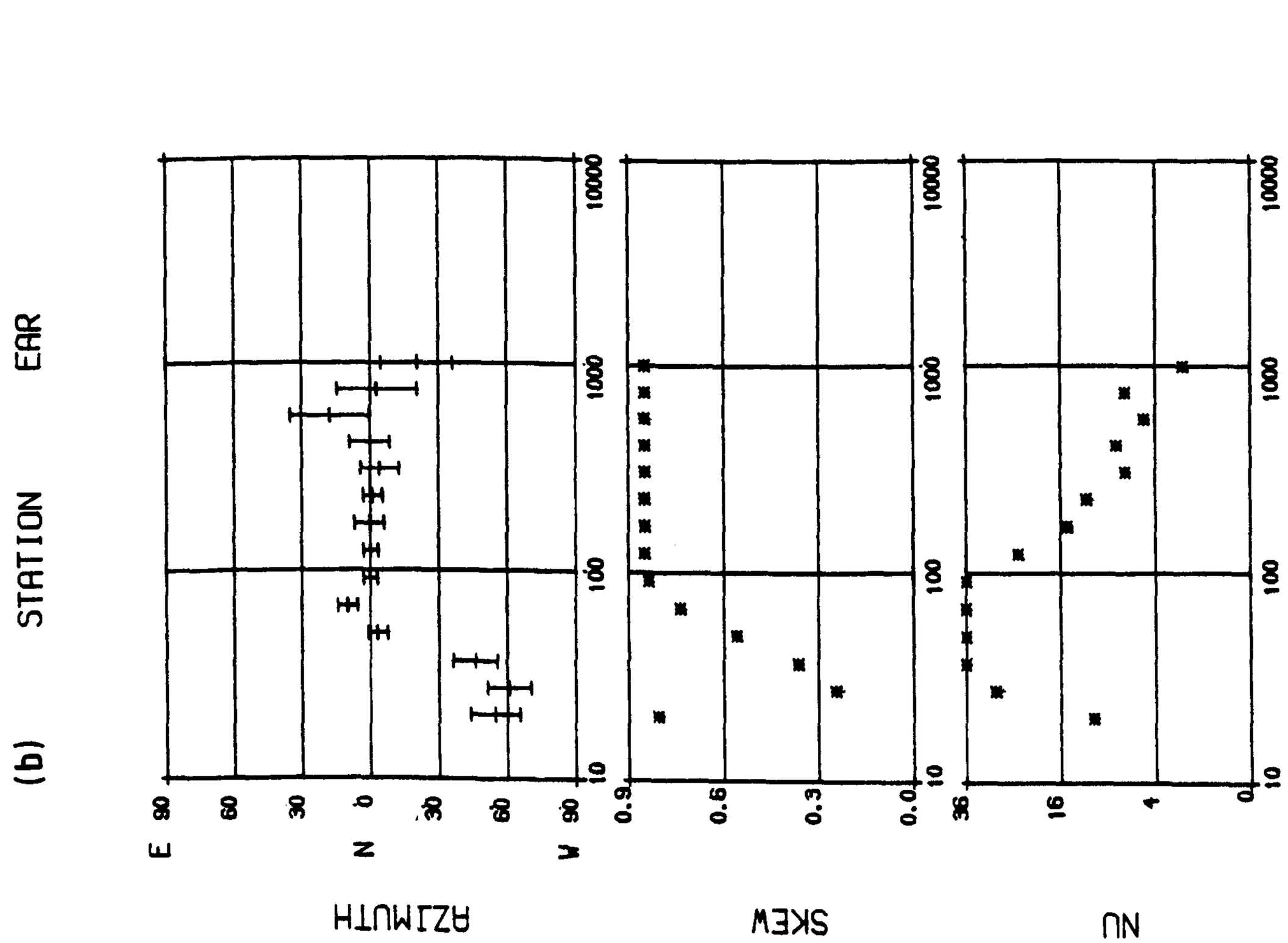
STATION
EAR
(b)
10000
1000
100
10
E 90
60
30
0
30
60
W 90
AZIMUTH
0.9
0.6
0.3
0.0
SKEW
36
16
4
0
NU
PERIOD IN SECONDS

Figure 5·7.

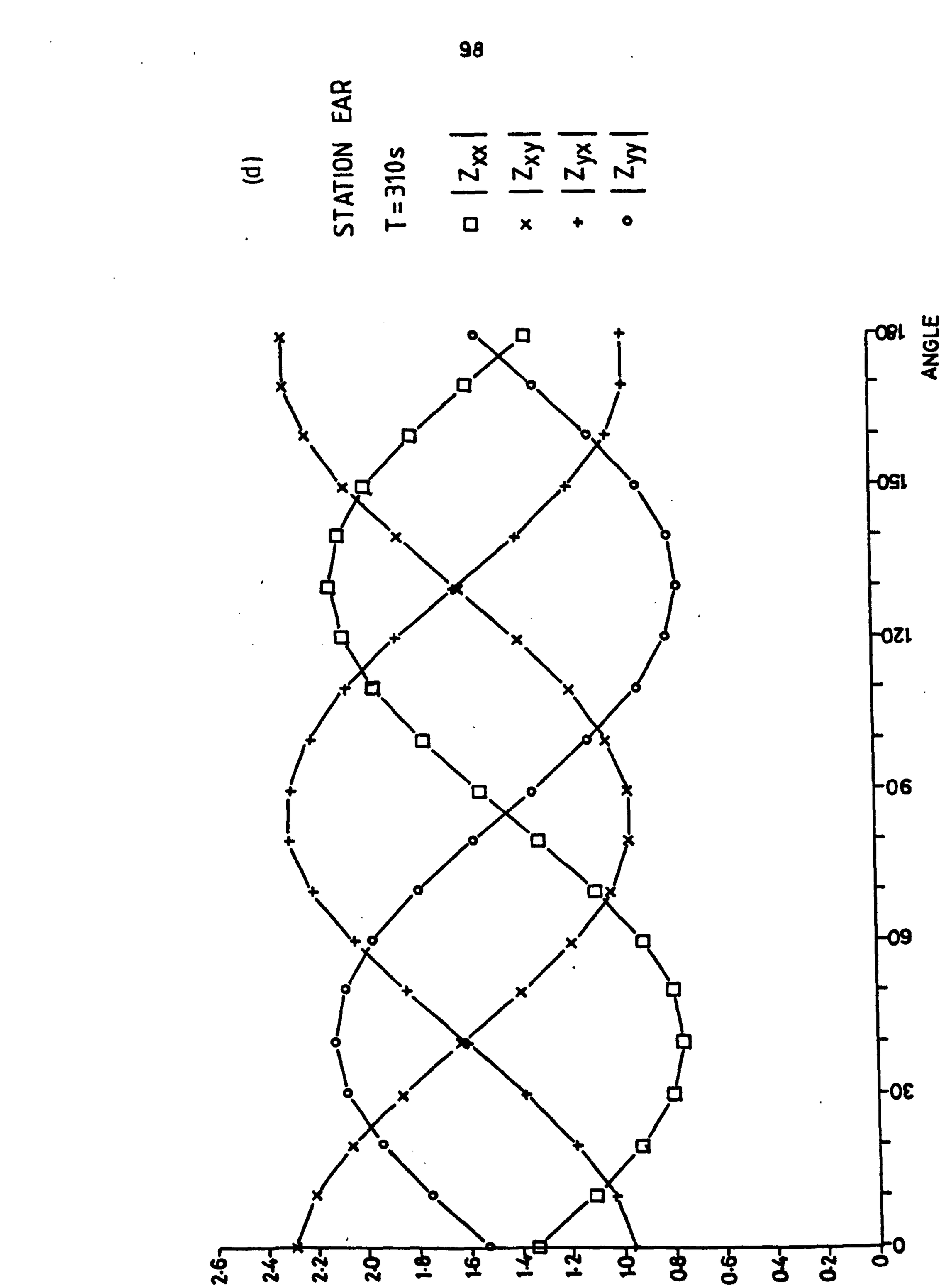
(d)
STATION EAR
T=310s
□ |Zxx|
× |Zxy|
+ |Zyx|
° |Zyy|
ANGLE
180
150
120
90
60
30
0
2.6
2.4
2.2
2.0
1.8
1.6
1.4
1.2
1.0
0.8
0.6
0.4
0.2
0

Figure 5·7.

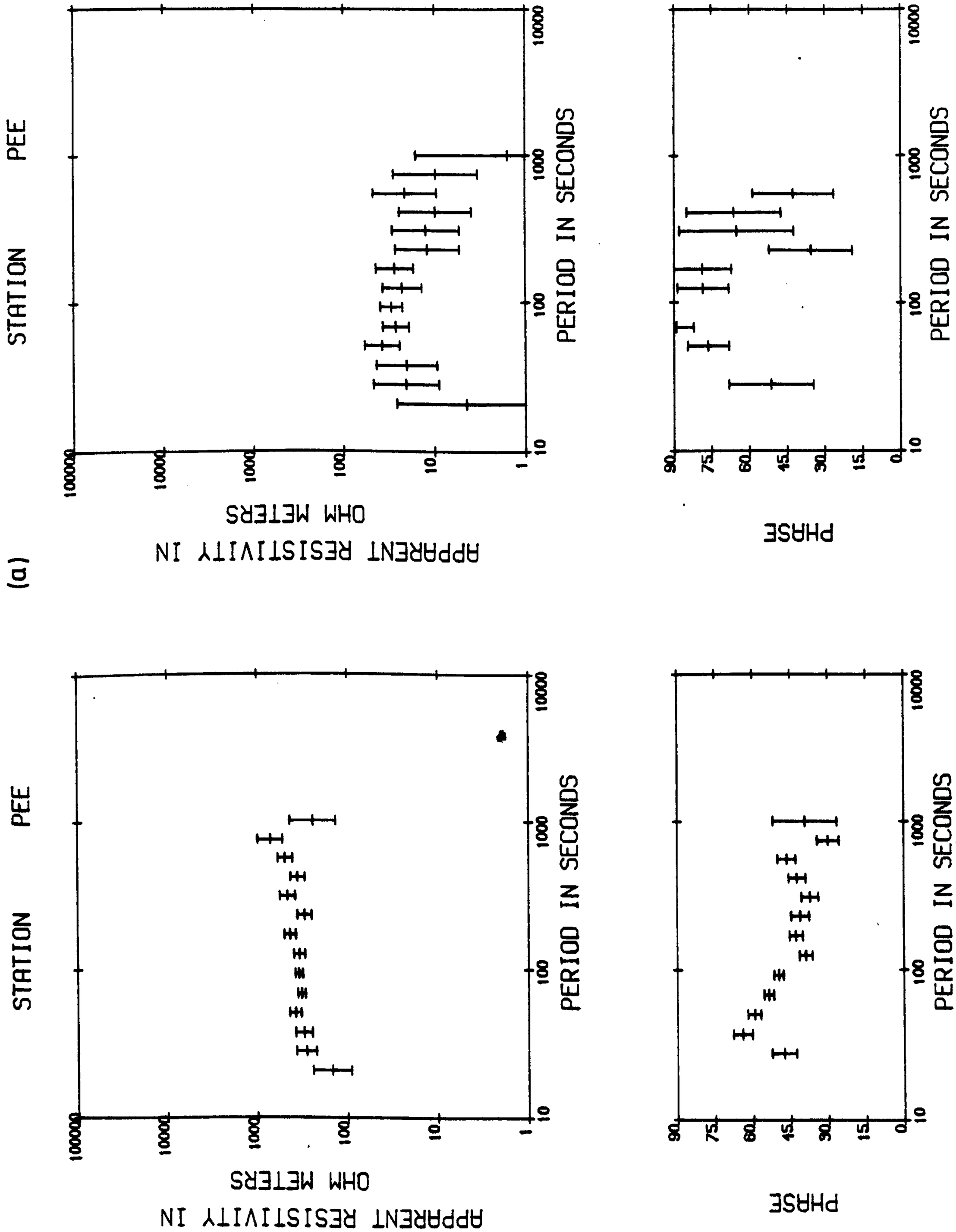
(a)
STATION PEE
APPARENT RESISTIVITY IN OHM METERS
100000
10000
1000
100
10
1
PERIOD IN SECONDS
10
100
1000
10000
PHASE
90
75
60
45
30
15
0

Figure 5·8.

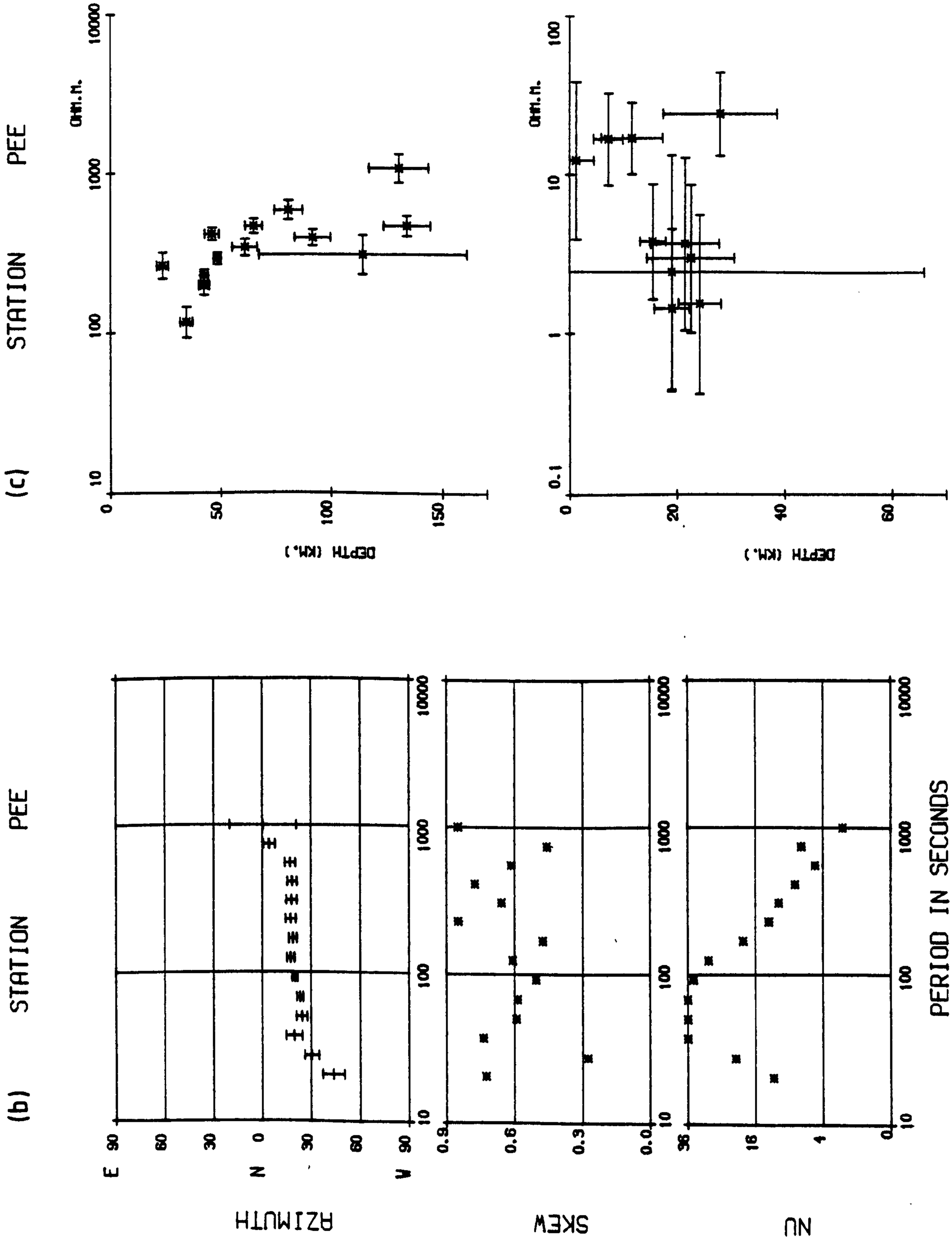
PEE
STATION
(c)
OHM.M.
10000
1000
100
10
0
50
100
150
DEPTH (KM.)
OHM.M.
100
10
1
0.1
0
20
40
60
DEPTH (KM.)
STATION
PEE
(b)
E 90
60
30
0
W 90
60
30
0
AZIMUTH
0.9
0.6
0.3
0.0
SKEW
90
10
1
0
NU
PERIOD IN SECONDS

Figure 5·8.

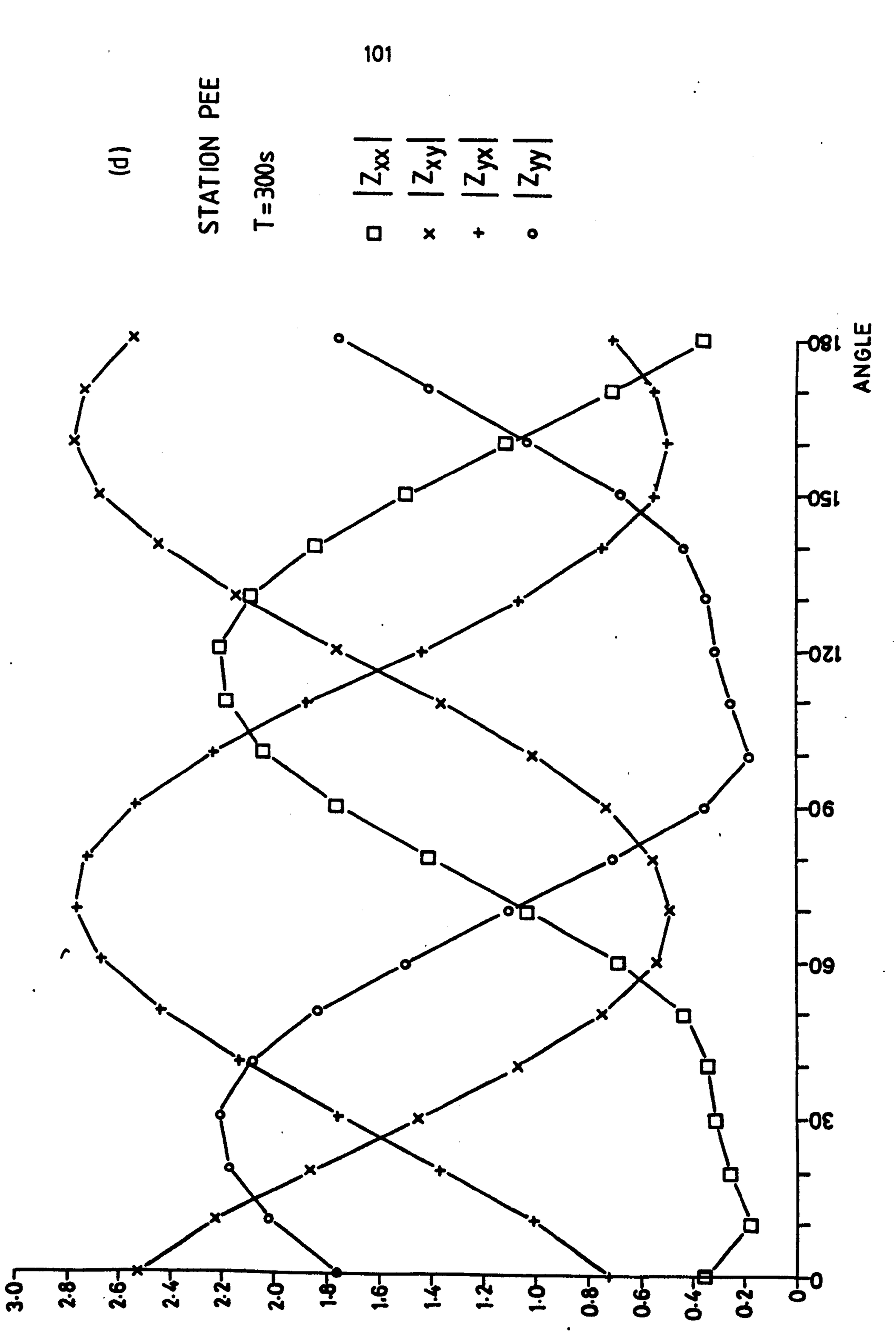
(d)
STATION PEE
T=300s
□ |Zxx|
× |Zxy|
+ |Zyx|
o |Zyy|
ANGLE
180
150
120
90
60
30
0
3.0
2.8
2.6
2.4
2.2
2.0
1.8
1.6
1.4
1.2
1.0
0.8
0.6
0.4
0.2
0

Figure 5·8.

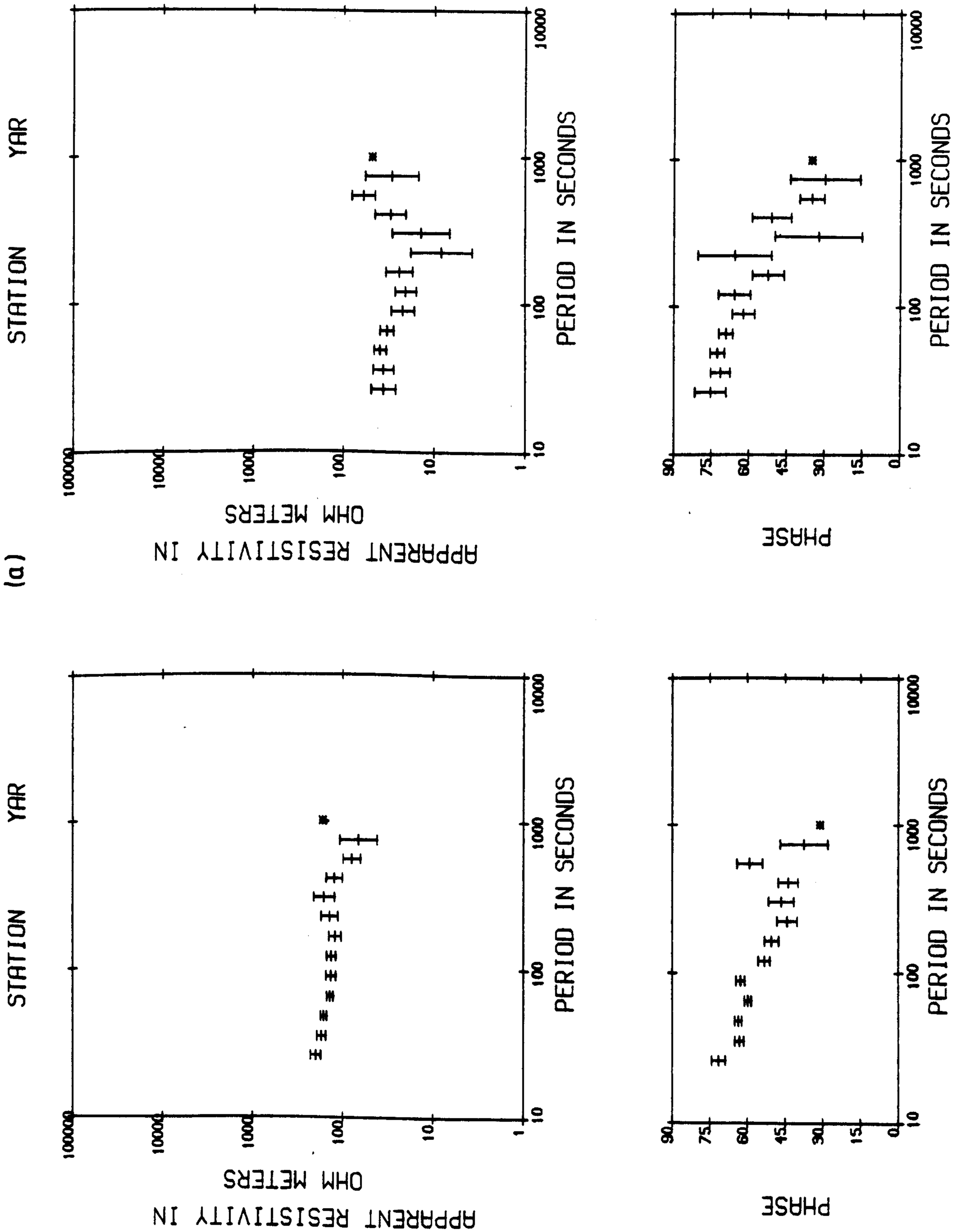
(a)
STATION YAR
APPARENT RESISTIVITY IN OHM METERS
100000
10000
1000
100
10
1
PERIOD IN SECONDS
10000
1000
100
10
PHASE
90
75
60
45
30
15
0

Figure 5·9.

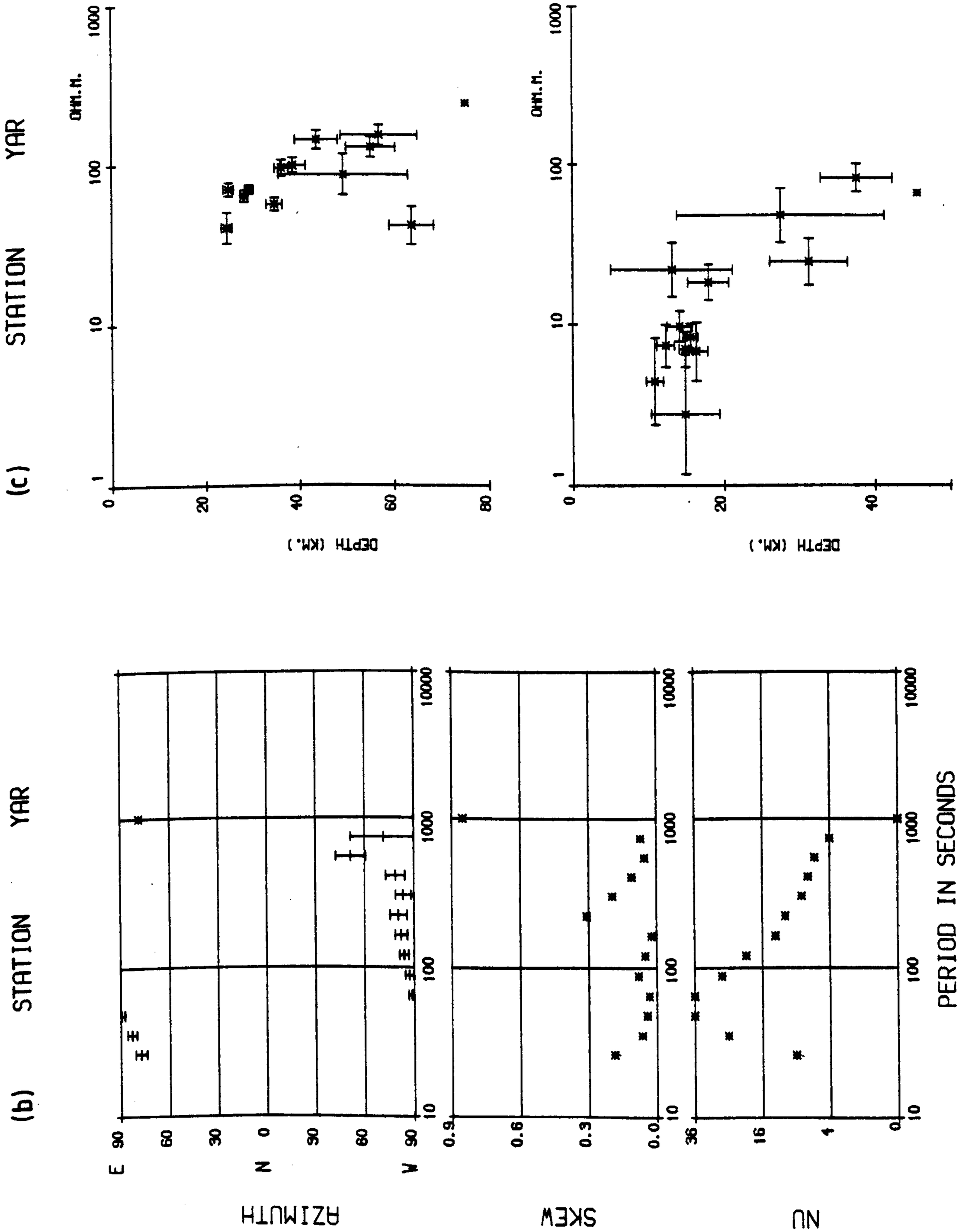
(c)
STATION
YAR
OHM.M.
1000
100
10
1
0
20
40
60
80
DEPTH (KM.)
OHM.M.
1000
100
10
1
0
20
40
DEPTH (KM.)
(b)
STATION
YAR
E 90
60
30
0
N
90
60
W 90
AZIMUTH
10000
1000
100
10
0.9
0.6
0.3
0.0
SKEW
36
16
4
0
NU
PERIOD IN SECONDS

Figure 5·9.

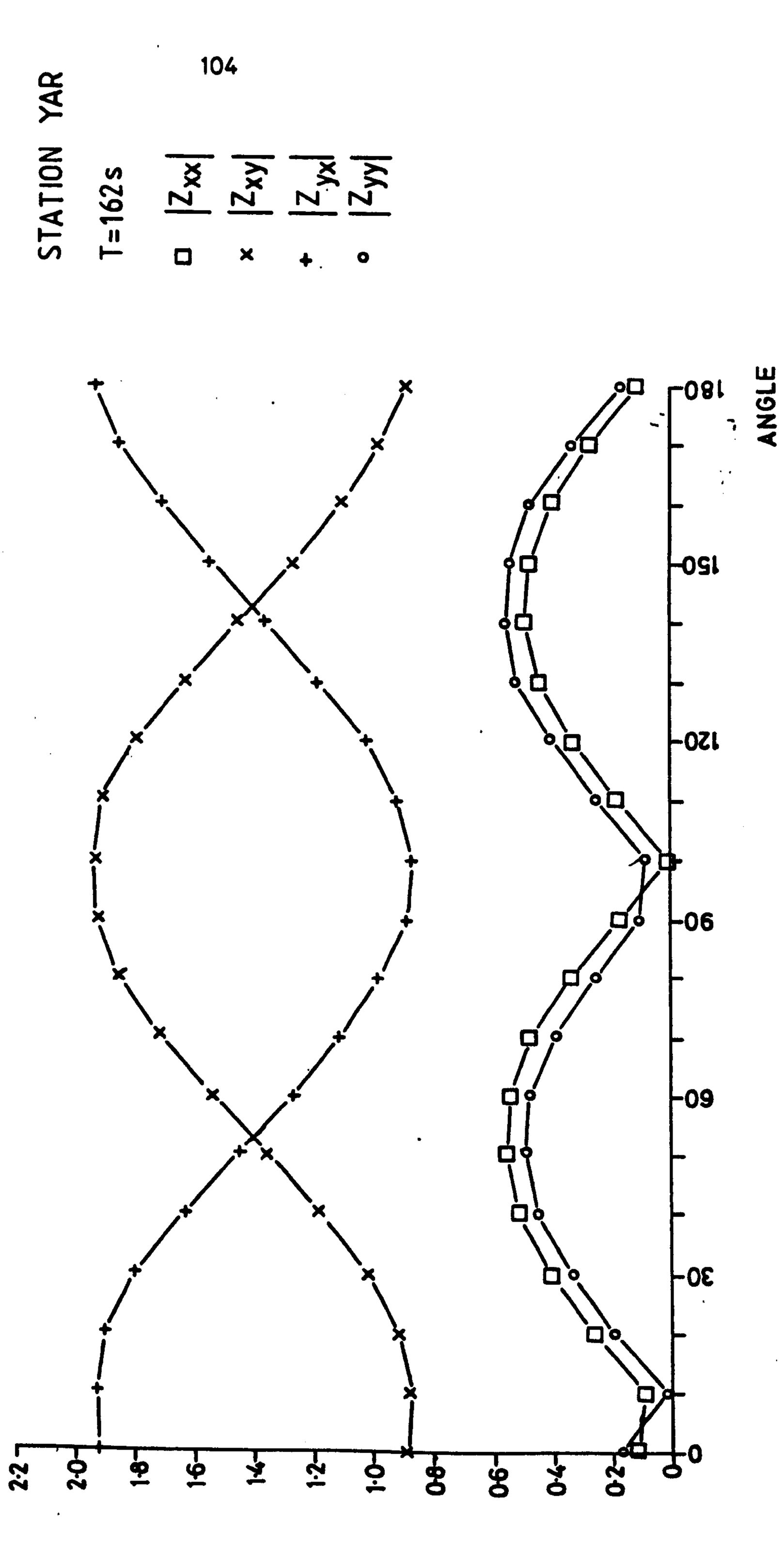
(d)
STATION YAR
T=162s
□ |Zxx|
× |Zxy|
+ |Zyx|
○ |Zyy|
ANGLE
180
150
120
90
60
30
0
2·2
2·0
1·8
1·6
1·4
1·2
1·0
0·8
0·6
0·4
0·2
0

Figure 5·9.

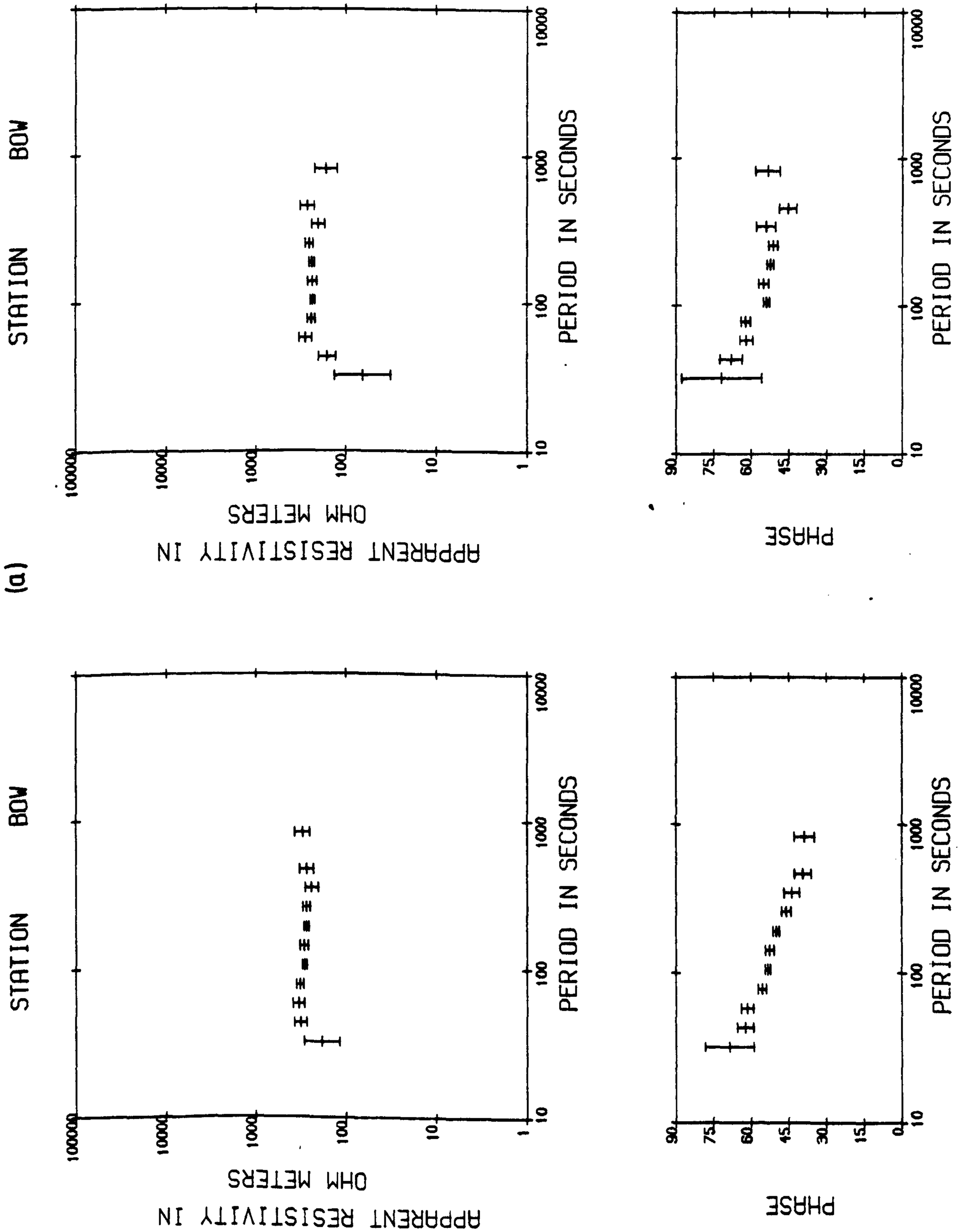
(a)
STATION BOW
APPARENT RESISTIVITY IN OHM METERS
100000
10000
1000
100
10
1
PERIOD IN SECONDS
10000
1000
100
10
PHASE
90
75
60
45
30
15
0

Figure 5·10.

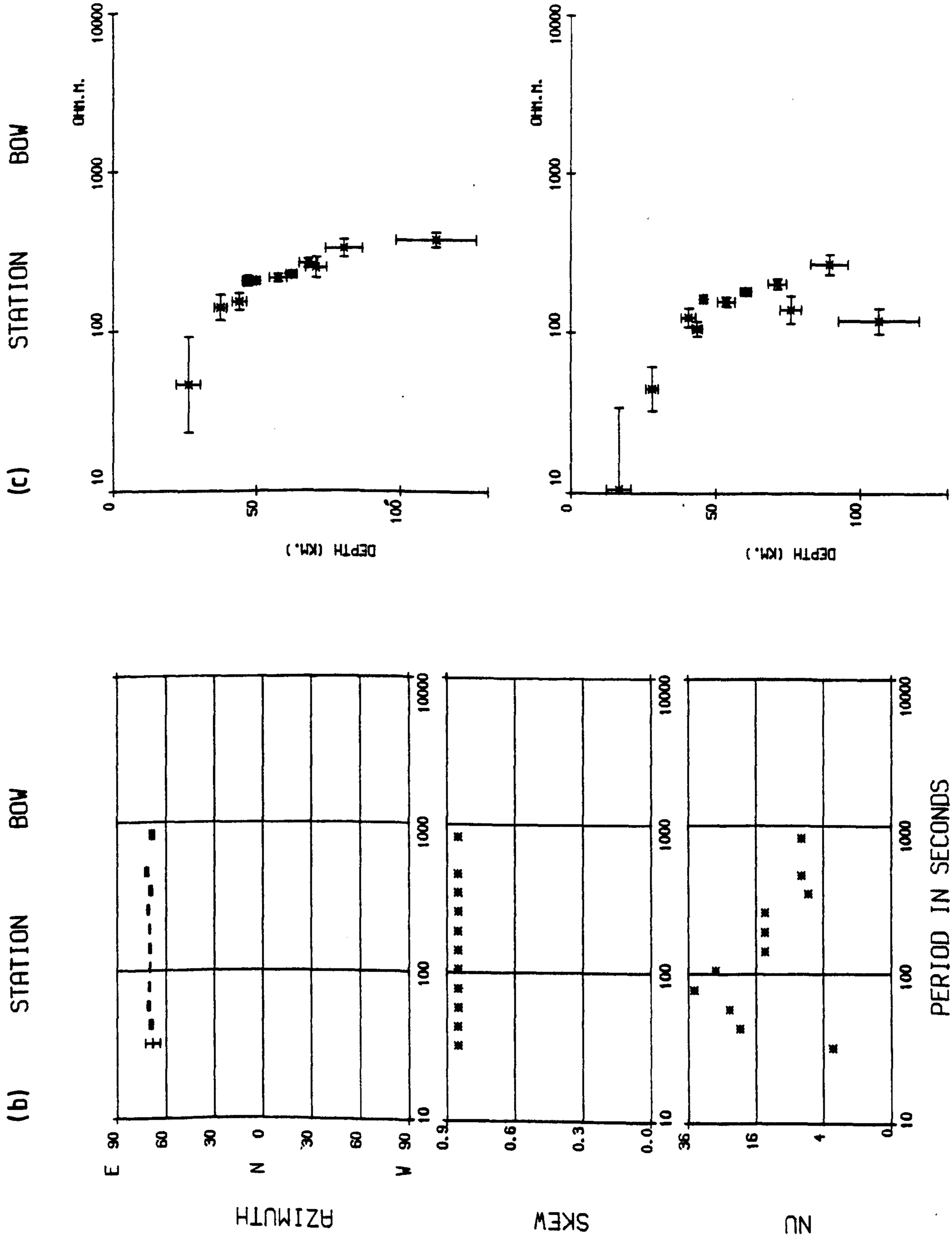
(c)
STATION
BOW
CM.N.
10000
1000
100
10
0
50
100
DEPTH (KM.)
(b)
STATION
BOW
PERIOD IN SECONDS
10000
1000
100
10
E 90
60
30
0
30
60
90 W
N
AZIMUTH
0.9
0.6
0.3
0.0
SKEW
36
16
4
0
NU

Figure 5·10.

(d)

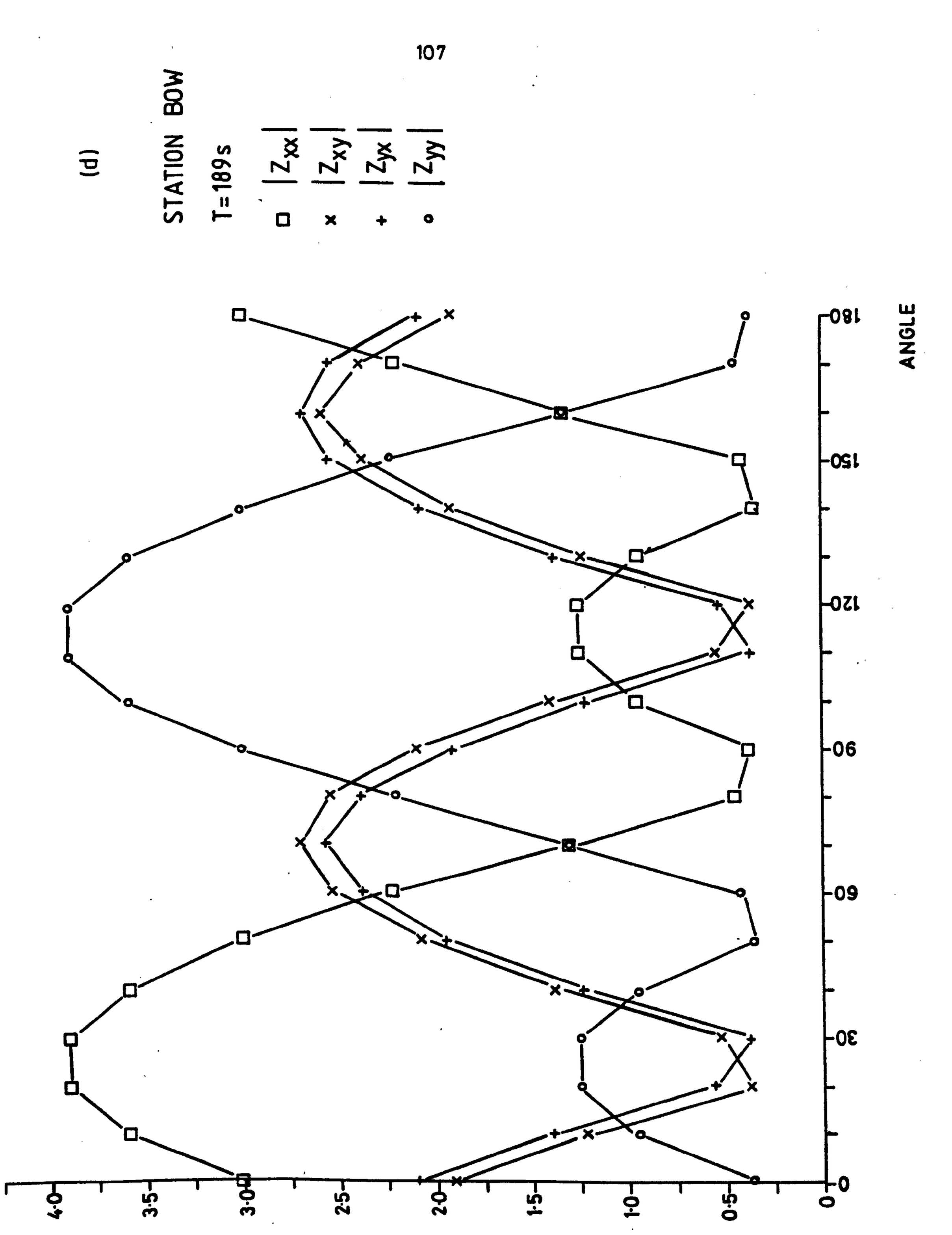
STATION BOW
T=189s
□ |Zxx|
× |Zxy|
+ |Zyx|
o |Zyy|
ANGLE
180
150
120
90
60
30
0
4·0
3·5
3·0
2·5
2·0
1·5
1·0
0·5
0

Figure 5·10.

and $\rho_\perp$ curves at N60°E strike direction as will be shown in chapter 6.

The dimensionality of the sites, as indicated by the skew and impedance tensor rotation, also changes from north to south. Both EAR and PEE appear roughly two-dimensional, YAR is a good two-dimen sional site and BOW, although having isotropic ρ_a curves, is strongly three-dimensional.

All the one-dimensional Schmucker inversions are similar for the Southern Uplands sites, suggesting a good conductor at a depth of around 50 km.

5.2:Magnetic results.

The magnetic results for each site consist of the unreversed real and imaginary induction vectors and Bank's maximum and minimum induction vectors. However, at all the sites the two sets of vectors are very similar, as can be seen for KLR, figure 5.11, allowing for reversal of the real induction arrow. Thus, for the other sites, only the real and imaginary induction vectors are presented (figures 5.12 to 5.14). The variations of the real and imaginary parts of the transfer functions A and B, with period, are plotted in figures 5.15 to 5.17, and allow an easier comparison between induction vectors at different sites as estimates can now be made at particular periods.

Maps of the reversed real and imaginary induction vectors at periods of 90, 180, 300 and 540 seconds, covering the whole of the South of Scotland are shown in figures 5.18 and 5.19. These have been constructed using the curves of A_r, A_i, B_r, and B_i in figures 5.11 to 5.13. The maps at periods of 90s and 180s also include the induction arrows for the sites of Jones (1977)

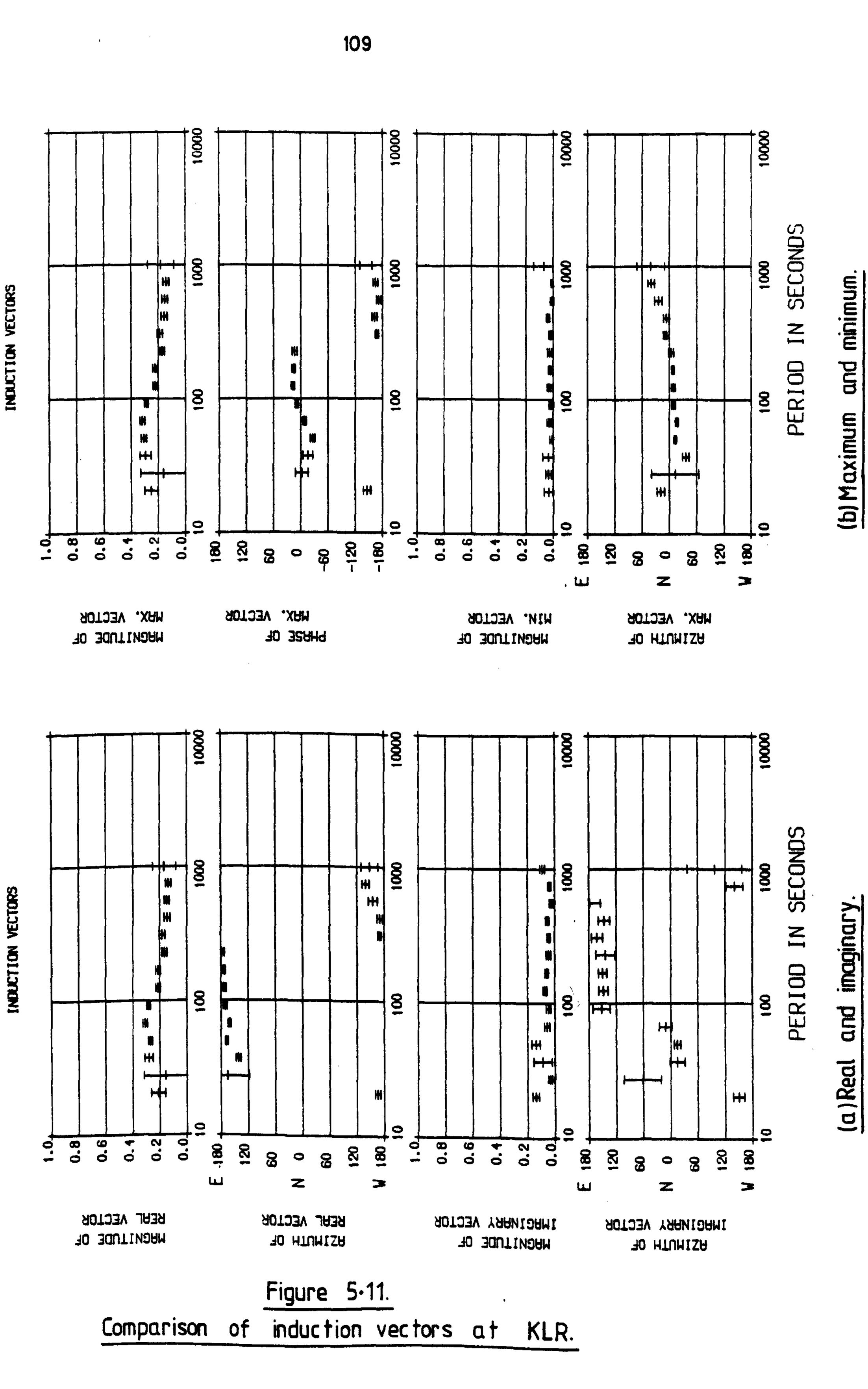

Figure 5·11.

Comparison of induction vectors at KLR.

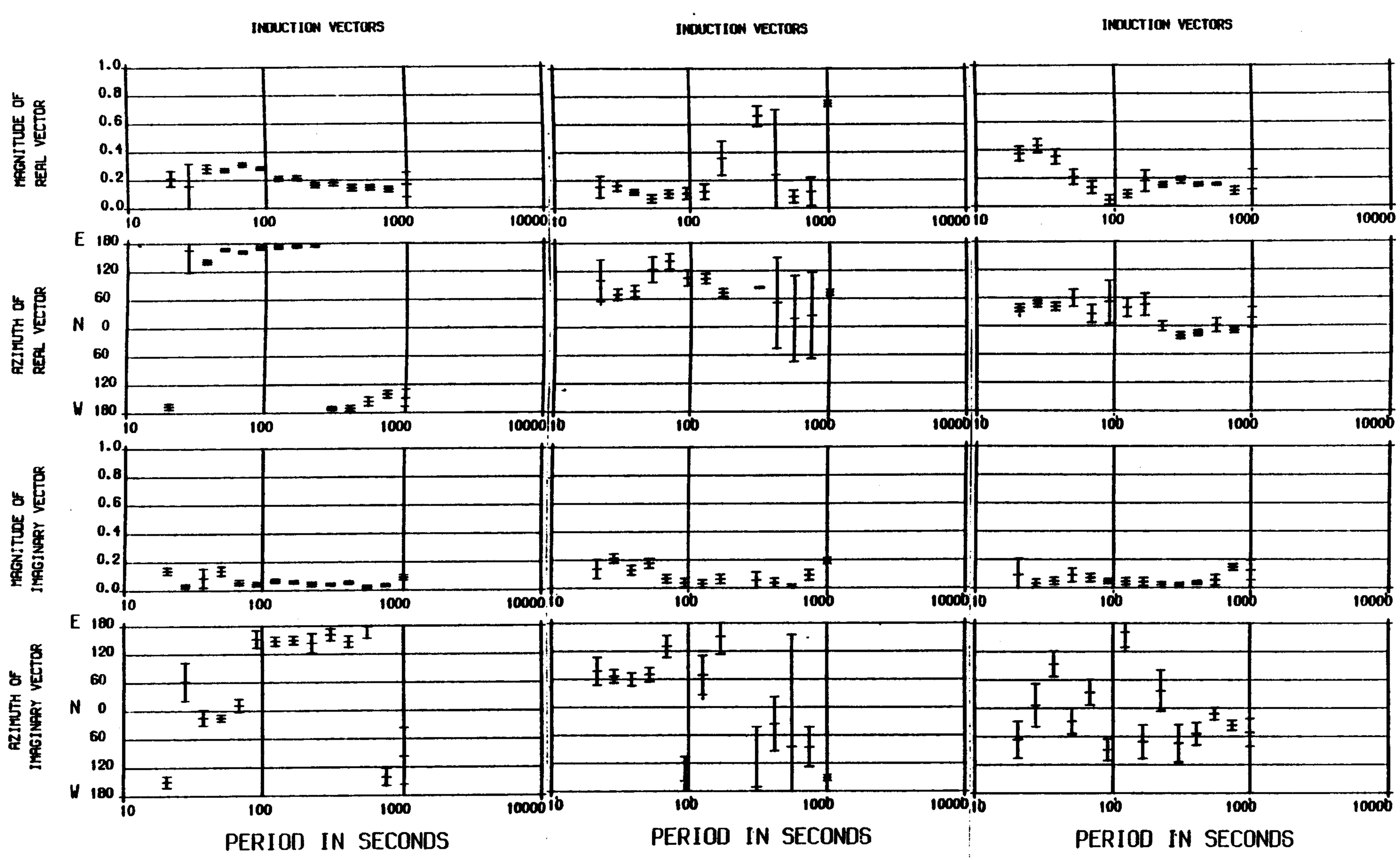

Figure 5-12.

Real and imaginary induction vectors at the Highland sites.

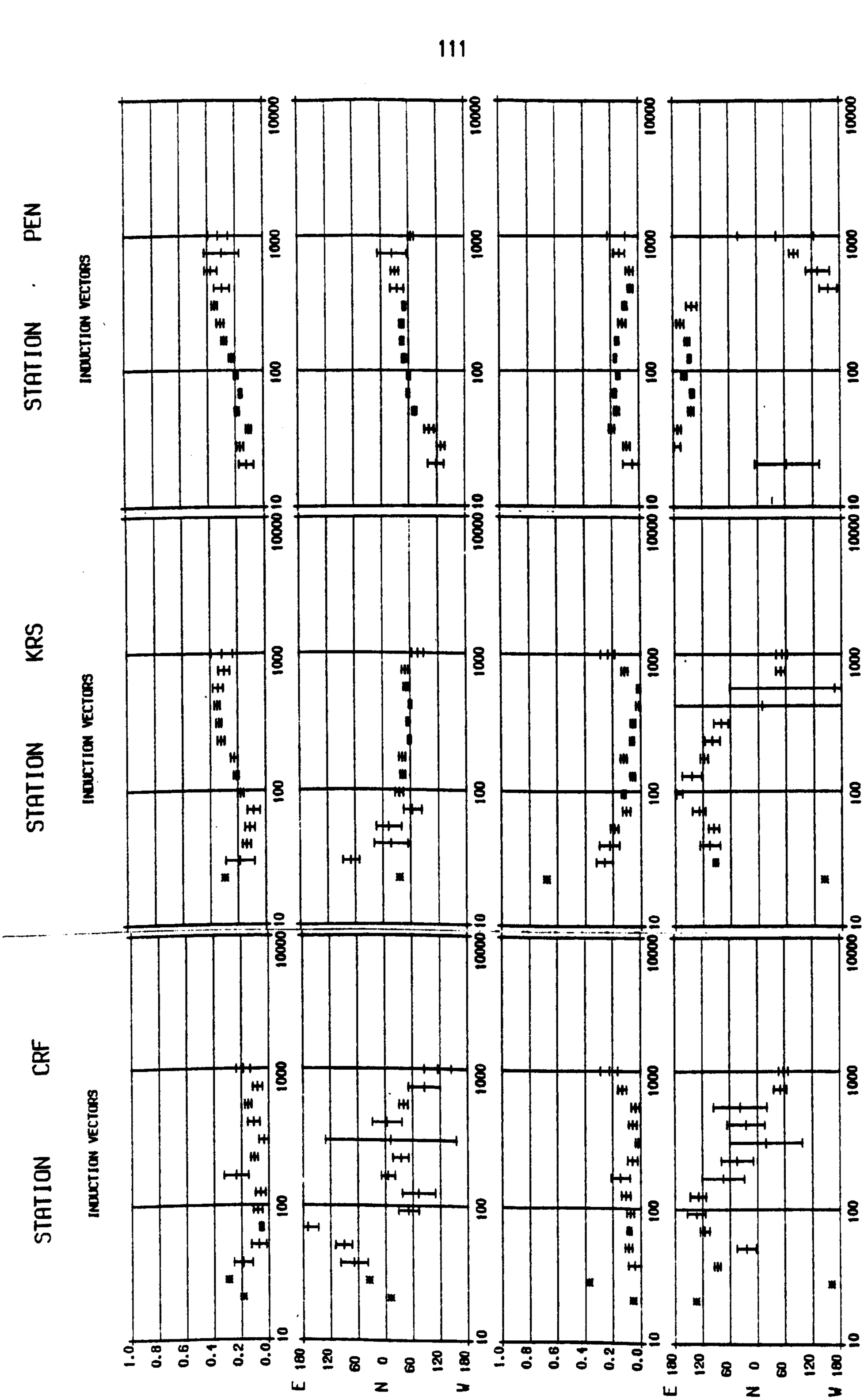

Figure 5·13. Real and imaginary induction vectors at the Midland Valley sites.

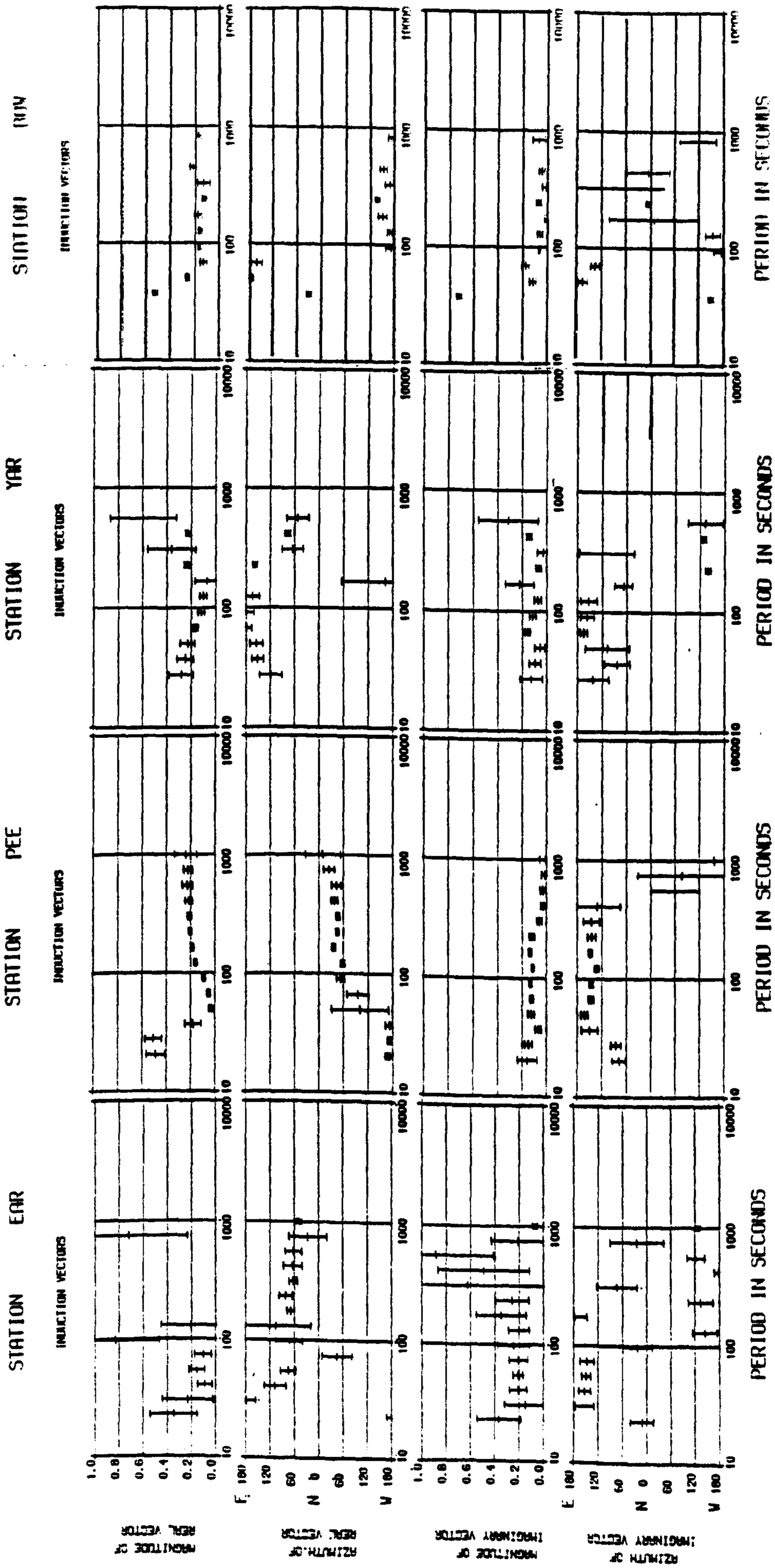

Figure 5·14.

Real and imaginary induction vectors at the Southern Uplands sites.

Figure 5.15.

Variation of A and B with period at Highland sites.

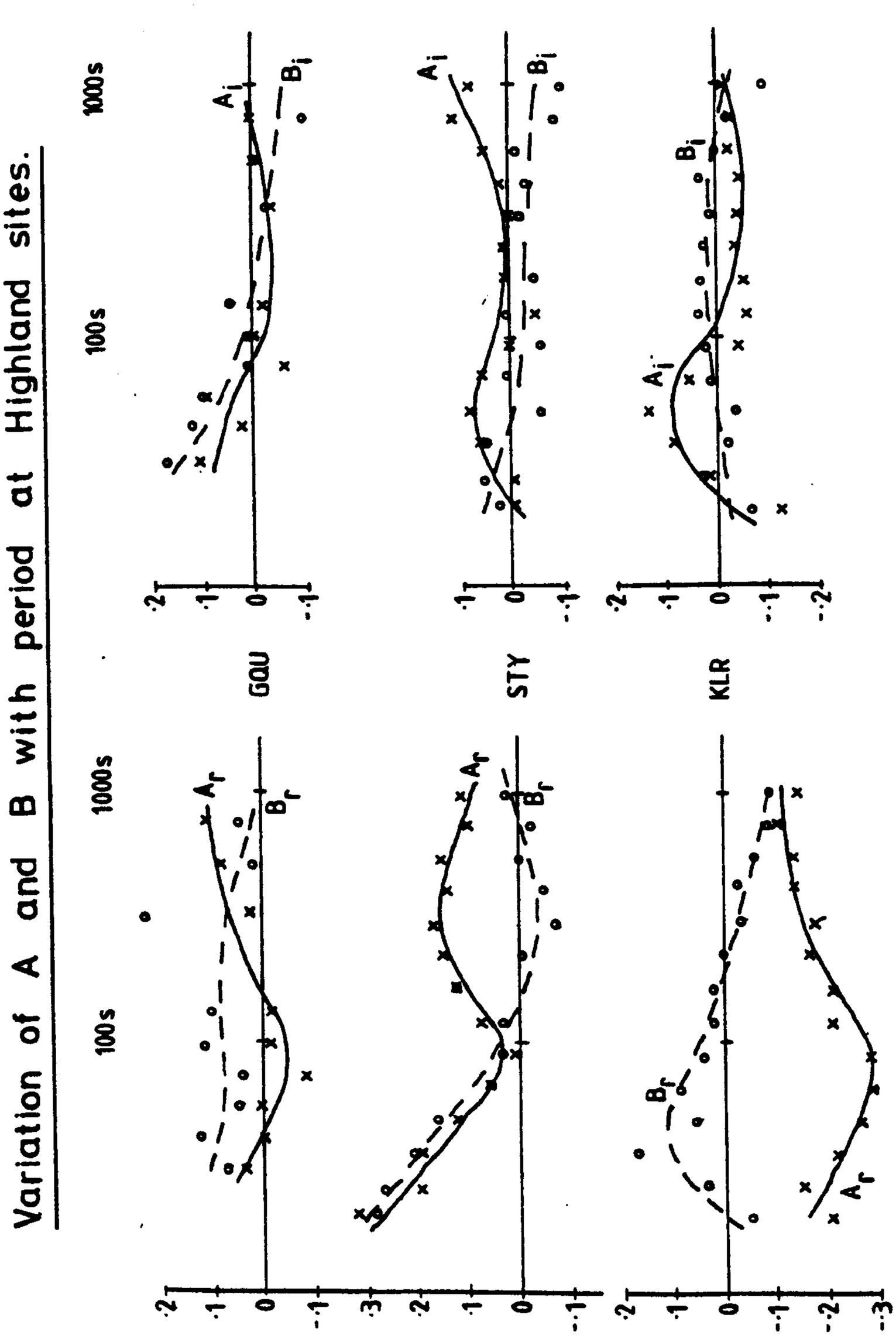

Figure 5·16.

Variation of A and B with period at Midland Valley sites.

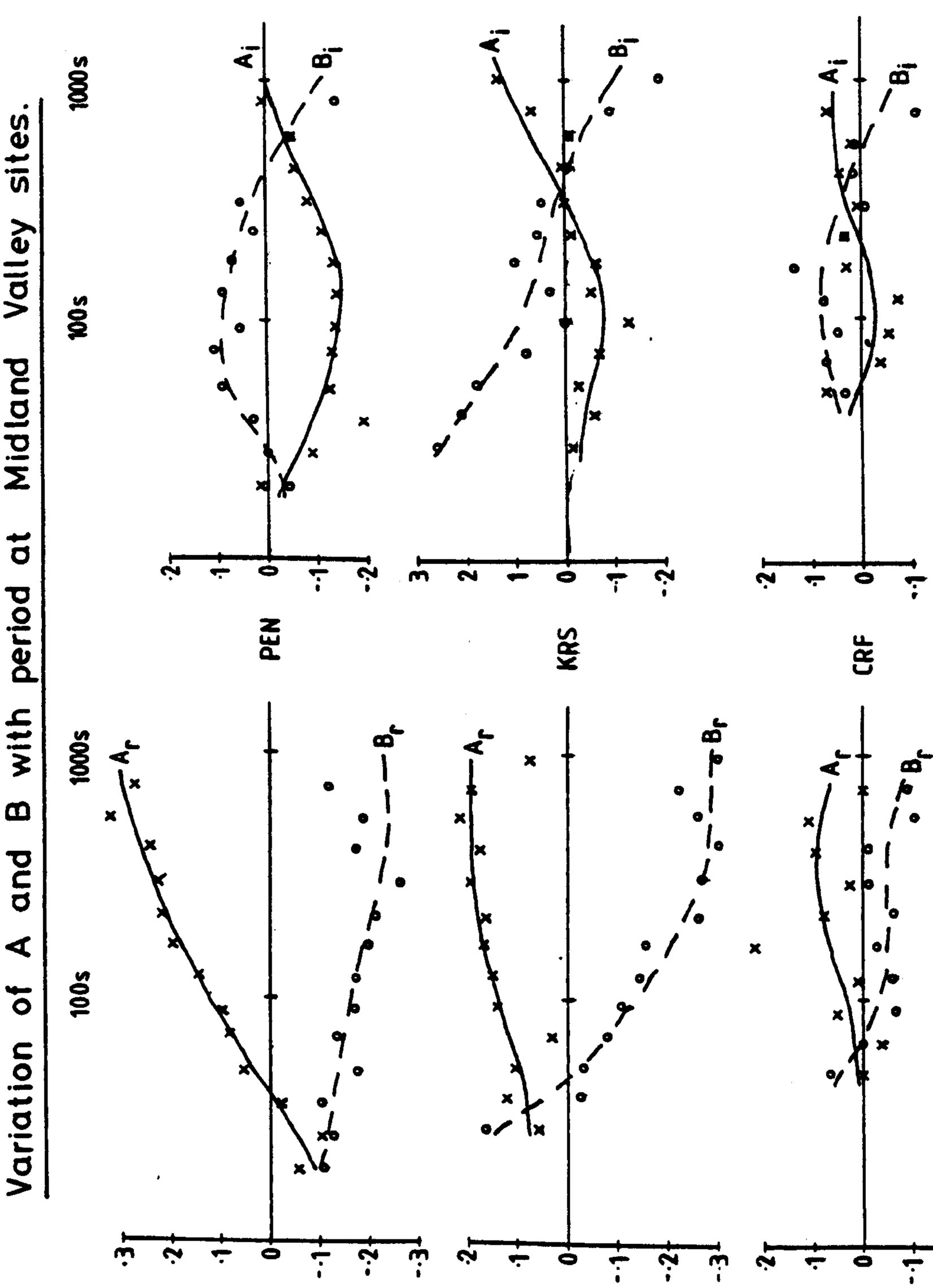

Figure 5·17.
Variation of A and B with period at Southern Uplands sites.

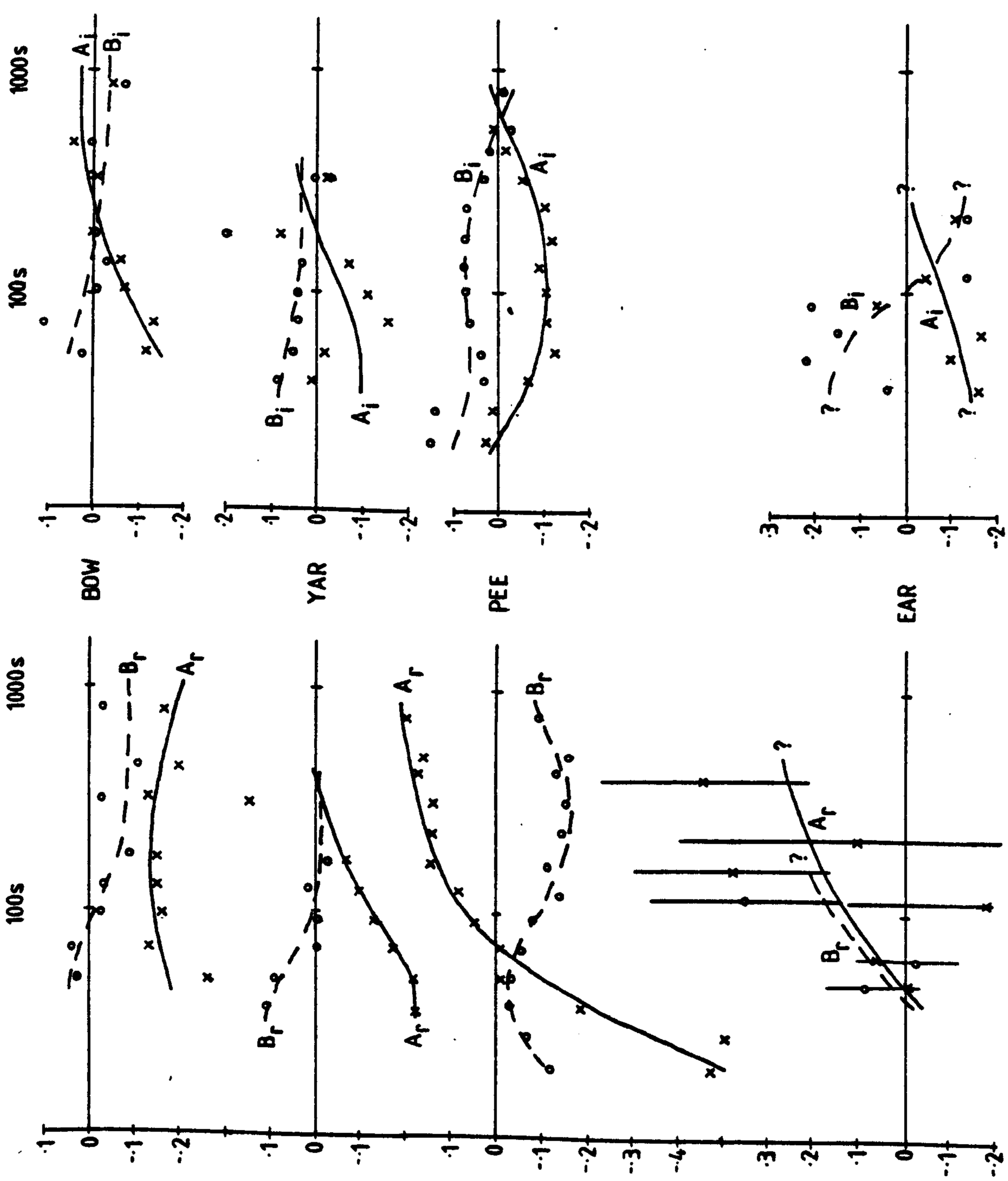

recalculated from the original data in the same way as the arrows for the new sites were obtained. The maps for the two longer periods include, as well as these sites, the other additional sites listed in table 4.2.

The main features which are apparent in figures 5.18 and 5.19 are listed below.

1)The real induction arrow at KLR, the most northerly station, points consistently north and is larger in magnitude than the arrows at the other Highland sites which tend to point south, across the Highland Boundary Fault, at longer periods.

2)In the Midland Valley the real arrows point south-east across the general geological trend of the area.

3)The magnitudes and directions of the arrows are very variable in the Southern Uplands although there tends to be a reversal in direction, which is across the Southern Uplands Fault at 60 seconds and moves progressively south-east with increasing period.

In all but the simplest cases, where a distinct reversal of the real arrow occurs across an anomaly, it can still be difficult to interperet maps of induction arrows. Bailey et al. (1974) introduced the technique of "hypothetical event analysis" in which the vertical field produced by a unit horizontal field in a particular direction is found from equation 2.65 at each of the sites, and the results contoured. For a situation which can be described in terms of an E-polarization and an H-polarization, the contributions to the vertical magnetic field from each polarization can be separated by taking orthogonal hypothetical magnetic fields orientated parallel and perpendicular to the main structural trend. Bailey and Edwards (1976) applied this tech-

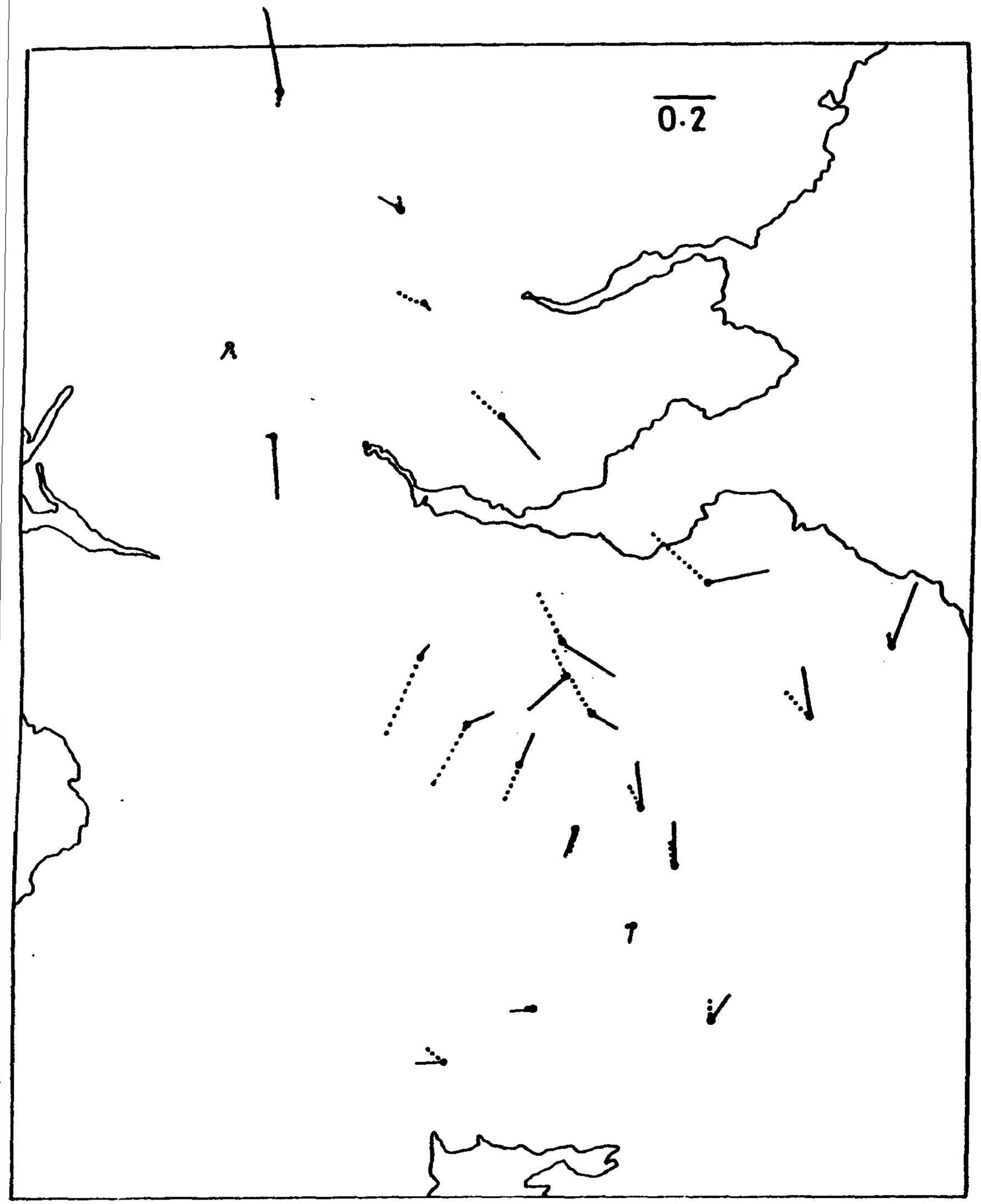

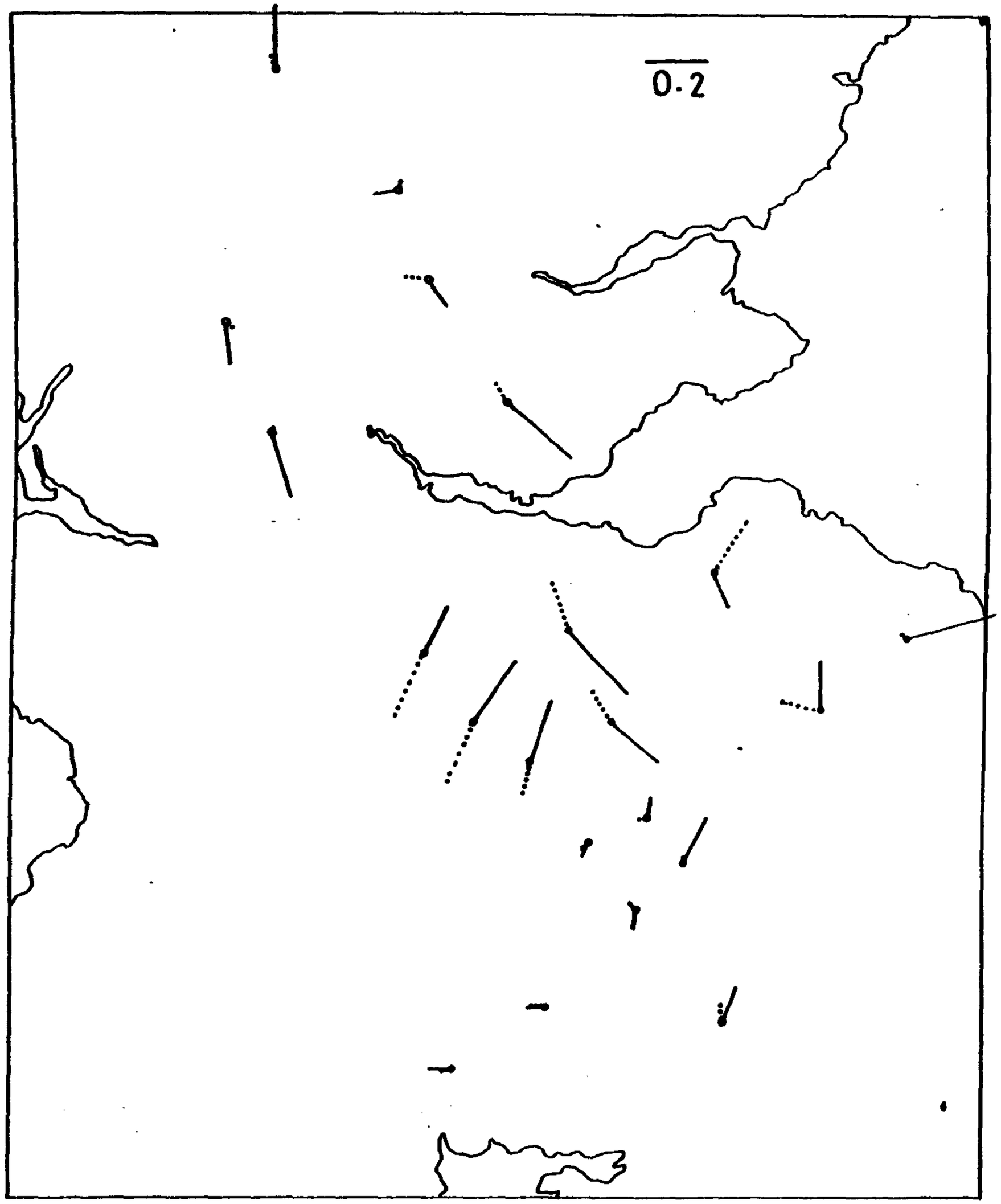

Figure 5·18. (a) T=90s Real (—) and imaginary (····) induction vectors across South Scotland. (b) T= 180s

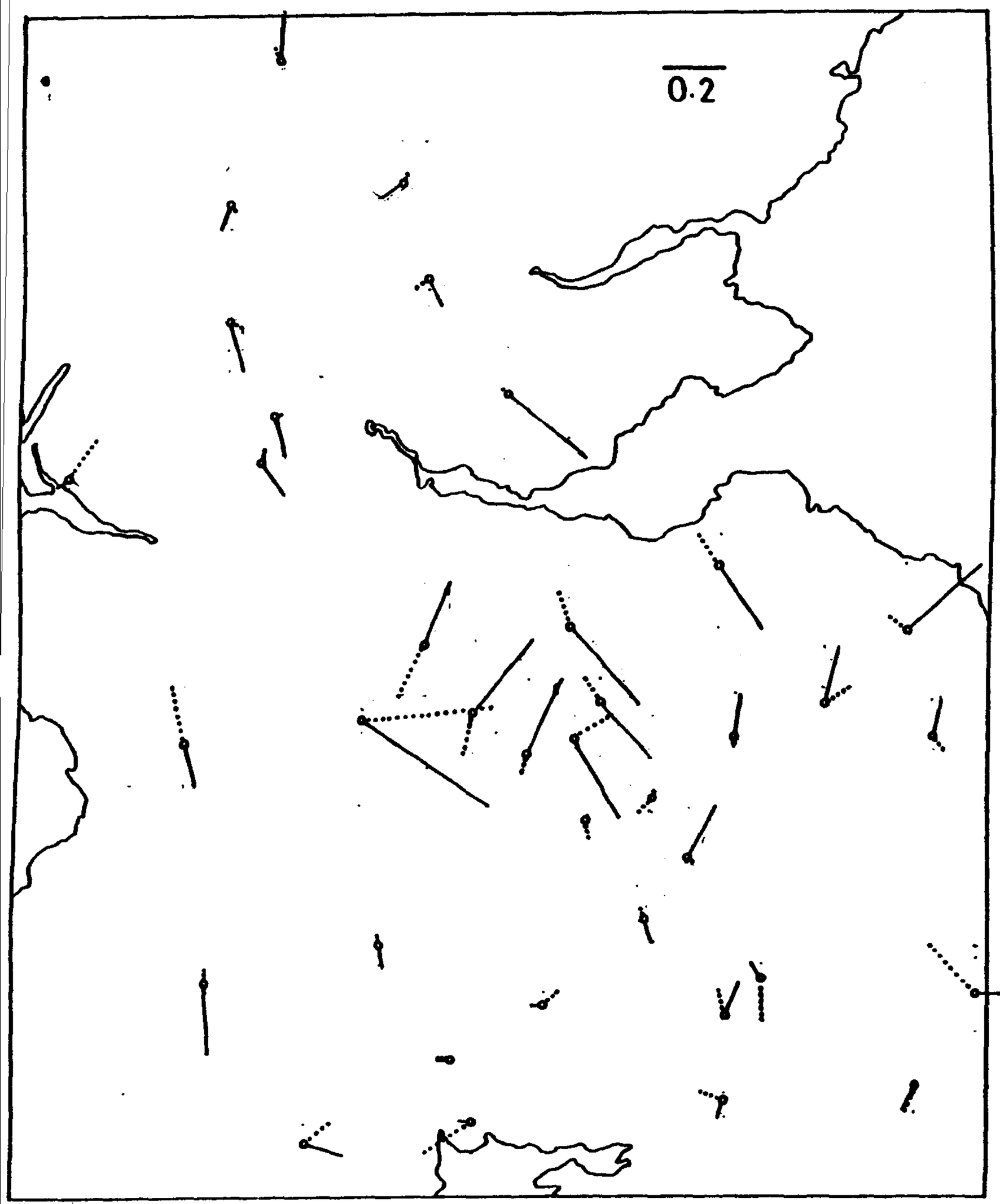

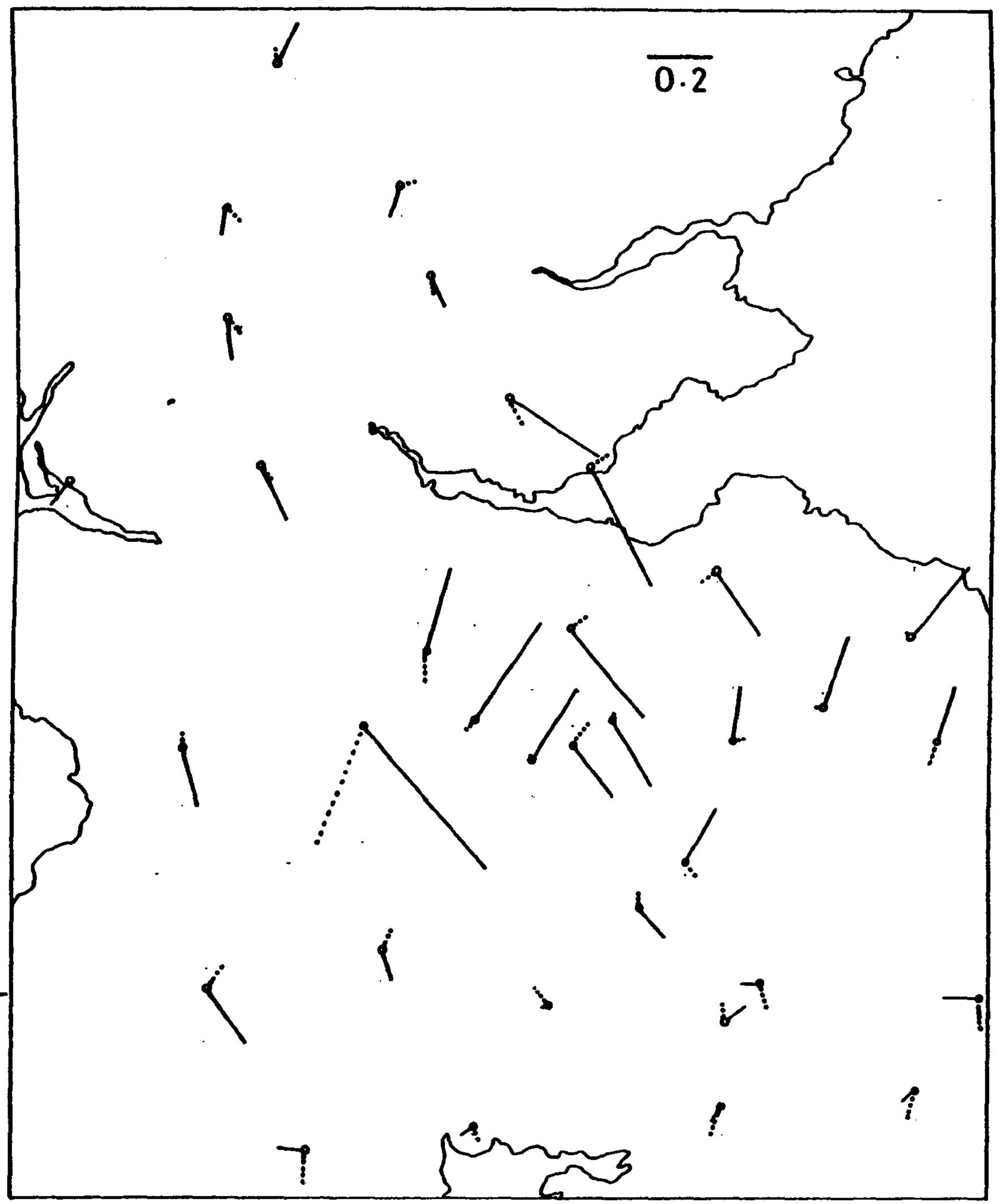

Figure 5·19. (a) T=300s Real (—) and imaginary (····) induction vectors across South Scotland. (b) T= 540s

nique to geomagnetic deep sounding data from south of the Midland Valley. As at the long periods they considered, the dominating structural trend is the N-S orientation of the continental shelf, they used regional magnetic fields directed westwards and northwards. The regional N-S electric current induced by the westwards magnetic field, as it flows parallel to the strike, is in phase with the field, whilst the regional E-W current is in quadrature with the northwards magnetic field which induces it. Thus the deflection of currents by conductivity anomalies can, in general, be identified from two contour maps:

1)the in-phase vertical field produced by a horizontal field perpendicular to the main conductivity contrast;

and 2)the quadrature field produced by a horizontal magnetic field parallel to the contrast.

The relevant contour maps for the South of Scotland, at a representative period of 300s, are shown in figure 5.20. Assuming that any conductivity contrast is parallel to the gross structural strike the fields which have been contoured are

1)the in-phase vertical field produced by a unit horizontal field at N45°W, figure 5.20a;

and 2)the quadrature vertical field produced by a unit horizontal field at N45°E, figure 5.20b.

Both contour plots show the same principal feature - a complicated change in the sign of the vertical field across the Southern Uplands, the reversal in sign being in the opposite direction for the two plots. The anomaly is more marked for the in-phase field and corresponds well with that observed at longer periods by Bailey and Edwards. However, the complicated structure evident around the central part of the Southern Uplands Fault, is

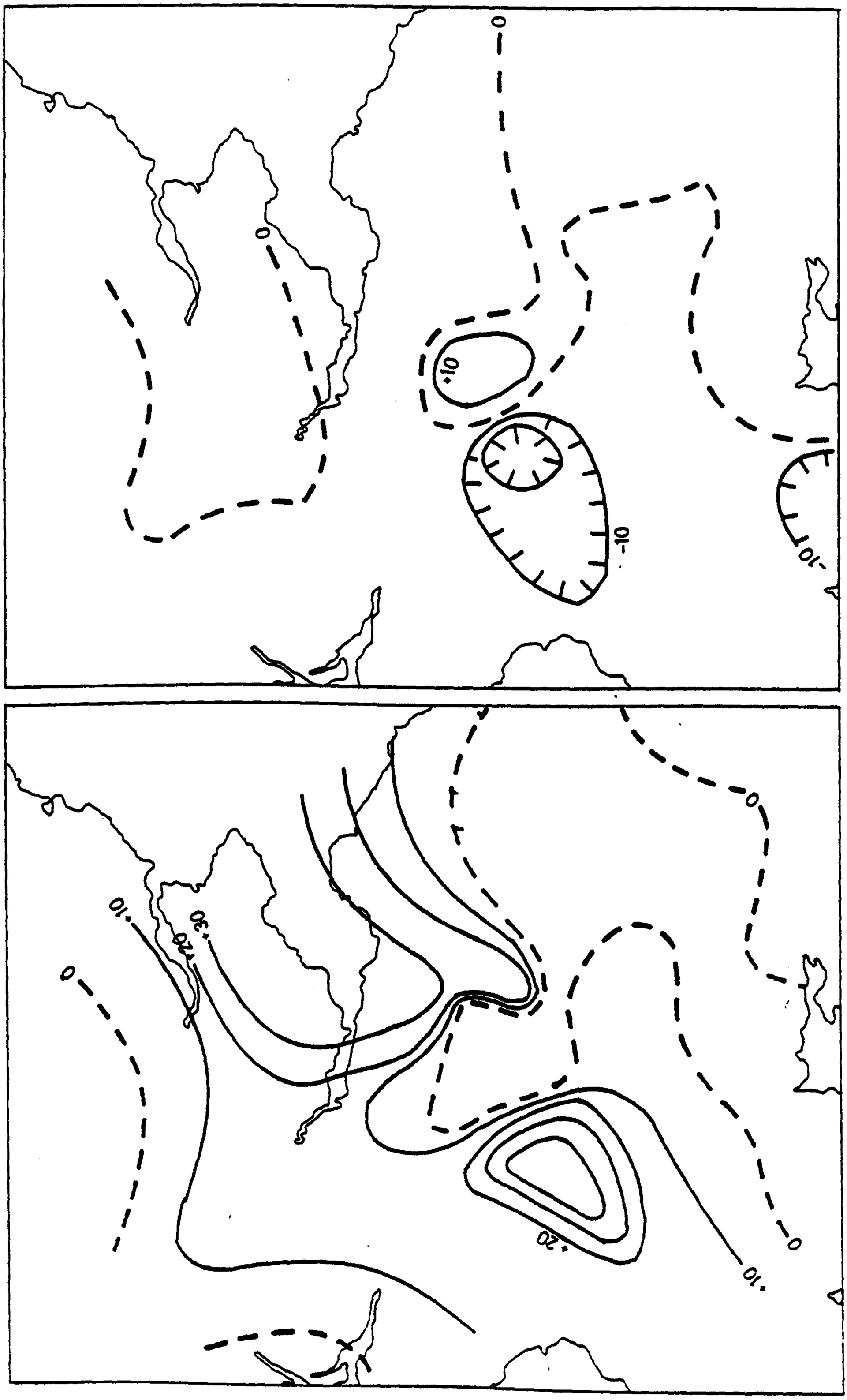

(b) Quadrature vertical field (x100) produced by a unit horizontal field at N45°E, T=300s.

(a) In-phase vertical field (x100) produced by a unit horizontal field at N45°W, T=300s.

Figure 5·20.

a previously unobserved feature presumably only detected because of the much greater station density used in the calculation. Both plots also show a zero in the vertical field further north, close to the Highland Boundary Fault, the gradients are not as steep however, as they are in the south.

5.3:Summary.

1)The magnetotelluric results from both the Highland and Southern Uplands areas appear to show features which are characteristic of each region.

2)There is a considerable variation in the magnetotelluric results from sites within the Midland Valley.

3)The magnetic results indicate a large conductivity anomaly beneath the Southern Uplands.

CHAPTER 6: MODELLING.

The modelling of the magnetotelluric and magnetic results presented in chapter 5 was carried out in five stages, which are listed below and subsequently discussed in more detail.

1) It was suggested in section 2.2.1 that the actual resisivity variation with period at a site is better represented by an average value of the maximum and minmimum apparent resistivities than by either of these two curves itself. For this reason average curves of ρ_a and φ_a were calculated for each site.

2) A one-dimensional modelling of the average ρ_a and φ_a curves from each site was carried out using the Monte-Carlo program of Jones (1977) in a slightly modified form.

3) The one-dimensional models for each site were used to construct a preliminary two-dimensional model along a traverse from north of the Highland Boundary Fault to the Borders. The line of the traverse was approximately N30°W - N150°E, (line AA' in figure 4.3), thus $\underline{E}$ and $\underline{H}$-polarization solutions correspond respectively to the curves of $\rho_{//}$ and $\rho_{\perp}$ for a strike direction of N150°W - N60°E - the general geological trend.

4)Two-dimensional modelling was carried out using the method of Brewitt-Taylor and Weaver (1976) in its diakoptic form (Brewitt-Taylor and Johns, 1980), the model being adjusted in stages to fit both the averaged magnetotelluric results at each site and the variations in Z/H along the traverse.

5) Once a fit for the averaged magnetotelluric curves at all sites had been obtained further model adjustment was aimed at fitting the actual curves of $\rho_{//}$, $\rho_{\perp}$, $\varphi_{//}$ and $\varphi_{\perp}$ at each site. The known geological structure of the area was also taken into

consideration when adjustments were being made to the model.

6.1: Averaging of the impedance tensor.

Before proceding to two or three-dimensional modelling, it is normal in magnetotelluric studies to undertake a one-dimensional inversion of the results from each site and to use the one-dimensional models as a basis for more complicated modelling. For sites which are not truly one-dimensional this presents a difficulty in that there are two possible sets of apparent resistivity and phase curves which may be modelled. As section 2.2.1 showed, neither set is a particularly good representation of the actual resistivity variation and it is clear from figure 2.3 that some kind of average would be more suitable. The apparent resistivity and phase are the magnitude and argument, respectively, of a complex number, thus a straight averaging of ρ_a and φ_a would be incorrect. The correct average is that of the impedance tensor elements from which the apparent resistivity and phase curves are calculated.

$$Z_{av} = \frac{1}{2}(Z'_{xy}(\emptyset) - Z'_{yx}(\emptyset)) \qquad 6.1$$

The important point to note about equation 6.1 is the appearance of a negative rather than a positive sign. This is necessary because, although physically the phase lies between 0° and 90°, it is a result of the calculation of $\underline{Z}$ that the phase of one of the principal impedances lies in the third rather than the first quadrant. Hence, using the minus sign is equivalent to restoring the phase to the first quadrant and adding the impedances. The correctness of Z_{av} given by 6.1 can be seen by substituting for $Z'_{xy}(\emptyset)$ and $Z'_{yx}(\emptyset)$ from equations 2.57 and 2.58 to get an average impedance which is invariant with angle of rotation.

Averaged apparent resistivities and phases can be calculated from Z_{av}.

Apart from giving single apparent resistivity and phase curves for one-dimensional inversion, the average curves are also of use for preliminary two-dimensional modelling. On a long traverse across a complicated tectonic region there are many changes in the relative magnitudes of $\underline{E}$ and $\underline{H}$ - polarization apparent resistivities. Rather than immediately attempting to construct a model to take account of these, it is simpler, and the logical step after one-dimensional inversion, to first find a two-dimensional model which fits the average curves from each site. Such a model can then be amended to fit both the $\underline{E}$ and $\underline{H}$ - polarization results along the traverse.

6.2: One-dimensional modelling.

One-dimensional modelling was carried out using a slightly modified form of the Monte-Carlo inversion program of Jones (1977). With the relatively short band-width available it was considered likely that three-layered models would be sufficient to represent the data from each site. Subsequent investigation of models with more layers showed that this was indeed the case and that using four or more layers is an over-resolution of the problem.

The theoretical curves of Srivistava (1967) were used to find a starting model for each site with resistivities ρ_{i_o} (i=1,3) and interface depths h_{i_o} (i=1,2). From each starting model between 1000 and 2000 further models were generated using the relationships

$$\rho_i' = \rho_i 10^r \qquad i=1,3 \qquad 6.2$$

$$h_i' = h_i 2^r \qquad i=1,2 \qquad 6.3$$

where ρ_i and h_i are the resistivities and interface depths of the previous best fitting model and r is a random number between 0 and 1. The fit of each model was calculated as a least squares deviation of the model ρ_a and φ_a curves from the actual field curves. At most of the sites little difference was found between the result when fitting solely the ρ_a or φ_a curve and fitting both at the same time.

At each site the 30 to 40 best fitting models to both the apparent resistivity and phase were selected. The results from the three regions; the Highlands, the Midland Valley and the Southern Uplands; are shown in figures 6.1, 6.2 and 6.3 respectively. For each site the upper part of the diagram shows the range of the best fitting models, and the lower part the fit of the single best model.

For the three Highland sites the models are all very similar. They show:

1) a resistive top layer extending to a depth of between 10 and 25 km.;

2) an intermediate, relatively conducting layer (200- 700Ω-m); and

3) a resistive basement from a depth of between 40 - 100 km.

However, as might be expected from the original data, there is not as great a similarity between the sites within the Midland Valley. At Crieff the models show a very good conductor, coming to within 5 - 15 km of the surface, and of very indeterminate thickness. A highly conducting layer is also very close to the surface at Penicuik, though here the resistive basement is at a slightly greater depth. At Kinross there is a considerable

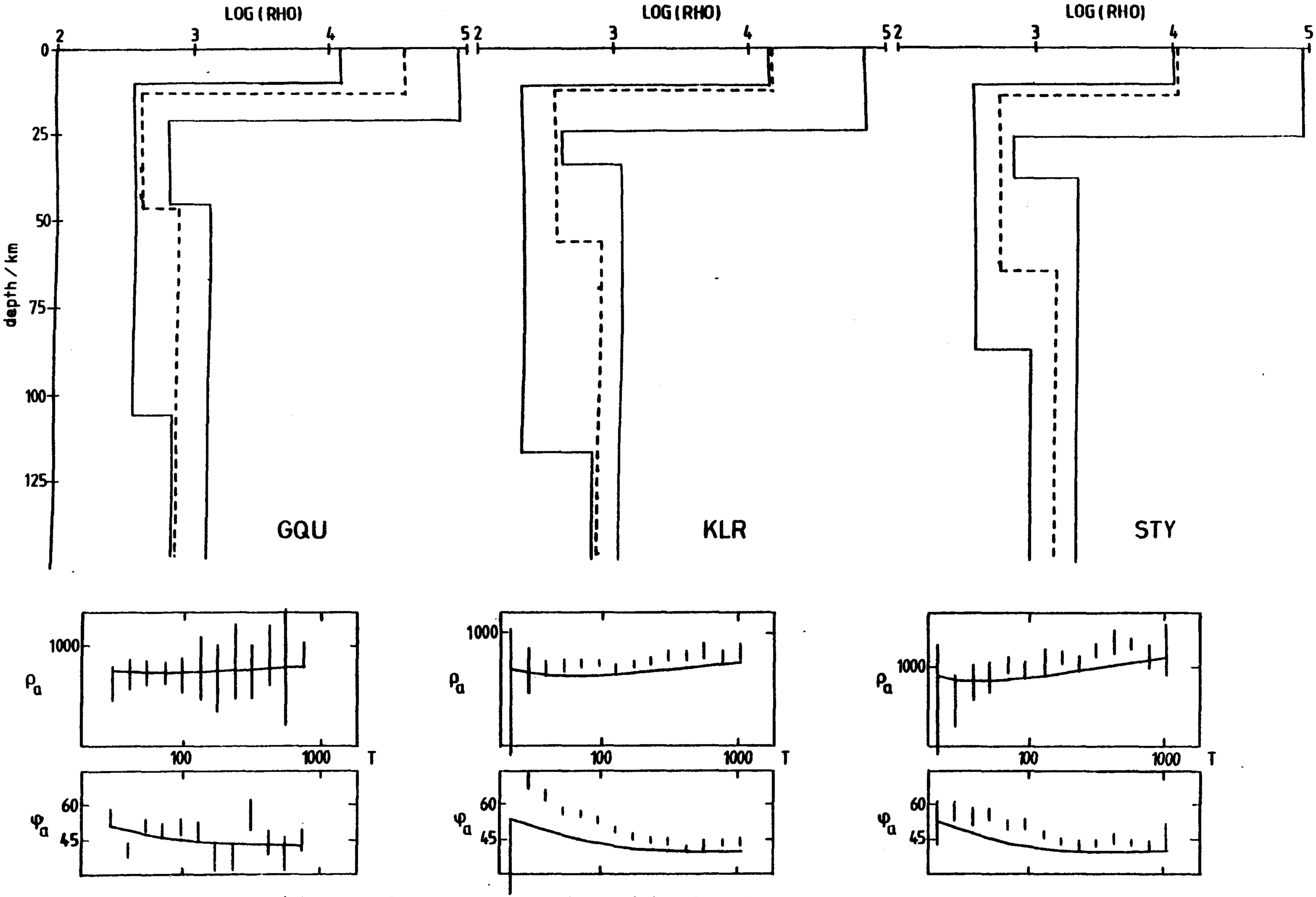

Figure 6·1. One-dimensional models for the Highland sites.

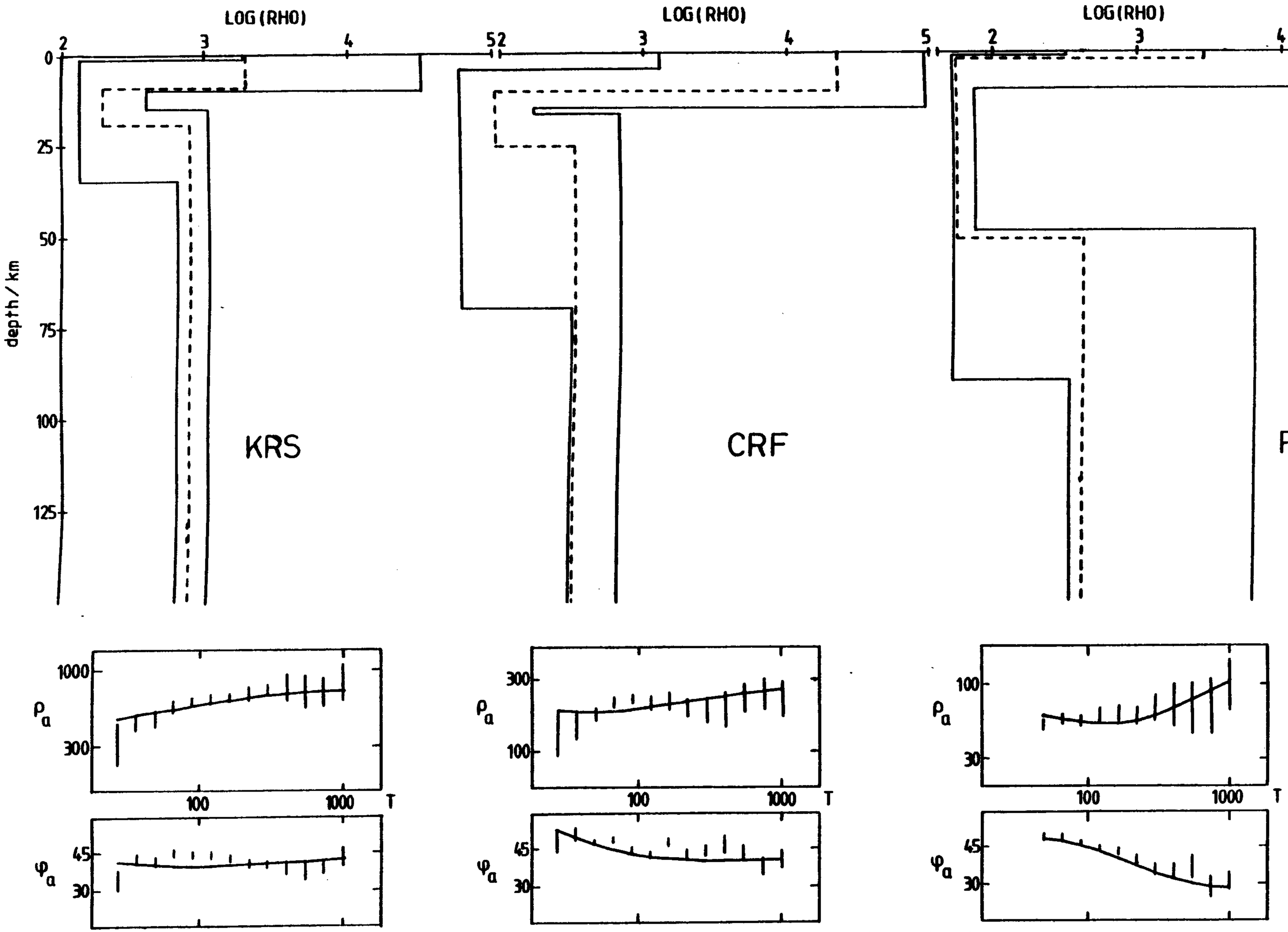

Figure 6·2. One-dimensional models for the Midland Valley sites.

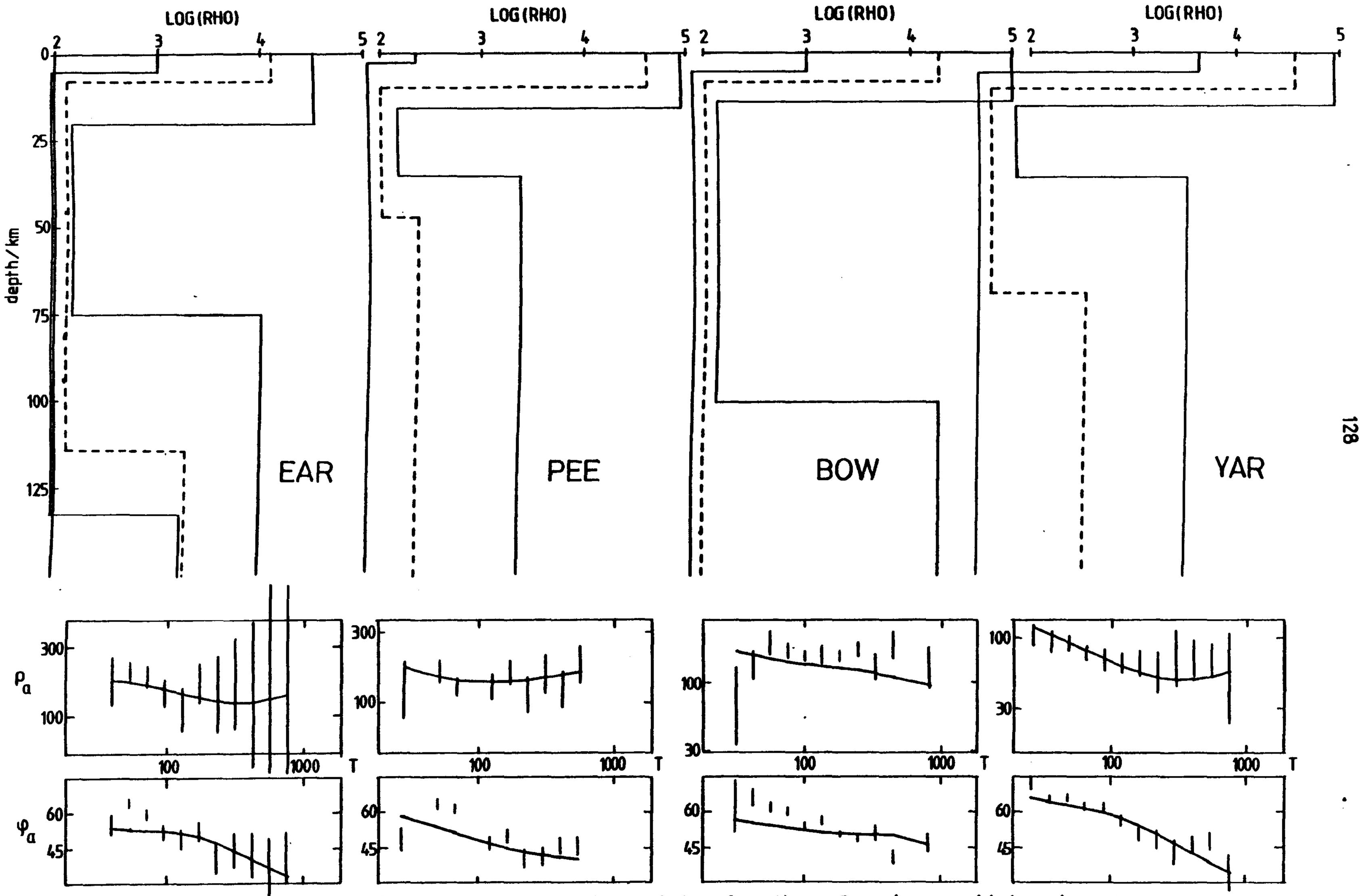

Figure 6·3. One-dimensional models for the Southern Uplands sites.

difference from the other two sites. The intermediate layer is not as conducting (200 - 400 Ω-m) and is much thinner, going to only 15 - 30 km depth. It is difficult to visualize a continuous structure across the Midland Valley.

The highly conducting layer at Penicuik also appears to be present at all four of the Southern Uplands sites. The top of the layer is slightly deeper than in the southern part of the Midland Valley, and it is possibly a little less conducting, but the main difference is that, beneath the Southern Uplands, the layer extends to a very great depth. The wide range of possible depths to the resistive basement may in fact be due to the failure to penetrate the overlying conductor.

For Penicuik and the Southern Uplands the model results are very similar to those obtained by Jones (1977) and shown in figure 3.4. Jones employed different data analysis techiniques to those used in this project and re-analysis of data from some of his other sites (figure 6.4), using the same programs as for the new sites, also shows good agreement between all the models in this part of the study area.

It is worth pointing out that all the models show the sequence resistor - conductor - resistor. In the cases where no initial decrease in apparent resistivity is observed the upper resistive layer is necessary to fit the phase curve, which has an initial maximum. The presence of a thin conducting, presumably sedimentary, layer at the surface was found to have either very little or no effect on the model curves. Such a layer could therefore be included at most of the sites without changing the basic features of the one-dimensional model.

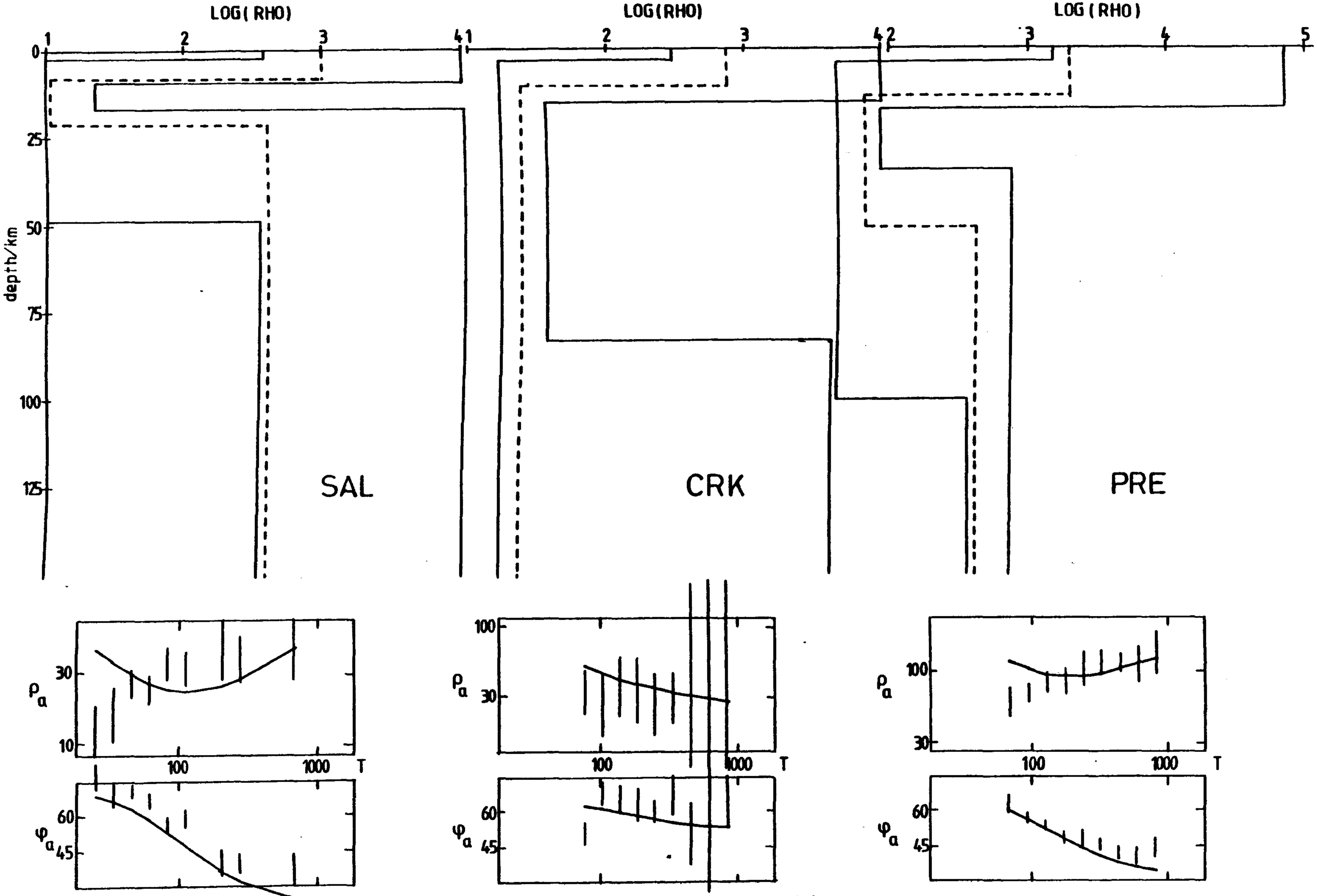

Figure 6·4. One-dimensional models at additional sites.

6.3: Two-dimensional modelling.

6.3.1: The numerical modelling program.

The program used for two-dimensional modelling was the diakoptic formulation (Brewitt-Taylor and Johns, 1980) of the finite difference method of Brewitt-Taylor and Weaver (1976).

Previous finite difference methods (Jones and Pascoe, 1971; Pascoe and Jones, 1972) have concentrated on the representation of conductivity changes as sharp boundaries (figure 6.5). To find the correct finite difference representation, 'ficticious' field values have to be introduced, and Brewitt-Taylor and Weaver showed that this leads to overdetermination of the solution. For example, for the E-polarization case the four finite difference equations for representing equation 2.33 are

$$\begin{aligned}
E_1 + E_2 + E_3^{(1)} + E_4^{(1)} &= (4 + i\nu_1 h^2)E_0 \\
E_1^{(2)} + E_2 + E_3 + E_4^{(2)} &= (4 + i\nu_2 h^2)E_0 \\
E_1^{(3)} + E_2^{(3)} + E_3 + E_4 &= (4 + i\nu_3 h^2)E_0 \\
E_1 + E_2^{(4)} + E_3^{(4)} + E_4 &= (4 + i\nu_4 h^2)E_0
\end{aligned} \qquad 6.4$$

where E_0, E_1, E_2, E_3, E_4 are the field values at grid points 0, 1, 2, 3 and 4, $E_i^{(j)}$ is the fictitious field at point i associated with region j and $\nu_i = \omega\mu_0\sigma_i$. h is the grid spacing, which is uniform. Applying the boundary condition that the tangential magnetic field must be continuous across the boumdaries gives

$$\begin{aligned}
E_4^{(1)} - E_2 &= E_4 - E_2^{(4)} \\
E_4^{(2)} - E_2 &= E_4 - E_2^{(3)} \\
E_1^{(2)} - E_3 &= E_1 - E_3^{(1)} \\
E_1^{(3)} - E_3 &= E_1 - E_3^{(4)}
\end{aligned} \qquad 6.5$$

and for the normal component to be continuous

$$E_1^{(2)} = E_1^{(3)}$$

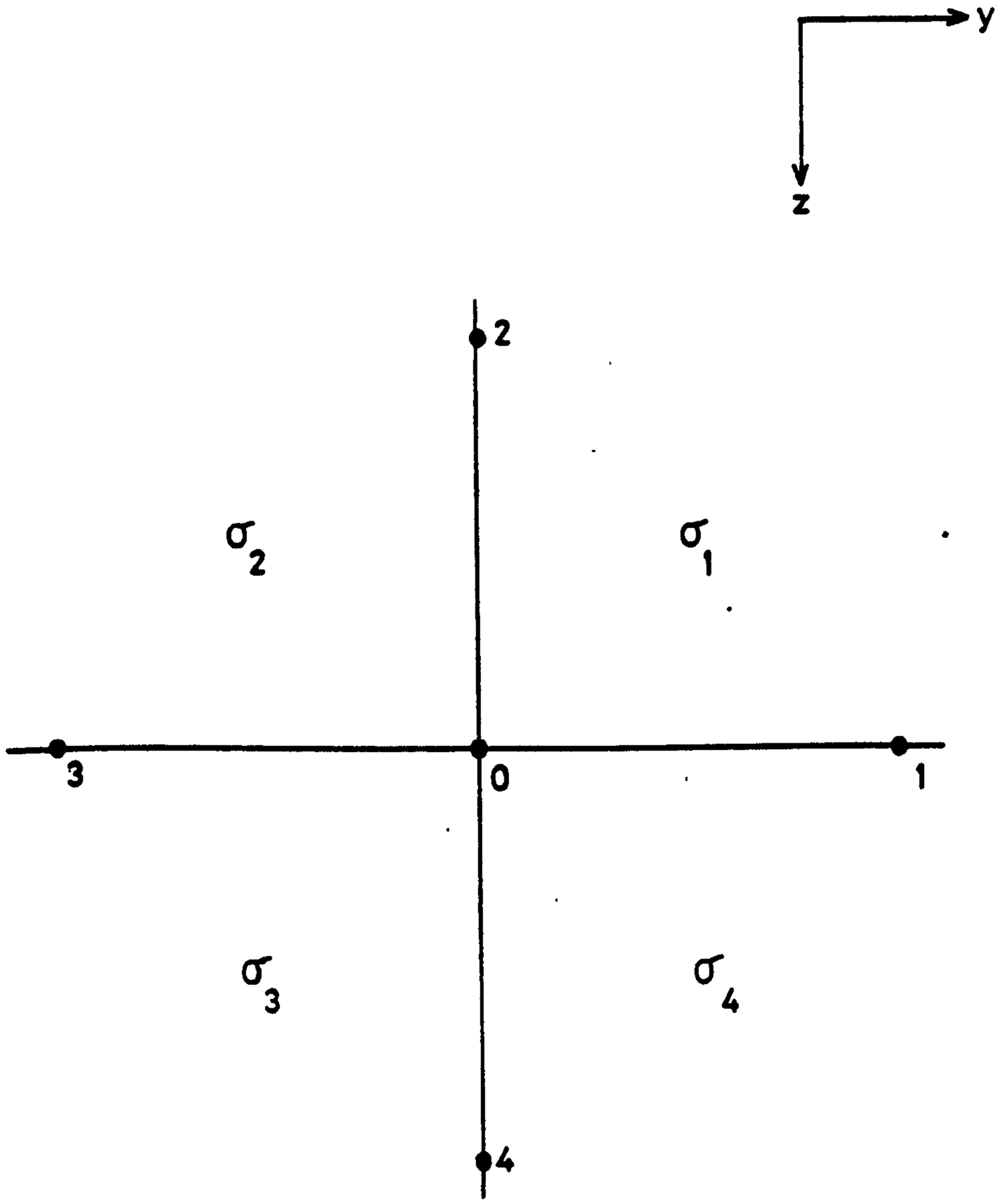

Figure 6·5.

Node at a junction of four regions of different conductivities.

$$E_2^{(3)} = E_2^{(4)}$$
$$E_3^{(4)} = E_3^{(1)} \qquad 6.6$$
$$E_4^{(1)} = E_4^{(2)}$$

Equations 6.4, 6.5 and 6.6 mean that the solution is overdetermined unless $\sigma_1 + \sigma_3 = \sigma_2 + \sigma_4$ i.e. unless the geometry is greatly simplified. Similar problems are also encountered in the H-polarization solution and when an irregular grid is used.

In their own analysis Brewitt-Taylor and Weaver allocated conductivity values at the centres of each grid element rather than at the grid points and allowed for a smooth variation in conductivity between the assigned values. Conductivity elements are represented as $\sigma_{m+\frac{1}{2}\,n+\frac{1}{2}}$ to indicate the assignation to the grid element with corners at (m, n), (m, n+1), (m+1, n), (m+1, n+1). Assuming that at the edges of the model the problem becomes one-dimensional ($y \to \pm\infty, \sigma \to \sigma(z)$) and allowing for variable grid spacings by defining

$$h_m = y_{m+1} - y_m \quad k_n = z_{n+1} - z_n \qquad 6.7$$

the central difference formula for the first and second derivatives of the electric field at the edges of the model are given by

$$\frac{\partial E_n}{\partial z} = \frac{E_{n+1}k_{n-1}}{k_n(k_n+k_{n-1})} + \frac{E_n(k_n-k_{n-1})}{k_nk_{n-1}} - \frac{E_{n-1}k_n}{k_{n-1}(k_n+k_{n-1})} \qquad 6.8$$

$$\frac{\partial^2 E_n}{\partial z^2} = \frac{2E_{n+1}}{k_n(k_n+k_{n-1})} - \frac{2E_n}{k_nk_{n-1}} + \frac{2E_{n-1}}{k_{n-1}(k_n+k_{n-1})} \qquad 6.9$$

These give a finite difference representation of equation 2.33, for E-polarization, applying the condition of continuity of $\partial E/\partial z$, of

$$\frac{E_{n+1}}{k_n(k_n+k_{n-1})} - \frac{E_n}{k_nk_{n-1}} + \frac{E_{n-1}}{k_{n-1}(k_n+k_{n-1})} = \frac{1}{2}i\mathcal{K}_nE_n \qquad 6.10$$

where

$$\nu_n = \frac{k_{n-1}\nu_{n-\frac{1}{2}} + k_n\nu_{n+\frac{1}{2}}}{k_n + k_{n-1}} \qquad 6.11$$

ν being related to σ by $\nu = \omega\mu_0\sigma$.

This finite difference representation is the same as that for the case where the conductivity at the grid point n is given by the weighted mean (6.11) of the assigned values above and below. The generalization into two dimensions gives a finite difference equation which represents a variation in conductivity such that the value at any grid point is given by a similar weighted mean of the four actual assigned values of conductivity surrounding the point

$$\nu_{mn} = \frac{K_{mn} + K_{mn-1} + K_{m-1n} + K_{m-1n-1}}{(h_m + h_{m-1})(k_n + k_{n-1})} \qquad 6.12$$

where $K_{mn} = h_m k_n \nu_{m+\frac{1}{2}\, n+\frac{1}{2}}$.

For $\underline{H}$-polarization a similar procedure can be followed using equation 2.35. The result, which defines not only the conductivity at a grid point but also its gradient (note the presence of $\underline{\nabla}\sigma$ in equation 2.35) is

$$\rho_{mn} = \frac{R_{mn} + R_{mn-1} + R_{m-1n} + R_{m-1n-1}}{(h_m + h_{m-1})(k_n + k_{n-1})} \qquad 6.13$$

$$\left(\frac{\partial\rho}{\partial z}\right)_{mn} = \frac{2}{(h_m + h_{m-1})(k_n + k_{n-1})}\left\{\frac{R_{mn} + R_{m-1n}}{k_n} - \frac{R_{mn-1} + R_{m-1n-1}}{k_{n-1}}\right\} 6.14$$

$$\left(\frac{\partial\rho}{\partial y}\right)_{mn} = \frac{2}{(h_m + h_{m-1})(k_n + k_{n-1})}\left\{\frac{R_{mn} + R_{mn-1}}{h_m} - \frac{R_{m-1n} + R_{m-1n-1}}{h_{m-1}}\right\} 6.15$$

where $\rho_{mn} = 1/\nu_{mn}$ and $R_{mn} = h_m k_n \rho_{m+\frac{1}{2}\, n+\frac{1}{2}}$.

The smoothly varying conductivity functions 6.12 and 6.13 lead, with suitable boumdary conditions, to relatively simple

finite difference formulations for the fields in both the E and H-polarization cases. Three boundary conditions are applicable in both cases. They are:

1) the assumption made earlier - that at the sides of the model the problem becomes one-dimensional. That is, as $y \to \pm\infty$, $\sigma \to \sigma(z)$.

2) In the region above the surface of the Earth ($z<0$) the magnetic field is a constant (H_c) at the edges of the model.

3) The magnetic field does not penetrate the bottom of the model, i.e. as $z \to \infty$, $H \to 0$.

Two further boundary conditions are applicable to the E-polarization problem:

4) As $y \to \pm\infty$ in the region $z>0$, $E \to E^{\pm}$ and $\mathcal{H} \to \mathcal{H}^{\pm}$, so that

$$\frac{\partial^2 E^{\pm}}{\partial z^2} = i\mathcal{H}^{\pm} E^{\pm}$$

subject to the conditions that $E^{\pm} \to 0$ as $z \to \infty$ and that $(\partial E/\partial z)_{z=0} = i\omega H_c$.

5) Finally, at large distances $(y^2 + z^2)^{1/2}$ the electric field in the region $z<0$ satisfies

$$E \sim \bar{E} - i\omega H_c z + \left(\frac{\Delta E}{\pi}\right)\arctan\left(\frac{y}{|z|}\right)$$

where $\bar{E} = \frac{1}{2}(E^{+} + E^{-})_{z=0}$ and $\Delta E = (E^{+} - E^{-})_{z=0}$.

The additional boundary condition for the H-polarization problem is equivalent to (4) above. Namely that $B \to B^{\pm}$ as $y \to \pm\infty$ so that

$$\rho^{\pm}\frac{\partial^2 B^{\pm}}{\partial z^2} + \frac{\partial \rho^{\pm}}{\partial z}\frac{\partial B^{\pm}}{\partial z} = iB^{\pm}$$

subject to $(B^{\pm})_{z=0} = H_c$, which follows from (2).

Supplementary to the conditions (1) - (5), it is also necessary that the tangential components of the fields within the

model are continuous across boundaries and that the normal component of $\underline{H}$ is also continuous.

Applying these conditions the finite difference expression for the interior points of the grid for $\underline{E}$-polarization is

$$\frac{2k_n}{h_m+h_{m-1}}\left(E_{m+1n}+\frac{h_m}{h_{m-1}}E_{m-1n}\right)+\frac{2h_m}{k_n+k_{n-1}}\left(E_{mn+1}+\frac{k_n}{k_{n-1}}E_{mn-1}\right)$$

$$=\left(\frac{2k_n}{h_{m-1}}+\frac{2h_m}{k_{n-1}}+ih_mk_n\mathcal{H}_{mn}\right)E_{mn} \qquad 6.16$$

Once the solution for the electric field has been obtained the magnetic field solution can be found by using equation 2.36. Similarly, once the finite difference solution for the $\underline{H}$-polarization case has been found equation 2.37 gives the electric field. From the field solutions at the surface of the Earth impedances and hence apparent resistivites and phases can be calculated.

Programs to calculate these quantities from the electric field values (for the $\underline{E}$-polarzation) and magnetic field values (for the $\underline{H}$-polarization) output by the modelling program, were written by E. Mbipom (pers. comm.) and the author respectively.

The diakoptic form of the program (Brewitt-Taylor and Johns, 1980) which was actually used, draws an analogy between the two-dimensional induction problem and a transmission surface network such as that shown in figure 6.6. For the $\underline{E}$-polarization case the following equivalences are used:

V_{ij} = voltage at (i,j) ≡ E_{ij} = electric field at (i,j)

TR = (transverse components) ≡ inductors with L = μ_o Henry

CG = (components to ground) ≡ resistors, R = $1/h^2\sigma$ Ohms

In the $\underline{H}$-polarization case

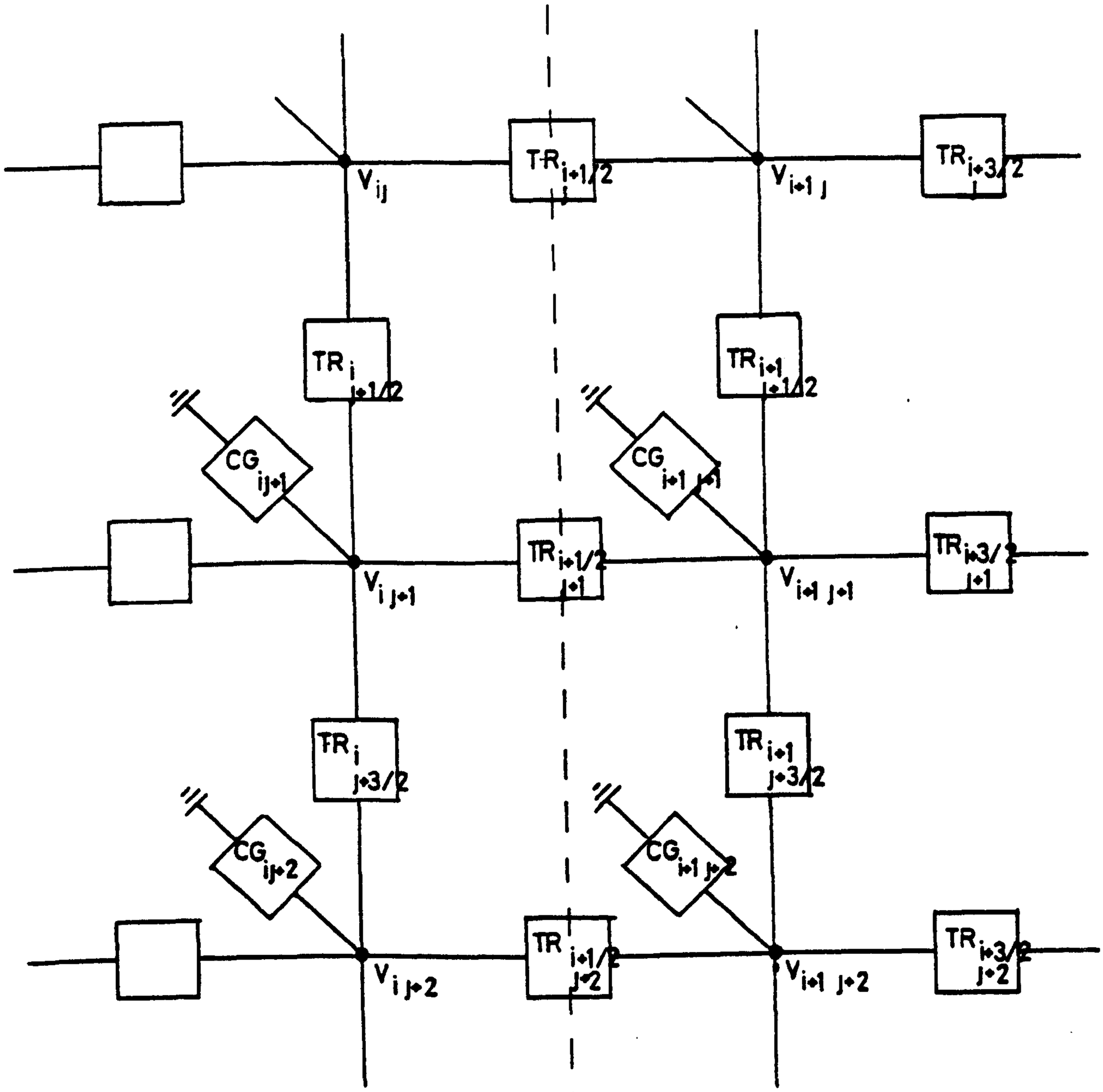

V_{ij}	=	E_{ij}	H_{ij}
TR_{ij}	=	$L_{ij} = \mu_o$ Henrys	$R_{ij} = \sigma$ Ohms
CG_{ij}	=	$R_{ij} = 1/h^2\sigma$ Ohms	$C_{ij} = 1/h^2\mu_o$ Farads

Figure 6·6.

Transmission surface analogy for the solution of 2-D induction problems.

$V_{ij} \equiv H_{ij}$ = magnetic field

TR ≡ resistors, R = σ Ohms

CG ≡ capacitors, C = $1/h^2\mu_o$ Farads.

Averaged values are used when the grid is irregular. The principal feature of the program is the facility allowing the problem to be sub-divided into sections, each of which can be solved individually. The complete solution can then be obtained by adding all the section solutions together. The main advantage of this method of analysis is that when alterations are made to only one part of the model the solutions to other sections can be left unchanged.

However, for the models constructed in this study, vast amounts of computer time and storage were not necessary and the models were treated as a single problem rather than being sub-divided.

6.3.2: Modelling procedure and results.

The evolution of the conductivity model is best described by considering the process at each of the five stages illustrated in the block diagram of figure 6.7.

1) Stage 1.

The results of the one-dimensional modelling were used to construct a conductivity profile across the South of Scotland, this profile is shown in figure 6.8a. Average values from the 1-D model ranges were taken for the conductivities and depths of the layers, and smooth boundaries drawn along the profile. From the profile the initial two-dimensional model, Model A - figure 6.8b, was produced. Figure 6.8b represents Model A on a grid point scale, thus one unit is one grid spacing and not indicative of an actual physical scale. The positions of the grid points, in

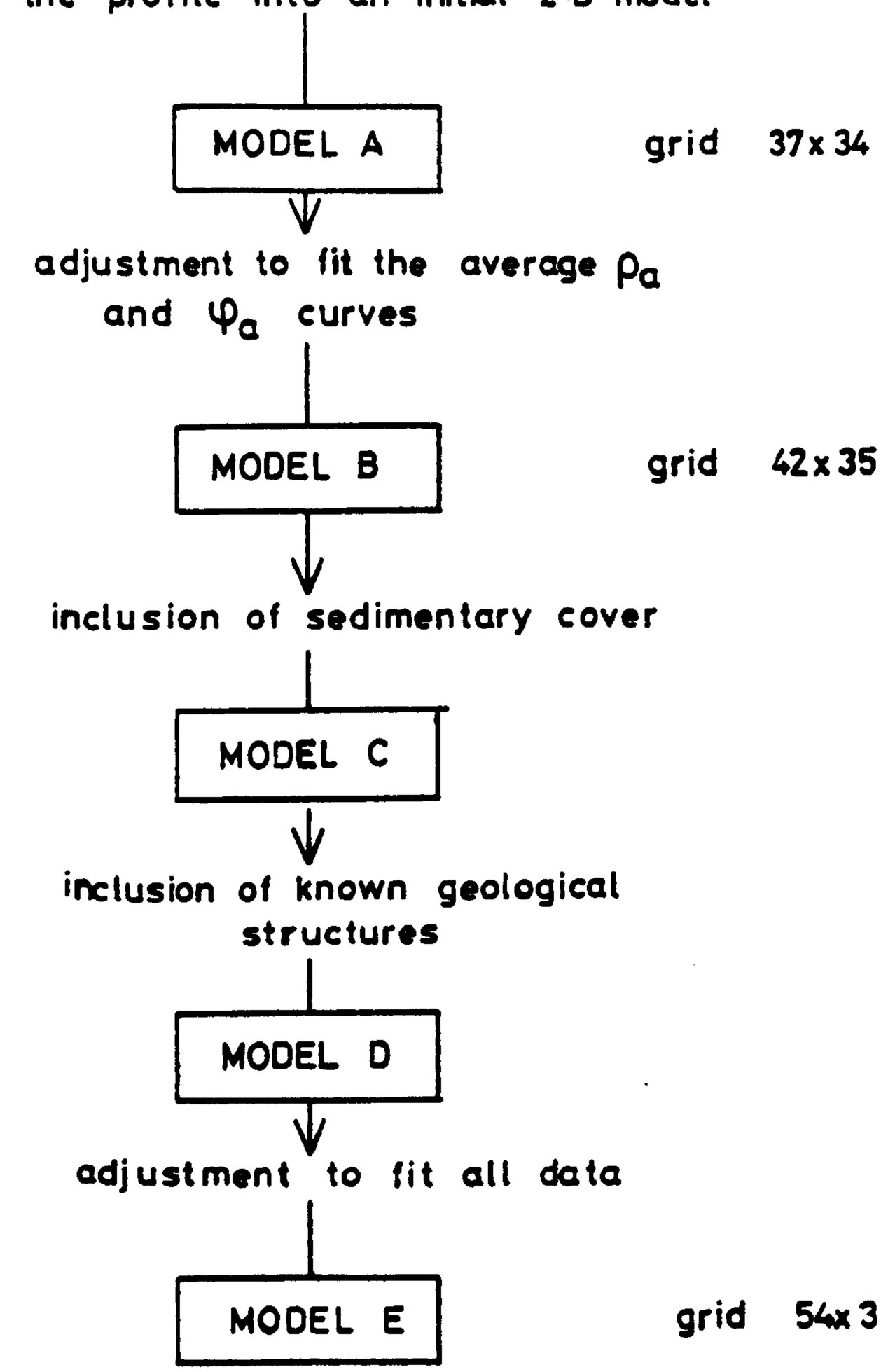

Figure 6-7.
Two-dimensional modelling procedure.

kilometers, centred on Kinross at (0, 0) are tabulated on the right of the model. The Highland Boundary Fault, Southern Uplands Fault and the positions of the sites are all marked. For comparison figure 6.8c shows the model on a true physical scale.

Model A is a relatively simple representation of the conductivity profile in figure 6.8a, containing only four conductivities and three major vertical discontinuities, all close to the faults. Thus, as there were few parameters initially, model improvement tended to lead to more complicated models.

2) Stage 2.

The second stage in the two-dimensional modelling process was the adjustment of Model A to fit the averaged resistivity and phase values at each site, and as far as possible, the variation in Z/H along the traverse. As a guide to the kind of model alteration required, sets of one-dimensional model curves were produced, each set having one variable parameter. Thus an indication could be obtained of how the model should be adjusted to bring about a desired change in apparent resistivity and phase. The following variations were investigated

i) In a three layer one-dimensional model of the type resistor - conductor - resistor, increasing the depth to the basement resistor (i.e. making the conducting layer thicker) lowers the apparent resistivity at longer periods and increases the phase.

ii) In the same kind of model, increasing the resistivity of the middle layer increases the apparent resistivity at all periods and lowers the phase at short periods.

iii)Increasing the thickness of the surface resistor increases both the phase and apparent resistivity at short periods.

iv) The presence of a thin conducting layer at the surface has

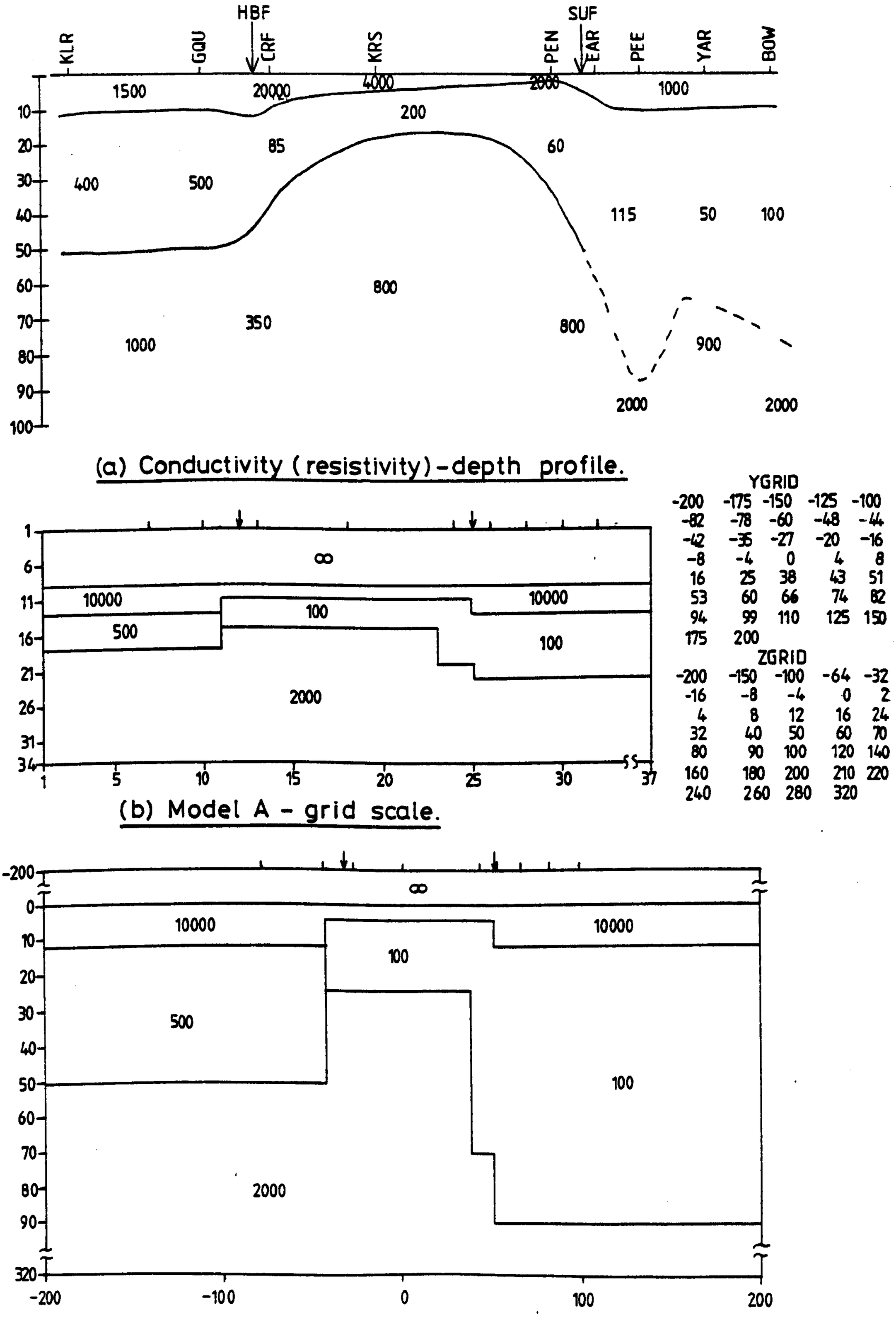

Figure 6·8.

Resistivities in Ω-m.
Distances / depths in km.

very little effect on the apparent resistivity but decreases the phase at short periods.

Examples of (ii) and (iii) are shown in figure 6.9.

The main conclusions arrived at from the generation of the kinds of one-dimensional models discussed above, are that, firstly, the general amplitude of the apparent resistivity curve is fixed by the conductivity of the intermediate conducting layer, and secondly, the shape of the phase curve depends on conductivity contrasts rather than actual values.

A reasonable general fit to the data was obtained from Model B, which is shown in figure 6.10a on a grid point scale as in figure 6.8b. In the course of arriving at Model B the size of the grid was expanded to 42 x 35, the grid points are also listed in figure 6.10.

3) Stages 3 and 4.

Having obtained a fit to the averaged magnetotelluric data and the Z/H variation, Model B was adjusted to take into account known geological structures. Initially a superficial sedimentary layer was included to the depths indicated by the LISPB profile (figure 3.5). This was then changed to take account of thinner sediments over the Ochil Hills (grid points 18 to 23) and deeper sediments in the other parts of the Midland Valley. The resulting model, Model C, is shown in figure 6,10b.

From (iv) above it is clear that the existence of a thin sedimentary layer has relatively little effect on the apparent resistivity and phase at the periods involved in this study. Thus the representation of sedimentary cover in the models is very schematic and it is really an integrated conductivity, rather than the actual conductivuty, that matters. For example, the

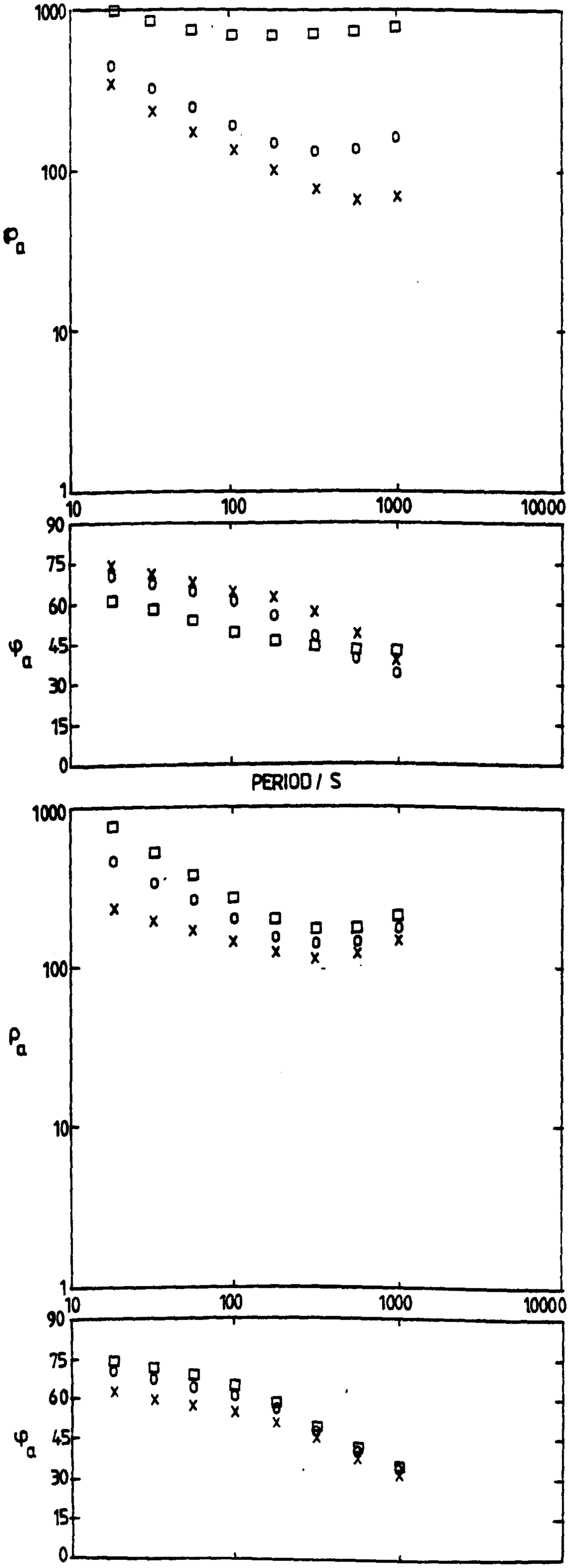

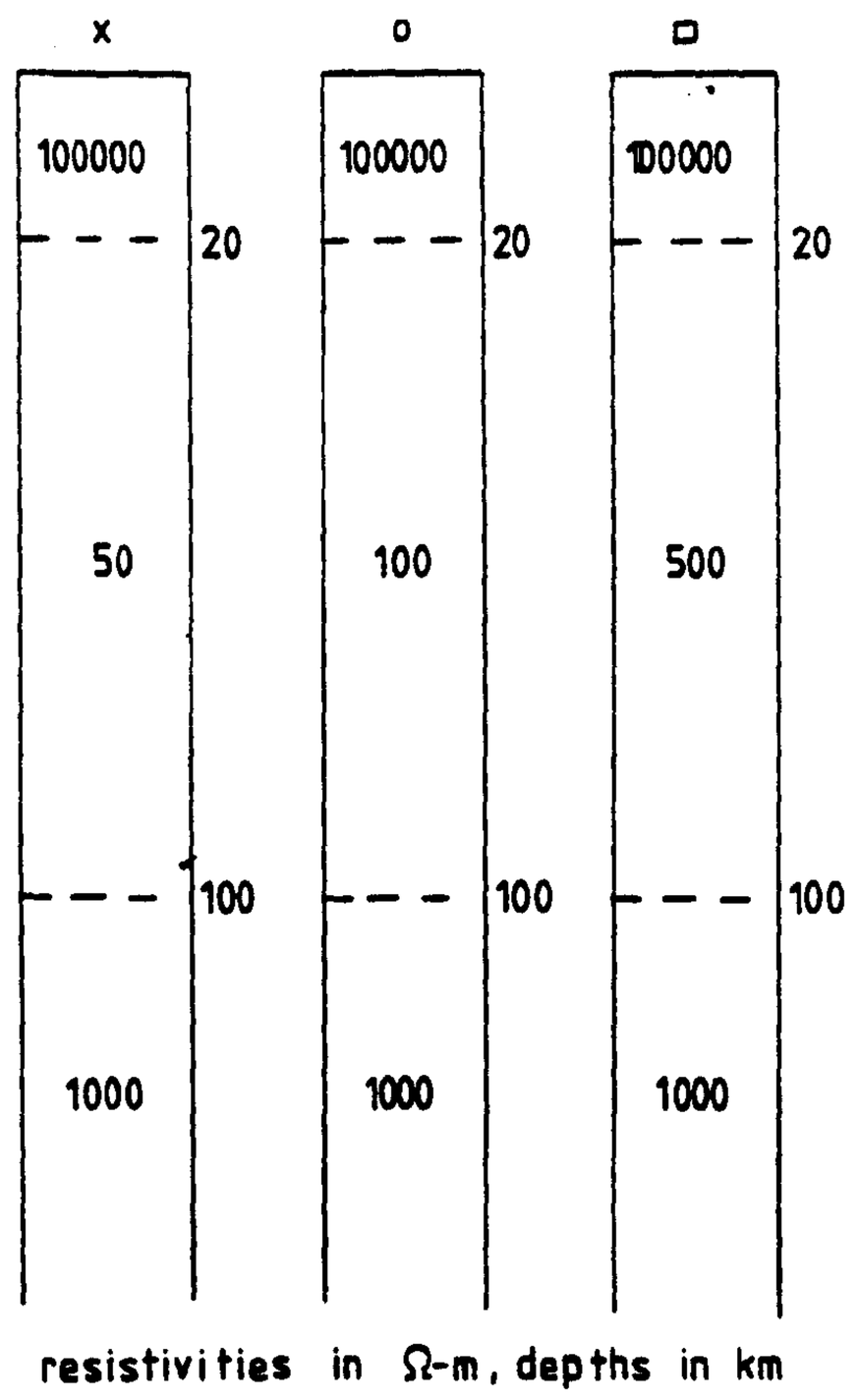

resistivities in Ω-m, depths in km

(a) Effect of an underlying conducting layer on ρ_a and φ_a.

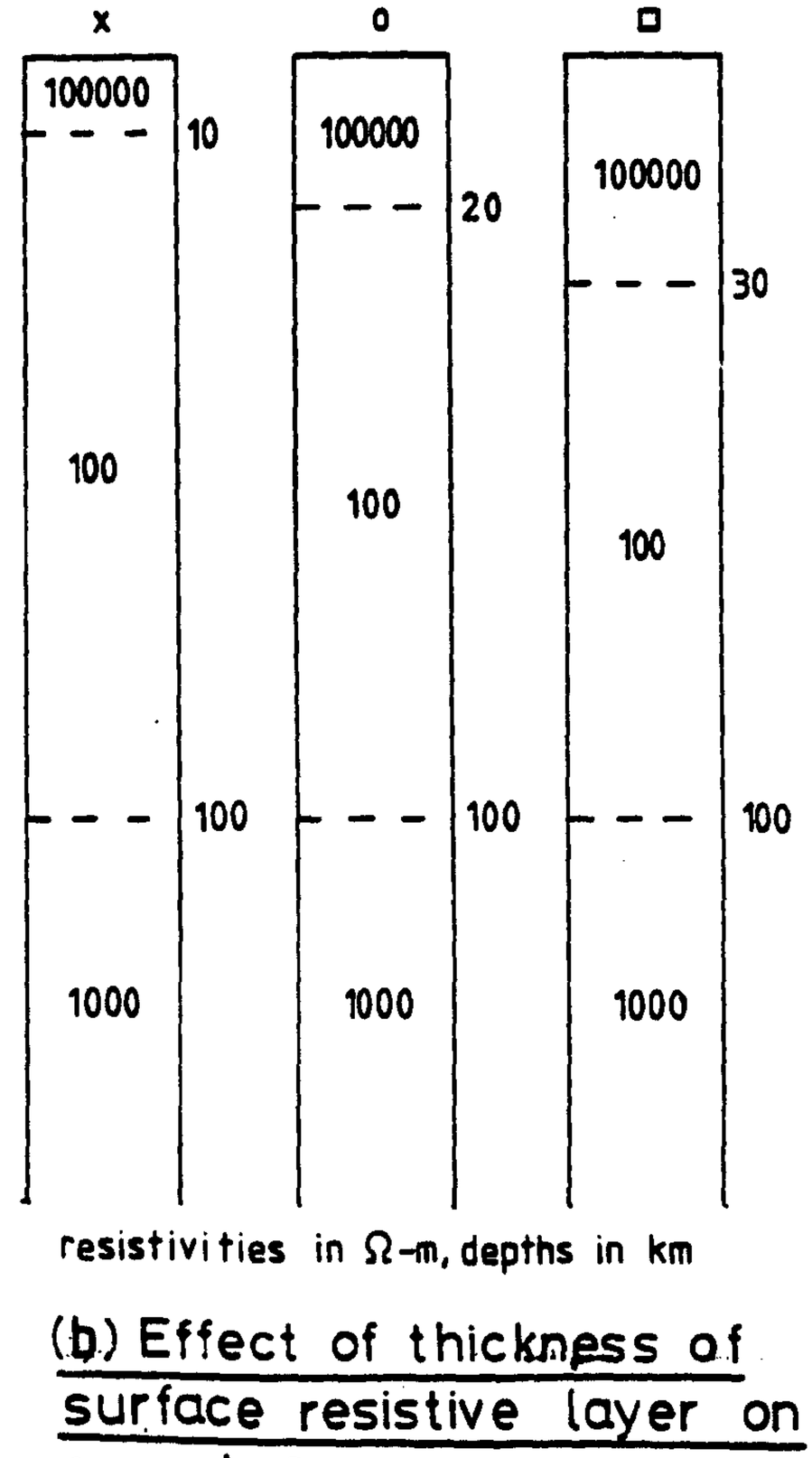

resistivities in Ω-m, depths in km

(b) Effect of thickness of surface resistive layer on ρ_a and φ_a.

Figure 6·9.

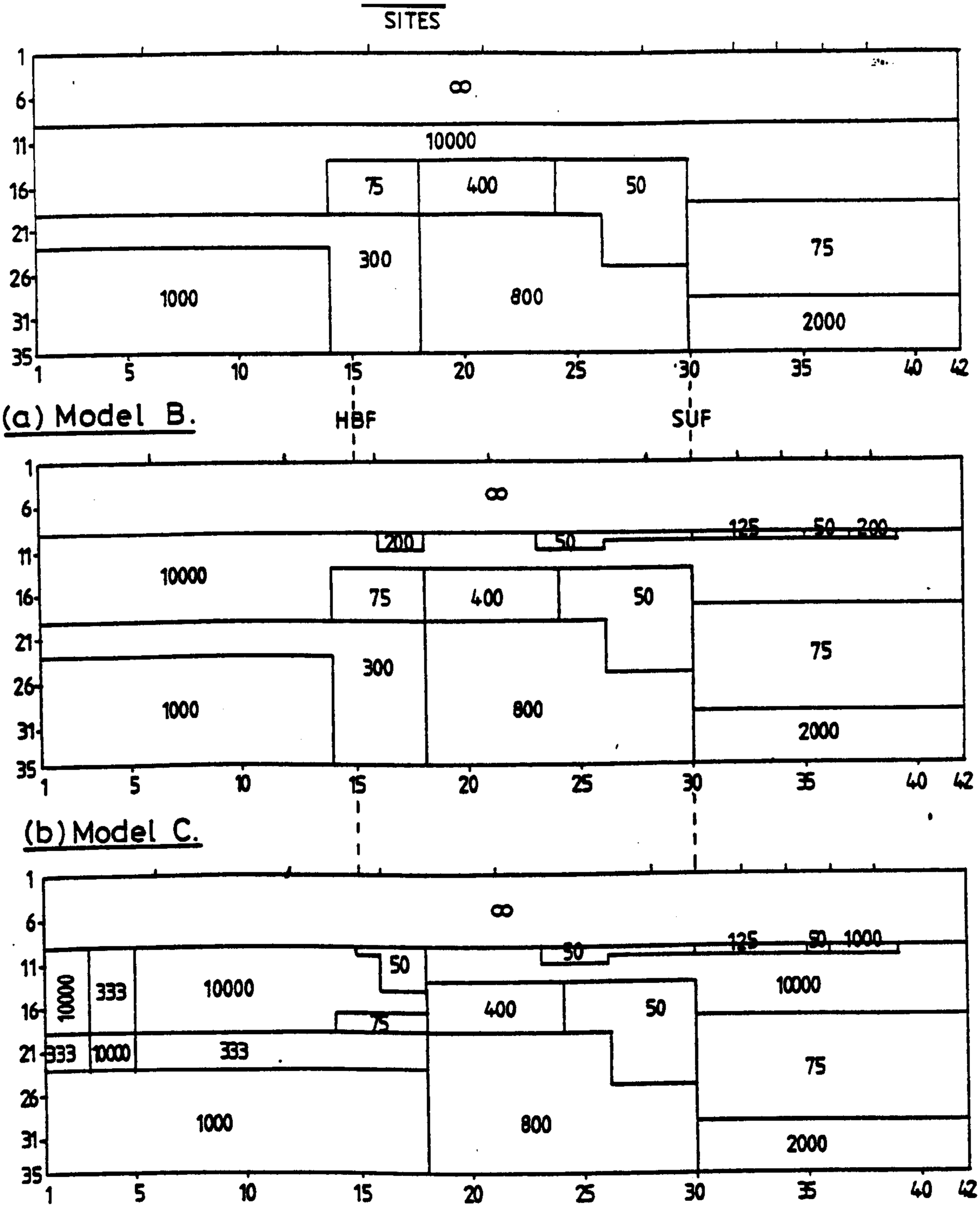

Figure 6·10.

Two-dimensional models of S.Scotland.

resistive layer of 125 Ω-m extending to 1 km depth (the minimum depth on the grid used), in the northern part of the Southern Uplands, could be replaced by either a layer 2 km thick of 250 Ω-m or a half kilometer layer of 62.5 Ω-m. Similarly the absence of a surface conducting layer does not imply that no such layer exists but that it is neither thick enough nor conducting enough to affect the model results. The appendix deals with audiomagnetotelluric measurements which were used to investigate the sedimentary cover in the Midland Valley and the Southern Uplands.

Model D (figure 6.10c) was derived by alteration of Model C to take account of the possibility of deep sediments between the Ochil Hills and the Highland Boundary Fault and a conducting zone of graphitic schists to the north of the fault. The inclusion of these two features did in fact improve the overall fit of the model by changing the relative magnitudes of the $\rho_{//}$ (E-polarization) and $\rho_{\perp}$ (H-polarization) curves at both KLR and CRF so that they correspond better to the field curves from these sites.

4) Stage 5.

A good fit to the averaged magnetotelluric results, taking into account known and probable geological structure, was provided by Model D. However, the fit of this model to the Z/H variation, although reasonable, was not particularly good at the NW end of the traverse. Furthermore, the final model should fit the apparent resistivities and phases both parallel and perpendicular to the geological strike (with the E- and H-polarizations respectively) at all the sites. This was not the case with Model D.

The final stage of the modelling procedure therefore, was further adjustment of Model D to fit the actual apparent

resistivity and phase curves rather than the average, and to provide a better fit to Z/H. This involved a further expansion of the grid size to 54 x 35 and a considerable increase in the complexity of the model. The final model, Model E, is shown in figure 6.11 on a physical scale. The fit of the model curves for both E- and H-polarizations at all sites, and the fit of the Z/H variation along the traverse at periods of 60, 120 and 300 seconds is shown in figures 6.12 and 6.13.

The model has a general form similar to the one-dimensional models of resistor - conductor - resistor. The conducting layer is most marked in the south and penetrates to its deepest extent beneath the Southern Uplands. The layer thins considerably in the central part of the Midland Valley and is much more resistive to the north where it again becomes thicker and deeper. The upper crustal structure of the model is complex with many vertical boundaries. The reasons for some of these features are listed below.

i) The 50Ω-m block at a shallow depth between -155 and -115 km represents the conducting anomaly associated with the Great Glen, detected by Kirkwood (pers. comm.) and Mbipom (1980). Despite its distance from the sites in this study, the Great Glen anomaly is necessary to produce the positive values of Z/H observed at the north-west end of the traverse. Although the anomaly does in fact have considerable structure, delineated by Mbipom, its inclusion as a rectangular block in Model E is sufficient to have the desired effect on Z/H.

ii) The resistive block of 33333Ω-m beneath KLR represents the Cairngorm granite and is required to produce sufficient contrast with the region of 2000Ω-m to the south-east, to make the value

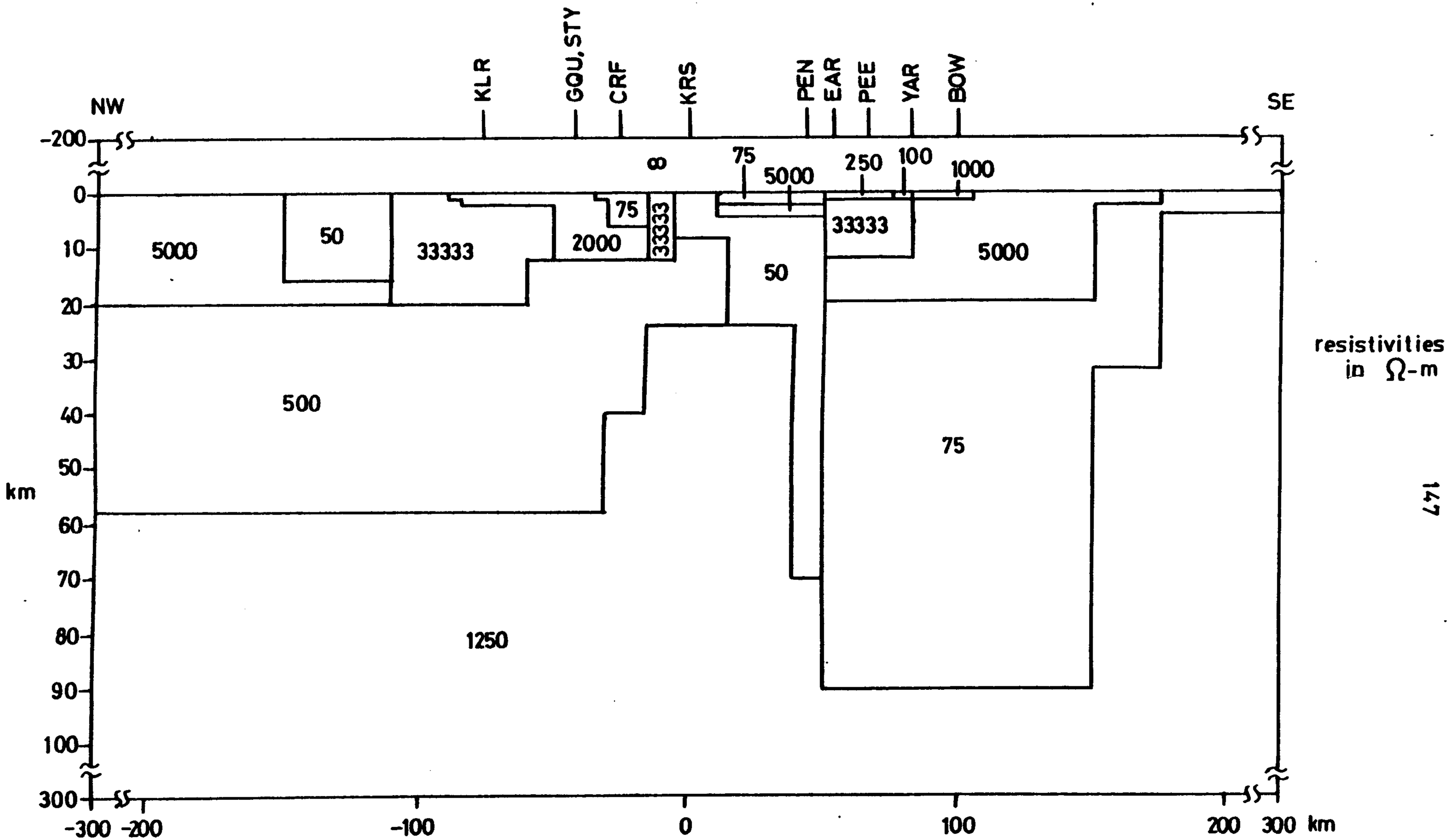

Figure 6·11. Model E.

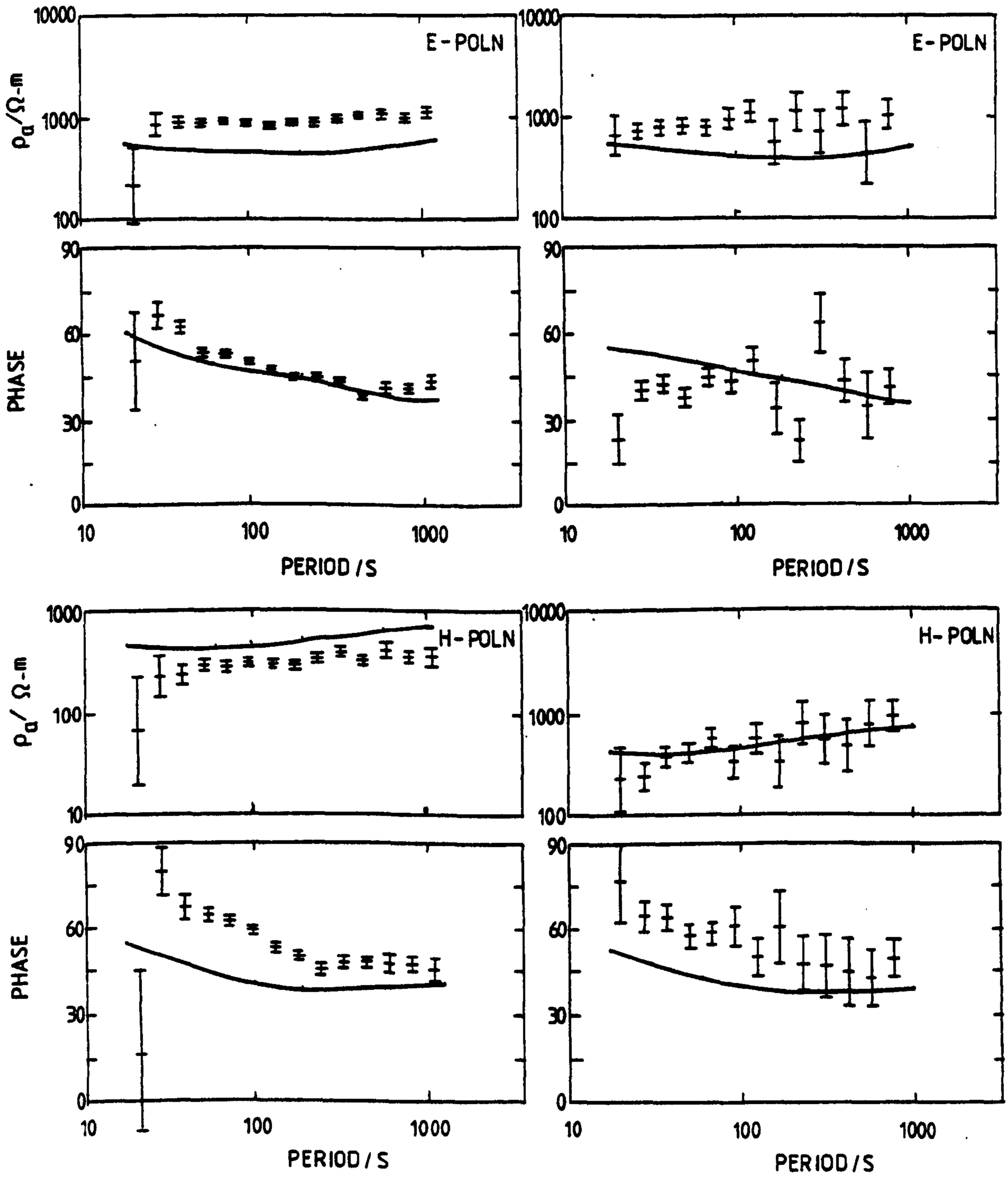

Figure 6·12.

Fit of Model E to field data.

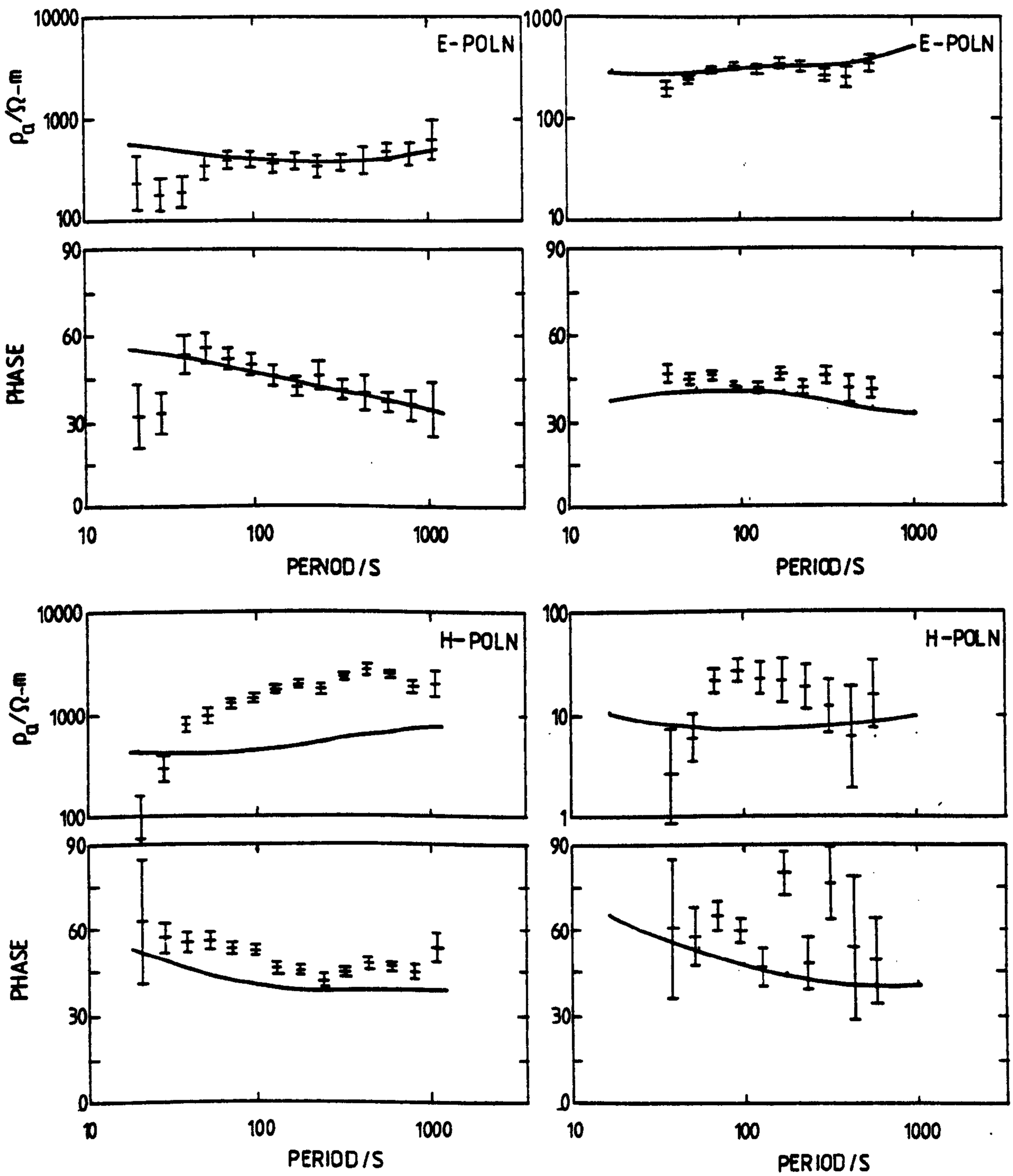

Figure 6·12.

Fit of Model E to field data.

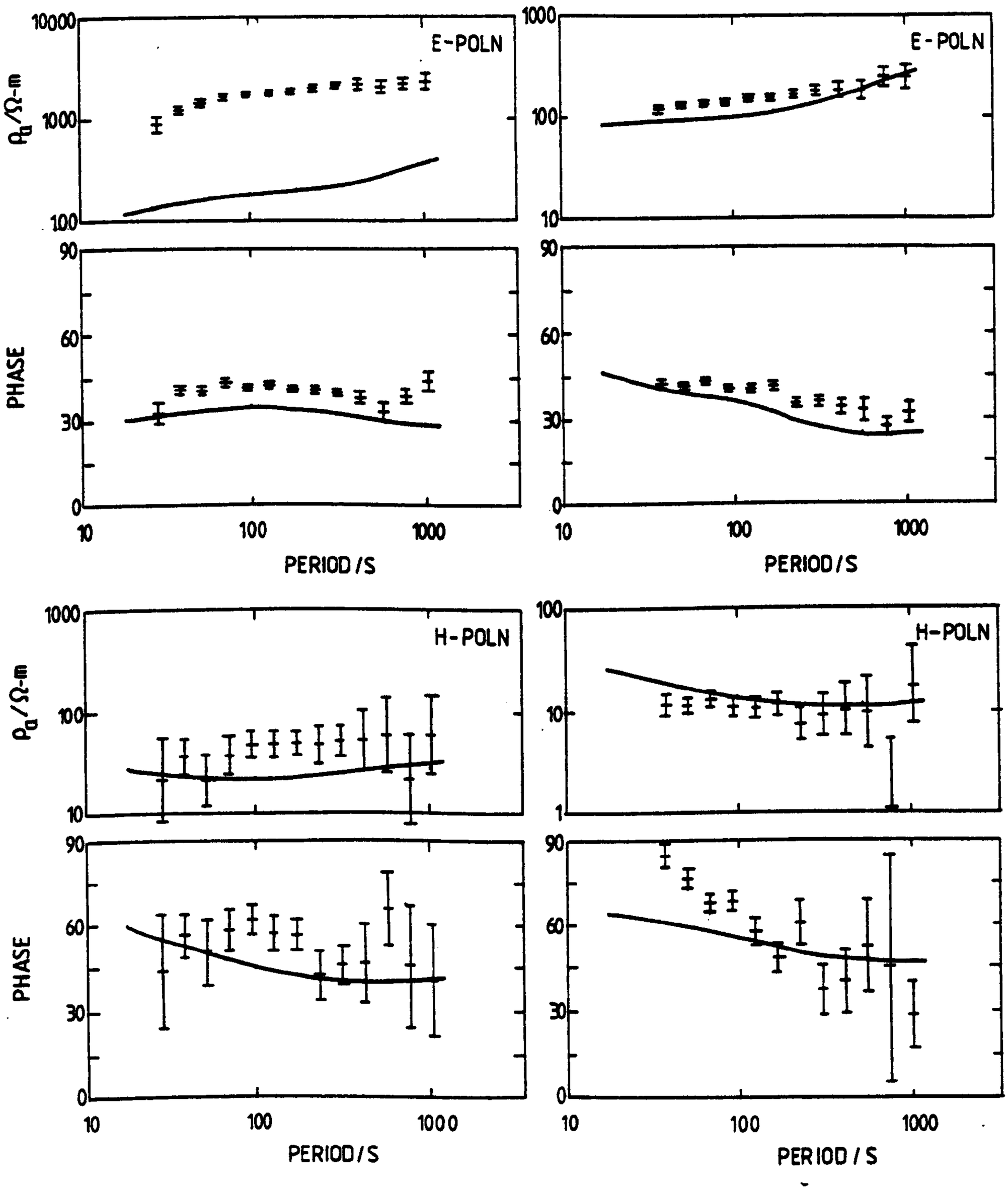

Figure 6·12.

Fit of Model E to field data.

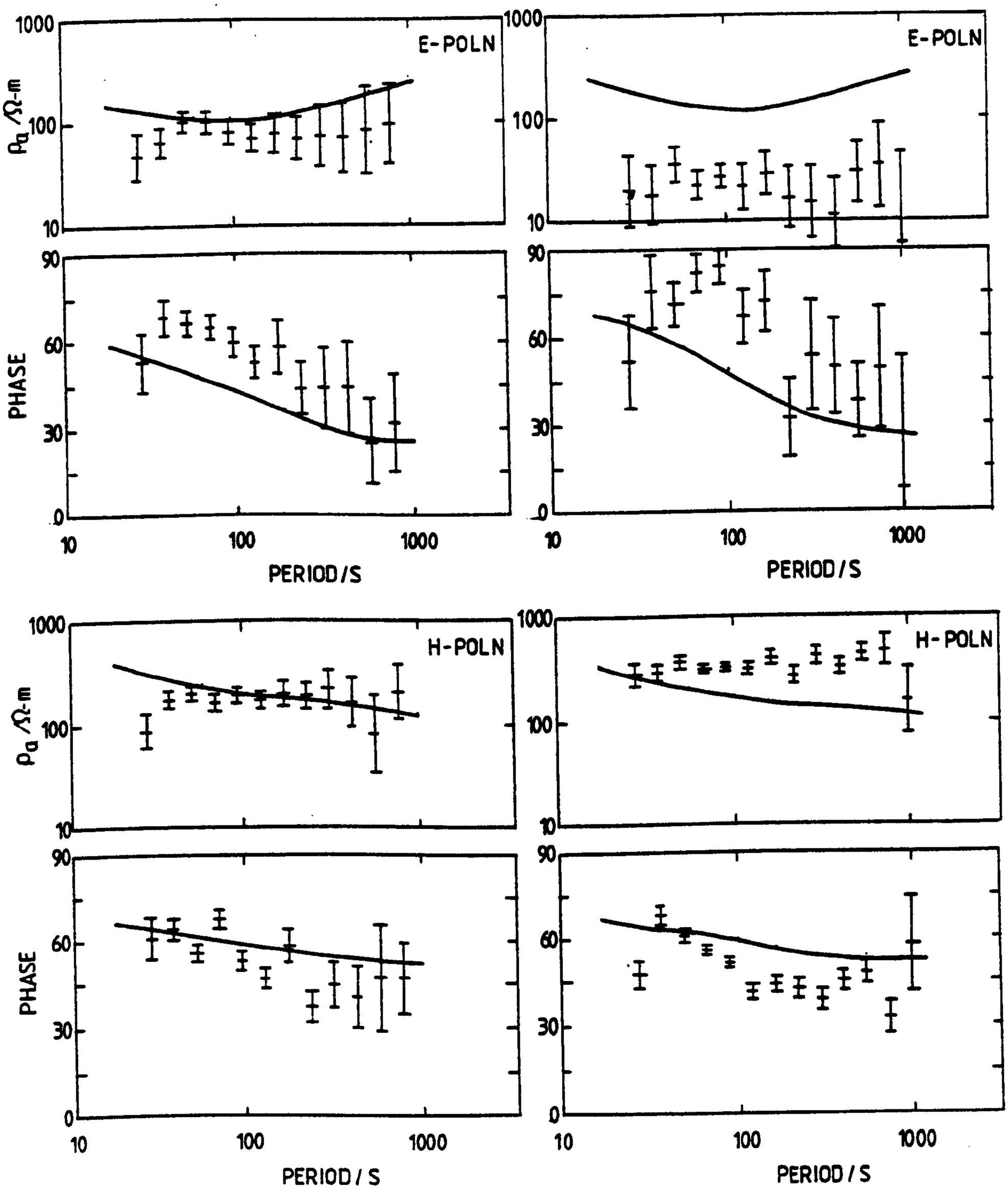

Figure 6·12.

Fit of Model E to field data.

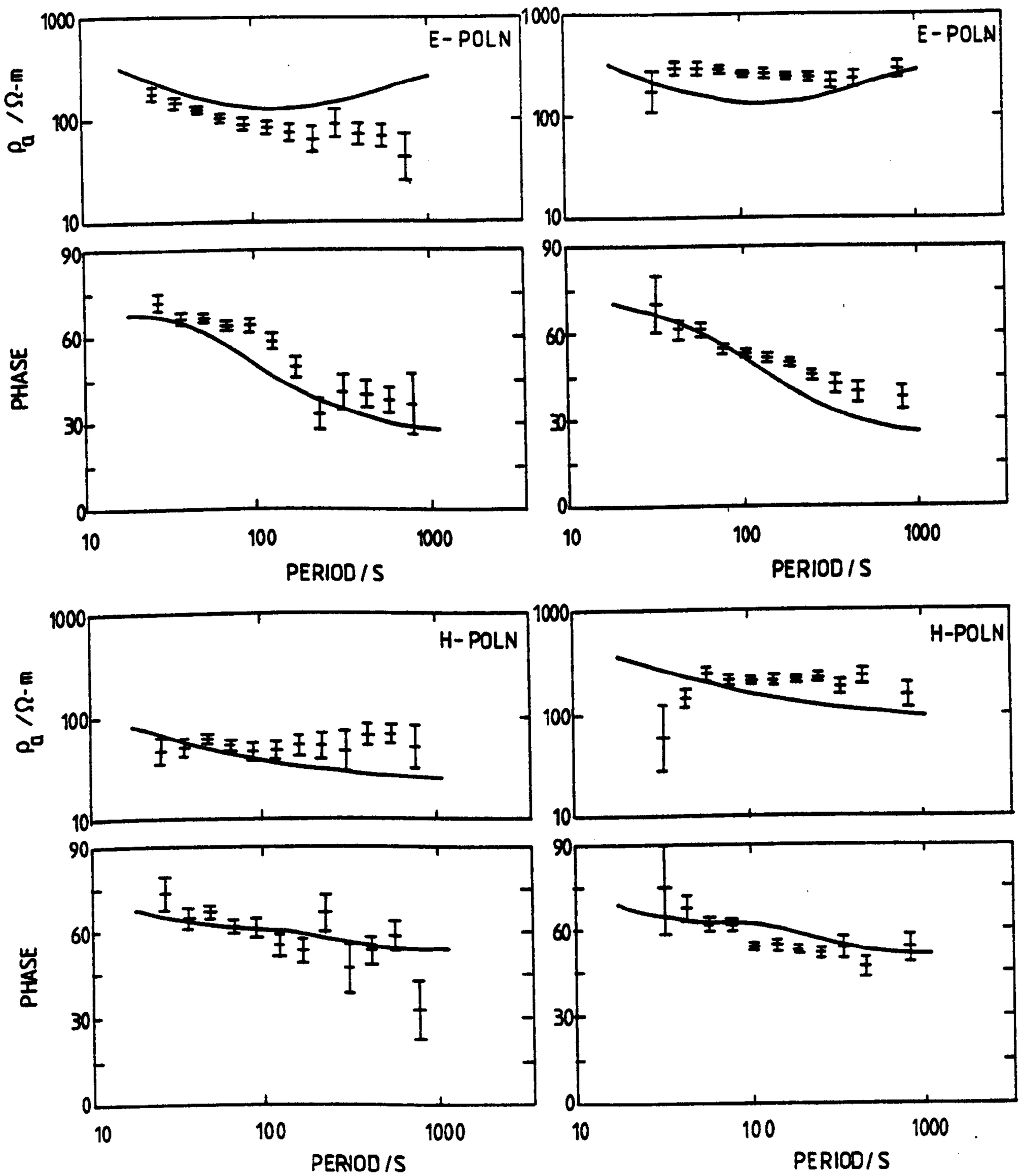

Figure 6·12.

Fit of Model E to field data.

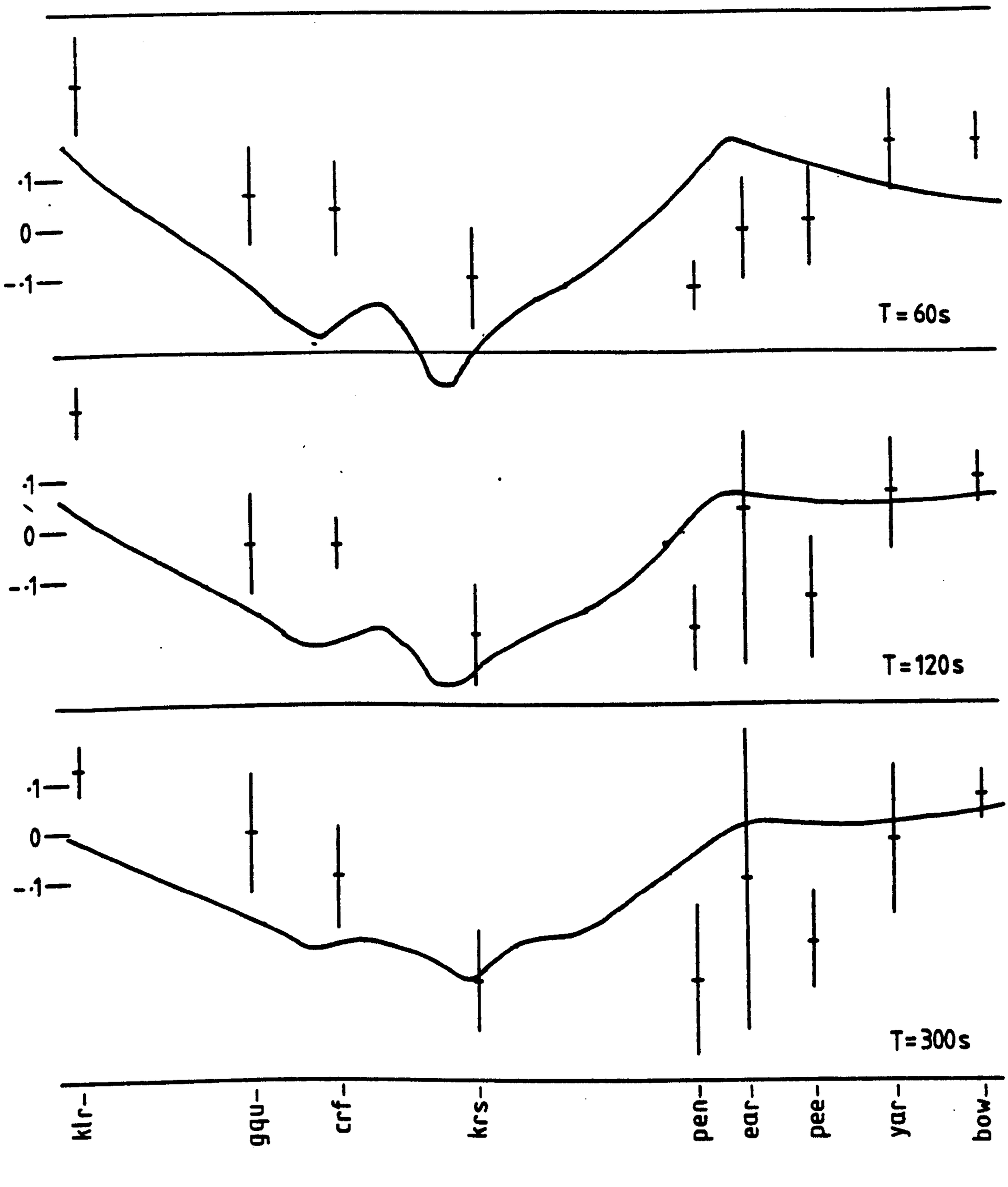

Figure 6·13.

Z/H variation across South Scotland for a horizontal field in the direction N150°E.

\+ observation

—— model

of $\rho_{//}$ greater than $\rho_{\perp}$, as observed, at both KLR and GQU. The latter, more conducting region replaces the belt of graphitic schists in Model D. It was noted in chapter 5 that a difference exists between the relative magnitudes of $\rho_{//}$ and $\rho_{\perp}$ at GQU and STY even though the two sites are in a similar situation with respect to the Highland Boundary Fault. This difference can be interpreted as being due to local deviations from two-dimensionality, close to the Fault (chapter 7).

iii) The highly resistive (33333Ω-m) and conducting (50Ω-m) sections, coming to the surface between CRF and KRS are needed to produce the anisotropic apparent resistivities observed at KRS. As can be seen from figure 6.12c, though the low H-polarization resistivity is modelled satisfactorily, the E-polarization value is still low by a factor of 10. However, such a structure was the only one found which could produce even this amount of anisotropy and it is possible that using a finer grid, so that KRS could be positioned closer to the boundary, would increase the anisotropy in the way that might be expected from figure 2.3. The resistive zone coincides with the surface extent of the lavas of Old Red Sandstone age associated with the Ochil Hills.

iv) The Tweedale granite proposed by Lagios (1979) and Lagios and Hipkin (1979) is represented by the third highly resistive block beneath EAR, PEE and YAR. However, the period of variations used in this study are not really short enough to differentiate between near-surface resistors of 33333Ω-m and 5000Ω-m, both of which can be considered as very resistive compared to the underlying 75Ω-m region. Therefore the distinction between these two values is not a requirement of the magnetotelluric data and is made for compatibility with the gravity results. A more

detailed study of this part of the profile, using audiomagnetotellurics, is discussed in the appendix.

v) The 100Ω-m surface layer at YAR corresponds to the valley of the Yarrow Water, in which the site was situated, and is necessary to model the low values of $\rho_{\perp}$. At PEE, on the edge of the Tweed Valley, it is the $\rho_{/\!/}$ curve which has the low apparent resistivities and again, reference to figure 2.3 suggests that a finer grid, placing the site on the resistive side of a boundary, would give a better fit for the E-plarization curve.

vi) The rise to the surface of the 75 Ω-m layer, in the south-east, is based on Jones' 1-dimensional interpretation of results from Towhouse in the Northumberland Basin, and has no direct effect on the model results. However, the extension of this conducting zone beyond BOW is confirmed by the model fit to Jones' site at Newcastleton approximately 35 km to the south-east.

The overall fit of the model results to the field data has not been quantified. However, from examining figure 6.12, apart from STY, which does not lie directly on the line AA' (figure 4.3), only the $\rho_{/\!/}$ curves at KRS and PEE, both of which have been discussed above, are obvious misfits. The Z/H profile is less well modelled in detail, but the general shape, particularly in the north-west, has been matched. The discrepancy in the Southern Uplands may be rectified by a change in structure further to the south-east, where data has only recently been obtained (Novak, pers. comm.). However it is possible that the misfit in the southern part of the profile may be a result of conduction as well as induction. This will be dealt with in the next section.

The sensitivity of the model results to variations in

resistivities and depths was faily well established during the modelling process and the effects of some variations have already been discussed. As a further example, the depth to the good conducting layer, beneath the Southern Uplands is quite well defined by the high values of phase at short periods. Changing the depth produces a significant change in phase.

The principal boundary which was not well defined during the modelling is the lower boundary of the same conductor. To test the effect of changing the depth to this boundary, further models were tried. The conductor - resistor boundary was first put at 125 km and this resulted in apparent resistivity values at the longer periods which were too low. Raising the boundary to 58 km also failed to fit the data as it increased the magnitude of the apparent resistivity at all periods. This was rectified to a certain extent by lowering the resistivity of the conducting layer to 50Ω-m, however, the fit was not as good as for Model E.

An attempt was also made to represent the conducting layer by two conductors separated by a resistor. The presence of the intermediate resistor raised the value of apparent resistivity considerably, however, and did not provide a good fit to the data.

In the absence of longer period data to delineate the lower boundary better it was concluded that the optimum depth is as in the model.

It must be appreciated that some trade-off is possible between the depths and resistivities shown in figure 6.11, and that the resistivities are an indication of the order of magnitude rather than of the actual value. In particular the uniform basement of 1250 Ω-m could be split into several

different values; however, in the regions of the model containing good conductors, the basement resistivity has very little effect on the results and it has been kept uniform for convenience. A simplified version of Model E showing resistivity ranges and possible depth variations for the principal horizontal boundaries is shown in figure 6.14.

6.4: Equivalent line current modelling of the magnetic results.

In section 6.3 the modelling of the Z/H profile along the traverse was considered as an induction problem. This is not the only posibility however. Banks (1979) suggested that so many conductive regions have been identified in the upper 400 km of the Earth that it is unlikely that each region can be considered as isolated from its neighbours. Each conducting region should instead, be considered as modifying the regional electric currents experienced by other anomalous zones around it. The normal regional electric currents can be assumed to be induced in such widespread good conductors as the oceans; local conducting anomalies then deflect and channel these currents.

The general method of identifying such electric currents is to use the magnetic transfer functions A and B to construct hypothetical event contour maps, as indicated in chapter 5. Equivalent sheet or line currents, which model the contour plots, can then be calculated, and used as a guide to the delineation of complex conducting structures. Banks did this for geomagnetic array data from Kenya, whilst other examples are for the Pyrenees (Babour et al., 1976) and the Rhinegraben (Babour and Mosnier, 1979).

Ideally, as single station transfer functions are likely to

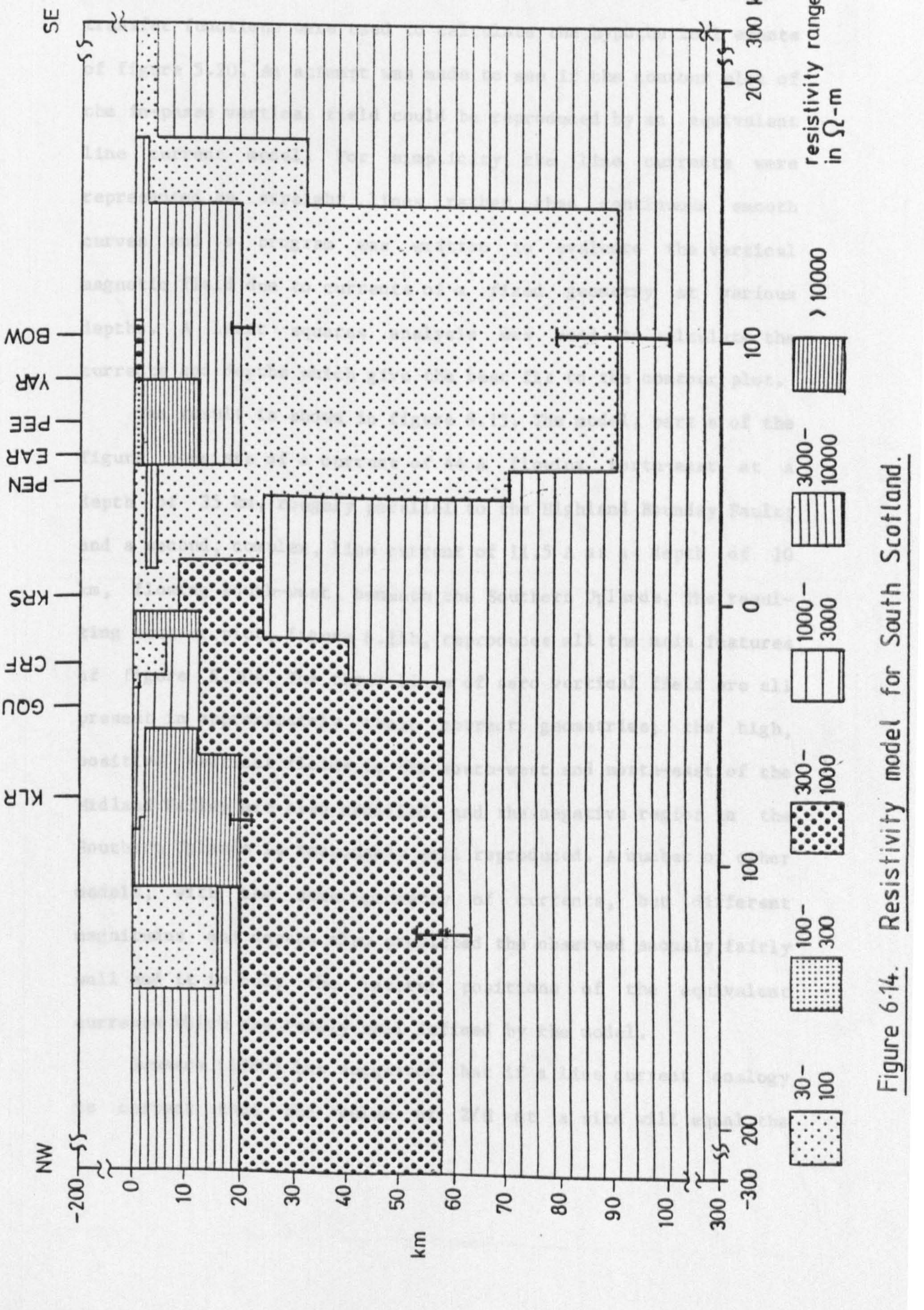

Figure 6·14. Resistivity model for South Scotland.

be biased by polarization effects (chapter 4), inter-station transfer functions should be used. However for the South of Scotland simultaneous data are not available and single station transfer functions were used to calculate the hypothetical events of figure 5.20. An attempt was made to see if the contour plot of the in-phase vertical field could be reproduced by an equivalent line current model. For simplicity the line currents were represented as straight lines rather than continuous smooth curves and a program was written to evaluate the vertical magnetic field due to currents of a fixed geometry at various depths. A least squares analysis was used to calculate the currents and depths which give the best fit to the contour plot.

The result is shown in figure 6.15. The model, part a of the figure, consists of a current of 44 A flowing north-east at a depth of 35 km, roughly parallel to the Highland Bounday Fault; and a second, complex, line current of 11.5 A at a depth of 10 km, flowing south-west, beneath the Southern Uplands. The resulting contour plot, figure 6.15b, reproduces all the main features of figure 5.20a. The three lines of zero vertical field are all present in approximately their correct geometries; the high, positive vertical fields to the south-west and north-east of the Midland Valley are also modelled, and the negative region in the Southern Uplands is reasonably well reproduced. A number of other models, with the same geometry of currents, but different magnitudes and depths also predicted the observed anomaly fairly well and it is only the lateral positions of the equivalent currents which are really well defined by the model.

Summers (1980) has suggested that if a line current analogy is correct then the value of Z/H at a site will equal the

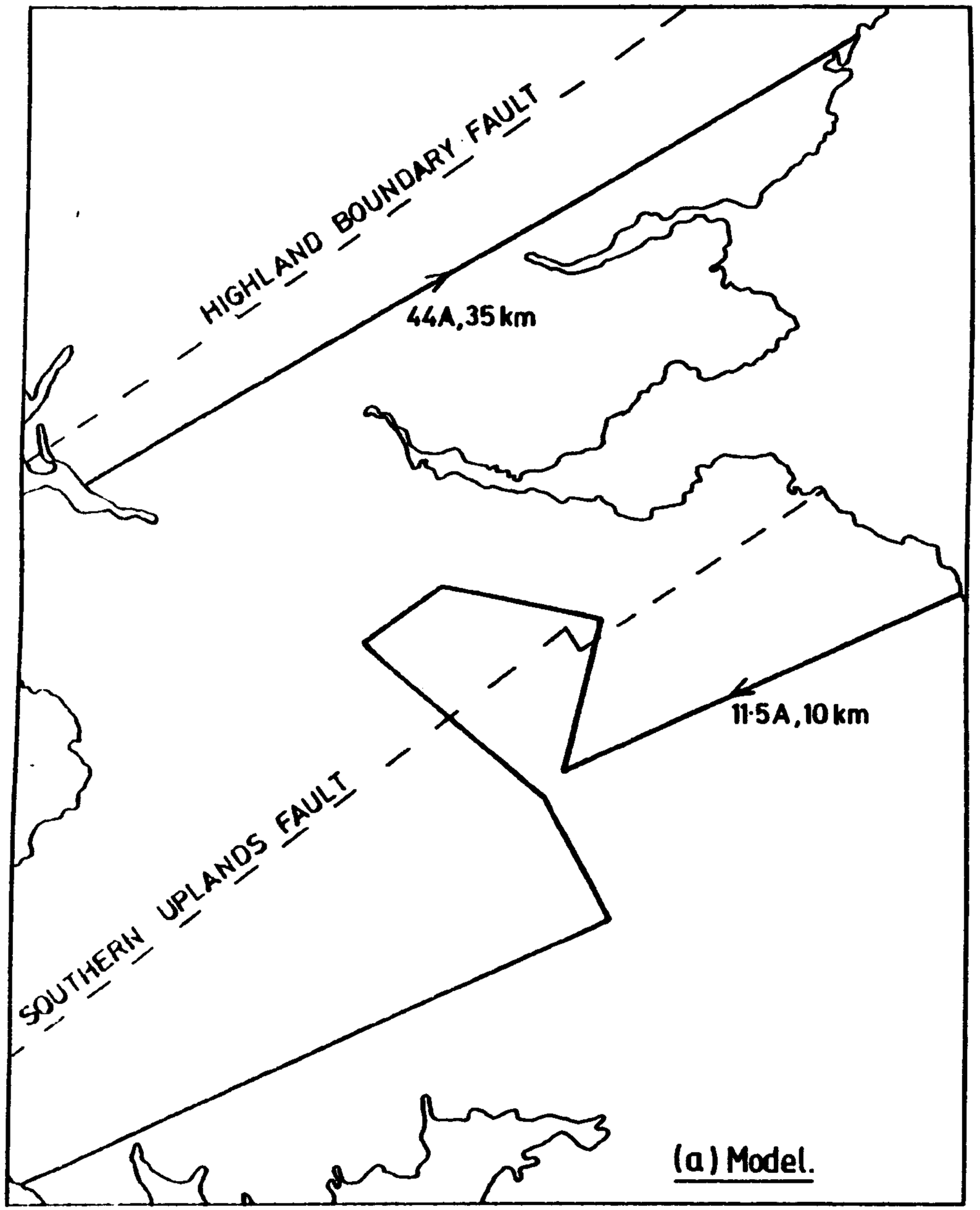

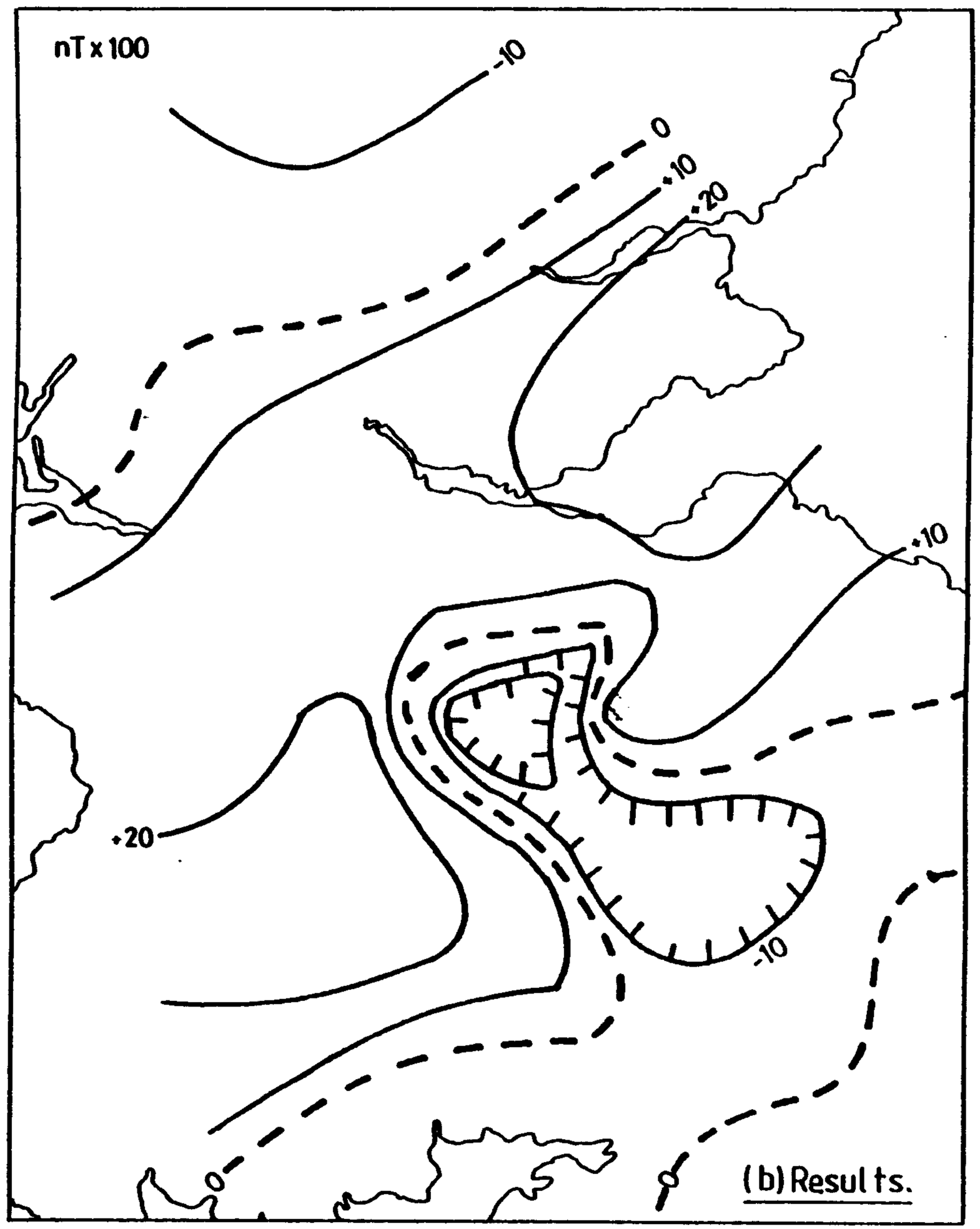

Figure 6·15. Equivalent current model of the in-phase vertical field at T = 300 s.

cotangent of the angle θ between the surface and the radial joining the current line to the site. Thus, values at several sites can be used to indicate the depth to an equivalent current flowing in a good conductor beneath the area. If this is done for the Southern Uplands sites, using figure 6.13, it indicates, for a period of 60 s, a depth of not less than 60 km to the equivalent currents. This is not incompatible with the existence of the deep conducting zone of Model E. At longer periods the intersection of radials calculated from $\cot \theta = Z/H$ occurs progressively further to the south-east in accordance with the line of reversal of the induction arrows noted in section 5.2.

Although the magnetic results have been treated in terms of conduction and induction anomalies separately, it seems likely that the Z/H profile is due to a combination of both effects. One way of investigating this would be to subtract the Z/H profile due to the model from the field values and to model the residues as a conduction anomaly. However, if the existence of a conduction anomaly is accepted it is perhaps more important to consider how this would affect the magnetotelluric results. Intuitively it seems likely that a conduction anomaly possibly connecting the North and Irish Seas would have its greatest effect at long periods and indeed the work of Bailey and Edwards (1976) involved variations of period 2400 seconds. Furthermore it is only at periods of 300 seconds and above that a major feature associated with the Southern Uplands Fault becomes evident in the hypothetical event contour plots, although this is perhaps partly due to the smaller number of stations at shorter periods. At periods greater than 300 seconds any distortion in the apparent resistivity is most likely to be evident in the H-polarization curves,

particularly in this case those for the Southern Uplands sites. The magnitude of the H-polarization resistivities for these sites is around 100Ω-m and if the impedance were to change by +30% the apparent resistivities would still only rise to 250Ω-m. It is unlikely therefore that the existence of a conduction anomaly would significantly change the final model.

6.5: Summary.

1) One-dimensional modelling of the apparent resistivities and phases gives characteristic structures for both the Highlands and the Southern Uplands. Considerable lateral variation is evident across the Midland Valley. The models for the Southern Uplands and the southern part of the Midland Valley agree well with those of Jones (1977).

2) Two-dimensional modelling of a profile across South Scotland resulted in the model of figures 6.11 and 6.14, which gives a good overall fit to the data.

3) An equivalent current model for the vertical magnetic fields observed suggests a line current between the Firth of Forth and the Solway Firth at depth, and a second current close to the Highland Boundary Fault.

CHAPTER 7: DISCUSSION, INTERPRETATION AND CONCLUSIONS.

7.1: Comparison of the geoelectric section with other geophysical results.

7.1.1: Comparison with other geophysical models of South Scotland.

Prior to this work the only deep crustal profile across the south of Scotland was that of LISPB (Bamford et al., 1978) shown in figure 3.5. Although there is no general physical reason why resistivity boundaries should coincide with seismic ones, there are several common points between the two models.

1) The top of the conducting layer beneath the Highlands and the Southern Uplands coincides with the seismic boundary between the Pre-Caledonian basement and the lower crust. Such conducting zones in the crust have been associated with the transition from amphibolitic to granulitic facies at the Conrad discontinuity.

2) A general thinning of the upper crustal layers beneath the Midland Valley is observed although there is no direct correlation between electric and seismic boundaries.

3) Probably the most interesting feature of the geoelectric section, the deep zone of high electrical conductivity beneath the Southern Uplands, corresponds to the zone which the seismic results could not resolve, (Bamford et al.,1978; Assumpcao and Bamford, 1978).

The southern part of the profile across the north of Scotland constructed by Mbipom (1980) overlaps the northern end of the profile presented here and there is an excellent correspondence between the two models for the region just to the north of

the Highland Boundary Fault. Mbipom's profile, further to the north-east, does however give a slightly lower resistivity for the conducting layer beneath his site Kirkmichael, which is in an equivalent position to GQU and STY. This result can be seen as a continuation of the trend of a lowering in resistivity along the fault line and can be interpreted as being due to zones of mineralization trending NNE - SSW rather than parallel to the main geological strike. Further to the north, Mbipom's model confirms the resistive and conductive structures respectively of the Cairngorm granite and the Great Glen and delineates them in detail.

The results of the two-dimensional modelling for the southern part of the Midland Valley and for the Southern Uplands agree closely with the one-dimensional interpretation of Jones (1977), (figure 3.4). This lends considerable weight to the validity and usefulness of one-dimensional modelling even in complicated tectonic regions.

The hypothetical event analysis and the line current modelling of the vertical magnetic field agree well with the longer period work of Bailey and Edwards (1976) and the more recent study of Hutton and Jones (1980).

7.1.2: Comparison with geoelectric models from other regions.

It is useful to compare the geoelectric section with the results of similar studies in other parts of the world. Because of the parallel tectonic histories outlined in chapter 3, the most meaningful comparison is with the results from Atlantic Canada. Of these, those of Kurtz and Garland (1976) are probably the most pertinent. Their model and the traverse which it

represents are shown in figure 7.1. The principal resistivity contrast is between the conducting lower crust and resistive mantle beneath the Grenville Shield and the resistive lower crust and conducting upper mantle beneath the Appalachians. The authors suggest a possible connection between this contrast and the Iapetus Ocean Suture and indicate that serpentinized peridotite and micaceous schists have properties which are comparable with both the conducting zones and the seismic studies of Jordan and Frazer (1975).

In western Canada magnetotelluric measurements in the Pemberton Volcanic belt of British Columbia (Dragert et al., 1980) detected a good conductor (100Ω-m) at a depth of approximately 20 km. The thickness of the conductor has been estimated to be at least 20 km. The highly resistive zone above it has been associated with granitic and metamorphic complexes.

Many Russian studies have detected anomalously good conductors in the crust and mantle (Berdichevsky et al., 1972) and Adam (1976) concluded that these indicate that there are in general three possible regions of anomalous conductivity; one in the crust and two in the mantle.

It is more difficult to find counterparts for the presence of a good conductor at depths less than 15km beneath the southern part of the Midland Valley.Most of the shallow conducting regions detected have been in either thermal areas (Stanley et al., 1977) or active rifts (Rooney and Hutton, 1977; Hermance and Pedersen, 1980), neither of which appears to exist in the south of Scotland. However, high resistivity structures in the upper crust have been found in many areas and generally linked with igneous and metamorphic zones (e.g. Dragert et al., 1980; van

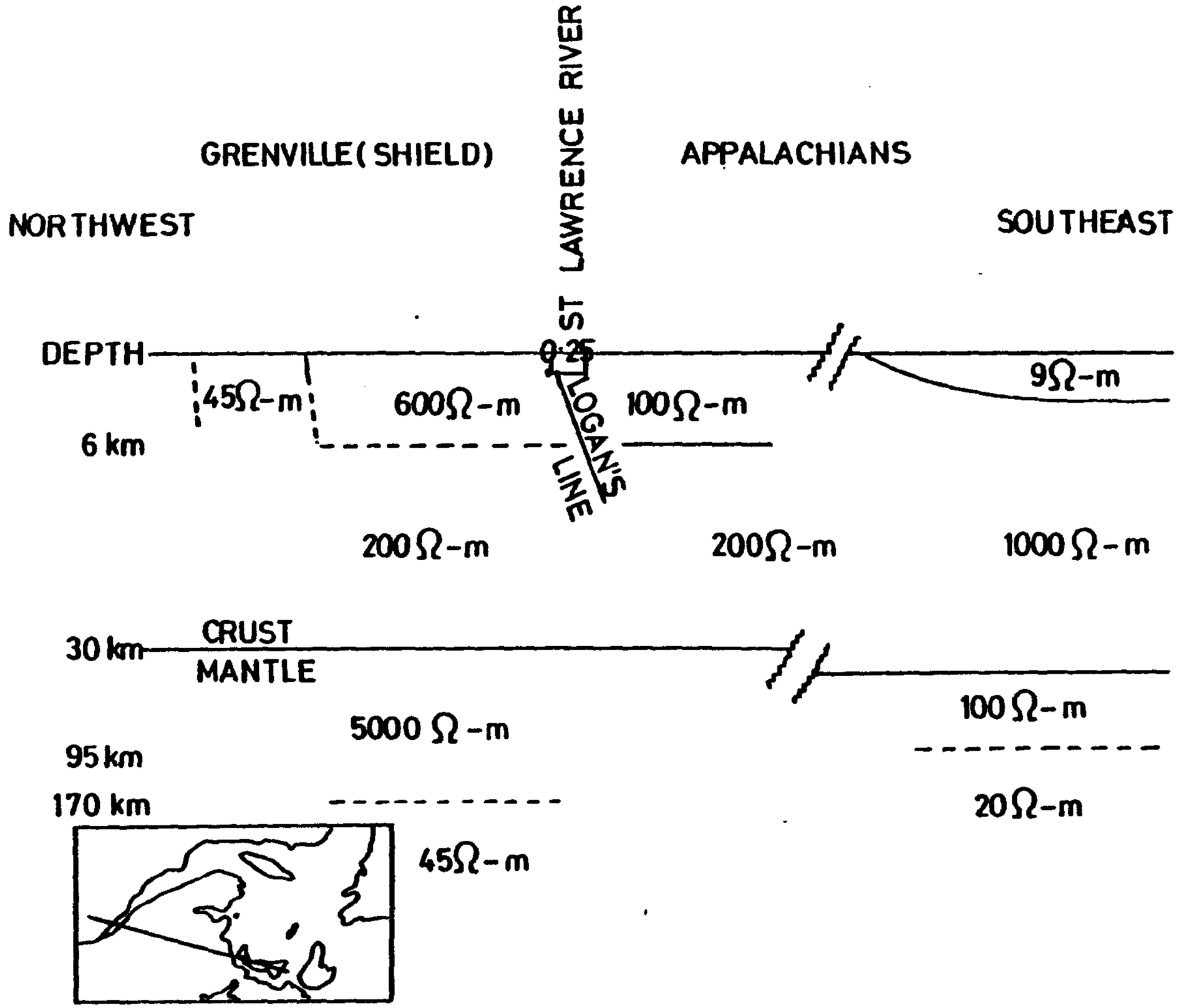

Figure 7-1.

Resistivity section across N.E. Canada (Kurtz and Garland, 1976).

Zijl, 1977).

Thus, as well as being in agreement with many of the previous geophysical studies in this region, the geoelectric section has counterparts in other studies for practically all of its features. It is the interpretation of these features in terms of the petrology of the crust and upper mantle which will now be discussed.

7.2: Conductivity models for the crust and upper mantle.

Global electrical conductivity profiles have been constructed by several authors (Keller et al., 1966; Banks, 1969, 1971; Brace, 1971; Dvorak, 1975) using various techniques. Banks fitted theoretical geomagnetic responses generated from conductivity models to the actual variations of the responses with period. The analysis concentrated on the longer period end of the geomagnetic spectrum and the result for the upper mantle was a background conductivity of between 10^{-3} and 10^{-1} Sm^{-1} down to 400 km depth.

Braces's model was based on laboratory measurements of electrical conductivity. The effects of porosity, pore fluid resistivity and salinity, pressure and temperature were all taken into accoumt to produce a distribution which showed a range of conductivities between 10^{-5} and 10^{-3} Sm^{-1} in the upper 40 km of the Earth. Brace's work was extended by Dvorak to take into account different kinds of crust: continental, sub-continental and oceanic. The typical continental crust considered by Dvorak was constituted of 3.4 km of sediments, 20.1 km of granitic rocks and 20.1 km of deeply metamorphosed basaltic rocks. This was underlain by a mantle containing peridotite, residual durite, eclogite, gabbro and basalt. Both dry and "wet" (in which solid

conduction and electrolytic conduction were added in parallel) models were constructed and the conductivity profiles that resulted are shown in figure 7.2. Whereas the dry model generally confirms the low conductivities of Braces's model, the "wet" model shows a possible increase in conductivity associated with the Conrad discontinuity which agrees well with field observations.

The problem of the validity of assuming water in the lower crust and upper mantle is very controversial and will be dealt with in section 7.3. However, although many geologists believe that all cracks and pores are likely to be closed by pressure within the top 15 km of the Earth, it is worth noting the comment of Dvorak:

"...any geologic material will be probably highly permeable to fluids when considered over geological times (Healey, 1971)."

The principal result that comes of the construction of global conductivity profiles is that the average conductivity of the upper part of the Earth is low, of the order of $10^{-5} - 10^{-3}$ Sm^{-1} . In the light of this result the detection by field studies of regions of considerably higher conductivity is significant and the necessity to explain the occurrence of such zones is of paramount importance.

7.3: Causes of high electrical conductivity within the Earth.

The causes of high values of conductivity within the Earth's crust and upper mantle have been put into four categories by Stanley et al. (1977). These are:

1) solid (or electronic) conduction;

2) electrolytic conduction, i.e. due to the presence of

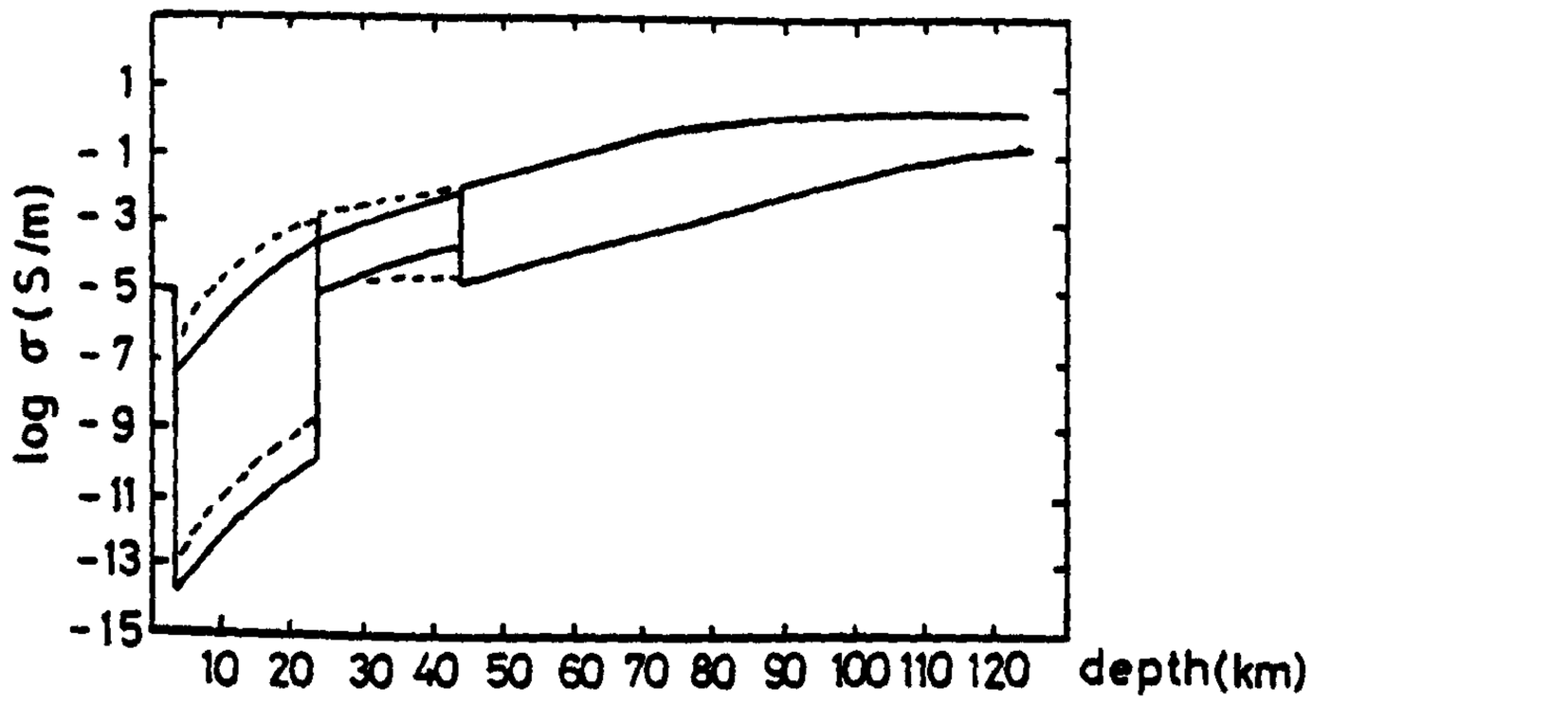

(a) Dry model.

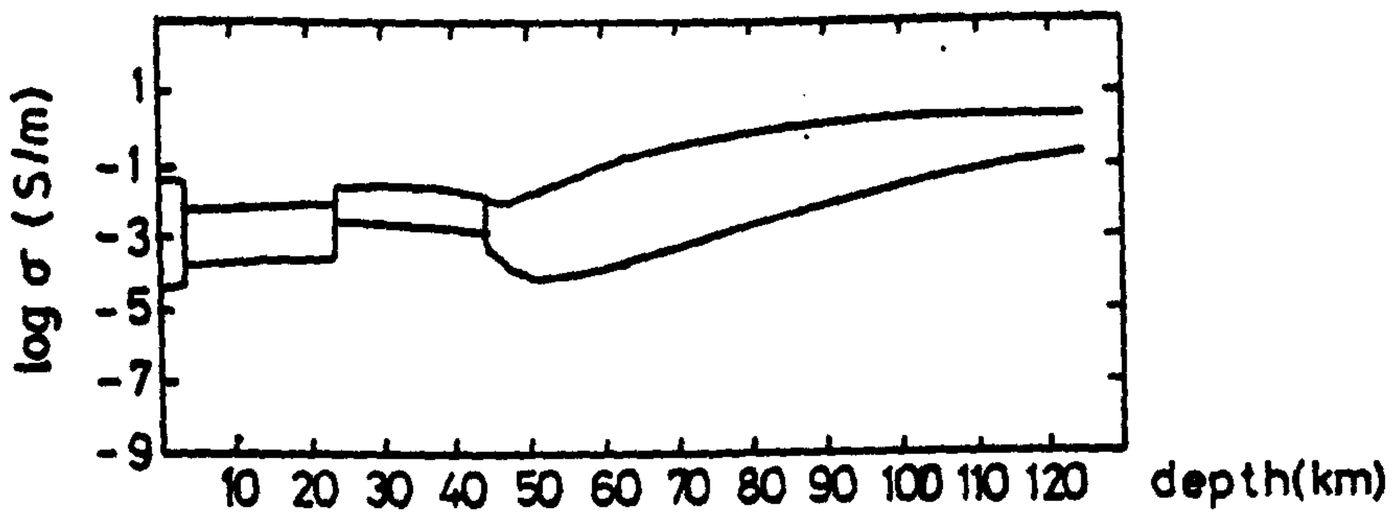

(b) Wet model.

Figure 7·2.

Conductivity - depth models for continental crust (Dvorak, 1975).

conducting fluids;

3) partial melting; and

4) the effects of alteration of the rocks.

However, the effects of each of these categories on conduction within the Earth can only be investigated by extrapolating the results of laboratory measurements on small samples and short time scales to the larger scales of the crust and mantle and geological times. There must therefore be doubts as to the validity of such measurements as a guide to conduction within the Earth (Duba, 1976), particularly as so many individual constraints (such as temperature, pressure and oxygen fugacity) affect each method of conduction that it is extremely difficult to obtain conditions representative of the crust and upper mantle. Nevertheless the results of laboratory measurements are the only guide to the mechanisms of good electrical conductivity, although it should be remembered that the results of such studies may be in error by, in some cases, at least two - three orders of magnitude.

7.3.1: Solid conduction.

The process of electronic conduction through rocks is basically that of a typical semiconductor and follows an equation of the form

$$\sigma = \sum_i \sigma_i e^{-E_i / kT} \qquad 7.1$$

The summation is over different semiconducting mechanisms in the rock, each with an activation energy E_i, of which one will dominate at any particular temperature. Typical values of activation energies are of the order of an electron- volt so that solid

conduction is often unimportant below temperatures of around 700 °C. Brace (1971) calculated the maximum and minimum effects of electronic conduction in a variety of rocks (figure 7.3a) and it seems conclusive that at the temperatures characteristic of the crust this mechanism can be discounted as a means of producing high conductivity. At deeper levels, within the mantle, where the temperature is high it is possible that other processes are more efficient at providing an increase in conductivity.

7.3.2: Electrolytic conduction.

Conduction by pore fluids in rocks obeys Archie's Law (Archie, 1942) which states that

$$\sigma_r = \sigma_f \eta^n \qquad 7.2$$

where σ_r is the overall conductivity of the rock, σ_f the conductivity of the fluid, η the porosity and n an exponent which is generally taken as being between 1 and 2 (Keller, 1966). The critical factor in equation 7.2 is the porosity, the variation of which with depth has been calculated by Dvorak (1975) and is shown in figure 7.3b. Hermance (1973) has calculated how the effect of temperature and pressure on porosity control the actual conductivity σ_f of the pore fluid and his result is shown in figure 7.3c.

From these calculations it is apparent that conduction by pore fluids is likely to be very low beneath a maximum depth of about 15 km. However, Berdichevsky et al. (1972) have argued that water can be released from hydrated minerals in the course of metamorphism.. They estimate that minerals of amphibolitic facies contain about 1-5% water and that dehydration at the boundary with granulitic facies releases all of this. The water released

Figure 7·3.

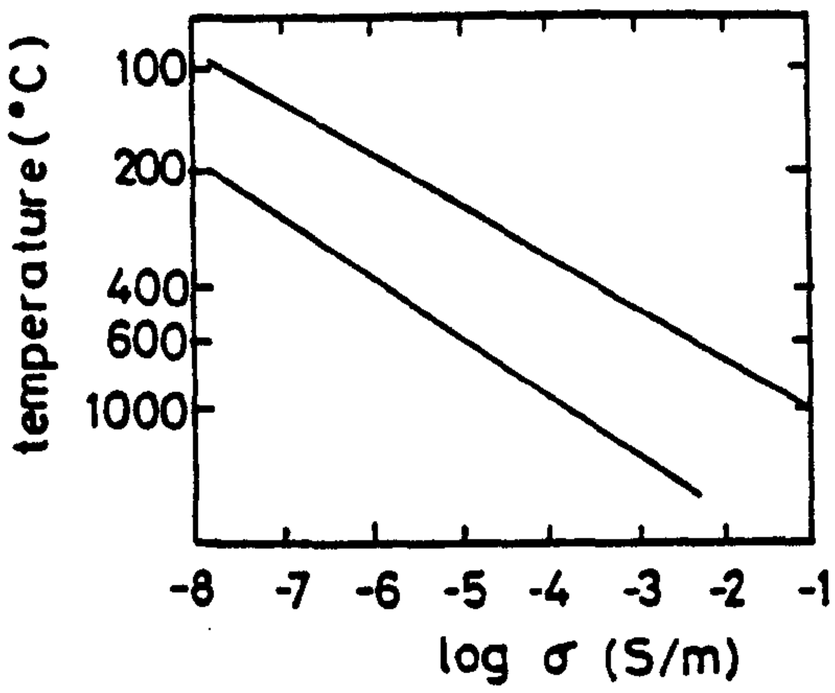

(a) Minimum and maximum boundary lines for electronic conduction effects (Brace, 1971).

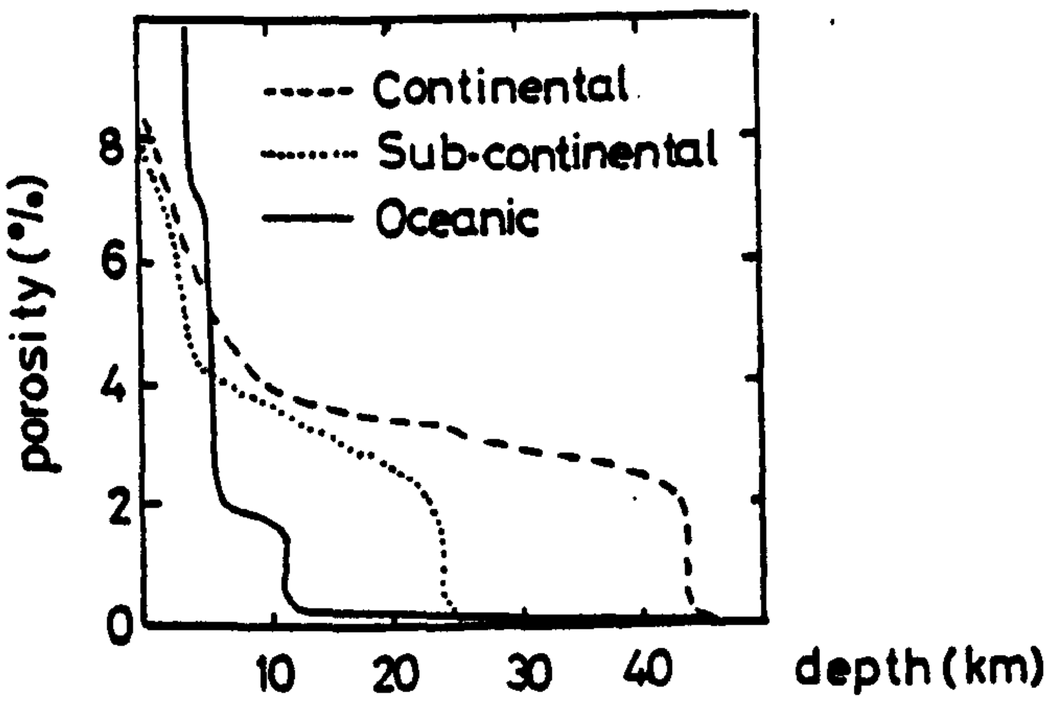

(b) Porosity vs. depth (Dvorak, 1975).

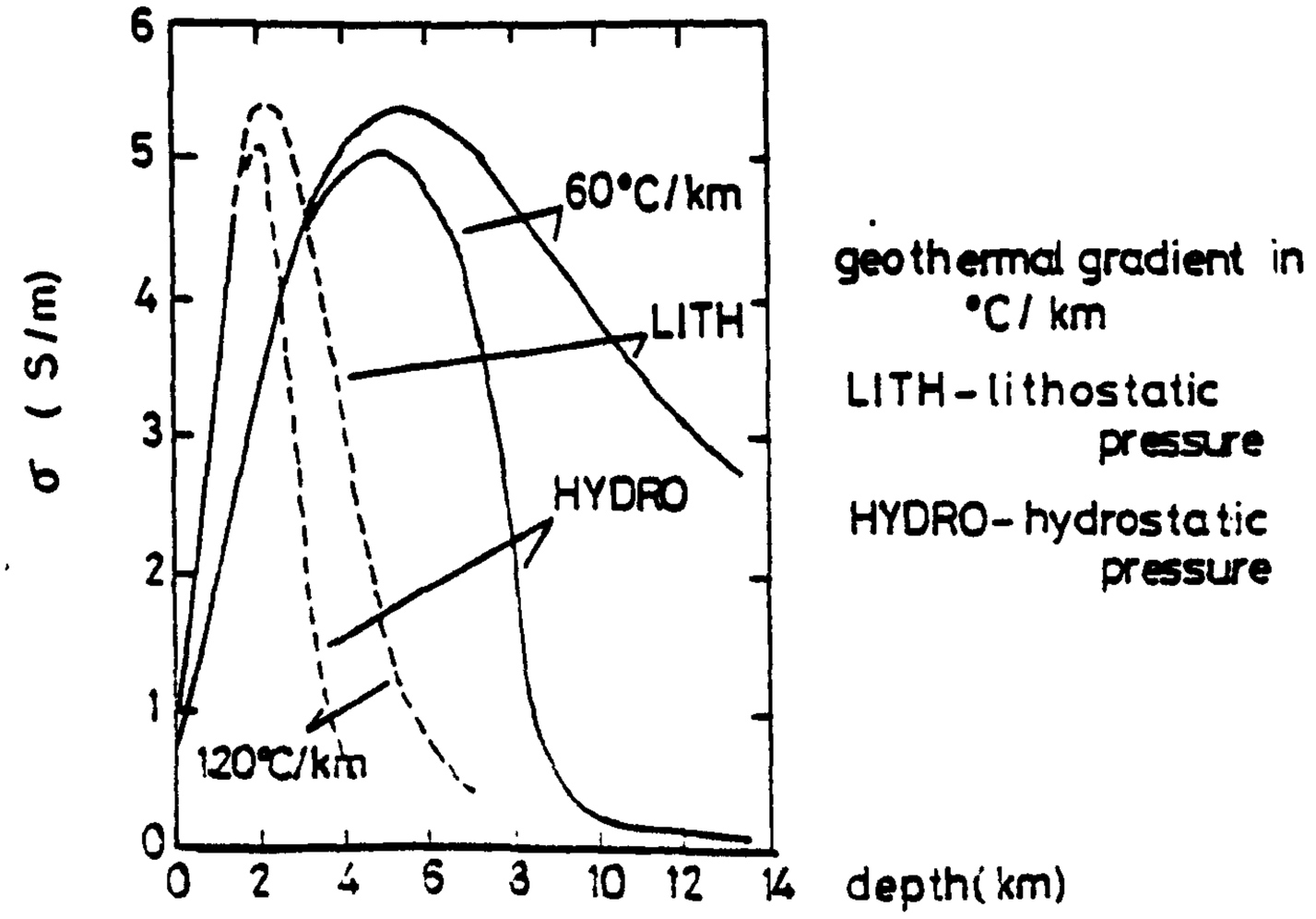

(c) Pore fluid conductivity vs. depth (Hermance, 1973).

is distributed intergranularly in a network pattern (Zadridze, 1967) and can produce conductivities of the same order of magnitude as a liquid phase. Zablocki (1964) has studied the process of dehydration in serpentinous peridotites and reported tenfold increases in conductivity associated with the release of water of crystallization at 400 - 600 °C. Similar observations have been made by Feldman (1976).

Sternberg (1979) has made a compilation of resistivity versus temperature curves from Keller (1971) and used the result to conclude that only hydrated rocks can produce the resistivities which are interpreted at 20 - 30 km depth in the southern extension of the Canadian Shield, at an estimated temperature of 300 - 400°C. The increase in conductivity for hydrated rocks at this temperature in Sternberg's diagram (figure 7.4) compares with that at the onset of dehydration found by Zablocki.

Thus, although pore fluids are likely to be expelled by the closure of cracks and pores in the upper crust it is possible that low resistivities may be produced in the lower crust by that process of dehydration of hydrated minerals. This may also lead, as will be discussed below, to the onset of partial melting.

7.3.3: Partial melting.

The melting of rocks in the upper mantle and in localized areas of the lower crust can significantly increase the electrical conductivity and is a possible explanation of not only conductivity anomalies but also of zones of low seismic velocity.

Hyndman and Hyndman (1968) have suggested that partial melting in the presumably anhydrous upper mantle will only occur at depths of 100 to 200 km, i.e. depths which are significantly

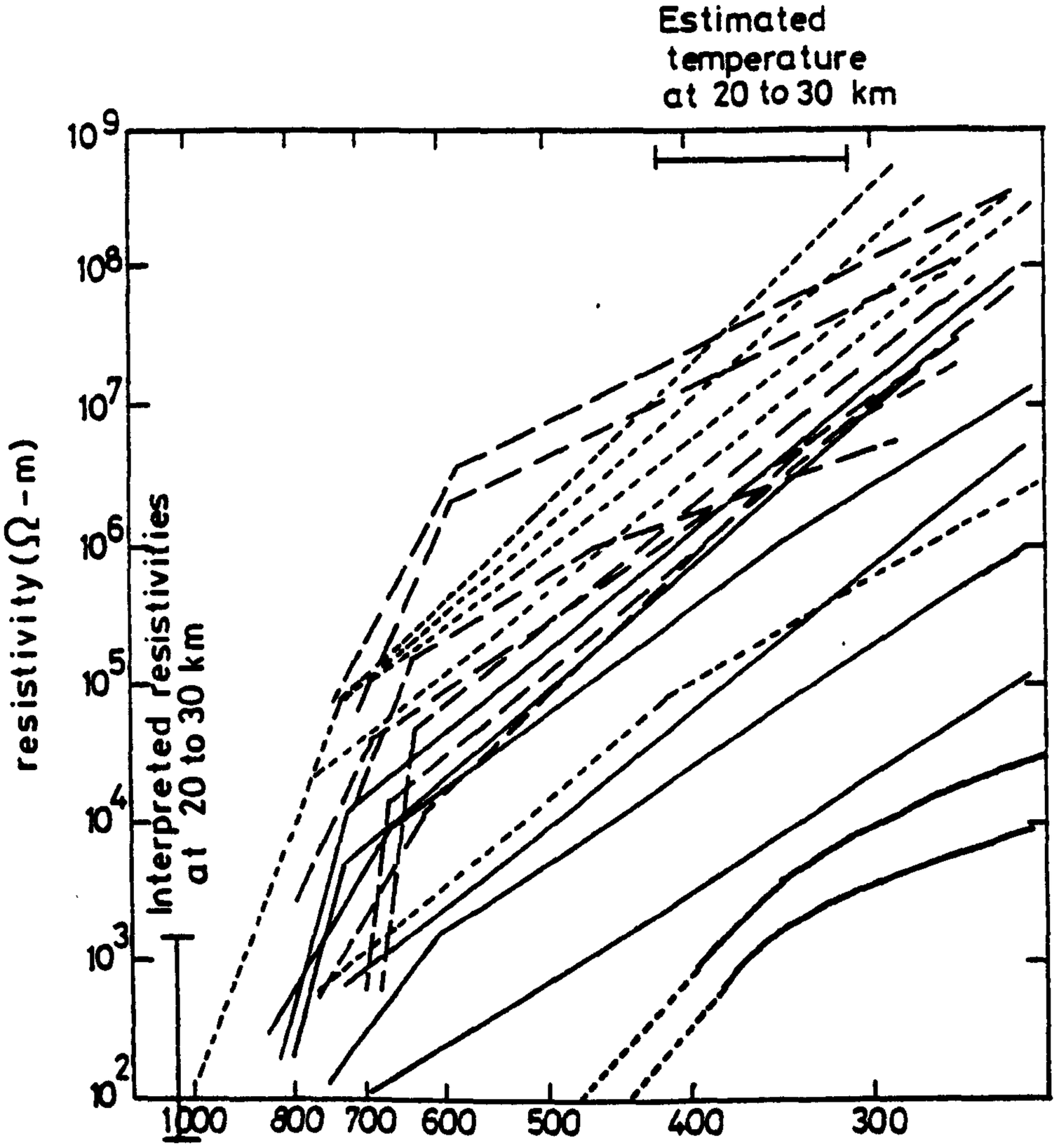

Figure 7·4.

Resistivity as a function of temperature for a variety of rock types (Sternberg, 1979).

deeper than many zones of anomalously high conductivity. However, they also indicate that partial melting occurs during the advanced stages of metamorphism and that the presence of water in the lower crust can significantly lower the temperature at which it commences. Wet granites have commonly been found to have the lowest melting point of all rocks (Wyllie, 1971) and Lebedev and Kitarov (1964) have measured the position of the solidus at a range of pressures. Their results (figure 7.5a) have been used by Stanley et al. (1977) in a carefully worded argument to speculate that the 500°C isotherm can be identified with the onset of partial melting in a wet granitic crust, whereas the top of the melting zone in a drier basaltic lower crust is marked by the 700 °C isotherm. A model drawn up using this proposal (figure 7.5b) was used to explain the results of magnetotelluric measurements in the Snake River Plain.

Various rock-water systems have been investigated by Lambert and Wyllie (1970) in an attempt to produce a model for the low velocity zone. Their results for tonalite-water and gabbro-water systems, and those af Boettcher and Wyllie (1968) for granite-water and Kushiro et al. (1968) for peridotite- water are shown in figure 7.6a. The curves show that the granite, tonalite and gabbro systems all have solidi which for pressures corresponding to about 40-50 km depth in the Earth lie at temperatures of 600-700°C. The conductivities of dry basalts have been studied by Khitarov et al. (1970), figure 7.6b, and found to increase by two to three orders of magnitude on melting at 1200-1400°C. Similar results have been obtained by Presnall et al. (1972) and by Shankland and Waff (1977) who used a synthetically constituted basalt.

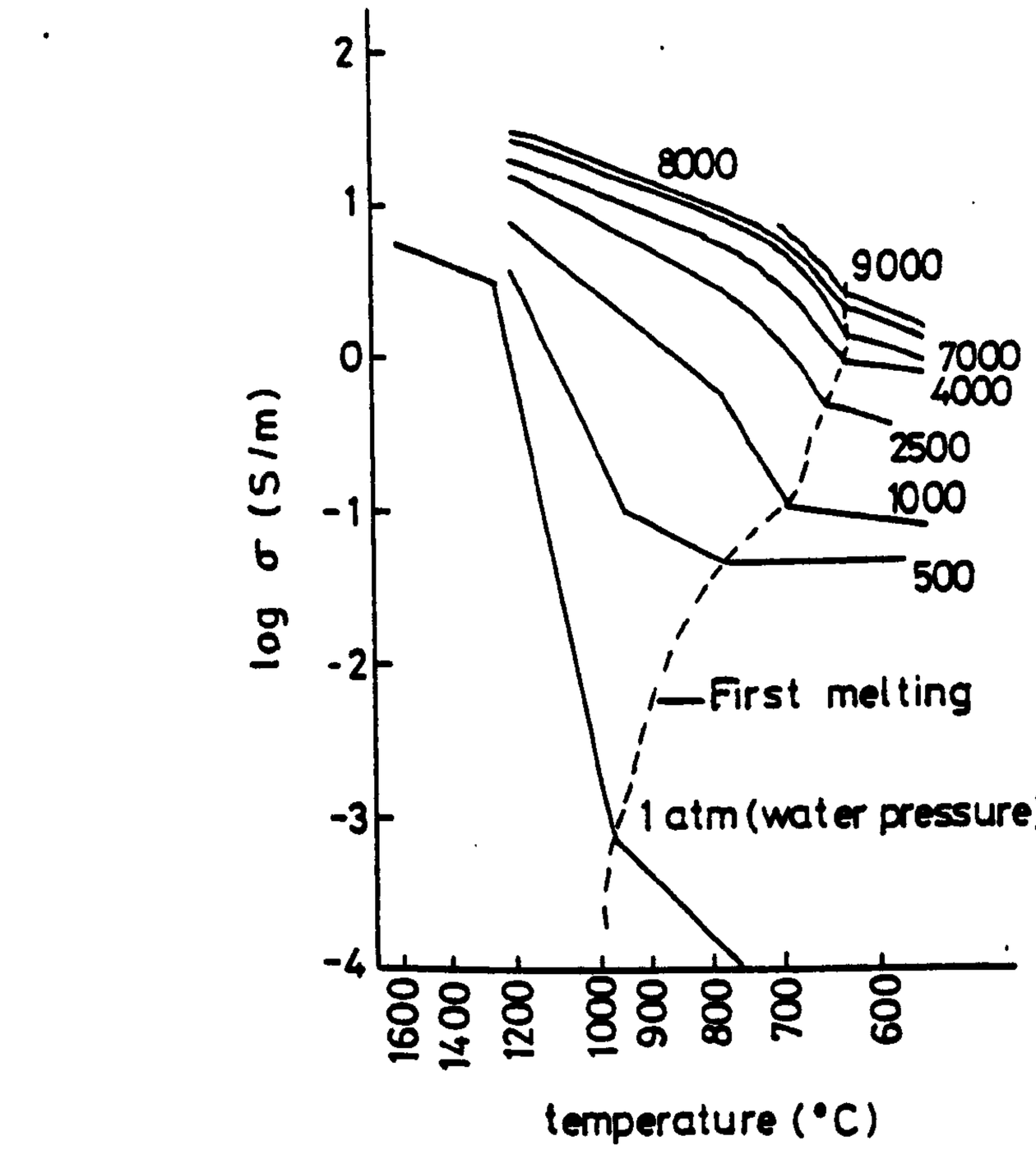

(a) Conductivity of granite (Lebedev and Khitarov, 1964).

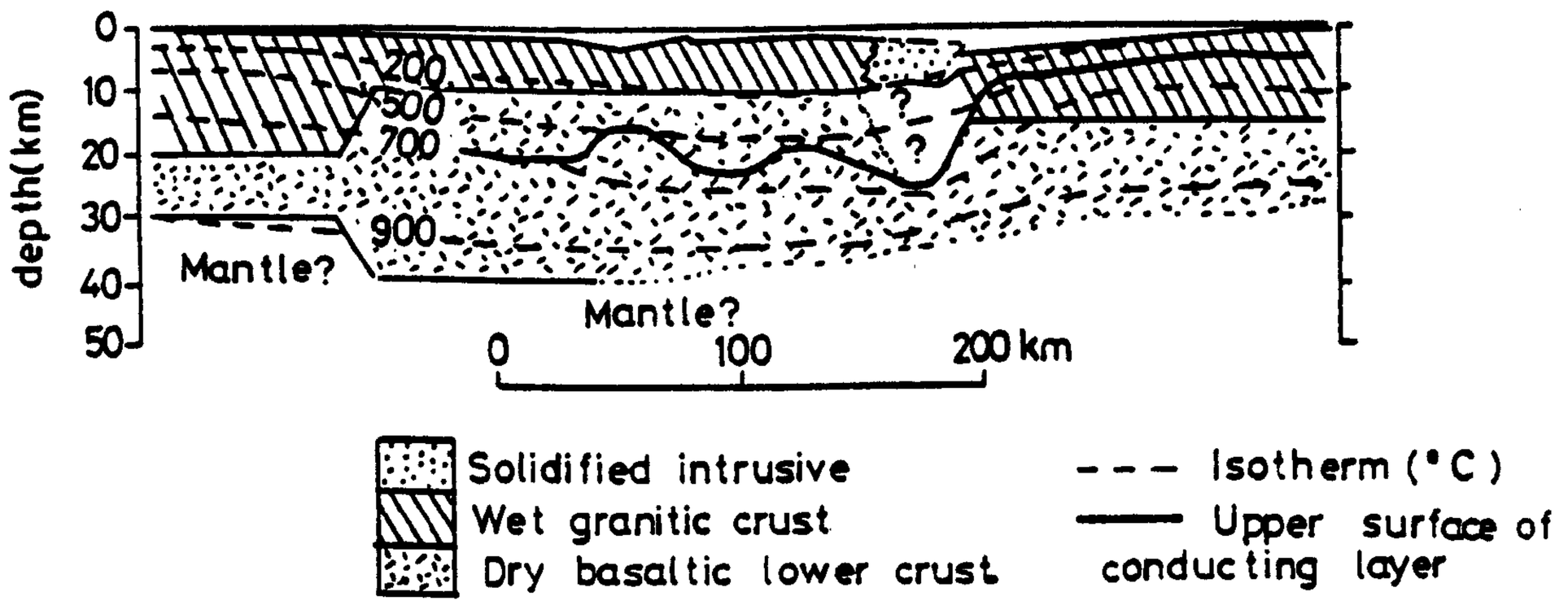

(b) Isothermal and geoelectric model across the Snake River Plain (Stanley et al., 1977).

Figure 7·5.

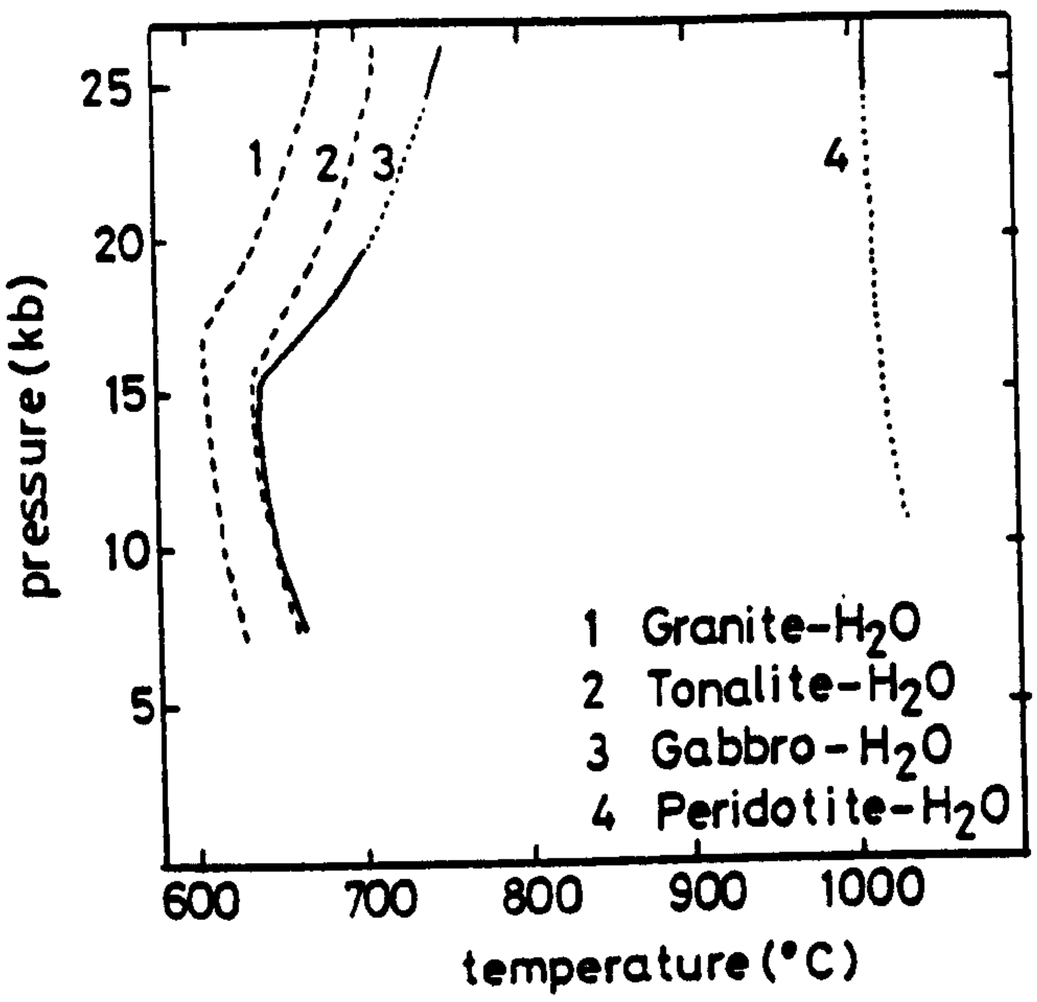

(a) Beginning of melting curves for rock-water systems (Lambert and Wyllie, 1970).

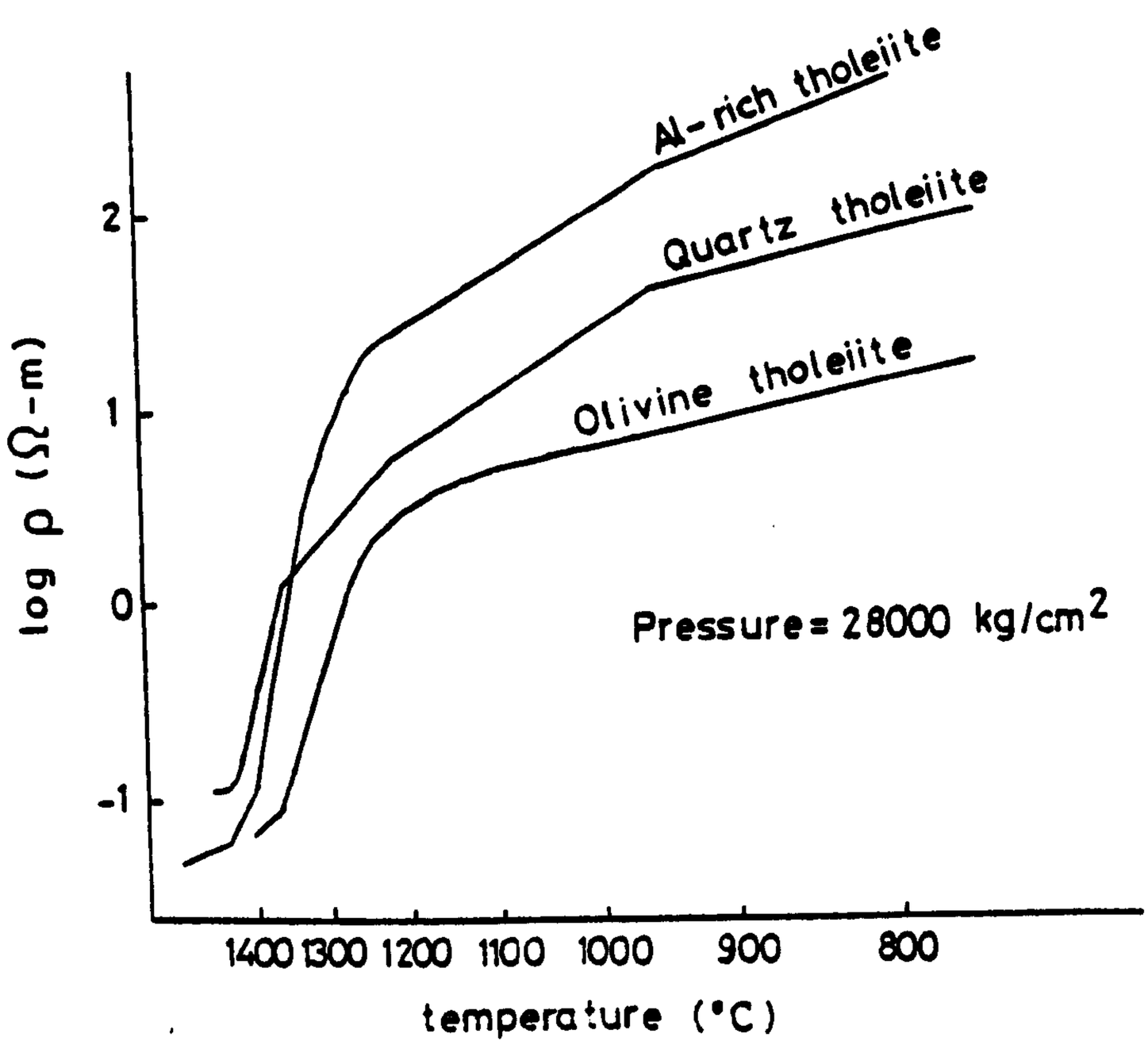

(b) Resistivity vs. temperature for basalts (Khitarov et al., 1970)

Figure 7·6.

In some areas the lack of surface manifestations such as hot springs and abnormally high heat flow have been cited as an argument against the explanation of conductivity anomalies by partial melting. However, Berdichevsky et al. proposed that even 1-2% of liquid phase, too little for the formation of magma proper,is sufficient to provide a conducting pathway through solid rock by a means similar to pore fluid conduction.

Several authors have estimated how the electrical conductivity varies with the concentration of partial melt. Waff (1974) and Madden (1976) placed bounds on the effect of partial melting on the conductivity - the Hashin - Shtrikman bounds. These represent the difference in bulk conductivity between the cases of a highly conducting melt connected along the grain boundaries of the solid phase and of pockets of melt isolated from each other by the solid phase. These two cases are equivalent to solid and liquid conductivities being in parallel and series respectively. By analogy with Archie's law, Hermance (1979) produced an intermediate model in which the melt is replaced by a conductor in parallel with the solid phase but having a reduced conductivity to that of the pure melt. Thus the bulk conductivity (σ^*) is given by

$$\sigma^* = \sigma_s + (\sigma_m - \sigma_s) C_m^2 \qquad 7.3$$

where σ_s is the solid conductivity, σ_m the melt conductivity and C_m the melt fraction. Equation 7.3 is valid for either of the two cases of the Hashin - Shtrikman bounds, and for a solid conductivity of 0.02 Sm^{-1} and a melt conductivity of 2 Sm^{-1} gives a σ^* versus C_m curve as shown in figure 7.7.

Although it is clear from the above that partial melting is a possible cause of the high conductivities found in the lower

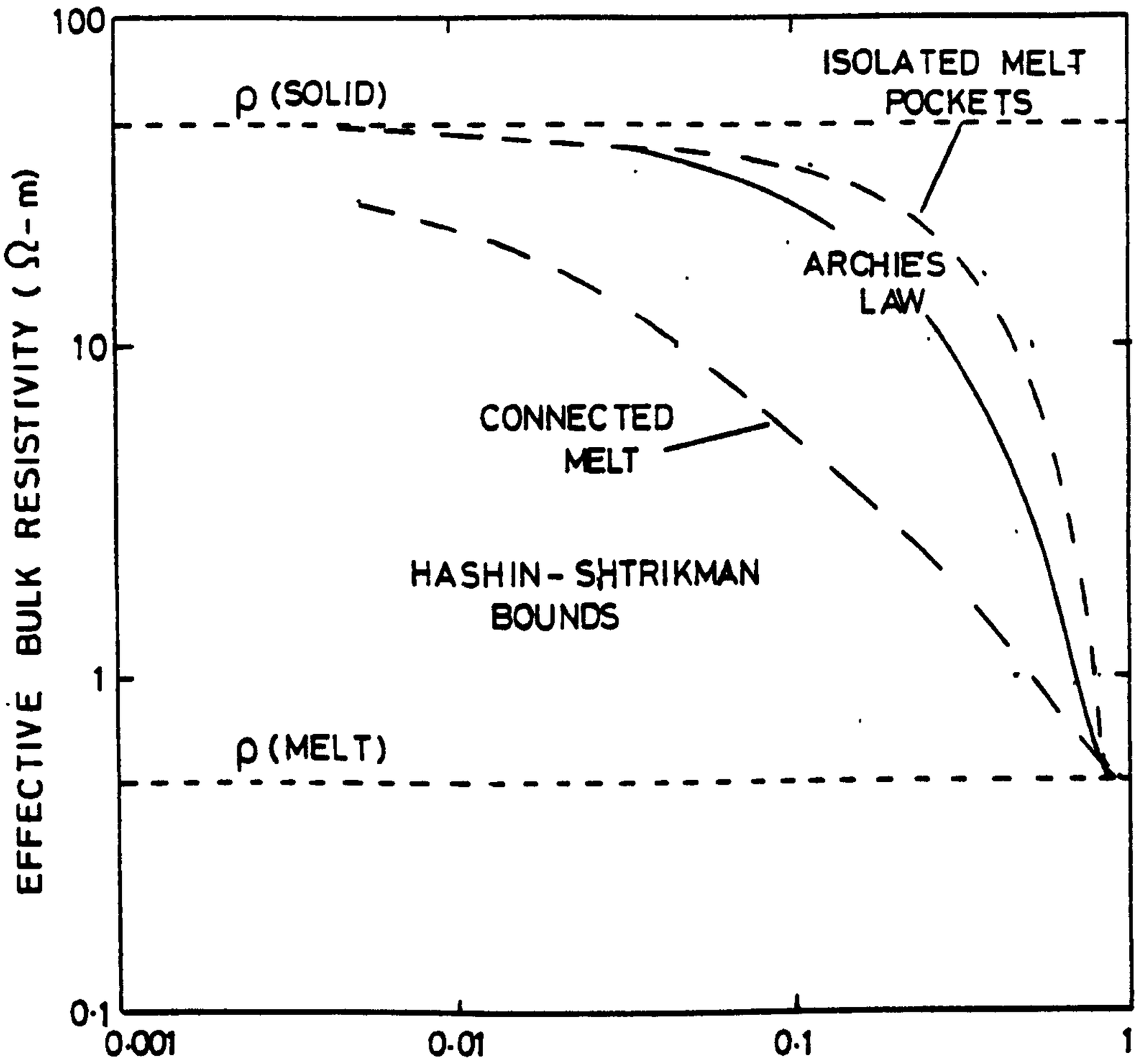

Effective bulk resistivity calculated from a modified Archie's law for T = 1200°C, ρ_m = 0·5 Ω-m, ρ_s = 50 Ω-m, compared with the Hashin-Shtrikman bounds (Hermance, 1979).

Figure 7·7.

crust and upper mantle, it should be noted (from figures 7.5a and 7.6b) that conductivities of the order of magnitude of $10^{-2} Sm^{-1}$ can be obtained by solid conduction. A further point has been raised by Piwinskii and Duba (1974) who reported, that at temperatures lower than the solidus, albite exhibits a conductivity which increases 2-3 orders of magnitude with time. The phenomenon seems to be characteristic of order-disorder systems on a time scale of about 1500 hours and has been reported, for example, in basalts containing plagioclase (Duba et al., 1975). It is of importance because it suggests that laboratory measurements made on short time scales may seriously underestimate rock conductivities developed over geological time.

7.3.4: Alteration.

It has been suggested by Stanley ey al. (1977) that high electrical conductivities may also be produced by the alteration of rocks. The lining of pore walls by alteration products may lower the resistivity, in a similar manner to fluid conductivity, by providing pathways of lower resistance, and pore fluids themselves may be sealed into the rock (Zobacki, 1975). The importance of this is that it provides another mechanism whereby fluids may be retained at depths greater than 20 km and lead either by electrolytic conduction or by lowering of the melting temperature, to enhanced conductivities.

7.4: Interpretation of the geoelectric section for South Scotland.

As the preceding section has shown, the electrical conductivities of rocks are very dependent on temperature. Because of this a knowledge of the temperature distribution in the crust and

upper mantle beneath South Scotland would be very helpful in the interpretation of the geoelectric section. Unfortunately there are relatively few heat flow measurements in the United Kingdom, those that there are being concentrated mainly in England. However, Oxburgh et al. (1980) have presented a heat flow map for Britain which does include measurements of 60-65 mWm^{-2} in the Midland Valley of Scotland. The heat flow north of the Highland Boundary Fault does seem, from the few measurements available, to be smaller than this value, whilst the one measurement in the Southern Uplands, near Dumfries in the far south-west, has a value of 61 mWm^{-2}. If the existence of the Tweedale granite is accepted, however, it may be that heat flow in the part of the Southern Uplands relevant to this project is higher. This would also follow from the work of Blaxland et al. (1979) (chapter 3) who foumd that samples of granite from the Southern Uplands were more radiogenic than those from further north.

Oxburgh et al. have correlated the heat flow from Caledonian granites with heat production to give the equation

$$q_o = 27 + 16.6\ A_o \qquad 7.4$$

where q_o is the measured heat flow in mWm^{-2}, A_o the heat production in μWm^{-3} and 16.6 a scale length in km which corresponds to the thickness of heat producing rocks in the crust. The intercept, 27, is the background heat flow from depth.

Assuming uniform heat production in the top 16.6 km, the heat flow q(z) at depths less than this is

$$q(z) = q_o - A_o z \qquad z \leqslant 16.6 \text{ km} \qquad 7.5$$

where

$$A_o = (q_o - 27)/16.6 \qquad 7.6$$

The temperature gradient (dT/dz) at depth z is found from the

standard equation relating q, dT/dz and the thermal conductivity (λ):

$$q(z) = \lambda \, dT/dz \qquad 7.7$$

thus,

$$\frac{dT}{dz} = \frac{q_o - A_o z}{\lambda} \qquad z \leqslant 16.6 \text{ km} \qquad 7.8$$

For a layered earth, as shown in figure 7.8, with thermal conductivity changes at depths z_1, z_2, z_3 equation 7.8 can be integrated to give the temperature at any depth. The result is:

$$T(z) = \begin{cases} \dfrac{q_o z}{\lambda_1} - \dfrac{A_o z^2}{2\lambda_1} & z < z_1 \\ T(z_1) + \dfrac{q_o (z - z_1)}{\lambda_2} - \dfrac{A_o (z^2 - z_1^2)}{2\lambda_2} & z_1 < z \leqslant 16.6 \\ T(16.6) + \dfrac{27(z - 16.6)}{\lambda_2} & 16.6 < z \leqslant z_2 \\ T(z_2) + \dfrac{27(z - z_2)}{\lambda_3} & z_2 < z \leqslant z_3 \\ T(z_3) + \dfrac{27(z - z_3)}{\lambda_4} & z_3 < z \end{cases} \qquad 7.9$$

Equation 7.9 has been used to estimate temperature profiles for the Highlands, the Midland valley and the Southern Uplands. Possible constituents of the crust and upper mantle were drawn up for each region from the average compositions of continental crust of Dvorak (1975) and the suggestions of Hall and Simmons (1979). Likely variations indicated by the geoelectric section were also included and a Moho depth of 35km was assumed as indicated by the LISPB profile. Values of thermal conductivities for carboniferous sediments were taken from Richardson and Oxburgh (1978), for Caledonian granites from Bott et al. (1972)

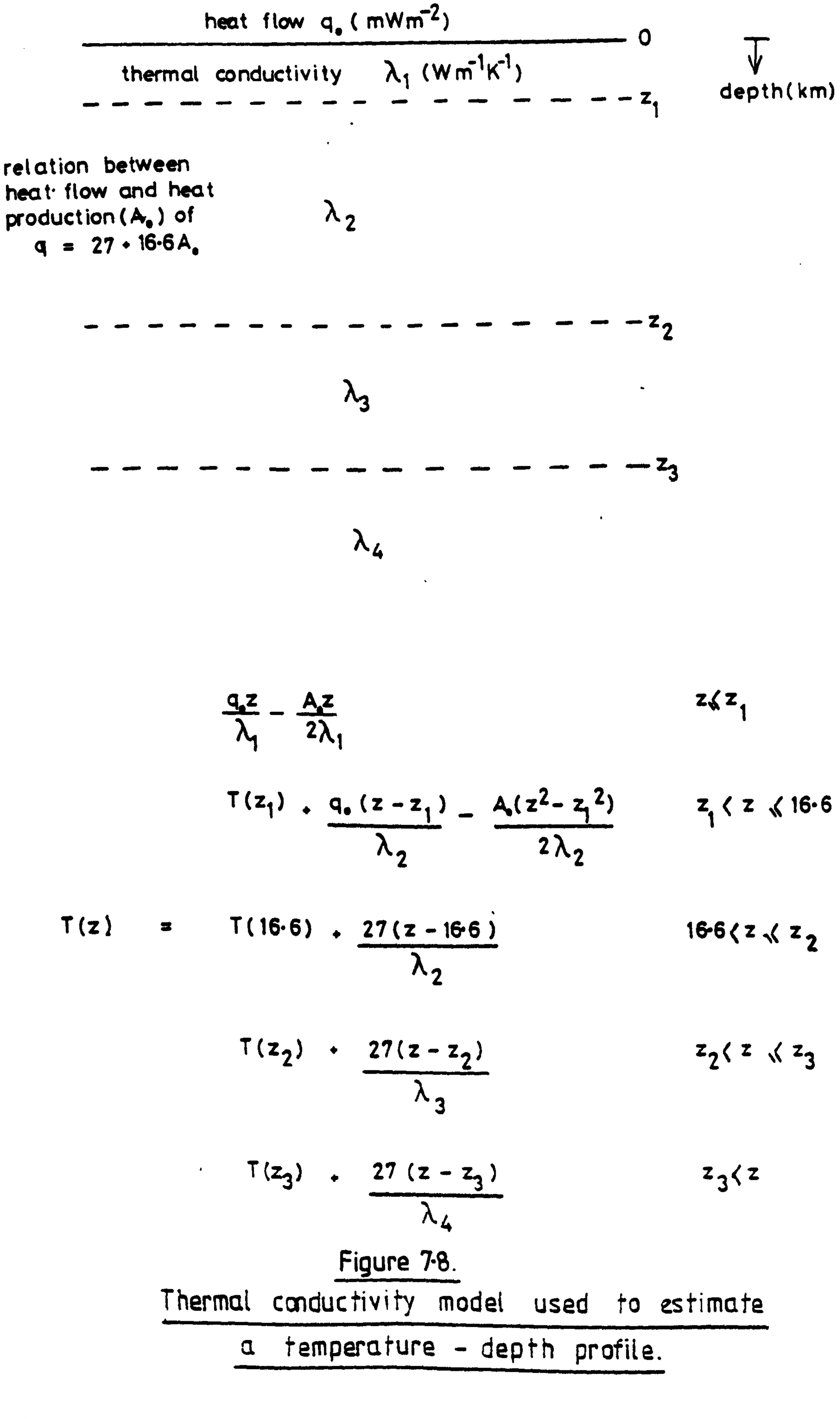

$$\frac{q_0 z}{\lambda_1} - \frac{A_0 z}{2\lambda_1} \qquad z \ll z_1$$

$$T(z_1) + \frac{q_0 (z - z_1)}{\lambda_2} - \frac{A_0 (z^2 - z_1^2)}{2\lambda_2} \qquad z_1 < z \ll 16{\cdot}6$$

$$T(z) = T(16{\cdot}6) + \frac{27(z - 16{\cdot}6)}{\lambda_2} \qquad 16{\cdot}6 < z \ll z_2$$

$$T(z_2) + \frac{27(z - z_2)}{\lambda_3} \qquad z_2 < z \ll z_3$$

$$T(z_3) + \frac{27 (z - z_3)}{\lambda_4} \qquad z_3 < z$$

Figure 7-8.

Thermal conductivity model used to estimate a temperature - depth profile.

and for other rocks from the Handbook of Physical Constants of the Geological Society of America. Estimates of the various thermal conductivities are given in table 7.1 and the models for the three regions are shown in figure 7.9. The heat flow in the Highlands was taken as 45 mWm^{-2}, that in the Midland Valley as 60 mWm^{-2} and in the Southern Uplands 70 mWm^{-2} .Whilst the value assumed for the Southern Uplands may seem speculative, a normal heat flow of 60 mWm^{-2} would only lower the temperature by 35 °C, and it does seem likely that the heat flow may be greater than the continental average for the United Kingdom.

Table 7.2 lists the calculated variation of temperature with depth for each region. Also listed in table 7.2 are very rough figures for temperature profiles from Pollack's (1975) correlation of temperature with heat flow and Ringwood's (1969) profile for PreCambrian regions. The profiles for the Midland Valley and Southern Uplands show considerable agreement with Pollack's profile for a heat flow of 60 mWm^{-2}. The proposed profile for the Highlands does, however, show a more rapid increase in temperature with depth than might be expected.

If the calculated temperature profiles are taken as giving at least an indication of the structure of the geotherms across the geoelectric section, they can be used to place constraints on the likely causes of the high conductivity zones. Reference to figure 7.5a shows that the temperatures at a depth of 20 km, which corresponds to the upper surface of the principal conducting zones beneath the Highlands and the Southern Uplands, are not high enough for the enhanced conductivity to be caused by the partial melting of wet granitic rocks. Beneath the Southern Uplands the depth of 20 km agrees well with that predicted by

Table 7.1

Thermal conductivities.

		Ref
Granites	2.59 ÷ 3.77 W $m^{-1}K^{-1}$	3
	2.93	
Caledonian granite		2
Serpentinized peridotite	2.38 - 2.93	3
Schists/gneisses	1.88 - 3.35	3
Amphibolite	2.55 - 3.81	3
Lavas	1.67 - 3.77	3
Tonalite	2.51	3
Basalts	1.67	3
Gabbro	2.09	3
Albitite	1.97	3
Dunite	3.35 - 5.02	3
Dolomite	3.35 - 5.02	3
Carboniferous sandstones	3.31	1
Carboniferous siltstones	2.22	1
Carboniferous mudstones	1.49	1
Coal	0.31	1

References:

1 Richardson and Oxburgh, 1978.

2 Bott et al., 1972.

3 Geol. Soc. America, Memoir 97, 1966.

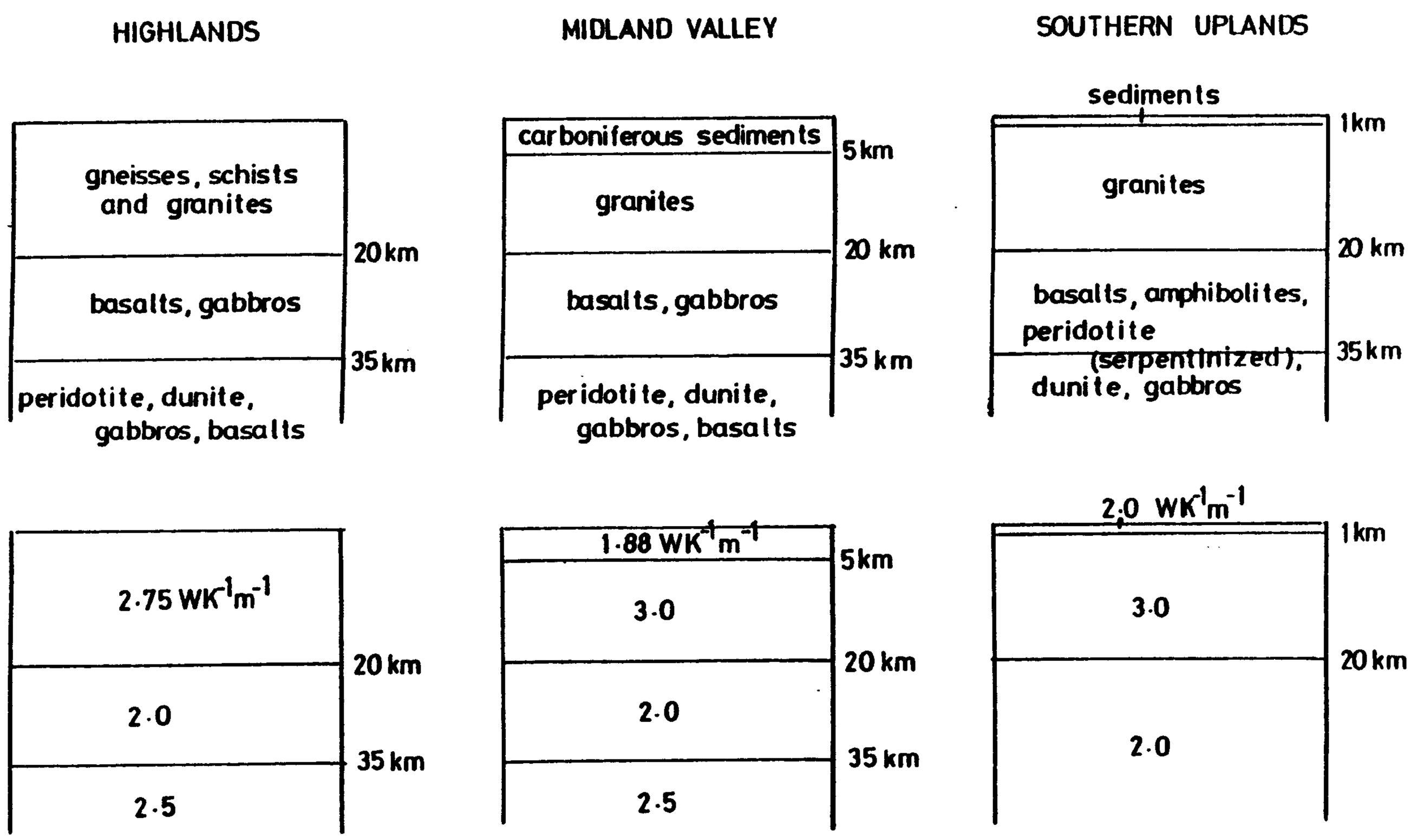

Figure 7·9.

Compositional and thermal conductivity models for South Scotland.

Table 7.2

Temperature profiles.

Depth (km)	Highlands	Midland Valley	Southern Uplands	Pollack (1975) HF=40mWm^{-2}	60	90	Ringwood (1969)	Pressure
10	144°C	221°C	177 - 202°C	125°C	170°C	225°C	125°C	3 kb
20	263	326	281 - 310	200	350	500	250	5
30	398	461	416 - 445	300	450	675	350	8
40	520	683	551 - 580	350	575	850	450	11
50	628	691	686 - 715	450	700	1075	550	15
60	736	799	821 - 850	500	800		650	17.5
70	844	907	956 - 985	575	900		725	20
80	952	1015	1090 - 1120	630	980		800	24
90	1060	1123	1226 - 1255	700	1100		850	27.5
100	1168	1231	1361 - 1390	775	1225		900	31

Adam (1976) for the depth to the conducting layer caused by release of water of hydration at the transition from amphibolitic to granitic facies, for a heat flow of 60-70 mWm^{-2}. Adam's equation relating the depth h_1 to this zone to the heat flow q (in heat flow units) is

$$h_1 = 35q^{-1.3} \qquad 7.10$$

which gives a value of h_1 of between 18 and 22 kilometres. For the lower heat flow of 45 mWm^{-2} in the Highlands, h_1 is 32 km which is close to the centre of the conducting zone. Above this at between 20 and 30 km depth the temperature is 250-400 °C and figure 7.4 suggests that the relatively high conductivities at this depth could be due to hydrated rocks still retaining their water of crystallization. The temperature and pressure at the deepest extent of the conducting zone under the Highlands are estimated to be 700°C and 17.5 kbar respectively, and from figure 7.6b it would seem unlikely even at this depth that the high conductivity is due to melting. A more likely explanation is that the temperature gradient has been overestimated and that the transition from amphibolitic to granulitic facies occurs at a greater depth than 32 km.

The difference in the resistivities of the conducting zones beneath the Highlands and the Southern Uplands presumably arises from the crustal rocks beneath the latter containing more water of crystallization. The presence of water saturated oceanic crust from the subduction of the Iapetus beneath the Southern Uplands would lead to a lower resistivity in this region; the suggestion of Blaxland et al. that the rocks beneath the Highlands and Midland Valley may contain a larger component of Lewisian crust would also indicate higher resistivities to the north.

Between the depths of 40 and 70 km beneath the Southern Uplands the high conductivity is probably due to electronic conduction in basaltic rocks. The estimated temperature of 600-1000°C in this depth range would give conductivities of the correct order of magnitude according to both figure 7.4 and figure 7.6b, particularly if there is an increase in conductivity with time as suggested by Duba. Below 70 km, at an estimated temperature of over 1000°C and a pressure of ~20 kbar, it is possible that partial melting is the cause of the high conductivity. Such conditions lie close to the beginning of the melting curve of the peridotite - water system in the P-T diagram of figure 7.6a. A depth of around 70 km to a zone of partial melting is also predicted by Adam's relationship between heat flow and the depth to the second characteristic zone of anomalously high conductivity. This equation:

$$h_2 = 155q^{-1.46} \qquad 7.11$$

gives values of 92 and 73 km for heat flows of 60 and 70 mWm respectively.

It must be remembered that the zone of 75Ω-m resistivity is likely to be an average over many zones of locally higher or lower resistivity. For a region in which the rock resistivity is 200Ω-m Hermance's modified form of Archie's law can be used to estimate the amount of partial melt required to give a resistivity of ~75Ω-m. If the figure of 2 Sm^{-1} used by Hermance is taken as representative of the conductivity of the melt, then a resistivity of 100Ω-m is produced by only 5% of partial melt. However, as it appears that the ambient solid resistivity may be less than 200Ω-m it must be stressed that partial melting, although it may occur to a locallized extent, is not a necessity

to explain the high conductivity beneath the Southern Uplands.

The absence of the deep conducting zone beneath the central part of the Midland Valley can be explained by the change in the nature of the Pre-Caledonian basement at the Southern Uplands Fault, indicated by the LISPB profile and remarked on by Blaxland et al.. The more resistive rocks north of the fault in the lower crust mean that the zone of dehydration at 20 km marks the base of the conducting zone rather than its upper surface as it does to the south. The northward dip of the conductor beneath the Highland Boundary Fault is possibly indicative of a subduction zone along the fault line with the "wet" oceanic crust being carried to a greater depth further north.

Between Kinross and Penicuik, as the actual resolution of the resistivity structure is less clear, the interpretation of the good conductor at very shallow depths is perhaps best left until more measurements have been obtained from the southern part of the Midland Valley.

The above interpretation of the zones of good conductivity is summarized in figure 7.10.

7.5: Structural and tectonic implications.

Although the interpretation of the last section was based on the initial assumption of the compositions of the crust and upper mantle in each region, it is not critically dependent on the chosen structures. The temperature estimates are primarily dependent on the assumed heat flow and would not be radically altered by making compositional changes which would give different thermal conductivity values. The following structural conclusions can however be drawn.

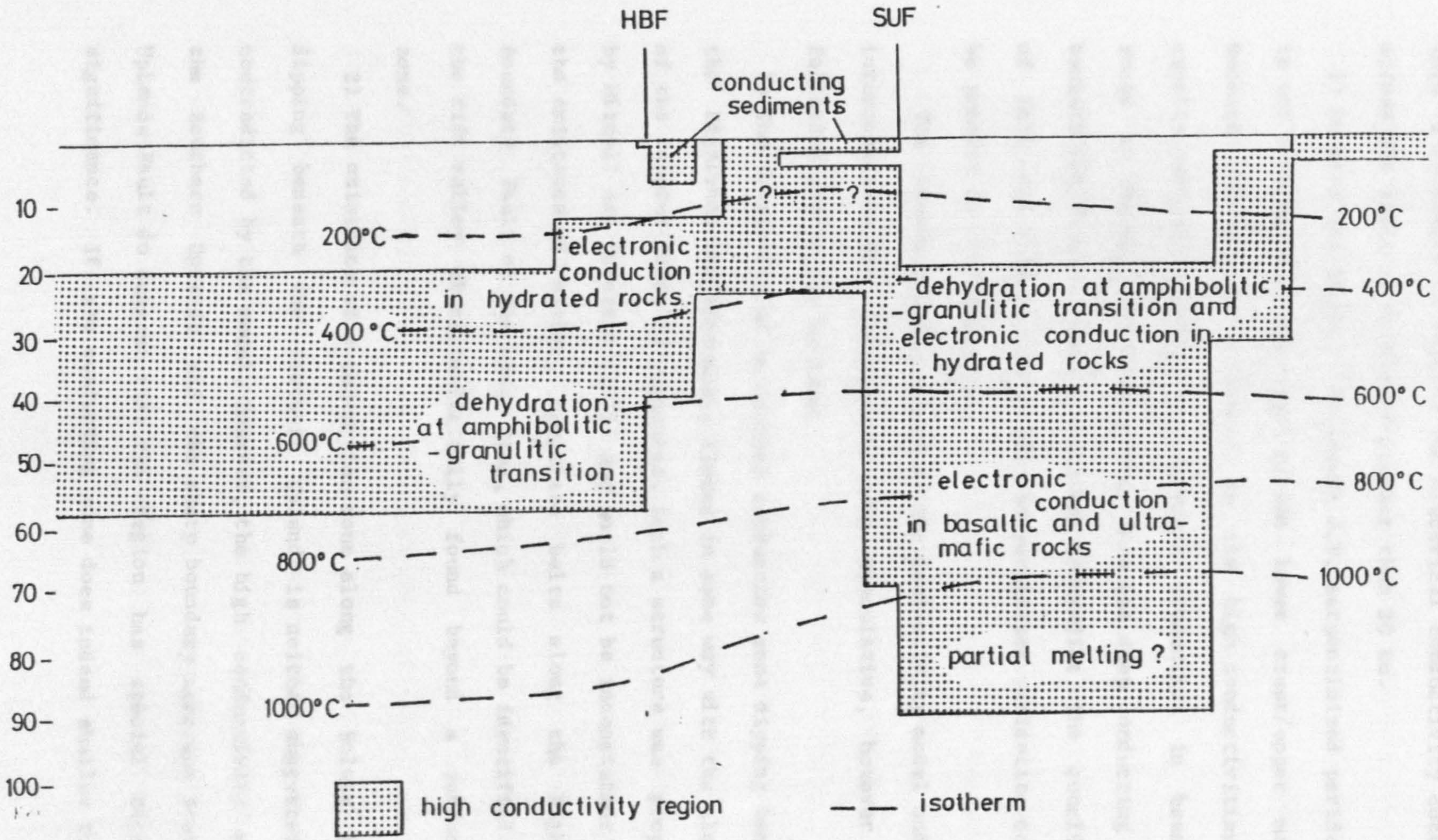

Figure 7·10.

Interpretation of the high conductivity region in South Scotland.

1) There is a fundamental difference in the lower crustal structure to the north and south of the Southern Uplands Fault. This is necessary to explain the electrical conductivity contrast across the fault at depths of greater than 20 km.

2) Despite its presence in figure 7.9, serpentinized peridotite is not a necessary constituent of the lower crust/upper mantle beneath the Southern Uplands as the high conductivities may equally well be explained by electronic conduction in basaltic rocks at temperatures above 600°C. Thus the deep conducting zone beneath the Southern Uplands does not contradict the conclusion of Hall and Simmons (1979) that serpentinized peridotite cannot be present in the deep crust.

The tectonic implications of the conductivity model and its interpretation are necessarily more speculative, however the following points can be made.

1) The possiblity of an ancient subduction zone dipping beneath the Highlands and presumably linked in some way with the closure of the Iapetus Ocean is suggested. Such a structure was proposed by Mitcell and McKerrow (1975) and would not be inconsistent with the existance of either, ophiolite belts along the Highland Boundary Fault or the Great Glen, which could be identified with the rift valley characteristically found beyond a subduction zone.

2) The existence of a subduction zone along the Solway Firth dipping beneath the Southern Uplands is neither suggested nor contradicted by the model. However, the high conductivity under the Southern Uplands and the sharp boundary near the Southern Uplands Fault do suggest that the region has special tectonic significance. If the conducting zone does indeed shallow to the

(see Sec. 7.7)
south, then it may well be that it is the result of the subduction of oceanic crust into the upper mantle beneath the Southern Uplands.

3) Because of the contrast in lower crustal structure close to the Southern Uplands Fault it is unlikely that the southward dipping conducting structure at the fault is the result of ancient subduction.

7.6: Summary and conclusions.

1) Five component magnetotelluric measurements were made at ten new sites in the South of Scotland. Nine of the sites lie on a linear traverse running N30°W - N150°E from Kinloch Rannoch in the Highlands to Borthwickbrae in the Southern Uplands.

2)Apparent resistivities and phases and vertical magnetic field response functions were calculated for each site.

3) Average apparent resistivities and phases were calculated from the field curves and used as a basis for one-dimensional modelling. Subsequent two-dimensional modelling showed that this procedure does in general give a valid resistivity structure even when the site is two rather than one-dimensional. One-dimensional modelling of the average curves is still a useful starting point in three-dimensional situations.

4) The one-dimensional models for each site were used to construct a two-dimensional model along the traverse. This was then altered in stages to fit the E and H-polarization apparent resitivities and phase curves at each site and the variation of Z/H along the traverse. Although a perfect fit was not obtainable at all the sites the overall general fit of the final model to the field curves was good.

5) The resulting model indicated a zone of very low resistivity (75 Ω-m) between 20 and 90 km depth beneath the Southern Uplands and a somewhat poorer conductor (~ 500Ω-m) between 20 and 58 km beneath the Highlands. The structure beneath the Midland Valley was less well resolved but it suggested that the conducting structure comes very close to the surface and only extends to around 20 km depth. Various resistivity contrasts were required in the upper crust to model particular features of the field curves.

6) Heat flow measurements and thermal conductivity estimates for different rock types were used to produce temperature-depth profiles along the traverse. These were then used as an aid in the interpretation of the zones of good conductivity.

It was concluded that:

7) beneath the Highlands the high conductivity between about 20 and 40 km is due to electronic conduction in hydrated rocks and that below this it is the result of the release of water of crystallization during dehydration at the boundary of the amphibolitic and granulitic facies.

8) The lower part of the conducting zone beneath the Midland Valley is also a result of dehydration at this boundary. At greater depths than 20 km the absence of a good conductor is explained by the inclusion of a greater percentage of Lewisian rocks in the lower crust than there is to the south of the Southern Uplands Fault.

9) The good conductor beneath the Southern Uplands is due to a combination of many effects - hydrated rocks and dehydration at the amphibolitic/granulitic transition in the upper part of the conducting zone, electronic conduction in basaltic and ultramafic

rocks at deeper depths and possibly partial melting below 70 km.

10) Tectonic implications were drawn regarding the possible existence of an ancient subduction zone dipping northwestwards beneath the Highlands and the possiblity of ancient oceanic crust underlying the Southern Uplands.

11) Line current modelling of the "hypothetical event" vertical magnetic field Z at the sites along the traverse and at additional sites, indicated that the magnetic results could be explained by direct line currents flowing northwest along the Highland Boundary Fault and southeast beneath the Southern Uplands. The latter current could be the result of the deep conductor beneath the Southern Uplands providing a conducting link between the North Sea and the Solway Firth. It is likely however that the vertical magnetic field is a result of the combined effects of conduction and induction.

7.7: Suggestions for further work.

Although a considerable amount of work has now been undertaken in South Scotland there are still several lines of research which should be investigated.

1) A considerable amount of geomagnetic data is available from the South of Scotland. This should be subjected to a much fuller analysis in an attempt to see if the line current representation of the vertical field is a realistic one. In particular the separation of the vertical field into components due to induction and conduction should be attempted. By paying particular attention to the longer period data it ought to be possible to place better limits on the depth of the lower surface of the high conductivity zone.

2) More magnetotelluric soundings are required to help delineate the complex conductivity structure within the Midland Valley. Measurements along the length of the valley ought to indicate whether the structure inferred here is truly two-dimensional or not.

3) More heat flow measurements are needed from all over the survey area. These would enable a better resolution of the possible conduction mechanisms and indicate the correctness or otherwise of the assumptions made in section 7.4.

4) The extension of the profile southwards, which is already in progress, will confirm or deny the speculation as to the behaviour of the conducting zone to the south of the Southern Uplands. A shallowing of the zone would tend to confirm the subduction of oceanic crust associated with the closing of the Iapetus Ocean. However, recent measurements by Novak (pers. comm.) suggest that the results from Towhouse, upon which the shallowing of the conductor to the south, in the model, is based, are not representative of the Northumberland Basin.

APPENDIX: AUDIOMAGNETOTELLURIC MEASURMENTS.

To supplement the magnetotelluric measurements discussed so far audiomagnetotelluric measurements in the period range 1-100 milliseconds were made at six sites in the Midland Valley and Southern Uplands. The sites are listed in table A1.1 and shown in figure A1.1. The object of taking the AMT measurements was twofold. Firstly to investigate the sedimentary cover which was not resolved by the normal magnetotelluric measurements and was included in the two-dimensional model purely on geological grounds. Secondly it was hoped that by taking a series of measurements between the MT sites PEE and YAR it might be possible to detect the proposed Tweedale Granite of Lagios and Hipkin (1979).

The AMT system has been described by Novak et al. (1980). The data were recorded in analogue form on magnetic tape and digitized using the facilities of the Global Seismology Unit at the Institute of Geological Sciences, Edinburgh. Events were selected and processed in a similar manner as for the longer period data and a routine one-dimensional modelling program, written by G.Dawes, applied to the averaged apparent resistivities at each site. Unfortunately, at the present time, the phase data obtainable is not of a sufficiently high quality to use for modelling purposes.

A1.1:Sedimentary cover in the Midland Valley and Southern Uplands.

Two sites at which measurements were taken, Penicuik and Harlawmuir, were in the southern part of the Midland Valley. The ranges of the one-dimensional models which fit the apparent resistivity curves at these sites are shown in figure A1.2.Both sites

Table A1.1

Audiomagnetotelluric sites.

Site	Altitude	Grid reference
Glenkerry	925'	32836104
Glensax	1100'	32656344
Harlawmuir	925'	31876552
Longmoor End	1300'	32536192
Muttonhall	1050'	32706281
Penicuik	900'	32176609

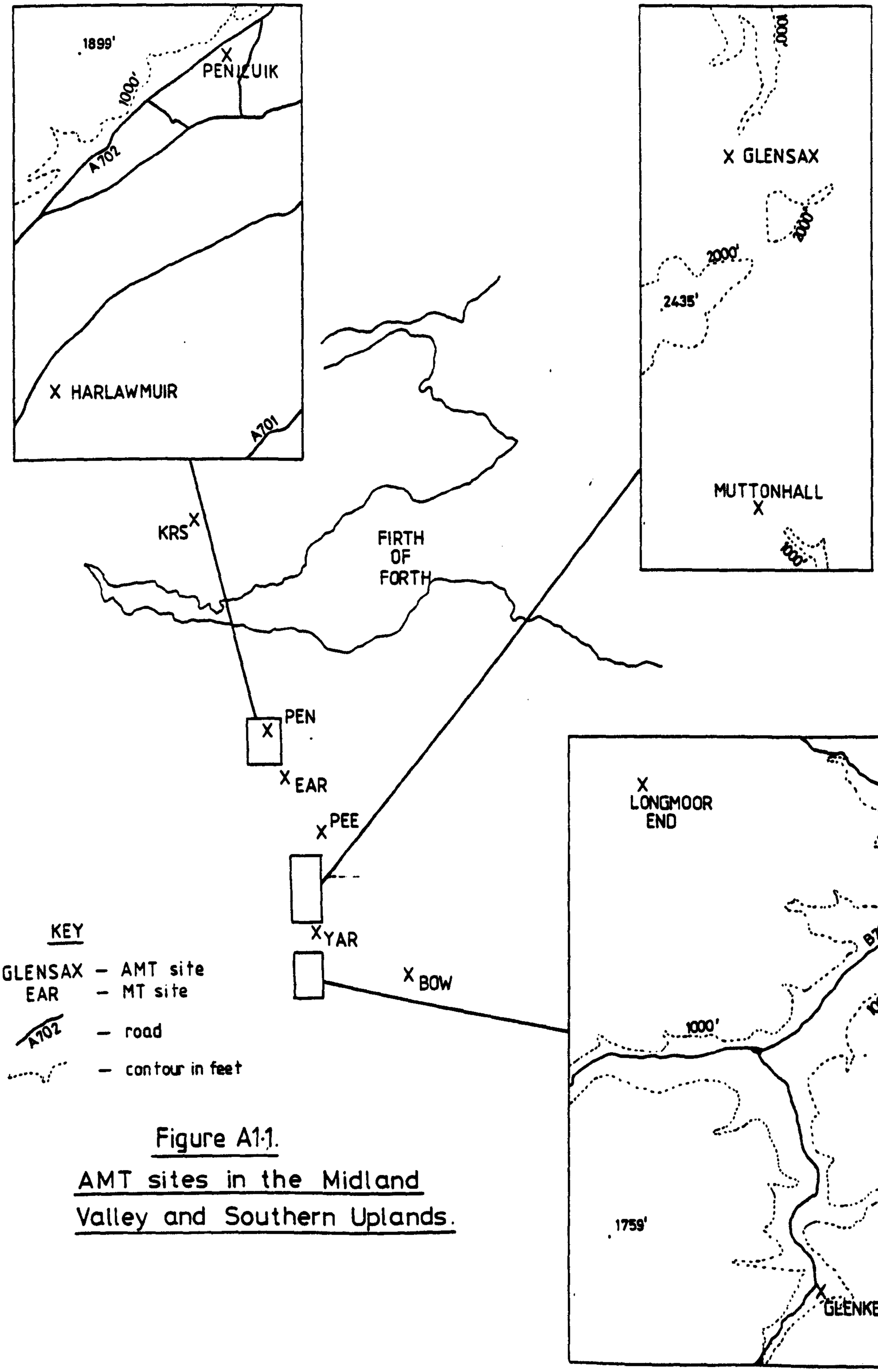

Figure A1.1.

AMT sites in the Midland Valley and Southern Uplands.

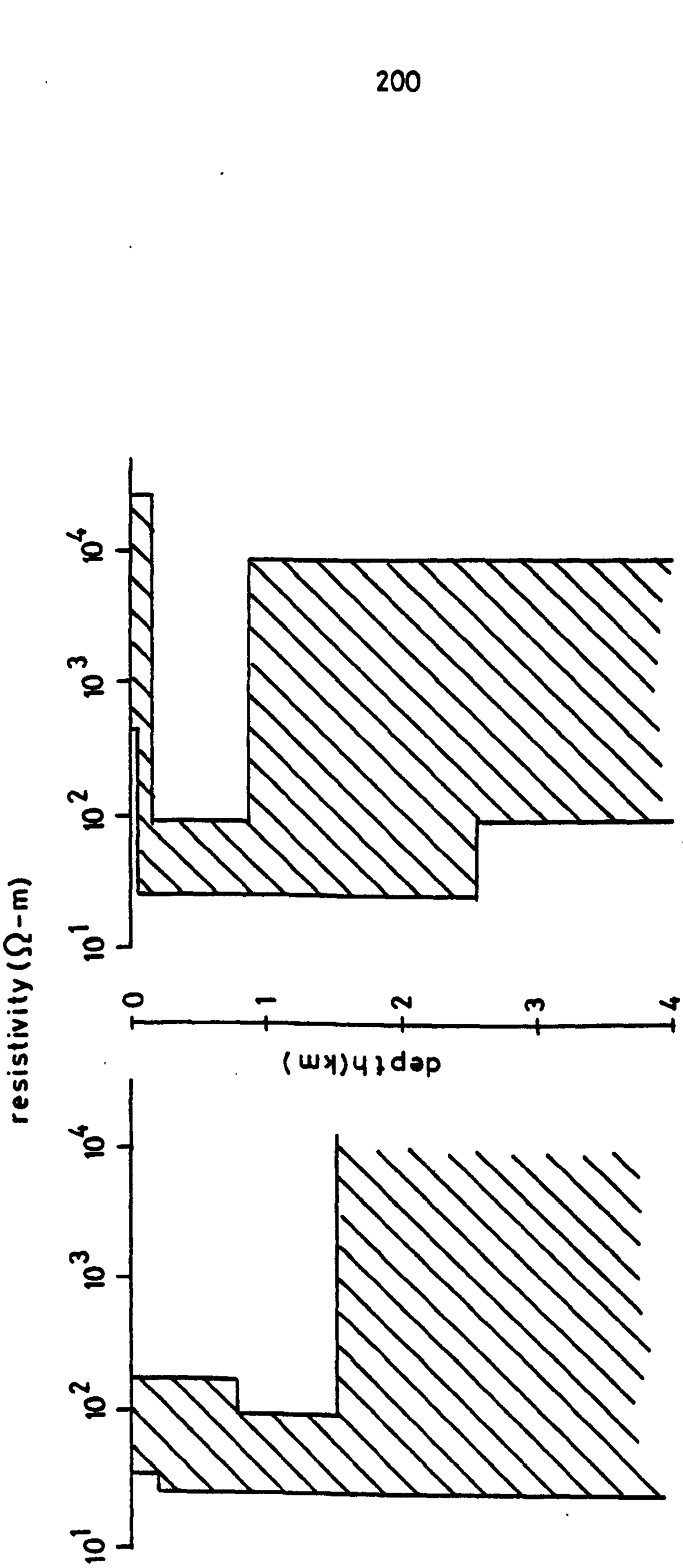

Figure A1·2.

One-dimensional models for AMT data from the Midland Valley.

have a low resistivity ($\sim$100 Ω-m) to a depth of around 1-1.5 km, below which the resistivity is very indeterminate.This presumably represents sediments, to a minimum of 1.5km depth, which are sufficiently conducting for there to be no penetration to deeper depths at the short periods involved. This is in agreement with the 2 kilometres of 75 Ω-m sediments used in the two-dimensional modelling.

The site at Penicuik was in fact the same as that at which magnetotelluric measurements were made and it is interesting to combine the results of the two soundings as has been done in figure A1.3.Both the maximum and minimum apparent resistivities have orders of magnitude in the two period bands which are comparable, a fact which encourages the belief that the curves are continuous across the gap in the period band without any major maxima or minima. The combined one-dimensional models for the site are also shown and illustrate the continuity which the use of both systems gives between the near surface and lower crustal structures. It should be noted that the AMT results were more effected by cultural noise than the MT results. The biasing effects at 50 and 150 Hz can be clearly seen in figure A1.3.

The results from four sites in the Southern Uplands at Glensax, Muttonhall, Longmoor End and Glenkerry are presented in figure A1.4. The surface layer of between 200 and 700 Ω-m to about 1.5 km depth at Muttonhall compares well with the sedimentary cover included in the two-dimensional model,as does the very thin conductor at Glenkerry. The results for Glensax and Longmoor End, however, are more difficult to interpret. At Longmoor End it seems likely that the sedimentary cover is represented by the very thin

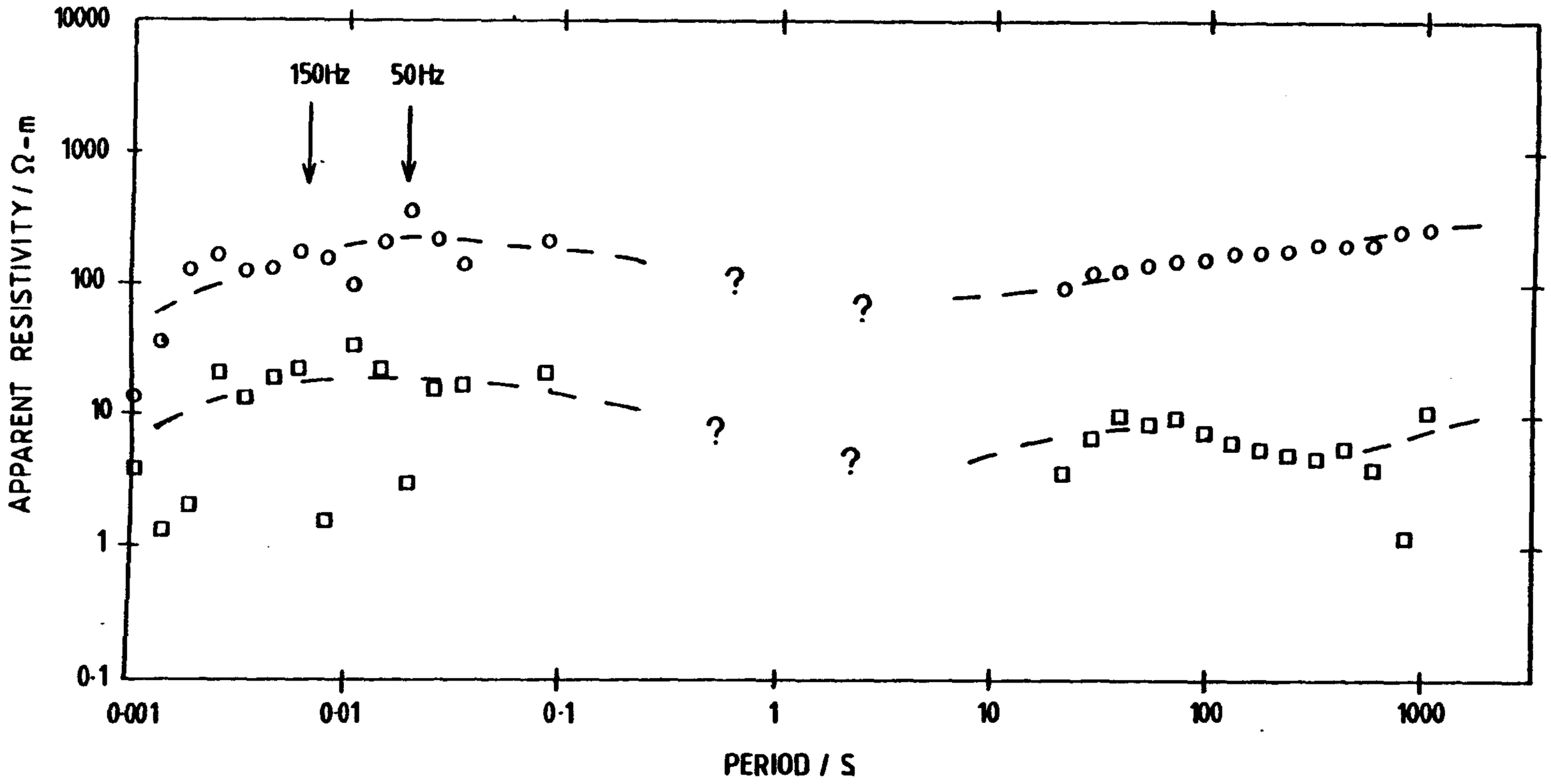

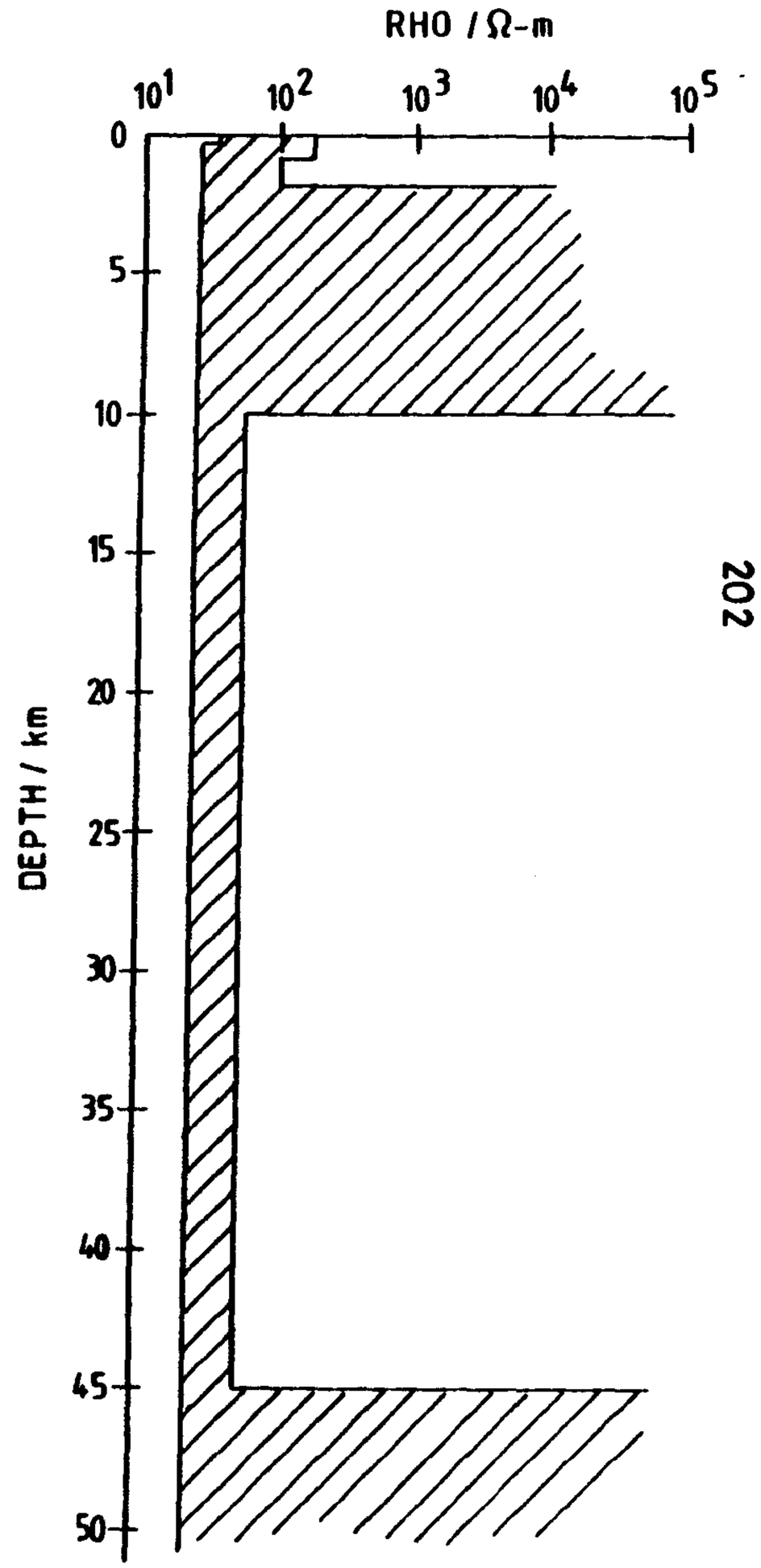

Figure A1-3.

Combined AMT and MT apparent resistivities and 1-d models for Penicuik.

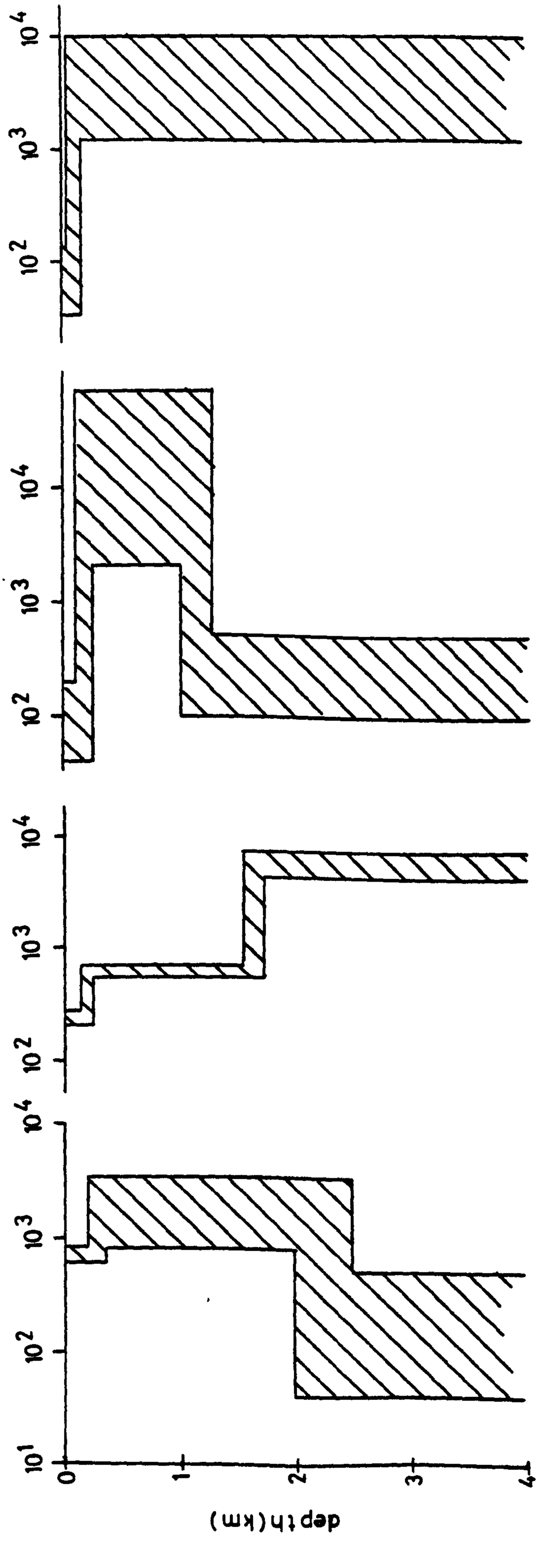

Figure A1.4. One - dimensional models for AMT data from the Southern Uplands.

conducting layer of around 100Ω-m resistivity. The 1km thick highly resistive structure is hard to understand and is discussed in the next section, although it is probable that slightly longer period data would resolve an increase in resistivity beneath the basement of the three-layer model. Similar commments apply to the results from Glensax.

Despite these difficulties, the overall impression is that the two-dimensional model for the magnetotelluric data includes a valid representation of the sedimentary cover in the Southern Uplands and the southern part of the Midland Valley. It is unfortunate that AMT measurements have not been made farther north as they may help to elucidate the upper crustal structure right across the Midland Valley.

A1.2: The Tweedale Granite.

The Tweedale Granite proposed on the basis of gravity and magnetic measurements by Lagios and Hipkin lies between the two MT sites at Peebles and Yarrow. The data from these sites were unable to resolve the structure however, and it was hoped that AMT measurements at intermediate sites might detect the intrusion at shorter periods. According to the gravity and magnetic model the granite comes to within 2.5 km of the surface at a point just to the north of Glensax, whilst to the south its upper surface shelves steeply to a depth of around 6 km beneath Muttonhall.

The result of the one-dimensional modelling for Glensax does show a boundary at 2-2.5 km, however the change is to a more conducting layer rather than the more resistive substratum one would expect for a granite. Novak (pers. comm.) has found resistivities of just less than a 1000 Ω-m for the Weardale granite using AMT

measurements and it is possible that the highly resistive layer from 0.25-2 km may represent rocks metamorphosed locally at the time of the intrusion. However, it is probably more likely that at the periods used the depth of penetration does not reach the surface of the granite. At Muttonhall, although there is a continuous increase in resistivity with depth the same is almost certainly true.

To investigate the possibility that the AMT measurements do not penetrate deep enough to detect the granite,a two-dimensional model was constructed and E and H-polarization apparent resistivities calculated for five periods between 0.001 and 0.1 seconds. The shape of the granite used in the model comes from a combination of the isodepth contours of figure 3.6 and the magnetic model of Lagios(1979). The model is shown in figure A1.5 with the positions of the two audiomagnetotelluric sites at Glensax and Muttonhall marked. An effective way of illustrating the variation in apparent resistivity with period across the model is to use resistivity pseudosections. In these distance along the traverse is plotted horizontally and period vertically; the apparent resistivity values at each point on the traverse at each period are then contoured. The shape of the contours indicates qualitatively the gradients in the actual resistivity structure. Variations in apparent resistivity with period at a particular site can be studied by examining the pseudosection along a vertical line and variations across the traverse at a particular period by considering a horizontal line.Pseudosections for both E and H-polarizations for the model of figure A1.5 are shown in figure A1.6.

The diagram shows that for both polarizations it is only at the longest periods, close to where the granite reaches its shal-

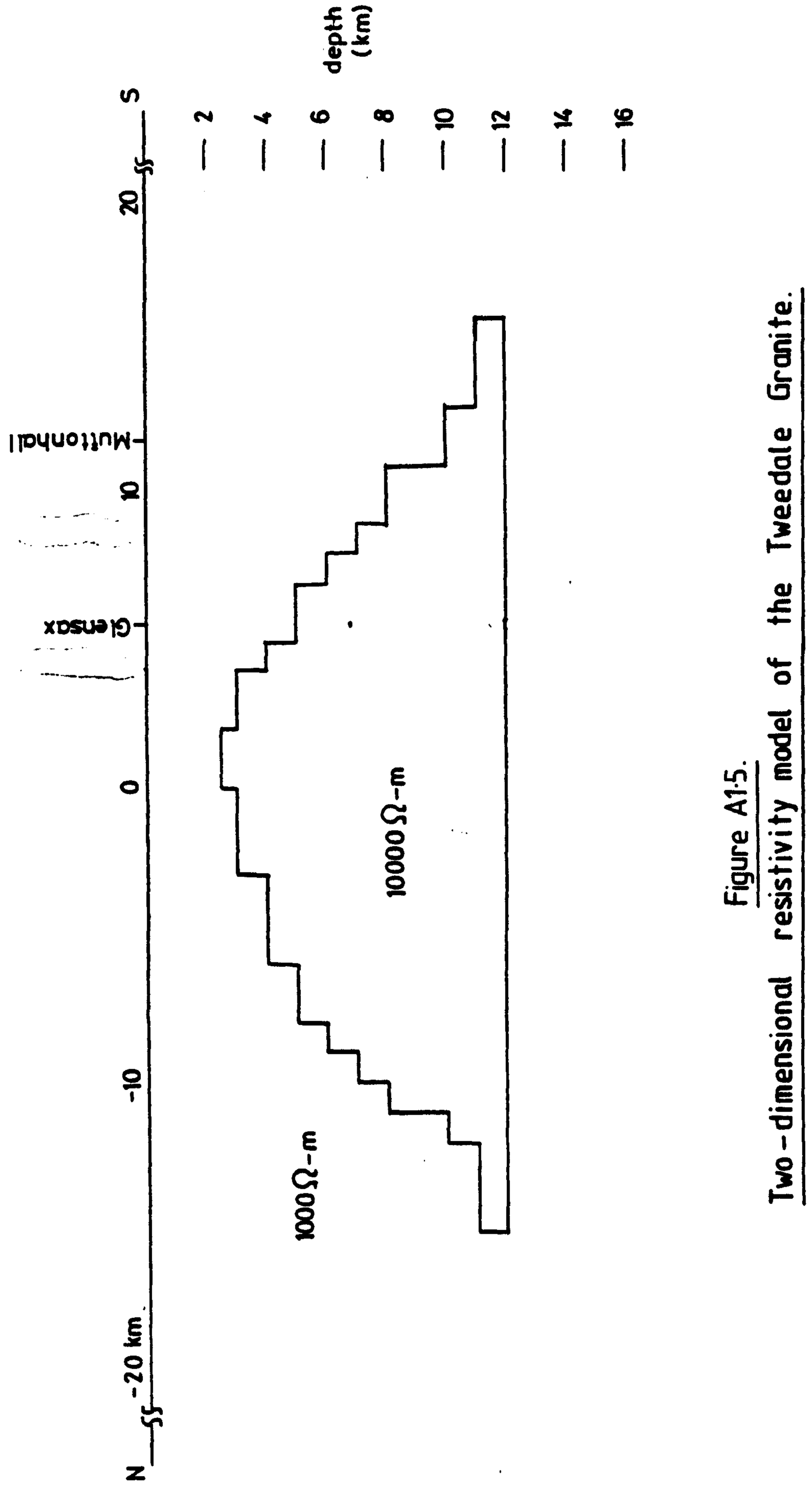

Figure A1.5.
Two-dimensional resistivity model of the Tweedale Granite.

Figure A1·6.

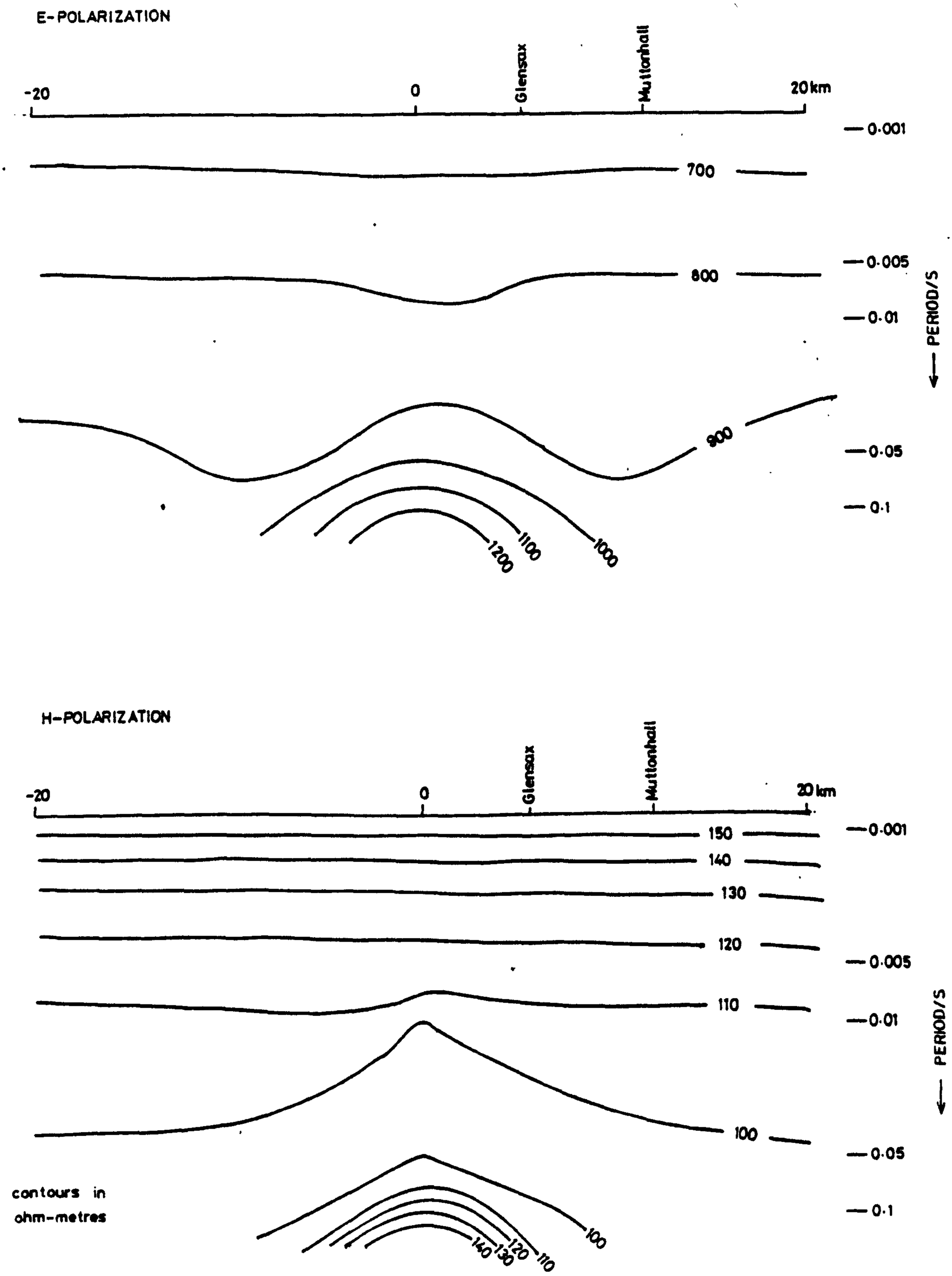

2-D model apparent resistivity pseudosections across the Tweedale Granite.

lowest depth, that there is any distortion from the plane layered contours of a one-dimensional model. The principal effect of the deviation from 1-dimensionality is the anisotropy of the apparent resistivities, those for E-polarization being 10 times the H-polarization values. The main conclusion from figure A1.6 is that for such a model, only at the two most northerly sites would the granite be detected by a sharp rise in resistivity at longer periods. However, the anisotropic effects due to the deviation from 1-dimensionality would be observable at all four of the sites.

When a 200 metre thick sedimentary layer of resistivity 300 Ω-m was included in the model the result was a plane layering of the contours at all periods, with only a very slight resistivity increase at 0.1 seconds close to the centre of the model.Moreover the values for E and H-polarizations were isotropic suggesting that the inclusion of the conducting cover prevents penetration to the underlying granite. The characteristics of the two models are summarized in table A1.2.

The conclusion that can be drawn from the models is that it does in fact seem unlikely that the AMT measurements are of sufficiently long period to penetrate to the granite at either Muttonhall or Glensax. It might, however, be possible to detect the intrusion slightly to the north of Glensax.

Table A1.2

2-d Models of the Tweedale Granite.

Comment \ Model	Figure A1.5	Figure A1.5 + 200m of 300Ω-m sedimentary cover
Magnitude of ρ_E	From 600-1000Ω-m	From 300 - 1000Ω-m
Magnitude of ρ_H	~100Ω-m with a minimum at 0.01 s	From 300 - 1000Ω-m
Isotropy	Anisotropic	Isotropic
Increase of ρ at long period	Yes for values of y of -6km _ +6km	Very small increase for -2km < y < 3km
Penetration to granite?	Yes for -6km < y < 6km but effect seen.	No

REFERENCES

Adam, G.A., 1976. Quantitative connections between regional heat flow and the depth of conductive layers in the Earth's crust and upper mantle., Acta. Geodet. Geophys. et Mont., 11, 503-509.

Albouy, Y., Godivier, R. and Perichon, P., 1971. Le sondage magnetotelluric., O.R.S.T.O.M., Paris.

Anderton, R., Bridges, P.H., Leeder, M.R. and Sellwood, B.W., 1979. A dynamic stratigraphy of the British Isles., Published by George Allen and Unwin. London.

Archie, G., 1942. The electrical resistivity log as an aid in determining some reservoir characteristics., Trans. Am. Inst. Min. Metall. Engrs., 146, 54-61.

Assumpcao, M. and Bamford, D., 1972. LISPB - V: Studies of crustal shear waves., Geophys. J. R. astr. Soc., 59, 539-552.

Babour, K. and Mosnier, J., 1979. Differential geomagnetic sounding in the Rhinegraben., Geophys. J. R. astr. Soc., 58,135-144.

Babour, K., Mosnier, J., Daignieres, M., Vaseur, G., le Mouel, J.L. and Rossignol, J.L., 1976. A geomagnetic variation anomaly in the Northern Pyrenees., Geophys. J. R. astr. Soc. 45, 583-600.

Banks, R.J. and Ottey, P., 1974. Geomagnetic deep sounding in and around the Kenya Rift Valley., Geophys. J. R. astr. Soc., 36, 321-335.

Bailey, R.C. and Edwards, R.N., 1976. The effect of source field polarization on geomagnetic anomalies in the British Isles., Geophys. J. R. astr. Soc., 45, 97-104.

Bailey, R.C., Edwards, R.N., Garland, G.D. and Greenhouse, J.P., 1978. Geomagnetic sounding of eastern North America and the White Mountain heat flow anomaly., Geophys. J. R. astr. Soc. 55, 499-502

Bailey, R.C., Edwards, R.N., Garland, G.D., Kurtz, R. and Pitcher, D.H., 1974. Electrical conductivity studies over a tectonically active area in Eastern Canada., J. Geomag. Geoelectr., 26, 125-146.

Bamford, D., Nunn K., Prodehl, C. and Jacob, B., 1978.LISPB - IV: Crustal structure of Northern Britain., Geophys. J. R. astr. Soc.,54, 43-60.

Banks, R.J., 1969. Geomagnetic variations and the elecrical conductivity of the upper mantle., Geophys. J. R. astr. Soc., 17, 457-487.

Banks, R.J., 1971. The overall conductivity distribution of the Earth., J. Geomag. Geoelectr., 24, 337-351.

Banks, R.J., 1973. Data processing and interpretation in geomagnetic deep sounding., Phys. Earth Planet. Inter., 7, 1-10.

Banks, R.J., 1979. The use of equivalent current systems in the interpretation of geomagnetic deep sounding data., Geophys. J. R. astr. Soc.,56, 139-157.

Bannister, J.R. and Gough, D.I., 1977. Development of a polar magnetic substorm. A two-dimensional array study., Geophys. J. R. astr. Soc., 51, 75-90

Bannister, J.R. and Gough, D.I., 1978. A study of two polar magnetic substorms with a two-dimensional magnetometer array. Geophys. J. R. astr. Soc., 53, 1-26.

Beamish, D., 1979. Source field effects on transfer functions at mid-latitudes., Geophys. J. R. astr. Soc., 58, 117-134.

Bentley, C.R., 1973. Error estimation in two-dimensional magnetotelluric analyses., Phys. Earth Planet. Inter., 7, 423-430.

Berdichevsky, M.N., 1960. Principles of magnetotelluric profiling theory., Applied Geophys., (Prikl. Geofiz.), 28.

Berdichevsky, M.N., 1963. Linear relationships in the magnetotelluric field., Applied Geophys., (Prikl. Geofiz.), 38.

Berdichevsky, M.N., Vanyan, L.L., Feldman, I.S. and Porstendorfer, G., 1972. Conducting layers in the Earth's crust and upper mantle., Gerlands. Beitr., Geophysik., 81, 187-196.

Blaxland, A.B., Aftalion, M. and van Breeman, O., 1979. Pb isotopic composition of feldspars from Scottish Caledonian Granites, and the nature of the underlying crust., Scott. J. Geol., 15, 139-151.

Boettcher, A.L. and Wyllie, P.J., 1968. Melting of granite with excess water to 30 kilobars pressure., J. Geol., 76, 235-244.

Bott, M.P.H., Johnson, G.A.L., Mansfield, J. and Wheildon, J., 1972. Terrestrial heat flow in north-east England., Geophys. J. R. astr. Soc., 27, 277-288.

Brewitt-Taylor, C.R. and Johns, P.B., 1980. Diakoptic solution of induction problems., J. Geomag. Geoelectr., In press.

Brewitt-Taylor, C.R. and Weaver, J.T., 1976. On the finite difference solution of two-dimensional induction problems., Geophys. J. R. astr. Soc., 47, 375-396.

Brace, W.F., 1971. Resistivity of saturated crustal rocks to 40 km based on laboratory measurements. AGU monograph, 14, 243-255.

Caignard, L., 1953. Basic theory of the magnetotelluric method of geophysical propecting., Geophys., 18, 605-635.

Church, W.R. and Gayer, R.A., 1973. The Ballantrae ophiolite., Geol. Mag., 110, 497-510.

Cochrane, N.A. and Hyndman, R.D., 1974. Magnetotelluric and magnetovariational studies in Atlantic Canada., Geophys. J. R. astr. Soc., 38, 385-406.

Cochrane, N.A. and Wright, J.A., 1977. Geomagnetic sounding near the northern termination of the Appalachian system., Can. J. Earth Sci., 14, 2858-2864.

Dawson, T.W. and Weaver, J.T., 1979. Three-dimensional induction in a non-uniform thin sheet at the surface of a uniformly conducting earth., Geophys. J. R. astr. Soc., 59, 445-462.

Dewey, J.F., 1969. The evolution of the Appalachian- Caledonian Orogen., Nature, 22, 124.

Dewey, J.F., 1971. A model for the Lower Palaeozoic evolution of the southern margin of the early Caledonides of Scotland and Ireland., Scott. J. Geol., 7, 219-240.

Dewey, J.F. and Pankhurst, R.J., 1970. Evolution of the Scottish Highlands and their radiometric age pattern., Royal Soc. Edinburgh Trans., 68, 361-389.

Dosso, H.W., 1973. A review of analogue model studies of the coast effect., Phys. Earth Planet. Inter., 7,294-302.

Dragert, H., Law, L.K. and Sule, P.O., 1980. Magnetotelluric soundings across the Pemberton Volcanic Belt, British Columbia., Can. J. Earth Sci., 17, 161-167.

Duba, A., 1976. Are laboratory conductivity data relevant to the Earth ?, Acta Geodet. Geophys. et Mont., 11,485-495.

Duba, A., Ho, P. and Piwinskii, A., 1975. Electrical conductivity studies of igneous rocks: fusion of basalt., Abstract in EOS, 56, 1075.

Dvorak, Z., 1975. Electrical conductivity models of the crust., Can. J. Earth Sci., 12, 962-970.

Edwards,R.N. and Greenhouse, J.P., 1977. Geomagnetic variation in the eastern United States: evidence for a highly conducting lower crust?, Science, 188, 726-728.

Edwards, R.N., Law, L.K. and White, A., 1971. Geomagnetic variations in the British Isles and their relation to electric currents in the ocean and shallow seas., Phil. Trans. Roy. Soc. Lond., 1204, 289-323.

El-Batroukh, S.I., 1975. Geophysical investigations on Loch Doon granite, south-west Scotland., PhD thesis, University of Glasgow.

Everett, J.E. and Hyndman, R.D., 1967. Magnetotelluric investigations in south-western Australia., Phys. Earth Planet. Inter., 1, 49-54.

Faber, S. and Bamford, D., 1979. Lithospheric structural contrasts across the Caledonides of Northern Britain., Tectonophysics, 56, 17-30.

Feldman, I.S., 1976. On the nature of conductive layers in the Earth's crust and upper mantle., KAPG Geophys. Monograph, 721-730.

Fitton, J.G. and Hughes, D.J., 1970. Volcanism and plate tectonics in the British Ordovician., Earth Planet. Sci. Lett., 8, 223-228.

Fowler, R.A., Kotick, B.J. and Elliott, R.D., 1967. Polarization analysis of natural and artificially induced geomagnetic micropulsations., J. Geophys. Res., 72, 2871-2883.

Green, C.A., 1975. An induction study at micropulsation periods in the British Isles., Geopyhs. J. R. astr. Soc., 40, 225.

Greig, D.C., 1971. The South of Scotland., British Regional Geology Series, HMSO.

Gunn, P.J., 1973. Location of the Proto-Atlantic Suture in the British Isles., Nature, 242, 111-112.

Haak, V., 1978. Interpretation procedure for magnetotellurics with particular consideration of laterally varying electrical conductivity in the Earth and a spatially inhomogeneous inducing field., Munchen Ak-Abh. maths-nat., 158.

Hall, J. and Simmons,G., 1979. Seismic velocities of Lewisian metamorphic rocks at pressures to 8 kbar: relationship to crustal layering in North Britain., Geophys. J. R. astr. Soc., 58, 337-347.

Harris, F.J., 1978. On the use of windows for harmonic analysis with the discrete Fourier Transform., Proc. IEEE, 66, 1.

Healey, J.H., 1971. Discussion of T.R. Madden's paper, in The structure and physical properties of the Earth's crust., AGU monograph, 95.

Hermance, J.F., 1973. An electrical model for the sub-Icelandic crust., Geophysics, 38 (1), 3.

Hermance, J.F., 1979. The electrical conductivity of materials containing partial melt: asimple model from Archie's Law., Geophys. Res. Lett., 6, 613-616.

Hermance, J.F. and Pedersen, J., 1980. Deep sructure of the Rio Grande Rift: a magnetotelluric interpretation., J. Geophys. Res., In press.

Hipkin, R.G. and Lagios, E., 1978. A gravity survey of south-east Scotland: The Southern Uplands., abstract in Geophys. J. R. astr. Soc., 53, 160.

Honkura, Y., Kurtz, R.D. and Niblett, E.R., 1977. Geomagnetic deep sounding and magnetotelluric results from a seismically active region north west of Quebec city., Can. J. Earth Sci., 14, 256-267.

Hutton, V.R.S., Sik, J. and Gough, D.I., 1977. Electrical conductivity and tectonics of Scotland., Nature, 266, 617-620.

Hutton, V.R.S. and Jones, A.G., 1980. Magnetovariational and magnetotelluric investigations in South Scotland., J. Geomag. Geoelectr., In press.

Hyndman, R.D. and Cochrane, N.A., 1971. Electrical conductivity structure by geomagnetic induction at the continental margin of Atlantic Canada., Geophys. J. R. astr. Soc., 25, 425-466.

Hyndman, R.D. and Hyndman, D.W., 1968. Water saturation and high conductivity in the lower continental crust., Earth Planet. Sci. Lett., 4, 427-431.

Jain, S. and Wlson, C.D.V., 1967. Magnetotelluric investigations in the Irish Sea and Southern Scotland., Geophys. J. R. astr. Soc., 12, 165-180.

Jeans, P.J.F., 1973. Plate tectonic reconstruction of the Southern Caledonides of Great Britain., Nature Phys. Sci., 245, 120-122.

Johnstone, G.S., 1966. The Grampian Highlands., British Regional Geology Series, H.M.S.O.

Jolivet, J., 1966. PhD thesis, University of Paris.

Jones, A.G., 1977. Geomagnetic induction studies in Southern Scotland., PhD thesis, University of Edinburgh.

Jones, A.G. and Hutton, V.R.S., 1979a. A multi-station magnetotelluric study in Southern Scotland - I. Fieldwork, data analysis and results., Geophys. J. R. astr. Soc., 56, 329-349.

Jones, A.G. and Hutton, V.R.S., 1979b. A multi-station magnetotelluric study in Southern Scotland - II. Monte-Carlo inversion of the data and the geophysical and tectonic implications., Geophys. J. R. astr. Soc., 56, 351-368

Jones, F.W. and Pascoe, L.J., 1971. A general computer program to determine the perturbation of alternating electric currents in a two-dimensional model of a region of uniform conductivity with an embedded inhomogeneity., Geophys. J. R. astr. Soc., 24, 3-30.

Jones, F.W. and Vozoff, K., 1978. A calculation of magnetotelluric quantities for three-dimensional inhomogeneities., Geophys., 43, 1167-1175.

Jordan, T.H. and Frazer, L.N., 1975. Crustal and upper mantle structure from Sp phases., J. Geophys. Res., 80, 1504-1518.

Kanasewich, E.R., 1973. Time sequence analysis in geophysics., Univ. of Alberta Press, Edmonton, Alberta, Canada.

Keller, G.V., 1966. Electrical properties of rocks and minerals., Handbook of Physical Constants., Geol. Soc. Amer. Mem., 97, 553-577.

Keller, G.V., 1971. Electrical properties of the Earth's crust, a survey of the literature., ONR Contract N000-14-70-C-0290, Colorado School of Mines, Golden.

Keller, G.V., Anderson, L.A. and Pritchard, J.F., 1966. Geological survey investigations of the electrical properties of the crust and upper mantle., Geophysics, 31, 1078-1087.

Khitarov, N.I., Slutsky, A.B. and Pugin, V.A., 1970. Electrical conductivity of basalts at high T-P and phase transitions under upper mantle conditions. Phys. Earth Planet. Inter., 3, 334-342.

Kurtz, R.D., 1973. A magnetotelluric survey of Eastern Canada., PhD thesis, University of Toronto.

Kurtz, R.D. and Garland, G.D., 1976. Magnetotelluric measurements in Eastern Canada., Geophys. J. R. astr. Soc., 45, 321-348.

Kushiro, I., Syono, Y. and Akimoto, S., 1968. Melting of a peridotite nodule at high pressures and high water pressures., J. Geophys. Res., 73, 6023-6029.

Lagios, E., 1979. Gravity and other geophysical studies relating to the crustal structure of south-east Scotland., PhD thesis, University of Edinburgh.

Lagios, E. and Hipkin, R.G., 1979. The Tweedale Granite - A newly discovered batholith in the Southern Uplands., Nature, 280, 672-675.

Lambert, I.B. and Wyllie, P.J., 1970. Melting in the deep crust an upper mantle and the nature of the low velocity layer., Phys. Earth Planet. Inter., 3, 316-322.

Lebedev, E.B. and Khitarov, N.I., 1964. Dependence of the beginning of melting of granite and the electrical conductivity of the melt on high water vapor pressure., Geochemistry International., 1, 193-197.

Leggett, J.K., McKerrow, W.S. and Eales, M.H., 1979. The Southern Uplands of Scotland: A Lower Palaeozoic accretionary prism., J. Geol. Soc. Lond., 136, 755-770.

Lines, L.R. and Jones, F.W., 1973a. The perturbation of alternating geomagnetic fields by three-dimensional island structures., Geophys. J. R. astr. Soc., 32, 133-154.

Lines, L.R. and Jones, F.W., 1973b. The perturbation of alternating geomagnetic fields by an island near a coastline., Can. J. Earth Sci., 10, 510-518.

MacGregor, M. and MacGregor, A.G., 1948. The Midland Valley of Scotland., British Regional Geology Series, H.M.S.O.

Madden, T.R., 1976. Random networks and mixing laws., Geophysics, 41, 1104-1125.

Madden, T.R. and Swift, C.M., 1969. Magnetotelluric studies of electrical conductivity structure of the crust and upper mantle. In: The Earth's crust and upper mantle., (ed. P.J. Hart). AGU Monograph, 469-479.

Matsushita,. S., and Campbell, 1967.
Editors: Physics of Geomagnetic Phenomena, Academic Press, New York.

Mbipom, E.W., 1980. Geoelectric studies of the crust and upper mantle in Northern Scotland., PhD thesis, University of Edinburgh.

Mbipom, E.W. and Hutton, V.R.S., 1978. Electromagnetic induction studies in Northern Scotland.

McKerrow, W.S. and Cocks, L.R.M., 1977. The location of the Iapetus Ocean Suture in Newfoundland., Can. J. Earth Sci., 14, 488-495.

McLean, A.C. and Qureshi, I.R., 1966. Regional gravity anomalies in the western Midland Valley of Scot;and., Trans. Roy. Soc. Edin., 66, 267-283.

Mishin, V.M., Bazarzapov, A.D., Matveev, M.I. and Nemtsova, E.I., 1975. On nature of Sq variations., Siberian Instit. of Terr. Mag., USSR.

Mitchell, A.H.G. and McKerrow, W.S., 1975. Analogous evolution of the Burma Orogen and the Scottish Caledonides., Bull. Geol. Soc. Am., 86/3, 305.

Moseley, F., 1977. Caledonian plate tectonics and the place of the English Lake District., Bull. Geol. Soc. Am., 88, 764-768.

Nekut, A., Connerney, J.E.P. and Kuckes, A.F., 1977. Deep crustal electrical conductivity; evidence for water in the lower crust., Geophys. Res. Lett., 4, 239-242.

Novak, M., Dawes, G.J.K. and Hutton, V.R.S., 1980. Audio-magnetotelluric investigations in North-east England., abstract in Geophys. J. R. astr. Soc., 61, 205.

Orr, D., 1973. Magnetic pulsations within the magnetosphere - a review., J. Atmos. Terr. Physics, 35, 1-50.

Osemeikhian, J.E.A. and Everett, J.E., 1968. Anomalous magnetic variations in S.W. Scotland., Geophys. J. R. astr. Soc., 15, 361-366.

Oxburgh, E.R., Richardson, S.W., Wright, S.M., Jones, M.Q.W., Penney, S.R., Watson, S.A. and Bloomer, J.R., 1980. Heat flow pattern of the United Kingdom., E.E.C. 2nd International Seminar on Geothermal Energy, 149-152.

Parkinson, W.D., 1959. Directions of geomagnetic fluctuations., Geophys. J. R. astr. Soc., 2, 1-14.

Parkinson, W.D., 1962. The influence of continents and oceans on geomagnetic variations., Geophys. J. R. astr. Soc., 6, 441-449.

Pascoe, L.J. and Jones, F.W., 1972. Boundary conditions and calculation of surface values for the general two-dimensional electromagnetic induction problem., Geophys. J. R. astr. Soc., 27, 179-193.

Phillips, W.E.A., Stillman, C.J. and Murphy, T., 1976. A Caledonian plate tectonic model., J. Geol. Soc. Lond., 132, 576-609.

Piwinskii, A.J. and Duba, A., 1974. High temperature electrical conductivity of albite., Geophys. Res. Lett., 1, 209-211.

Powell, D.W., 1971. A model for the Lower Palaeozoic evolution of the Southern margin of the early Caledonides of Scotland and Ireland., Scott. J. Geol., 7, 369-372.

Presnall, D.C., Simmons, C.L. and Porath, H., 1972. Changes in electrical conductivity of a synthetic basalt during melting., J. Geophys. Re., 77, 5665-5672.

Price, A.T., 1950. Electromagnetic induction in a semi-infinite conductor with a plane boundary., Quart. J. Mech. Appl. Math., 3, 385-410.

Price, A.T., 1962. The theory of magnetotelluric fields when the source field is considered., J. Geophys. Res., 67, 1907.

Raiche, A.P., 1974. An integral equation approach to three-dimensional modelling., Geophys. J. R. astr. Soc., 36, 363-376.

Reddy, I.K. and Rankin, D., 1972. On the interpretation of magnetotelluric data in the plains of Alberta., Can. J. Earth Sci., 9, 514-527.

Richardson, S.W. and Oxburgh, E.R., 1978. Heat flow , radiogenic heat production and crustal temperatures in England and Wales., J. Geol. Soc. Lond., 135, 323-337.

Rooney, D., 1976. Magnetotelluric measurements across the Kenyan Rift Valley., PhD thesis, University of Edinburgh.

Rooney, D. and Hutton, V.R.S., 1977. A magnetotelluric and magnetovariational study of the Gregory Rift Valley, Kenya., Geophys. J. R. astr. Soc., 51, 91-119.

Schmucker, U., 1970. Anomalies of geomagnetic variations in the South-western United States., Bull. Scripps Inst. Ocean., Univ. of Calif., 13.

Schuster, A., 1889. The diurnal variation of terrestrial magnetism., Phil.Trans. Roy. Soc. London, Ser. A, 180, 467-518.

Shankland, T.J. and Waff, H.S., 1977. Partial melting, and electrical anomalies in the upper mantle., J. Geophys. Res., 82, 5409-5417.

Srivistava, S.P., 1967. Magnetotelluric two- and three-layered master curves., Publ. of Dominican Observatory, Ottawa, Vol 35, No. 7.

Stanley, W.D., Boehl, J.E., Bostick, F.X. and Smith, H.W., 1977. Geothermal significance of magnetotelluric sounding in the Eastern Snake River Plain - Yellowsone Region., J. Geophys. Res.

Sternberg, B.K., 1979. Electrical resistivity structure of the crust in the southern extension of the Canadian Shield - layered earth models., J. Geophys. Res., 84, 212.

Summers, D.M., 1980. Interpreting the magnetic fields associated with two-dimensional induction anomalies., Geophys. J. R. astr. Soc., In press.

Swift, C.M., 1967. A magnetotelluric investigation of an electrical conductivity anomaly in the south-western United States., PhD thesis, M.I.T.

Trigg, D.F., 1972. An amplifier and filter system for telluric signals., Publ. Earth Phys. Branch, 41, 66.

Waff, H.S., 1974. Theoretical considerations of electrical conductivity in a partially molten mantle and implications for geothermometry., J. Geophys. Res., 4003-4010.

Weaver, J.T., 1973. Induction in a layered plane earth by uniform and non-uniform source fields.,Phys. Earth Planet. Inter., 7, 266-281.

Wiedelt, P., 1972. The inverse problem of geomagnetic induction., Zeitschrift Fur Geophysik., 38, 257-289.

Wiedelt, P., 1975. Electromagnetic induction in three-dimensional structures., J. Geophys., , 85-109.

Williams, A., 1975. Plate tectonics and biofacies evolution as factors in Ordovician correlation., In The Ordovician System : Proceedings of a Palaeontological Association Symposium, Cardiff, Univ. of Wales Press and Nat. Mus. Wales, 18-53.

Wilson, J.T., 1966. Did the Atlantic close and then re-open?, Nature, 211, 676-681.

Wyllie, P.J., 1971. Experimental limits for melting in the Earth's crust and upper mantle., A.G.U. monograph, 14, 279-301.

Zablocki, C.I., 1964. Electrical properties of serpentinite from Mayaguez, Puerto Rico., In A Study of Serpentinite, Washington.

Zaridze, G.N., 1967. On the problem of the connection of magmatism, metamorphism and tectonics., Geotectonics, 4.

van Zijl, J.S.V., 1977. Resistivity and the continental crust on Southern Africa, Nature, 265, 614.

Zobacki, M.D., 1975. High pressure deformation and fluid flow in sandstone, granite and granular materials. PhD thesis, Stanford University.

Sarson, P.H., 1973. Instrumentation for induction studies on land., Phys. Earth Planet. Int., 7, 313-322.

Reprinted from Nature, Vol 287, No. 5777, pp. 30-33, September 4 1980

An electrical model of the crust and upper mantle in Scotland

V. R. S. Hutton, M. R. Ingham & E. W. Mbipom

Department of Geophysics, University of Edinburgh, Mayfield Road, Edinburgh EH9 3JZ, UK

Magnetotelluric and magnetovariational studies in southern Scotland[1–4] have been followed by deep electrical soundings at an additional 30 sites. These lie on an approximately linear traverse extending from Kinlochbervie in the Lewisian Foreland to Borthwickbrae in the Scottish Borders (Fig. 1*a*). This traverse crosses the main geological zones of Scotland and follows reasonably closely the line of the LISPB[5] seismic project (Fig. 1*b*). Full details of these geo-electric studies will be published elsewhere. We present here results of two-dimensional modelling of both the magnetotelluric and geomagnetic response functions[6,7] obtained along the traverse.

The model was derived as follows. The digital data from each site were analysed in similar ways to those adopted in refs 8–10. The resulting magnetotelluric response functions, apparent resistivity and phase, were found to be anisotropic at all sites. This indication of lateral variations in conductivity structure was supported by the behaviour of the geomagnetic response functions.

A one-dimensional inversion[11] of the average apparent resistivity and phase data was obtained for each site. These were then used as the basis for applying a two-dimensional modelling programme[12] to each of the sections AA′ and BB′ of the total traverse.

Successive adjustments were then made to the initial two-dimensional models to obtain models which fitted not only both the maximum and minimum apparent resistivity data but also the geomagnetic response functions.

Finally, due to the similarity in the two best-fitting models in the region of overlap to the north of the Highland Boundary Fault, a single geo-electric model was constructed to represent the complete traverse. Observations at Newcastleton and Towhouse[11] have been taken into account to provide a very provisional model across the probable region of the Iapetus suture.

The resulting geo-electric model is given in Fig. 2*a*. This model provides reasonably good agreement between observed and computed response functions for the sites along the traverse marked by arrows in Fig. 1*a*. For traverse AA′, the modelling has been discussed by Mbipom[13] and for traverse BB′ a similar account is in preparation. Here we compare examples of observed and model responses (Figs 3, 4). The model suggests that the electrical structure of the crust and upper mantle in Scotland is, as one might expect from the surface geology, very complex and that there seems to be a distinctive conductivity–depth profile associated with each of the major geological zones along the traverse. For example, the Precambrian fragment to the west of the Moine Thrust is characterized by a resistive crust overlying a less resistive upper mantle, while in the Caledonian metamorphic belt, only the upper 10–15 km of the crust is resistive and the lower crust and uppermost mantle are relatively conducting. The major granitic intrusions are particularly resistive and where the observational density is sufficient the electrical model seems to delineate their form with some success. At the Great Glen, there is a 10 km wide gap in the resistive upper crust where an upper conducting layer connects with the deeper conducting layer of the lower crust and upper mantle. Above average crustal conductivity is also found at shallow depths near the Highland Boundary, Southern Uplands and Stublick Faults. The section of this two-dimensional model covering the south of Scotland confirms and extends the previous one-dimensional interpretation of this region[4]. In the Southern Uplands, the crust is resistive to a depth of ~20 km, and overlies a highly conducting layer, $\sigma \approx 2 \times 10^{-2}$ S m^{-1}, of poorly defined thickness, 30–70 km. Observational data from the Midland Valley and Northumberland Basin are sparse but in both regions a good conductor exists in the upper crust and it overlies a more resistive layer with the interface between them shelving rapidly near the boundaries of these regions.

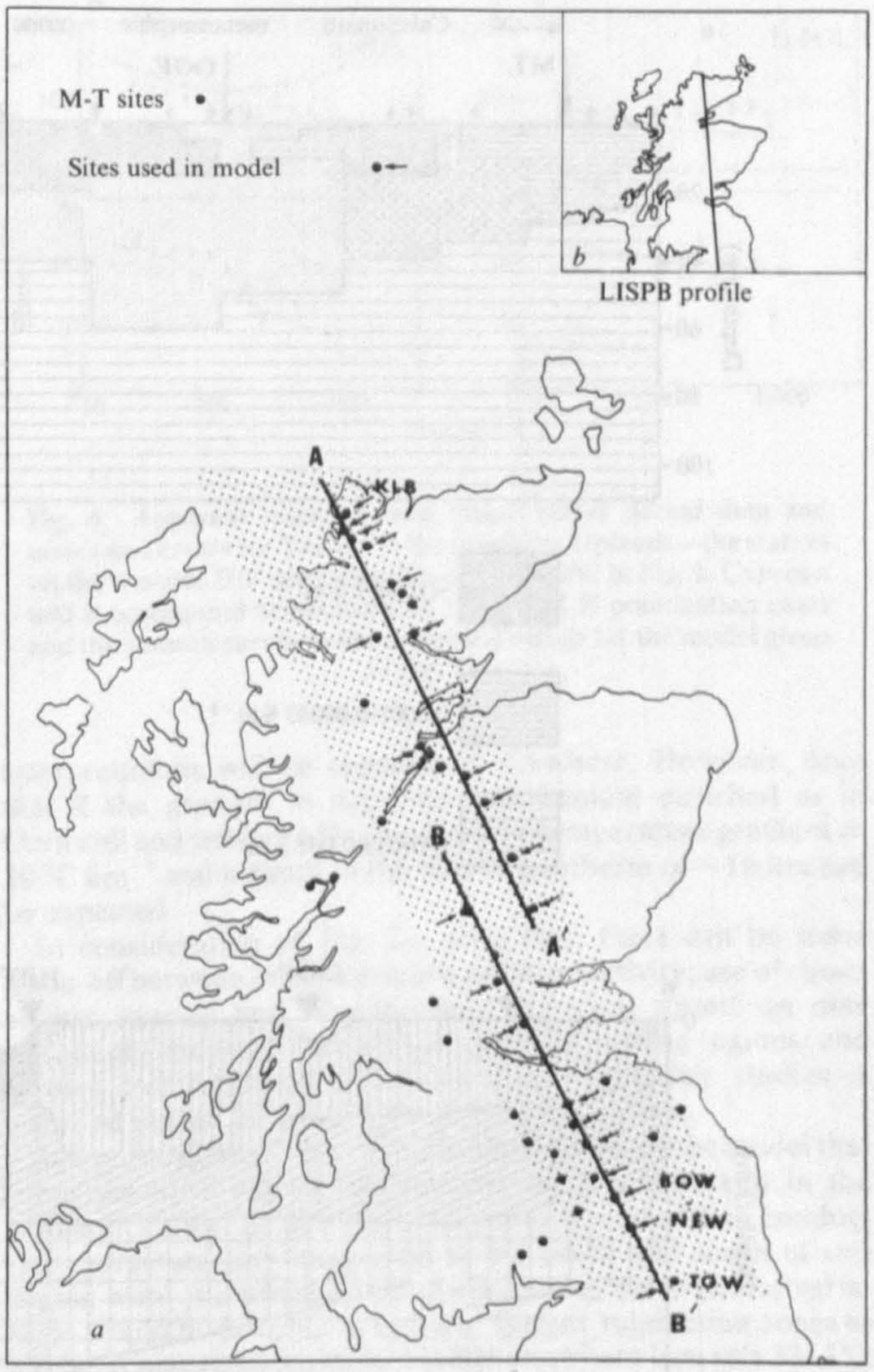

Fig. 1 *a*, Map of Scotland showing the location of the magnetotelluric (M–T) sites. KLB, Kinlochbervie; BOW, Borthwickbrae; NEW, Newcastleton; TOW, Towhouse. *b*, Map of Scotland showing the line of the LISPB study.

This Scottish electrical model can be compared with deep electrical soundings in other countries. Jones and Hutton[4] have already noted the similarity in the conductivity–depth profiles in the Southern Uplands and in the Canadian Appalachians, regions of common geological history. Further comparison of the Scottish model and that obtained from the Canadian study[14] for a traverse from the Grenville Province of the Canadian Shield to the Appalachians shows another common feature. The electrical conductivity of the lower crust in the neighbourhood of the St Lawrence river, that is the Logan line, where the basement was formed during the Grenville orogeny, is similar to that around the Great Glen, 5×10^{-3} S m^{-1}. In fact, a conductivity–depth profile consisting of a resistive upper crust, a more conducting lower crust and uppermost mantle and a relatively resistive upper mantle seems to be the most common profile in stable continental regions[15–24].

The average conductivity of near-surface continental crustal rocks is generally accepted to be in the range[25] 10^{-5} to 10^{-3} S m^{-1}, as found in the Scottish study along much of the traverse. In some locations, however, the conductivity within the

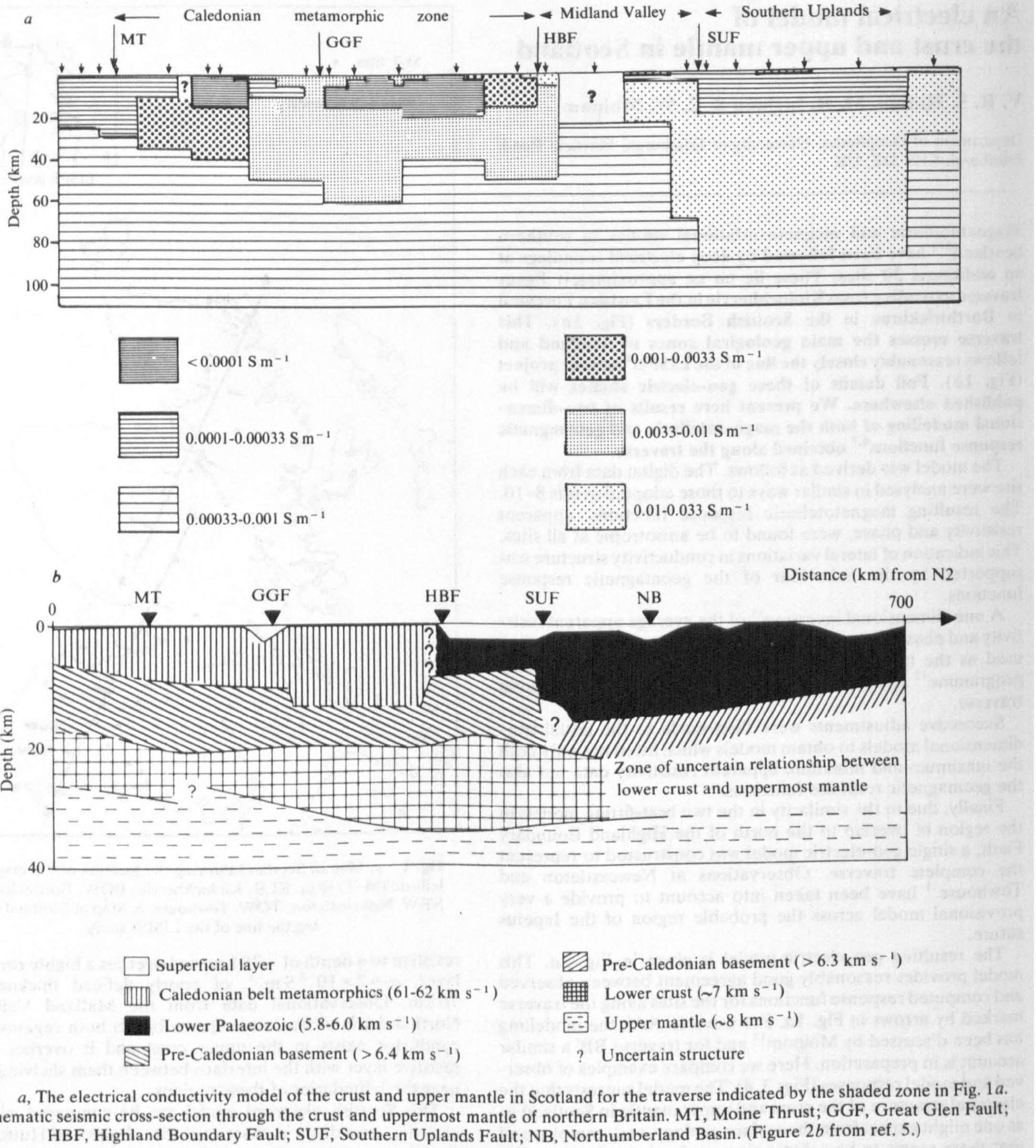

Fig. 2 *a*, The electrical conductivity model of the crust and upper mantle in Scotland for the traverse indicated by the shaded zone in Fig. 1*a*. *b*, Schematic seismic cross-section through the crust and uppermost mantle of northern Britain. MT, Moine Thrust; GGF, Great Glen Fault; HBF, Highland Boundary Fault; SUF, Southern Uplands Fault; NB, Northumberland Basin. (Figure 2*b* from ref. 5.)

top few kilometres is as high as 10^{-2} to 10^{-1} S m^{-1}. Conductivities of this order of magnitude have been found to be associated with the presence of graphitic schists, geothermal prospects or highly conducting fluids in loosely consolidated sediments.

Thus, in general, all sections of the Scottish model have their counterparts elsewhere. The lateral variation in structure over a distance of only 400 km is, however, probably more striking than in any previous study.

The only published model of the deep structure across Scotland, other than those inferred from studies of surface rocks, is that provided by the LISPB seismic study (Fig. 2*b*).

There is only partial agreement between the geometries of the seismic and electric models. For example, in the Lewisian, the boundary between the resistive crust and more conducting upper mantle occurs at a depth which corresponds well with the Moho as deduced from the seismic study. Further south, however, there is no boundary in the electrical model at Moho depths, but rather a boundary between the resistive upper crust and the more conducting lower crust. This boundary agrees reasonably well with the depth of the Conrad discontinuity. Sharp changes in depth of seismic boundaries, for example, at the Great Glen Highland Boundary and Southern Uplands Faults have their counterparts in the electrical model. The existence of a resistive crust of thickness about 20 km in the Southern Uplands is compatible with the absence of a seismic horizon at 10–15 km depth and a very good conductor in the uppermost mantle is compatible with the absence of a clearly defined signal from Moho depths.

Oxburgh *et al.*[26] have used a schematic crustal model to

explain their UK heat flow data. They propose that the variation in heat flow is due to variation in crustal heat production, with the higher heat flow belts including a higher proportion of granites than elsewhere. They require the granites to have a thickness of 16.6 km which is in reasonable agreement with that indicated for the Cairngorm granites in the geoelectric model.

The interpretation of the electrical model will be discussed in detail elsewhere. Here we briefly consider possible explanations of anomalously high conductivity. In the upper crust, it can arise, primarily, as a result of electrolytic conduction in pore fluids, of abnormally high temperature or of intense mineralization. Note that, along the Scottish traverse, the most conducting surface layers coincide with known sedimentary basins in which above average heat flow has recently been reported[26]. The relative contribution of porosity, salinity and temperature in these regions could thus be of interest to the UK geothermal programme. Moreover, similar electrical soundings might be useful to current studies of the deep sedimentary basins in England, especially as pore fluid data are already available from those regions[27].

In the lower crust, the increased pressure and hence crack closure make it unlikely that conduction in electrolytic pore fluids can account for the presence of a conducting zone at this depth. Solid conduction in dry rocks also seems improbable as extremely high temperatures—greater than 700 °C—would be required to provide conductivities of the order of magnitude found in this study. On the other hand, solid conduction through hydrated rocks may be a possibility. Laboratory measurements have also indicated that time-dependent increases in conductivity of up to four orders of magnitude can occur in the solid state due to phenomena such as order–disorder in crystals and rocks[28]. The presence of hydrated rocks with or without associated partial melting has, nevertheless, been the most frequent interpretation for conducting layers in the lower crust[15–24].

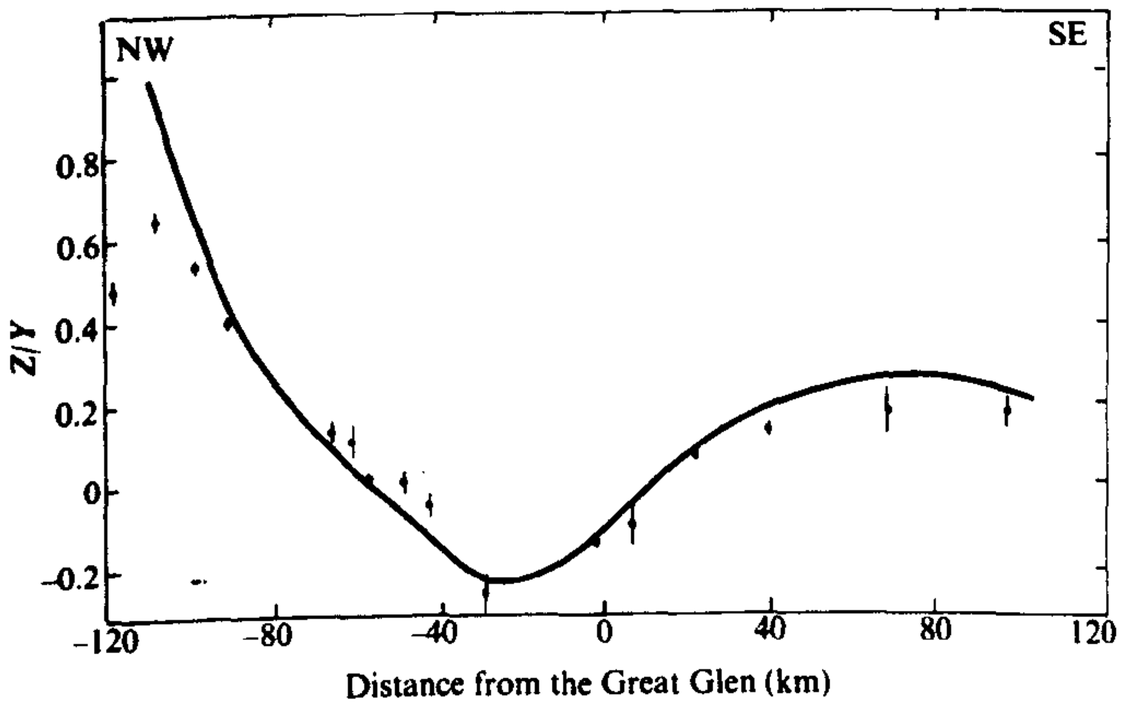

Fig. 3 The variation across the traverse AA′ of the vertical magnetic field transfer function Real (Z/Y), that is the E-polarization case, for a period $T = 95$ s. The solid curve represents the values computed for the model given in Fig. 2*a*. The dots and associated error bars refer to values computed from field data.

For example, Berdichevsky *et al.*[18] have discussed the increase in electrical conductivity of granite and other rock types on melting in the presence of water at temperatures of 400–600 °C. They have associated the zone of active granitization and melting with the transition zone between amphibolitic and granulitic facies, that is with the Conrad discontinuity, with the necessary few per cent of water being released as a result of the dehydration at this boundary. Stanley *et al.*[23] have used laboratory results[29–32] to argue that hydrated rocks, such as granite, tonalite, syenite and gabbro, in the upper crust will start melting at 500 °C, especially where the rocks have been subjected to rapid alteration processes. The 500 °C isotherm is, in this case, coincident with a large change in electrical conductivity.

The interpretation of the lower crustal conductor in Scotland in terms of hydrated rocks and partial melting and the other

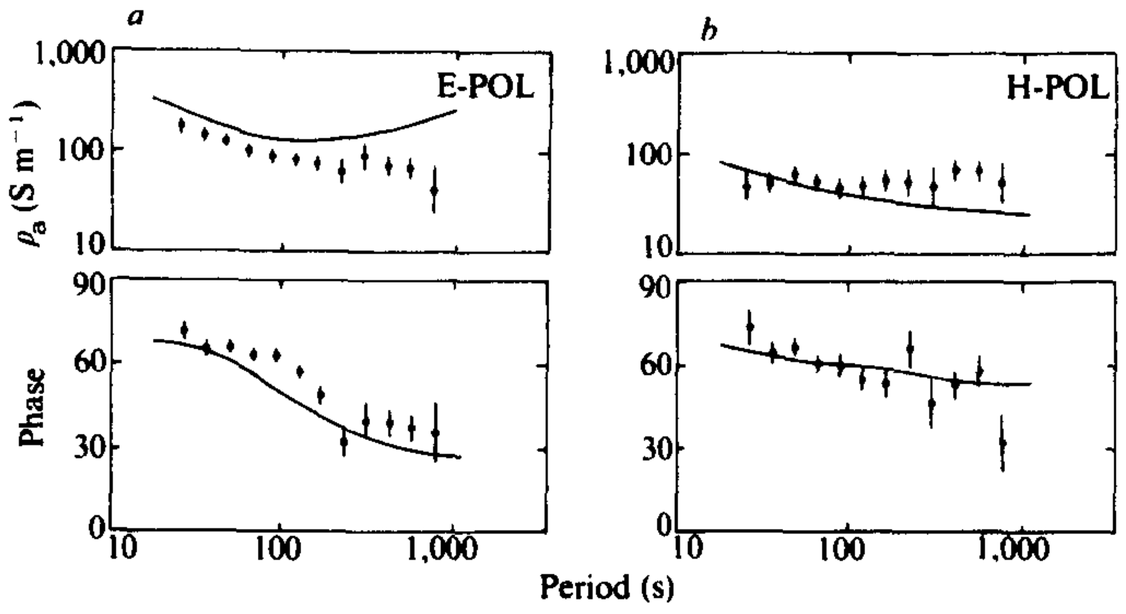

Fig. 4 Apparent resistivity and phase versus period data and associated errors for Yarrow in the Southern Uplands—the station on the traverse BB′ immediately north of BOW in Fig. 1. Curves *a* and *b* correspond respectively to the E and H polarization cases and the smooth curves to the computed values for the model given in Fig. 2*a*.

interpretations will be considered elsewhere. However, note that if the granites in Scotland are uranium enriched as in Cornwall and northern England, then a temperature gradient of 30 °C km^{-1} and a depth to the 500 °C geotherm of ~16 km can be expected.

In consideration of Fig. 2*a*, note that: there can be some trade-off between interface depth and conductivity; use of closer station spacing and broader-band electrical soundings may introduce significant changes to the model in some regions; and careful assessment of the validity of laboratory studies is required before further conclusions can be drawn.

It is unfortunate for the tectonic implications of the model that more electrical soundings have not been undertaken in the Midland Valley. If, however, the major boundaries in conductivity structure now suggested to the north and south of this region were confirmed an interpretation of these lateral variations would be possible in terms of former subduction zones as has been suggested in similar studies elsewhere (see refs 33–35). The location of a subsequent subduction zone and the nature of the Iapetus suture[36] may become clearer on the completion of current analyses of geomagnetic and geo-electric observations from northern England.

We thank the NERC for a research grant (GR3/2141) and a studentship for M.R.I., and the Federal Government of Nigeria for a studentship for E.W.M.

Received 2 May; accepted 3 July 1980.

1. Jain, S. & Wilson, C. D. V. *Geophys. J.R. astr. Soc.* **12**, 165–180 (1967).
2. Edwards, R. N., Law, L. K. & White, A. *Phil. Trans. R. Soc.* **270**, 289–323 (1971).
3. Hutton, V. R. S. & Jones, A. G. *J. Geomagn. Geoelec.* (in the press).
4. Jones, A. & Hutton, R. *Geophys. J.R. astr. Soc.* **56**, 329–368 (1979).
5. Bamford, D., Nunn, K., Prodehl, C. & Jacob, B. *Geophys. J.R. astr. Soc.* **54**, 43–60 (1978).
6. Schmucker, U. *Bull. Scripps Inst. Oceanogr.* **13**, 1–165 (1970).
7. Banks, R. J. *Phys. Earth planet. Inter.* **7**, 339–348 (1973).
8. Hermance, J. T. *Phys. Earth planet. Inter.* **7**, 349–364 (1973).
9. Haak, V., *Bayer. Akad. Wissen.* **158**, 1–105 (1978).
10. Rooney, D. & Hutton, V. R. S. *Geophys. J.R. astr. Soc.* **51**, 91–119 (1977).
11. Jones, A. G. thesis, Univ. Edinburgh (1977).
12. Brewitt-Taylor, C. & Johns, P. B. *J. Geomagn. Geoelec.* (in the press).
13. Mbipom, E. W. thesis, Univ. Edinburgh (1980).
14. Kurtz, R. D. & Garland, G. D. *Geophys. J.R. astr. Soc.* **45**, 321–348 (1976).
15. Hyndman, R. D. & Hyndman, D. W. *Earth planet. Sci. Lett.* **4**, 427–432 (1968).
16. Caner, B. *J. Geomagn. Geoelec.* **22**, 113–129 (1970).
17. Dowling, F. L. *J. geophys. Res.* **75**, 2683–2698 (1970).
18. Berdichevsky, M. N., Vanyan, L. L., Feldman, I. S. & Porstendorfer, G. *Beitr. Geophys.* **81**, 187–196 (1972).
19. Edwards, R. N. & Greenhouse, J. P. *Science* **188**, 726–728 (1975).
20. Van Zijl, J. S. V. *The Earth's Crust*, 470–500 (AGU Monograph No. 20, 1977).
21. Nekut, A., Connerney, J. E. P. & Kuckes, A. J. *Geophys. Res. Lett.* **4**, 239–242 (1977).
22. Sternberg, B. K. *J. geophys. Res.* **84**, 212–218 (1979).
23. Stanley, W. D., Boehl, J. E., Bostick, F. M. & Smith, H. W. *J. geophys. Res.* **82**, 2501–2514 (1977).
24. Hermance, J. F. & Pedersen, J. *Geophys. J.R. astr. Soc.* (in the press).
25. Duba, A., Piwinski, A. J., Santor, M. & Weed, H. C. *Geophys. J.R. astr. Soc.* **53**, 583–597 (1978).
26. Oxburgh, E. R. *et al. EEC 2nd int. Seminar on Geothermal Energy* 149–152 (1980).
27. Burley, A. J. *et al. EEC 2nd int. Seminar on Geothermal Energy*, 29–33 (1980).

28. Duba, A. *Acta geod. geophys. Montan.* **11**, 485–495 (1976).
29. Shankland, T. J. & Waff, H. S. *J. geophys. Res.* **82**, 5409–5417 (1977).
30. Wyllie, P. J. *Structure and Physical Properties of the Earth's Crust*, 279–301 (AGU Monograph No. 14, 1971).
31. Zobacki, M. D. thesis, Stanford Univ. (1975).
32. Lebedev, E. B. & Khitarov, N. J. *Geokhimiya* **3**, 195–201 (1964).
33. Law, L. K. & Riddihough, R. P. *Can. J. Earth Sci.* **8**, 1094–1106 (1971).
34. Gough, D. I. *Phys. Earth planet. Inter.* **7**, 379–388 (1973).
35. Garland, G. D. *Phys. Earth planet. Inter.* **30**, 220–230 (1975).
36. Phillips, W. E. A., Stillman, C. J. & Murphy, T. *J. geol. Soc. Lond.* **132**, 579–609 (1976).

Printed in Great Britain by Macmillan Production Ltd., Basingstoke, Hampshire